

**The Expedition ARKTIS XIX/1 a, b and XIX/2
of the Research Vessel „POLARSTERN“ in 2003**

**Edited by
Ursula Schauer and Gerhard Kattner
with contributions of the participants**

**Ber. Polarforsch. Meeresforsch. 481 (2004)
ISSN 1618 - 3193**

CONTENTS

ARK XIX/1: BREMERHAVEN - LONGYEARBYEN

U. Schauer pages 1 - 158

ARK XIX/2: LONGYEARBYEN - BREMERHAVEN

G. Kattner pages 159 - 190

ARK XIX/1

28.02. - 24.04.2003

Bremerhaven - Longyearbyen

WARPS - WINTER ARCTIC POLYNYA STUDY

Fahrtleiterin / Chief Scientist

Ursula Schauer

Koordinator / Coordinator

Eberhard Fahrbach

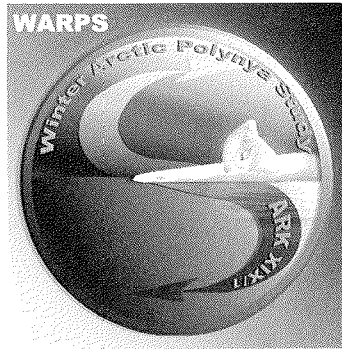
1.	EINLEITUNG UND FAHRTVERLAUF	5
	INTRODUCTION AND ITINERARY	8
2.	WEATHER CONDITIONS	10
3.	SEA ICE PHYSICS	13
3.1	Sea ice remote sensing, thickness profiling, and ice and snow analyses	13
3.1.1.	Outline	13
3.1.2.	General ice conditions	13
3.1.3	Remote Sensing	17
3.1.4.	Ice thickness measurements	26
3.1.5.	Laser profiling of pressure ridges	38
3.1.6.	Ice coring	40
3.1.7.	Snow measurements	40
3.1.8.	Wave measurements	41
3.2	Ice thickness determination using flexural gravity waves	43
4.	ATMOSPHERE PHYSICS AND CHEMISTRY	47
4.1	Convection Over Arctic Leads (COAL)	47
4.1.2.	Surface fluxes over leads and polynyas	49
4.1.3.	Ship borne continuous measurements	51
4.2	Arctic Boundary Layer and Sea Ice Interaction Study (ABSIS)	63
4.3	Determination of Arctic stratospheric ozone losses	67
4.4	Reactive trace compounds in sea ice and in the Arctic troposphere	69
4.5	Meridional aerosol optical depth distribution from 70°S to 80°N	72
5.	WATER MASSES AND CIRCULATION	72
5.1	Shelf convection in the western Barents Sea and Atlantic water north of Svalbard	72
5.3.	Technetium measurements	91

CONTENTS

6.	BIOLOGY IN THE SEA-ICE, IN THE WATER COLUMN AND AT THE SEA FLOOR	92
6.1	Arctic sea-ice biology in winter	92
6.2	Cryo-pelagic coupling in Arctic winter	97
6.3	Reproductive biology of calanoid copepods	99
6.4	The pelagic larvae of the invertebrate macrofauna in the Storfjorden and the adjacent Barents Sea	100
6.5	Ocean Optics	103
6.6	Ecophysiology	108
6.7	Arctic zooplankton	109
6.8	Sea ice microbiology	109
6.9	Benthos activities during winter	110
6.10	Seasonal investigations at a deep-sea long-term station	111
6.11	Methane plumes in the marginal Arctic Ocean - Pathways in the water column and documentation in specific biota	114
7.	SEDIMENTOLOGY	118
	APPENDIX	127
A.1	PARTICIPANTS	128
A.2	PARTICIPATING INSTITUTES	130
A.3	SHIP'S CREW	132
A.3	STATION LIST	133

1. EINLEITUNG UND FAHRTVERLAUF

Unsere Kenntnisse über physikalische, chemische und biologische Vorgänge in den Polargebieten stammen im Wesentlichen aus Beobachtungen im Sommer. Die meisten Prozesse in der Atmosphäre, dem Ozean und dem Meereis haben jedoch einen ausgeprägten Jahresgang, manche Prozesse, wie Eisbildung, finden fast ausschließlich im Winter statt. Um diesen Kenntnislücken Rechnung zu tragen, fand mit ARKXIX/1 im März/April 2003 zum ersten Mal seit 10 Jahren wieder eine Winterexpedition mit Polarstern in die Arktis statt

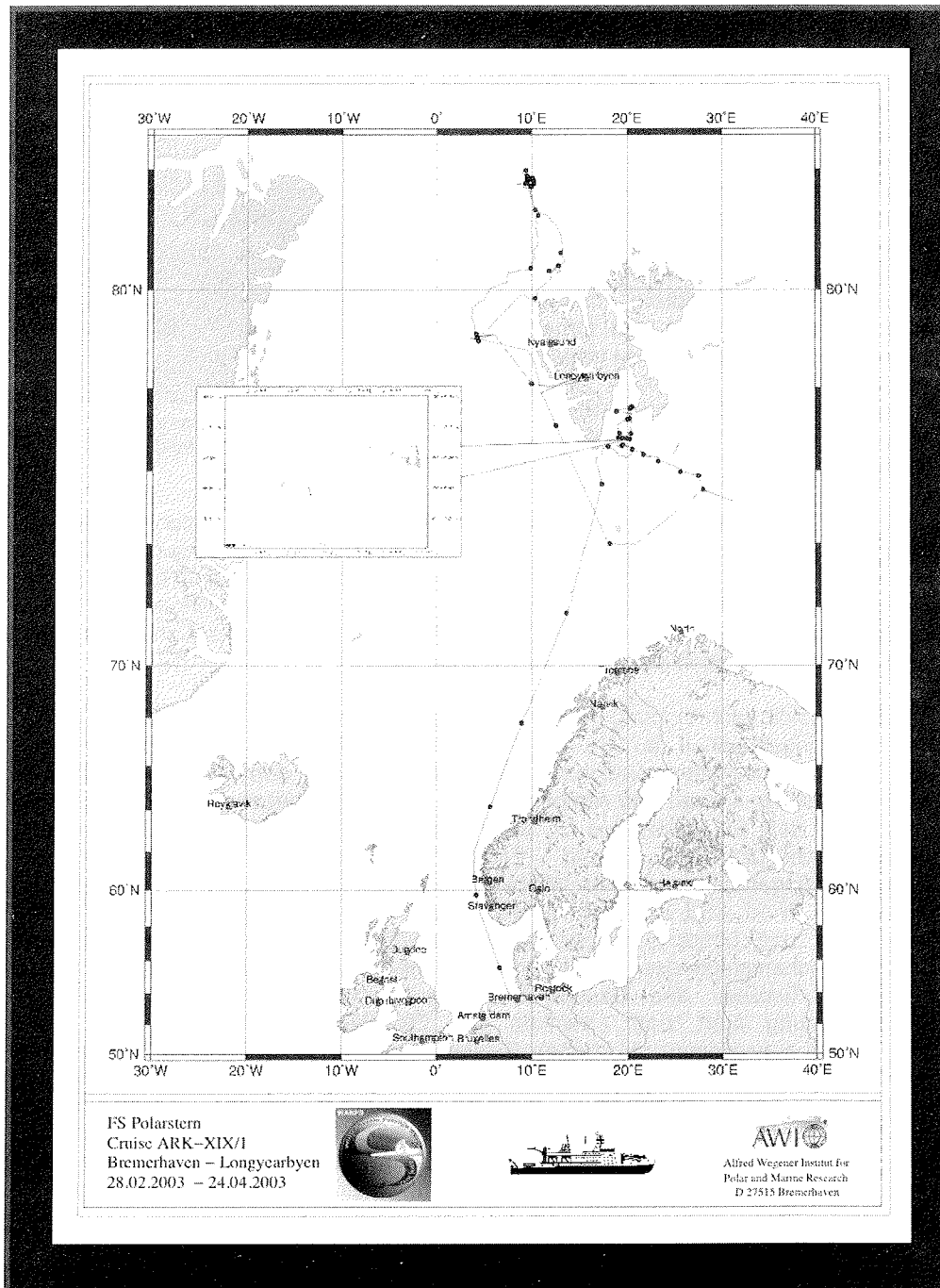


"Mr. Spock, take us to WARP 9 please!" (Star trek)

Polarer Winter bedeutet Verschwinden der solaren Einstrahlung, enormen Wärmetransfer vom Ozean zur Atmosphäre und Meereisbildung. Besonders viel Eis wird in „latent heat“-Polynjen gebildet, verbunden mit intensiver Wechselwirkung zwischen Eis, Ozean und Atmosphäre. Diese Wechselwirkungen haben weitreichende Auswirkungen sowohl auf die Zirkulation, als auch auf chemische und biologische Vorgänge in allen drei Kompartimenten.

Die Arktis spielt nach bisheriger Kenntnis eine entscheidende Rolle im Klimasystem. Der Strahlungshaushalt der Atmosphäre wird durch die hohe Reflektivität (Albedo) der Eisdecke modifiziert. Gleichzeitig behindert Meereis den Austausch fühlbarer Wärme zwischen Ozean und Atmosphäre. In Polynjen dagegen, wo auch im Winter wenig oder kein Eis vorhanden ist, weil es etwa durch den Wind verdriftet wurde, sind Wärme fluß und damit Eisbildung umso vehementer, da die Temperaturgegensätze zwischen Wasser und Luft 30 °C und mehr betragen können. Durch den Wind wird das dünne Neueis an den Rand der Polynja getrieben, zerbrochen und übereinandergeschoben. Dieser Prozess ist der dominierende Bildungsmechanismus des meterdicken Packeises der Arktis. Bei der Eisbildung bleibt der Großteil des Salzes im Wasser zurück. Die dort resultierende Dichteerhöhung führt zum Absinken des Oberflächenwassers. Obwohl dieser Prozess auf sehr kleinen räumlichen Skalen stattfindet, ist er Teil des Motors einer weltumspannenden Ozeanströmung, der thermohalinen Zirkulation, die Wärme und Stoffe über große Entfernungen umverteilt. Die unterschiedliche Eisbedeckung und die geringe Sonneneinstrahlung im Winter regulieren auch die Beschaffenheit der atmosphärischen Grenzschicht, die von stabiler Inversion über dem Packeis bis zu heftiger Konvektion über Polynjen und Rinnen reicht, die Wärme, Impuls und Feuchte in große Höhen verteilt.

1. EINLEITUNG UND FAHRTVERLAUF



1. EINLEITUNG UND FAHRTVERLAUF

Mehr als in niedrigeren Breiten unterliegen biologische Vorgänge in Polargebieten der extremen Saisonalität. Beobachtungen im Winter sind daher essentiell für unser Verständnis des arktischen Ökosystems. Die Besiedlung von neu gebildetem Eis mit Eisorganismen ist ebensowenig verstanden wie die Initiierung von Aktivität und Reproduktion und die Rekonstruktion des Nahrungsnetzes in und unter dem mehrjährigen Eis bei der Rückkehr des Sonnenlichts. Ebenso wenig ist der Einfluss der Jahreszeiten auf die Lebenswelt am Boden der Tiefsee bekannt.

„WARPS“ (Winter Arctic Polynya Study) war eine interdisziplinäre, internationale Studie der Wechselwirkungen von Atmosphäre, Meereis und Ozean und ihrer Konsequenzen für biochemische und biologische Prozesse in den Habitaten Meereis, Wassersäule und Meeresboden. Die Untersuchungen wurden in fünf Arbeitsgebieten durchgeführt:

- im Storfjord im Süden Svalbards
- über die Polarfront in der westlichen Barentssee
- in der Polynja nördlich von Svalbard (Whalers Bay)
- auf einer zwölf-tägigen Driftstation „Tomato Island“ im zentralen Packeis
- bei der Tiefsee-Langzeit-Station „Hausgarten“ in der Framstraße

ARKXIX/1 fand in zwei Abschnitten statt. Die Reise begann am 28. Februar 2004 in Bremerhaven. Nach der einwöchigen Anfahrt unter frühlingshaften Bedingungen trafen wir an der Meereisgrenze südlich von Svalbard auf den arktischen Winter. Ein dichter Brei aus Bruchstücken von mehrjährigen dicken Schollen und Splintern von Neueis bewegte sich südwestwärts und machte das Vordringen zum Storfjord zu einer langwierigen Angelegenheit im Zickzackkurs. Sowohl auf der Anfahrt als auch in der Polynja im äußersten Nordosten führten wir Stationen zu allen Forschungsprogrammen des ersten Teils durch und gewannen so einen Gradienten aller Parameter vom dichten, dicken Eis zur offenen Polynja.

Ein Schnitt vom polaren Wasser südlich Spitzbergen in den Bäreninsel-Trog, der von warmem atlantischen Wasser dominiert wird, diente dem Vergleich der Aktivität der planktischen und benthischen Fauna im Spätwinter in beiden Regimes.

Bei einem Zwischenstopp am 29. März in Longyearbyen wurde ein Teil des wissenschaftlichen Personals ausgetauscht. Das nächste Ziel war das Gebiet nördlich von Spitzbergen, wo der Einstrom warmen atlantischen Wassers die sogenannte „Whalers Bay“ zeitweise ganz eisfrei hält. Kurz vor unserer Ankunft war die warme Strömung von dickem Eis überschoben worden, so dass wir auf einer eintägigen Station den starken ozeanischen Wärmefluss mit heftigem Abschmelzen des Eises messen konnten. Die fast unmittelbare Verfügbarkeit von Eiskarten aus Satellitenmessungen ermöglichte uns, in einer breiten, abgesehen von „ein paar“ zähen Packeisbarrieren durchgängigen Rinne bis fast 82°N vorzudringen. Dort machte das Schiff an einer geeigneten Scholle, genannt „Tomato Island“, fest um mehrere Messmasten zu errichten, mit denen 12 Tage lang die stabile atmosphärische Grenzschicht über dem Packeis beprobt wurde. Zusätzlich wurde ein umfangreiches physikalisches und biologisches Meereisprogramm durchgeführt. Viele dieser Arbeiten waren Bestandteil von internationalen Programmen zur Validierung von Satelliten-Fernerkundung (CryoSat Validation Experiment CryoVex

1. INTRODUCTION AND ITINERARY

2003, GreenICE, SITHOS, and IRIS, siehe Abschnitt 3) oder meteorologischer Programme (ABSIS, Arctic Boundary and Sea ice Interaction Study, siehe Abschnitt 4.2). Unseren Weg aus dem Eis legten wir gemeinsam mit dem finnischen Forschungsschiff „Aranda“ zurück, das weiter südlich ein paralleles Messprogramm mit einer Driftstation absolviert hatte.

Die letzte Aktivität war ein Beitrag zu dem Langzeituntersuchungsprogramm an der Tiefseestation „Hausgarten“, wo zum ersten Mal seit dem Beginn 1999 das Benthos zwischen Schelfkante und Tiefsee im Winter beprobt wurde.

Polarstern beendete die Reise am 24. April 2004 in Longyearbyen. Die Fahrtteilnehmer möchten sich bei allen herzlich bedanken, die bei der Vorbereitung und Durchführung der Expedition durch ihre große Unterstützung zum Erfolg der Reise beitrugen.

INTRODUCTION AND ITINERARY

Our knowledge about physics, chemistry and biology of the polar oceans is to a large extent based on summer observations. Most polar processes within atmosphere, ocean and ice undergo, however, a strong seasonal cycle or, like icing formation, taking place only in winter. To redress this observational bias, in March and April 2003 Polarstern embarked on a winter expedition to the Arctic for the first time in 10 years.

Winter is the time of little to no solar radiation, huge heat transfer from the ocean to the cold atmosphere, and sea ice generation. Much of the ice is formed in latent heat polynyas and this process constitutes a momentous interaction between atmosphere, ice and ocean with far-reaching consequences for the circulation as well as for chemistry and biota in all three compartments.

According to present knowledge, the Arctic plays a decisive role in our climate system. The radiation budget of the atmosphere is modified by the high albedo (reflectivity) of the ice. At the same time, sea-ice slows the exchange of heat, moisture and gases between the air and the water. Where there is little ice, owing to wind-caused drifting, the heat flow is much stronger because the temperature difference between water and air can be more than 30°C. The wind drives the new ice to the edge of the polynya, breaks it and piles it up. This process is responsible for the generation of most of the thick pack ice of the Arctic. The different types of ice cover, in combination with the low insolation in winter, regulate the atmospheric boundary layer conditions from strong stability with a temperature inversion to vigorous convective motion over a polynya. During freezing, the majority of the salt remains in the surrounding water. The associated increase in water density causes the water to sink. Although this process occurs on very small spatial scales, it is part

1. INTRODUCTION AND ITINERARY

of the motor of a global current pattern, the thermohaline circulation, which distributes heat and substances over great distances.

Maybe more than elsewhere, in the ice and in ice-covered water of polar regions biological processes are subject to strong seasonality. Observations in winter are crucial to complete our understanding of the Arctic ecosystems. The colonization of newly formed ice is as poorly understood as the onset of biological activity and reproduction and the reforming of the foodweb in and below the pack ice with the return of sun light. Equally unknown is in which way the life at the bottom of the shelf and deep sea, the benthos, is subject to this seasonality.

“WARPS” (Winter Arctic Polynya Study) was an interdisciplinary, international study of the exchange between the atmosphere, ice and ocean and the consequences for biogeochemistry and biological processes in the habitats of ice, water and the sea floor. For these studies we worked in five areas:

- in the Storfjorden in southern Svalbard
- in the western Barents Sea
- in the sensible heat polynya north of Svalbard (Whalers Bay)
- on a two-week drift station in the central pack ice “Tomato Island”
- at the long-term deep-sea research site “AWI-Hausgarten”.

ARKXIX/1 was divided in two parts. The cruise began at 28 February in Bremerhaven. After a one-week transfer in friendly spring conditions we encountered winter and heavy ice south of Svalbard. A stream of crunched ice composed of thick multi-year boulders and newly formed chips moving southwestwards from east of Svalbard made our approach to the latent heat polynya inside the Storfjorden a slow and wiggled exercise. We measured atmosphere, ice and ocean properties, ice-ocean-atmosphere fluxes and chemical and biological parameters along several sections thus obtaining their distribution along a gradient from heavy ice into the open polynya.

A transect from the Polar Waters south of Svalbard into the Bear Island Trough with dominance of warm Atlantic Water enabled a comparison of the late winter zooplankton and benthos activities in the two different regimes.

On 29 March we had a stopover in Longyearbyen for an exchange of several participants. With the new group our destination were the waters north of Svalbard where the boundary current of warm Atlantic Water tends to maintain the Whalers Bay open during winter. Wind had, however, closed the sensible heat polynya with thick ice here as well so that we measured strong heat flux from the ocean and consequent rapid melting. Onboard availability of real-time SSIM images enabled us to find the entrance to an extended lead in northern Fram Strait along which we steamed towards north into the pack ice “only” interrupted by a few barriers of ridged ice. At almost 82°N, we tied Polarstern to a suitable large floe, named “Tomato Island” on which several masts were set up for 12 days to conduct atmospheric boundary layer measurements. In addition comprehensive investigations of sea ice physics and biology were carried out. Many of these studies were part of international programmes for the validation of sea ice satellite remote sensing (CryoSat Validation

Experiment CryoVex 2003, GreenICE, SITHOS, and IRIS, see Chapter 3) or for meteorology (ABSIS, Arctic Boundary and Sea ice Interaction Study, see Chapter 4.2). On our way back from the pack ice we joined the Finnish Research Vessel "Aranda" which operated further south at the ice edge.

The last activity focussed on the deep-sea benthic in the long-term station "AWI Hausgarten" in Fram Strait where in a series of surveys since 1999 the first winter observations were made.

The cruise ended in Longyearbyen on 24 April 2003.

The participants are grateful to all those who helped during the preparation and during the cruise to make the expedition a great success.

2. WEATHER CONDITIONS

Weiland, Gebauer, Buldt (DWD)

During the transit from Bremerhaven towards Spitsbergen (28.2. – 6.3.) a stationary high over Russia was dominating the weather in Europe. We had on the whole route a southerly wind between Bft 6 and 8 and temperatures about 6 °C. On the 5th of March Polarstern crossed the border between the mild Atlantic airflow coming from southwest and the polar air from east. The temperatures went down below the freezing-point, on the next day we had already -14 °C with easterly winds and snowdrift. On this day the scientific works began in the area around the Storfjord. Due to the further on stationary Eastern-European high the track of the lows did not change, they went from the area south of Iceland along the Norwegian coast to the Barents-Sea. On the 11th of March an upper trough crossed Western Europe from west to east causing an outbreak of cold air southward to Ireland. In connection with this trough low pressure systems shifted east across Central Europe, later a new high established over the Atlantic, which moved to the North-Sea with pressure about 1045 hPa. Now the Atlantic lows moved from Cape Farvel to Jan Mayen and further on to Bear Island. On the following days the frontal-zone moved further to the north, from 16th of march heavy developments took place near Western Greenland and due to upper troughs crossing Greenland, new lows established over the Greenland-Sea and moved east between Svalbard and the north-cape, developing rapidly from time to time. On 21st of March this circulation-type changed again, as the high over Central-Europe draw back to the south and the track of the lows shifted south again. During the whole cruise in the working-area of Polarstern the wind came predominantly from directions between east and north, so very cold air from the polar-ice arrived the area. Due to this situation the temperatures lay between -20 and -30 °C. Only if the wind came from south or southwest and brought Atlantic air, the temperatures rose up to -5 to -10 °C. Only on 21st of March the temperature reached the freezing-point for a short time. In case of a north-easterly airflow for several times in the southwest of the islands a lee-cyclone was remaining for a time, when a low had crossed in the south. These cyclones got their energy apparently from the temperature-differences between the cold air from the north which became warmed up over the Atlantic water and the extremely cold air coming from east from the polar-

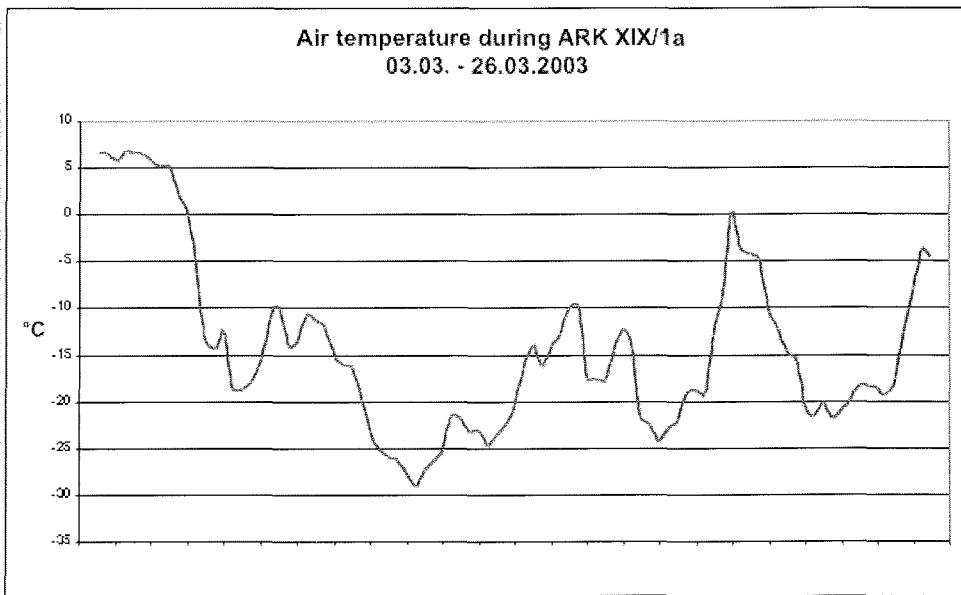
2. WEATHER CONDITIONS

ice. On the border-line between these air-masses sometimes "boundary-layer-fronts" were establishing containing mesoscale vortices. On 26th of March Polarstern started towards Longyearbyen,

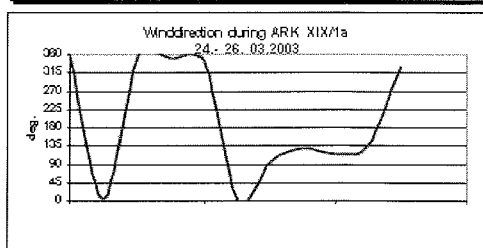
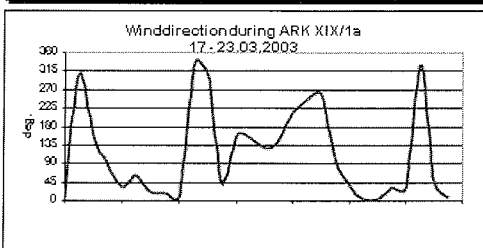
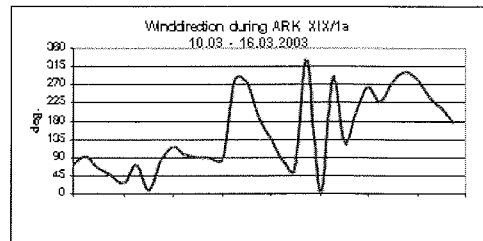
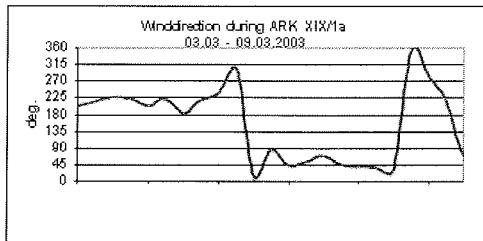
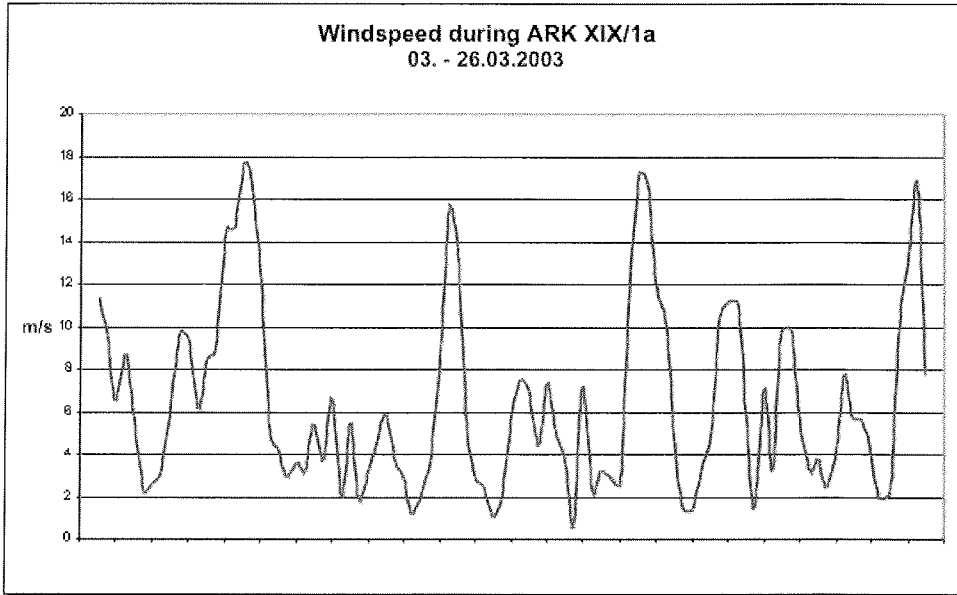
On 30th of March Polarstern left Longyearbyen again in order to reach the polar-ice north-west of Spitsbergen. A enduring northerly wind was blowing between an intensive high over the northern parts of Greenland and low pressure influence near the northern most part of Norway, mostly with wind force 4 to 6 Bft. Over open water it was foggy, over large areas covered with ice the visibility was fairly good.

On 6th of April the weather changed. A trough over Greenland migrated northeastward and lows moved along the eastern coast of Greenland in direction of Polarstern, which arrived at its destination on 82 °N. During the following ten days various lows passed along Polarstern. Wind speed und wind direction, visibility and ceiling varied over a long range, but frequently the wind blew from the south, accompanied by bad visibility. There was also intermediate high pressure influence with quite good flight weather.

Behind a cyclone, that intensified in the Fram Strait and in lee of Svalbard, the wind blew with 7 Bft from northerly directions and again the temperature sank below – 24°C. While working in the "Hausgarten" in open water (20 to 22 April) the wind speed decreased to 4 to 5 Bft.



2. WEATHER CONDITIONS



3. SEA ICE PHYSICS

3.1 Sea ice remote sensing, thickness profiling, and ice and snow analyses

Haas, Lieser, Lobach, Martin, Pfaffling, Willmes (AWI),
Alexandrov (NERSC), Kern (IfMH)

3.1.1. Outline

The main goal of the geophysical sea ice work was the determination of representative sea ice thickness distributions in Storfjord and the Barents Sea, as well as in Fram Strait, and the validation of a range of different satellite remote sensing data.

In Storfjord and the Barents Sea, the data were acquired to obtain estimates of the ice production in the Storfjord Polynya, as an independent assessment of oceanographic and meteorological salt and energy budget observations.

In Fram Strait, the geophysical field work was part of the CryoSat Validation Experiment CryoVex 2003 co-ordinated by the European Space Agency ESA. Coincident, synchronous helicopter flights were carried out with a Danish Twin Otter fixed-wing aircraft equipped with a synthetic aperture radar altimeter resembling the new-generation SIRAL radar altimeter on board ESA's upcoming CryoSat mission in 2004. CryoSat is dedicated to observe the ice thickness of the earth's land and sea ice masses.

Sea ice thickness measurements were complemented by a number of other observations including ice coring and snow sampling, visual ice observations and satellite image acquisition. The work was carried out in the framework of and supported by three EU projects GreenICE, SITHOS, and IRIS. Within these projects, real-time Envisat, ERS and QuickScat satellite imagery were transmitted to the ship as navigational support and for validation purposes by Norwegian (Nansen Environmental and Remote Sensing Center, Bergen) and Danish (Danish Technical University, Lyngby) partners.

3.1.2. General ice conditions

Hourly, standardised visual ice observations were performed in a joint effort by all 16 sea ice scientists during daylight hours when the ship was moving through ice. In total, 279 observations were performed.

On board, all observations and photographs were typed into Excel spreadsheets and linked html pages, and will be made available on the www after return to Bremerhaven.

3.1.2.1 Storfjord and Barents Sea

A diffuse ice edge with bands of pancake brash was crossed at about 8:00 UTC on March 6 between Björnøya and Svalbard (see cruise track; Fig. 3.1.1). From there,

3. SEA ICE PHYSICS

the ship passed in 70 to 90 % ice concentration with small thin floes < 20 m diameter to the southern tip of Svalbard. There, very heavy ice conditions were met requiring continuous ramming, lasting until March 21, when Storfjorden was left into the Barents Sea. Between March 7 and March 21, in outer Storfjorden Polarstern sailed in almost always 100 % ice concentration, with 0.4 to 1.8 m thick small floes (typically < 30 m diameter) covered with 20 to 30 cm of snow, embedded in heavily ridged and rubbled ice. As was interpreted from satellite radar imagery (Figs. 3.1.1, 3.1.2) and ice core analyses (Section 3.1.6), this ice was a mixture of second-year and multiyear floes from the Arctic Ocean, with deformed first-year ice in between.

Only few cracks and narrow leads led to the inner Storfjord region, where grey ice with thin or no snow prevailed and where Polarstern made good progress. As can be seen on the satellite images, this region of young and first-year ice formed in Storfjorden extended all along the western margin of the fjord. However, CTD work required a return into heavy ice soon again.

No opening of a large polynya occurred during our study. As can be seen on the near infrared image in Figure 3.1.3, open water and thin ice were confined to a narrow zone along the northern and north eastern coasts. However, as outlined above, by the end of March ice formed in Storfjorden could be tracked southward to the southern tip of Svalbard.

After March 21, in the Barents Sea with ice concentrations of 90 to 100% big floes (100-1000 m diameter) with less ridging but 20 to 30 cm snow were encountered. After March 24, fracturing due to ocean swell was observed, and bigger polynyas inside the closed pack covered with new ice and extensive amounts of frost flowers. After this, the marginal ice zone with heavy swell was left through a very diffuse ice edge into the open Barents Sea on March 26 to sail to Longyearbyen. On March 28, close to Svalbard ice exported from the Storfjord was encountered in the West Spitzbergen Current. Ice concentration was as high as 90 %, with small but thick deformed and snow covered floes.

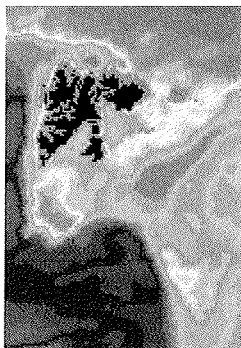


Figure 3.1.1: QuickScat HH backscatter image of Svalbard and the Barents Sea from March 06, 2003.

Dark tones represent low backscatter, bright tones represent high backscatter. The image shows the flow lines of older ice from the Arctic Ocean and first year ice formed leeward of Franz Josef Land and in Storfjorden. Image courtesy of L. Toudal, DTU.

Figure 3.1.2: Mosaic of ERS and Envisat SAR images acquired between March 17 and 21. Superimposed are the coastline of Svalbard and the actual cruise track until March 21 as well as planned stations. Different textures of second/multiyear ice and first-year ice can be seen and compared to Figure 1. Image courtesy K. Kloster, NERSC.

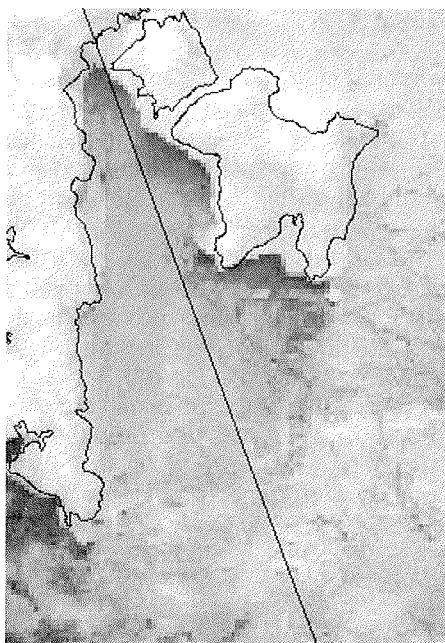


Figure 3.1.3: NOAA-AVHRR near infrared image of Storjorden received on board on March 19 (Section 3.1.1), showing the distribution of polynyas and thin ice areas, as well as the first-year ice exported from Storjorden

3. SEA ICE PHYSICS

3.1.2.2 Northwest of Svalbard

Kern (IFMH)

On March 29 the ship arrived in Isfjorden which was covered up to 90% with nilas and grey-ice and some smashed first-year ice. During and after leave of Isfjorden nilas and pancakes were encountered until March 30, 6 UTC, when last bands of almost completely melted brash ice were observed at 78°55'N, 7°35'E, while steaming westward. On March 31, steaming northeastward, the ship arrived at the ice edge at 80°05'N, 11°18'E. In between, isolated, almost completely melted second-year and multiyear ice floes were observed (e.g. at 79°04'E, 4°18'E); later, i.e. further north (around 79°50'N, 9°01'E and further east) bands of first-year ice floes and open water were observed. Typical ice (snow) thickness was 0.70 m (0.1-0.2 m) at the ice edge.

The ice coverage encountered during the next days until arrival at the drift station ice floe on April 6 at 81°54'N, 9°28'E, was between 90 and 100% comprising mostly first-year/second-year and multiyear ice floes (on average 100-200 m in diameter). These floes were separated by leads which were between 50 and 500 m (2000 m) wide. The leads were typically covered with nilas, grey, and grey-white ice, often covered by dense frost flower mats. Through these leads which can be seen in figures 3.1.5 and 3.1.8 quite clearly the ship was navigated to the drift station ice floe. Ice thickness in leads varied between 0.03 and 0.20 m whereas it was between 0.80 to 2.00 m otherwise. Observed snow depths ranged from 0.05 to 0.30 m on thick ice. Notable rubble fields (up to 30% of the total ice coverage) were observed on April 1 at around 80°26'N, 12°49'E. Typical ridge height and spacing was 1 m and 100 m, respectively. On the way to the drift station ice floe, the ship was stuck two times; the first time on April 3 at 80°42'N, 13°14'E for about six hours in a floe with a 3 m high ridge; the second time on April 4/5 for about 30 hours in a 0.8-1.2 m thick first-year ice floe which itself was stuck between two multiyear ice floes.

After leaving the drift station ice floe on April 18, at 81°38'N, 9°59'E, still heavy ice conditions were encountered with 90 to 100% of first-year/second-year and multiyear ice floes with an average diameter of 200 m, a snow depth of 0.15 to 0.30 m and average ridge height and spacing of 1 m and 100 m, respectively. Between these floes dark and light nilas was observed - almost without frost flowers. Rubble fields amounted up to 20% of the total ice cover. Between April 19 and 20, i.e. 81°15'N, 10°33'E and 80°35'N, 10°20'E, ice concentrations decreased to between 80 and 95%. The ice coverage comprised 1 to 2 m thick first-year/second-year and multiyear ice. Typical floe sizes decreased to between 20 and 50 m and looked like as if broken by recent swell activity. Floes were separated by brash ice rather than nilas. The ice type changed to mainly first-year ice around 80°19'N, 7°38'E with a decrease of the typical ice (snow) thickness to 0.40 to 0.60 m (0.05 to 0.10 m). Further to the southwest (80°12'N, 7°31'E) a mixture of such first-year ice and up to 2 m thick second-year/multiyear ice was observed together with some nilas and grey-ice as well as open water. Ice concentrations dropped to 60 to 90%. On April 21 at about 12 UTC the ship arrived in open water at about 79°20'N, 3°54'E, after steaming through 20 to 60% ice coverage with melting first-year ice.

3.1.3 Remote Sensing

3.1.3.1 NOAA-AVHRR imagery

(Lieser, Haas)

The satellite receiving system installed onboard RV POLARSTERN receives data from the polar orbiting NOAA-Satellites (National Oceanographic and Atmospheric Association, USA) NOAA-12, NOAA-15, NOAA-16 and NOAA-17. The satellites operate in a near-polar sun-synchronous orbit at a height of about 850 km. During the two legs of cruise ARK 19/1 more than 1000 passes have been captured and post-processed. The HRPT-Telemetry (High Resolution Picture Transmission) includes scans of the AVHRR-Sensor (Advanced Very High Resolution Radiometer) as well as information of the DCS-Platform (Data Collecting and Positioning System). AVHRR is a five channel radiometer operating in the visible (two channels) and near infrared (three channels) wavelength range with a nadir resolution of about 1.1 km. DCS receives environmental and GPS data (Global Positioning System) of either stationary or moving platforms, like ARGOS-buoys deployed on ice floes prior to the second leg of the cruise for meteorological data collection by the Met-Group from the University of Hamburg (see section 4.1). Positions and data of this buoy array were monitored via DCS and one buoy was successfully recovered after the drift-station.

More than 350 passes have been archived for further post processing. This will include exact geolocation of image data and analysis of information from the infrared channels in combination with data collected by the KT-15 infrared thermometer operated synchronously with SIMS (Section 3.1.4.1.2) in front of the ship. Only in cloud free scenes imagery was used for real time information about ice conditions around the ship and as a guiding information for Polarstern's bridge. Several SAR images (see Section 3.1.2) were also used to support the scientific cruise leader and the ship's bridge for decision making on the way through the ice. Especially while looking for an appropriate ice floe for the drift-station north of Svalbard and for finding a feasible way getting there and back again those images proved to be very helpful information.

A typical AVHRR infrared image is shown in Figure 3.1.4. Bright values indicate low temperatures, dark values correspond to higher temperatures. The scene was received on March 25, 2003 at 02:36 UTC from NOAA-16. It covers the Fram Strait, Svalbard, the Barents Sea, and the straits to Franz-Josef-Land, where a quite closed pack ice cover is present. Storfjord and the western Barents Sea appear ice covered as well but with smaller floes the signature is more diffuse. The darker values in the eastern part of Storfjord at the west coast of Edgeøya and Barentsøya indicate a polynya region with very thin ice cover or even open water. Because of the comparably warm water which is either directly exposed to the atmosphere or covered only with a very thin ice layer this region appears with darker tone. The black cross denotes the position of RV Polarstern at receiving time some days before the end of the first leg of the cruise.

Figure 3.1.5 shows an example of typical late winter / early spring sea ice conditions for the Fram Strait region. The image covers the same geographical area as Figure 3.1.4. It was received on April 05, 2003 at 08:19 UTC from NOAA-15. Again, large ice floes are clearly visible between Svalbard and Greenland. The ice edge follows approximately a line from 80°N 10°E to 75°N 10°W. South of this line a cold air outbreak from the North forms a typical cloud pattern over the open ocean. The

3. SEA ICE PHYSICS

Barents Sea appears to be mostly cloudy, but some ice is visible through the thin low cloud cover. Again the arched dark features north of 80 N show thin ice covers or open water mainly in lee of larger ice floes. Those fractures were used both on the way into the ice towards the location of the drift-station and back out of the ice towards the Hausgarten region (see Section 6.10). The black cross denotes the position of RV Polarstern at receiving time.

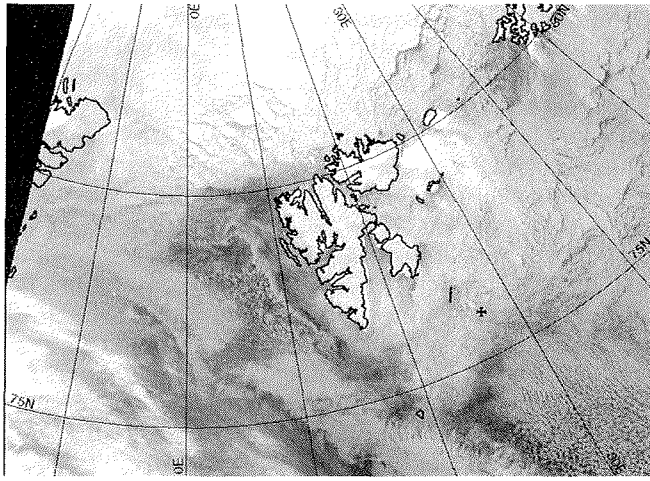


Figure 3.1.4: Image received on March 25th 2003 at 02:36 UTC from NOAA-16. The scene shows the area around Svalbard as seen from AVHRR channel 4.

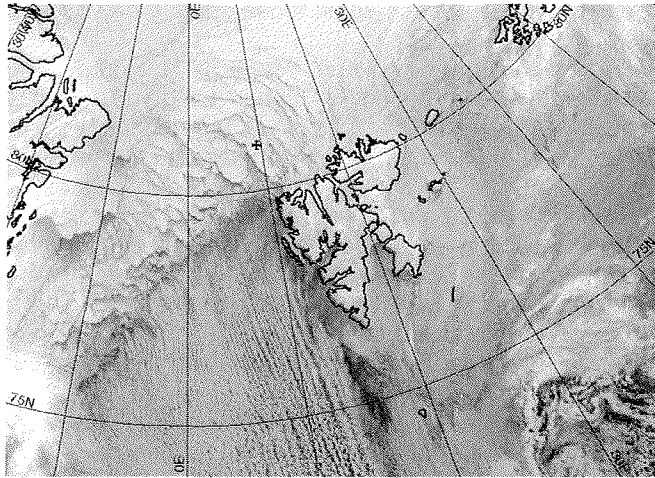


Figure 3.1.5: Image received on April 5th 2003 at 08:19 UTC from NOAA-15. The scene shows the area around Svalbard as seen from AVHRR channel 4.

3.1.3.2 Synthetic Aperture Radar (SAR) images

(Alexandrov, Haas, Lieser)

SAR images from different satellites have been ordered to cover the ARK 19 study regions: ENVISAT, RADARSAT, and ERS SAR. Some of these images have been acquired and archived at the Tromsø Satellite Station (TSS), and some of them have been acquired in near-real time and transmitted to Polarstern via INMARSAT and IRIDIUM communication systems. Onboard Polarstern SAR images were used both for navigation purposes and for planning field work. Radar signatures of different sea ice types and features have been investigated by means of comparison with subsatellite sea ice observations. ERS SAR scenes cover areas of 100 x 100 km with a resolution of 25 m.

Five ERS-2 SAR scenes were acquired onboard Polarstern during the first leg of the expedition. The first two images, dated February 27 and March 2, covering the area of Storfjord, were used for estimating sea ice conditions. The first ENVISAT ASAR image, covering Storfjord area, was received on March 14. This image was immediately used for navigation purposes and planning field work. This image is shown in Figure 3.1.6.

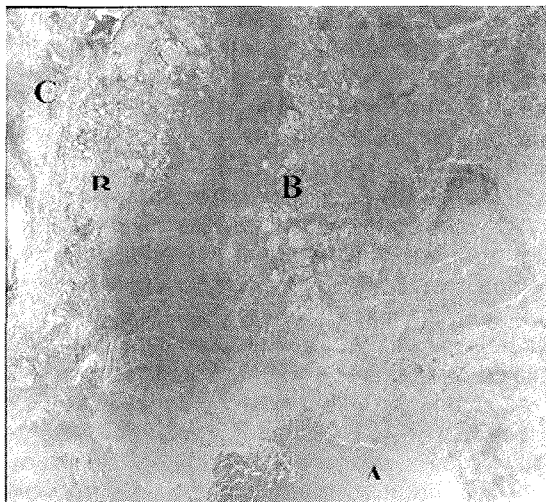


Figure 3.1.6: ENVISAT ASAR image for March 14, covering the area south and east of Storfjorden.

Ice edge position can be seen in the lower right part of this image (area A). The multiyear sea ice, which is imported from the central Arctic is evident in two areas, marked by B, with light tone, and rather level first-year ice located between these two areas is shown with dark tone. Rather bright image tone in Storfjorden (area C) is due to significant surface roughness.

3. SEA ICE PHYSICS

Three ERS-2 SAR images, acquired on March 16, 18, and 19 for the Storfjorden and eastward of it in the Barents Sea, were used for estimating sea ice conditions in this area, as well as ENVISAR ASAR image, dated March 20. Another ASAR for the same date covered Storfjorden and area west of Svalbard. The area west of Svalbard was also covered with ENVISAT image for March 25. In both these images a stripe of ice along the coast of Svalbard is clearly evident as well as young ice in Isfjorden and ice edge position north of the archipelago. From ASAR image for March 26 ice edge position in the north western part of the Barents Sea and Storfjorden can be easily determined. The ENVISAT ASAR image for March 28 covered Svalbard and area westward of it in the time when Polarstern approached Isfjorden. Near simultaneous in situ sea ice observations were compared with signatures of different new and young ice types in Isfjorden, and also in the area west of it.

After March 29 the second leg of the cruise to the north of Svalbard began. This area is characterized by significantly more complicated sea ice conditions than in the Barents Sea and remote sensing data were particularly important. ENVISAT ASAR image for March 30 covered this area and provided a possibility to estimate sea ice conditions there to plan how we can approach the needed area. This image is shown in Figure 3.1.7.

A diffuse ice edge is evident in area A. A mixture of first-year and multiyear ice persists in the transient area between ice edge and multiyear ice to the north. A number of giant multiyear ice floes are located to the north of Svalbard, and one of these floes is marked with B. They are shown with relatively bright tone, caused by volume scattering of radar signal in upper layer of multiyear ice, which is saturated with air bubbles. Fractures of different width, covered with new or young ice, are situated between these ice floes (in area C, for example). Their tone can vary from dark to bright, but in any case they could be detected among surrounding ice. Using these fractures a further route of the expedition was chosen. During the drifting stage SAR images have not been received onboard the Polarstern due to communication problems. Only in the final stage one SAR images was used for selecting return way. Figure 3.1.8 shows a Radarsat Narrow Swath image from April 04, covering some of Figure 3.1.7 and adjacent regions to the west. Svalbard is in the right margin. Some features can be identified on both images, enabling tracking of floes and detection of changes. Studies of ice signatures with different polarizations (Envisat: VV, Radarsat: HH) can also be performed. Three Radarsat images (March 26 and April 04 and 14) were purchased as navigational support for Polarstern. Unfortunately though, image ordering was not flexible enough so that the drift floe is not covered by any of the Radarsat imagery. However, some HEM flights are well within the images.

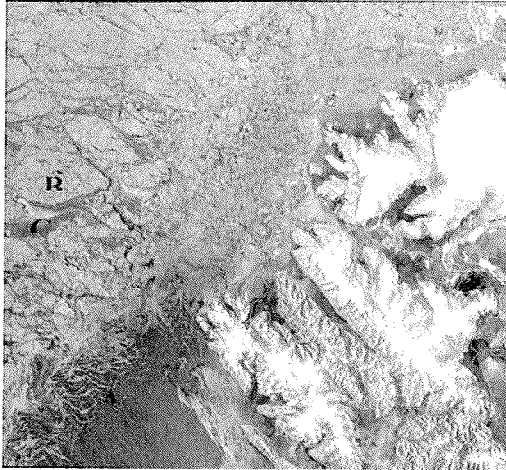


Figure SEAIC 3.1.7: ENVISAT ASAR image for March 30, covering sea ice northward of Svalbard.

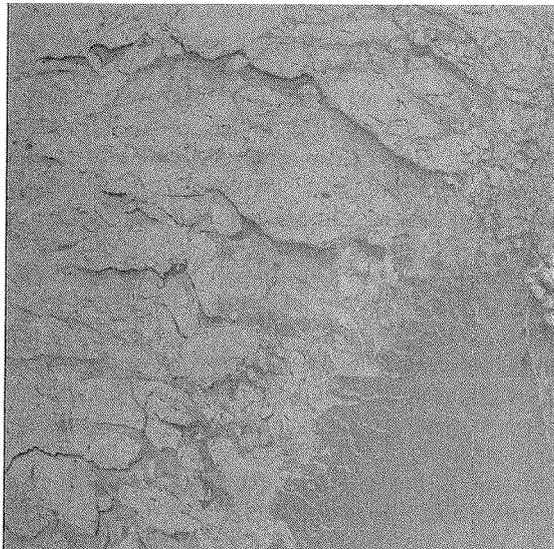


Figure 3.1.8: Radarsat Narrow Swath SAR image from April 04, showing Fram Strait northwest of Svalbard.

3. SEA ICE PHYSICS

3.1.3.3 Low resolution satellite data

(Haas)

As part of the GreenICE project, different ice products derived from passive microwave SSM/I and QuickScat Scatterometer were transmitted by email to Polarstern by the Danish Technical University (DTU, courtesy Leif Toudal) on a daily basis. All imagery was installed with a special browser on the ships public computer network and was accessible by all cruise participants. The data was very useful for estimating the overall ice situation, and in particular the ice edge position. Moreover, QuickScat provided some ice type information (see Figure 3.1.1 above) which was essential in guiding and interpreting the airborne and ground ice property measurements.

3.1.3.4 Helicopter Scatterometer Measurements

(HELISCAT; Kern)

A. The instrument:

The HELISCAT is a helicopter-based Scatterometer designed to measure quasi-simultaneous the surface radar backscatter at five different frequencies in the microwave frequency range (1.0, 2.4, 5.3, 10.0, 15.0 GHz, i.e. in the L-, S-, C-, X-, and Ku-Band, respectively), at HH-, VV-, and cross-polarization. It consists of the SCAT (five pulsed superheterodyne Doppler-Scatterometers) which generates, transmits and receives the signal, a parabolic broad-band dish antenna (1 m in diameter), a gyro, which measures pitch and roll of the helicopter, and a steering unit which controls the power supply, transmit and receive cycles, and which directs the signal to a tape-recorder for data storage. The gyro and the SCAT are mounted in an antenna rack which itself is mounted inside the helicopter. The antenna is aft-looking and is mounted outside the helicopter on an arm of the antenna rack which can be tilted during the flight so that the incidence angle can be varied between 20 and 70 degrees. A CCD-Camera is mounted on the same arm and is used together with a timer, a monitor and a video-recorder to observe the different surface types within the footprint of the antenna. This equipment is mounted together with the tape recorder, the steering unit, and two filters and amplifiers in a rack which is also placed inside the helicopter. The HELISCAT can be used from flight altitudes between about 50 and 1000 m. The size of the elliptical footprint depends on frequency, incidence angle and flight altitude and takes across-flight track values between about 3 m for Ku-Band (beamwidth: 0.9°) and about 50 m for L-Band (beamwidth: 13.6°) at a flight altitude of 150 m. The sampling rate is 100 μ s which ensures a continuous data acquisition along the flight track.

The measured parameter is the so-called normalised radar cross section (NRCS) which is roughly a measure for the amount of energy which is backscattered into the direction of the radar. The radar backscatter (or NRCS) of sea ice is determined by many different factors and properties: incidence angle, frequency (wavelength), and polarisation, snow properties such as wetness, density, grain size, and sea ice properties such as porosity, salinity, grain size, and roughness on the mm- to cm-scale. Young ice formed, for instance, under quiet conditions is level and has rather a low radar backscatter because its surface roughness is quite small which causes only a small amount of energy to be backscattered into the direction of the radar. In contrast, young ice formed as pancakes, i.e. under windy conditions, shows high NRCS-values due to the mm- to cm-scale rims on its surface which cause a fair

amount of surface scattering. Multiyear ice also has a high radar backscatter. The reason for this is twofold. At first this is due to a larger surface roughness compared to level sea ice. And secondly this is caused by many air pockets entrapped in the upper centimeters of the ice, which cause volume scattering.

The influence of snow on the backscatter measurements can be neglected as long as the snow is dry and free of ice layers with grain sizes that match the radar wavelength. In this case the radar penetrates the snow layer and the measured NRCS reflects the properties of the snow-ice interface and of the ice layer some centimeters thick below. In case of a wet snow surface, most of received energy stems from the upper millimeters to centimeters of the snow cover. In case of an icy layer of large-grained snow crystals buried in otherwise fine-grained dry snow, the measured NRCS-values are determined by the structure of this icy layer.

B. Goals

The goals of the HELISCAT measurements were twofold. The first one is to obtain a dataset of in situ and remotely sensed sea ice information for the Storfjorden, particularly its polynyas, in order to contribute to the evaluation of the sea ice part of micro- to meso-scale numerical ocean modelling of this area at the Institute of Oceanography, Hamburg (I. Harms). This includes detailed in-situ observations of the sea ice and snow properties on the one hand, in order to establish a data set to be used to evaluate both model and remote sensing data. And on the other hand, this includes sea ice backscatter measurements over sea ice with special emphasis on thin ice in order to improve current ice type classification schemes using satellite-based SAR imagery. The aim here is a SAR image classification scheme capable to routinely monitor the extent of polynyas in the Storfjorden area using Envisat ASAR and/or ERS2 SAR data. The second goal is to collect a data set of radar backscatter measurements for comparison/evaluation with/of Envisat ASAR imagery, and for modification of a current SAR ice classification method (L. Kaleschke, Uni Bremen). Here special emphasis will be put on as many as possible different sea ice types and surface properties. Again, these measurements will be accompanied by as many as possible in-situ observations of the sea ice and snow cover properties. For the aimed comparison/evaluation with/of SAR data only C-Band measurements are required. However the QuikSCAT Seawinds scatterometers obtains data at Ku-Band (13.4 GHz), the JERS-1 at L-Band (1.275 GHz) and the planned TERRASAR will use X-Band (9.8 GHz) for remote sensing of the surface at incidence angles within the range that is covered by the HELISCAT. Therefore it is intended to compare the data acquired with the HELISCAT at these frequencies with measurements of these sensors - at least JERS and QuickSCAT.

C. Measurements

In total 14 flights were carried out with the helicopter using the HELISCAT of which seven flights took place in the Storfjorden area/Barents Sea, and seven took place north of Svalbard. The typical flight pattern was a triangle with a total length of 60 nautical miles. This pattern was chosen in order to cover a wider area than with just a transect. Flight altitude was about 150 m for the first five flights and about 80 m for all other flights. The cruise speed changed from approximately 80 to 90 kn for the first four flights to about 100 kn during the rest of the cruise - except the tandem flight carried out on April 19. On this day the HEM-Bird (Section 3.1.4.1.3) and the

3. SEA ICE PHYSICS

HELISCAT were flown together along the same track. Cruising speed was 60 kn in this case due to the nominal cruising speed required for the HEM-bird.

Incidence angles were usually not varied during the flight. Depending on the satellite overpass of that particular day or the day before/after (Envisat ASAR or ERS2 SAR) the incidence angle was either set to 23° in case of an ERS2-SAR overpass or to 40° in case of an Envisat-ASAR overpass. During another flight which took place during the drift station, the incidence angle was changed systematically between 60° and 20° in steps of 10° while trying to overpass the same ice area in order to have measurements at different incidence angles over the same ice type.

For all flights latitude and longitude of the flight track were acquired with a handheld GPS - at least as long receiving conditions permitted. During some flights the GPS was not able to receive data from enough satellites to provide a proper flight track. In this case the GPS of the helicopter was used to obtain at least the corner coordinates of the flight pattern. During almost all flights pictures were taken with a digital camera at locations marked with the GPS.

Helicopter speed and flight altitude were taken from the instruments of the helicopter. Starting with the seventh flight, a laser altimeter (Section 3.1.5) was mounted on the left side of the helicopter. This vertically downward looking instrument provides the flight altitude very accurately at a sampling rate of 2 kHz. Furthermore, this altimeter allows to obtain ice ridge distribution and height accurately, which is a perfect combination to the NRCS measurements obtained with the HELISCAT.

D. Results

During all flights HELISCAT data were acquired at at least four of the five possible frequencies. Data have been stored on video tape and were subsequently digitised in the lab. It turned out already during the flights that the cold temperatures and/or the change between rather warm conditions inside the helicopter hangar and the cold conditions outside at least before/during the start have affected the reliability of some components of the HELISCAT.

A first quality check conducted on board Polarstern revealed that a) the amplifiers have caused problems during the first flights - particularly during the first part of the cruise and in C- and Ku-Band. This might be fixed later using some additional filters while re-digitising the data; b) the components are highly temperature sensitive and cause a substantial drift in the data, which, however, can be corrected for by performing the further data analysis step-by-step, assuming a rather constant temperature during shorter time intervals; c) the data acquired show a signal for all flights at least at two frequencies and that the last six flights were successful with a signal at all frequencies used during these flights.

Any further analysis will take place at the IfM in Hamburg once the equipment is back and will start with a further quality check of the already digitised data. Then the video data will be viewed and periods when the HELISCAT flew over distinct surface types (nilas with/without frost flowers, level ice, brash ice, first-year ice, multiyear ice, open water with/without grease ice) will be marked, selected and collected. On the basis of this supplementary information HELISCAT data will be analysed separately for each surface type discernible in the video in order to obtain the relative backscatter variation between different ice/surface types. The final step will be to use a sophisticated radar backscatter model developed at the University of Hamburg (R. Romeiser) to model NRCS values over open water according to HELISCAT flight

Sea ice remote sensing, thickness profiling, and ice and snow analyses

parameters and meteorological conditions encountered during HELISCAT flights over open water and by doing so to get an estimate of the absolute NRCS values.

Figures 3.1.9, 3.1.10, and 3.1.11 show one flight track and typical backscatter profiles along this track obtained from Envisat and HELISCAT.

E. Acknowledgements

We would like to thank the crew of R/V Polarstern as well as of Wasserthal-Helicopter Service and related people for perfect collaboration. Moreover, I very much benefited from the supplementary equipment (GPS, Laser-Altimeter) which was kindly provided by the AWI sea ice geophysics group. Thanks a lot.

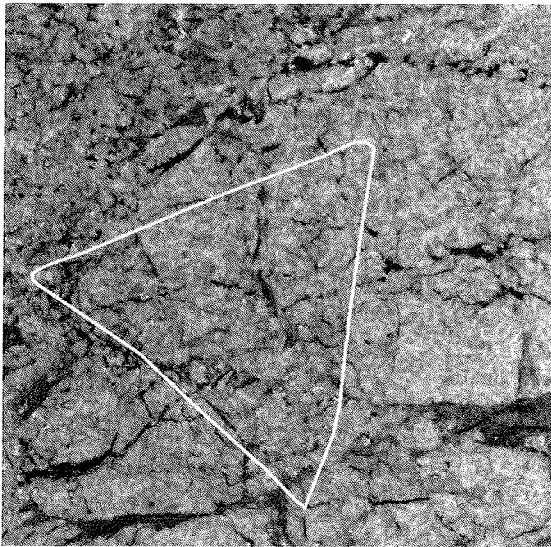


Figure 3.1.9: HELISCAT track on April 15, overlaid on Envisat VV SAR image.

3. SEA ICE PHYSICS

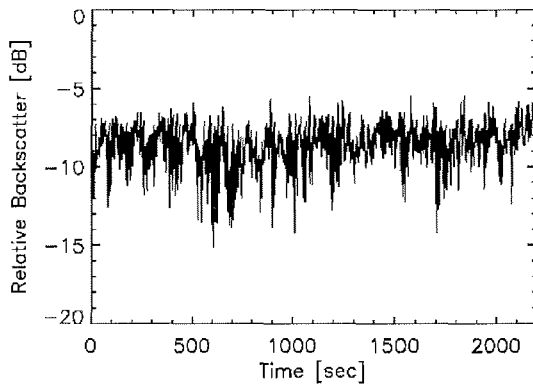


Figure 3.1.10: Envisat C-Band VV backscatter along flight track in Figure 3.1.10.

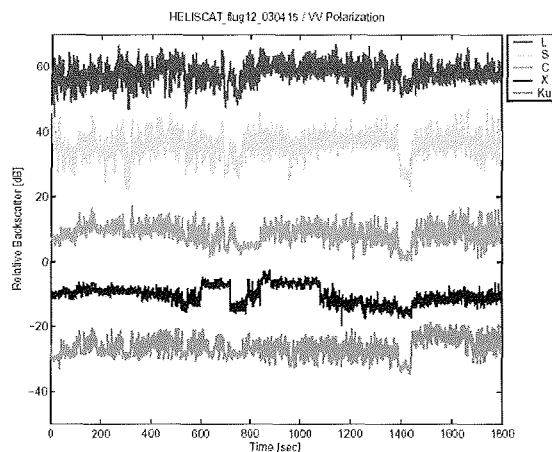


Figure 3.1.11: HELISCAT VV backscatter along flight track in Figures SEAIC 3.1.9&3.1.10.

3.1.4. Ice thickness measurements

The main goal of ice thickness measurements was to gain high resolution data to describe local and regional thickness distributions and surface morphology. Extensive ice thickness profiling was carried out by means of electromagnetic (EM) induction sounding. The technique allows for continuous high accuracy measurements, performed either directly from the ice surface or from above, e.g. by means of the ship or helicopters.

With EM sounding, a low-frequency EM field is generated by a transmitter coil. This field induces eddy currents in the water, which in turn result in a secondary EM field. The strength of this field is measured by a receiver coil. As the strength of any EM field decreases with distance to the source, the secondary field strength decreases

with increasing distance between the EM instrument and the water underneath the ice. Thus, the thicker the ice is, the weaker the secondary field becomes. Here, we deployed a hierarchy of different means of EM soundings: Ground-based measurements have proven to provide very accurate data (Section 3.1.4.1.1). Their calibration is evaluated by means of accompanying drill-hole measurements. However, ground-based measurements are only possible on single, thick floes, and the profile lengths are very limited. Another possibility is to perform continuous ship borne measurements along the ships track. These provide the most extensive data en-route without any extra requirement for ship time (Section 3.1.4.1.2). However, ice thicknesses along a ships track is never representative for a particular ice regime, as the ship usually follows leads with open water or new ice. At floe contacts, where the icebreaker has to break thicker ice, the ice is often deformed. Therefore we also carried out extensive helicopter borne surveys using a towed sensor, the EM bird.

3.1.4.1 Methods

3.1.4.1.1 Ground-based profiling using an EM31 thickness sensor (Haas)

Ground-based measurements have been performed on a daily basis on single ice floes using a Geonics EM31 instrument. Floes have been entered either from the ship or by helicopter during floe-hopping, when several floes were profiled during one flight. The EM31 operates at a frequency of 9.8 kHz with a coil spacing of 3.66 m. The EM31 provides high accuracy data and the procedures are well established. The EM31 was placed into a Prijon kayak serving as amphibic sledge, to enable measurements over melt ponds and to shelter the instrument. EM soundings were performed at a lateral spacing of 5 m. The profiles were laid along straight lines, including level and deformed ice. The EM profiles were occasionally validated by means of drill-hole measurements when time and weather allowed.

Along the EM profiles, also snow thickness was profiled using a ruler stick. This provided essential data e.g. for CryoSat validation, as the obtained data allow to distinguish between snow and ice thickness.

3.1.4.1.2 SIMS (Sea Ice Monitoring System): Continuous along-track ice thickness measurements (Haas)

Since 1994, continuous EM ice thickness measurements are performed along ship tracks. Since 2001 (Ark 17/2), a Geonics EM31 is used together with a Riegl laser profiler, and the system is integrated into Polarsterns PODAS system, called SIMS. During Ark 19/1, first tests were made integrating a KT15 infrared thermometer into the SIMS. The data were acquired with the turbulence measurements at the bow, and kindly provided by W. Cohrs (AWI).

Unfortunately, archiving of SIMS data into PODAS could still not be achieved, although the data were readily visible on the ships information monitors, including those on the bridge. Therefore, the navigation (GPS) data had to be joined with the thickness soundings only during post processing. However, synchronised and georeferenced thickness, speed, and surface temperature data are available shortly after the cruise.

SIMS was operated continuously from March 09 until April 19 when Polarstern was steaming in ice. Calibration is an important duty in EM thickness profiling, and is

3. SEA ICE PHYSICS

required to assess the system's stability. In the beginning, an old calibration from 2002 was used, because no actual calibration could be performed due to the lack of extensive water patches or leads.

The first calibration was therefore only carried out on March 23, 2003. During a five minute calibration experiment, SIMS was raised and lowered in a large lead above open water, and the according laser height and EM reading (apparent conductivity) was recorded (Fig. 3.1.12). The relationship between apparent conductivity and SIMS height above the water surface shows the well-known negative-exponential relation (Fig. 3.1.13). The curve has a very good signal-to-noise ratio except for some scatter between 4.5 and 6.0 m, which is due to some brash ice under the system. A calibration curve can be obtained by fitting a negative-exponential function to the data (Fig. 3.1.13). Inversion of this function yields a transformation equation to compute distance to the water surface from apparent conductivity. Ice thickness is then obtained by subtracting the laser-measured height above the ice surface.

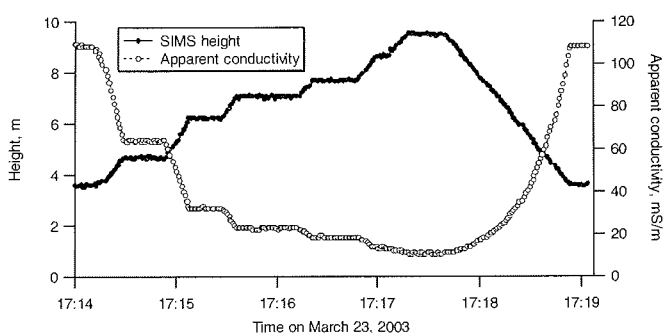


Figure 3.1.12: SIMS height and corresponding measured apparent conductivity during a calibration measurement, when SIMS was risen and lowered over open water.

The 2003 calibration agrees with the curve of Ark 11 in 1995 (Fig. 3.1.14), which was well explained by a one-dimensional model of a non-conductive ice cover overlying deep sea water with a conductivity of 2600 mS/m. The remaining discrepancy may be due to a different calibration factor of the particular EM31 used (e.g. a factor of 1.12 to account for instrument use at hip-height), but should be controlled by repeated calibration measurements.

Deviations from the 2001 curve are quite significant, and point to an outbalanced (tilted) SIMS during 2001. The scatter of the curves demonstrates how important repeated and careful calibration measurements are. They should be performed also with future SIMS realisations.

Sea ice remote sensing, thickness profiling, and ice and snow analyses

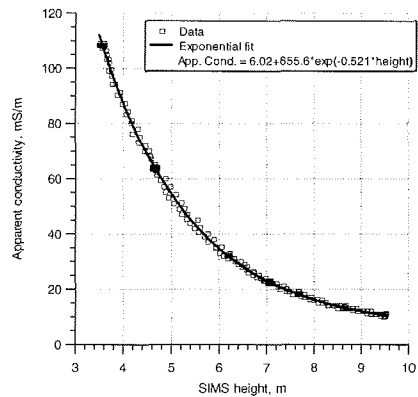


Figure 3.1.13: Apparent conductivity (EM31 reading) versus SIMS height during the calibration measurement of Fig. 3.1.12.

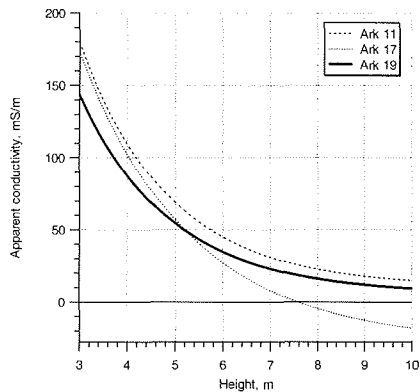


Figure 3.1.14: Comparison of different calibration curves obtained during Ark 11 (1995), Ark 17 (2001), and Ark 19 (2003).

A typical thickness profile is shown in Figure 3.1.15. The data were recorded during extensive ramming, showing the typical cycle of absent or thin ice and thick ice which brought the ship to a stop. Accordingly, the resulting thickness histogram shows two clear modes at 0 m and 1.6 m ice thickness (Fig. 3.1.16). The example illustrates the importance of co-registered GPS data, if the real thickness distribution of the regions shall be derived. This can only be obtained by removing all sections of the track when the ship was moving backwards or repeating a measurement over a formerly profiled spot. In fact, the typical thickness in the regions of the example was 1.6 m, explaining well the difficulties in straight moving forward.

3. SEA ICE PHYSICS

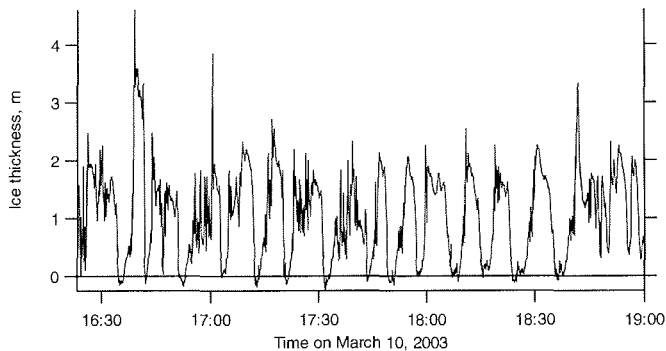


Figure 3.1.15: 2.5 hour recording of ramming cycles.

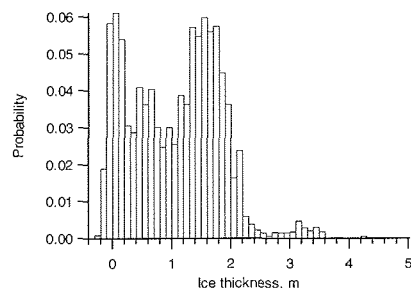


Figure 3.1.16: Thickness distribution for the example in Figure 3.1.15.

3.1.4.1.3 Airborne EM thickness profiling (Haas, Lobach, Pfaffling)

A helicopterborne EM ice thickness sensor (EM bird) was operated with the Polarstern BO-105 helicopters during 21 flights. The bird is 3.5 m long, has a diameter of 0.35 m, and weighs about 100 kg. It is towed 20 m below the helicopter, at a height of about 10 to 15 m above the ice surface. Take-off and landing were conducted from the helicopter deck. The bird was successfully landed directly into a special cart which could also be used for transport and storage on board.

The bird operates at 3.68 and 112 kHz, with coil spacings of 2.77 and 2.05 m, respectively. A GPS antenna and a laser altimeter are also included. Flights were performed along triangles with 40 km side length. At each turning point, the helicopter ascended to an altitude of 100 m to allow for internal calibration and nulling of the bird.

Some flights were complemented by ground validation along coincident short profiles on the longer ice stations close to the ship.

A nadir video camera was operated during all video flights to document ice conditions below the bird. However, on most flights videos were only recorded during the high

Sea ice remote sensing, thickness profiling, and ice and snow analyses

altitude sections to limit the amount of video data and to document general ice conditions in the region.

Geo-referenced digital still photographs were also taken to document general ice conditions. Subsequently they were included into an html linked map projection allowing for easy geocoded image browsing.

3.1.4.1.4 Ground penetrating radar (GPR; Pfaffling, Haas)

During ARK 19/1 a RAMAC GPR instrument (MALA GeoScience) was taken to the sea ice for the first time to assess the capability of the method to contribute information on the sea ice properties particularly ice thickness (Fig. 3.1.17).

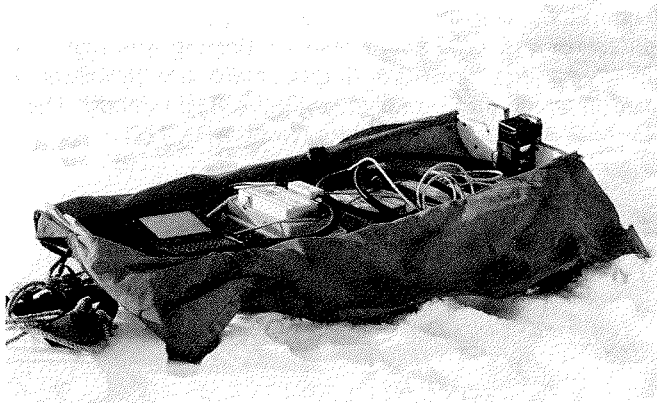


Figure 3.1.17: The RAMAC GPR mounted into a little Pulka.

In contrast to EM induction methods (EMI, Sections 3.1.4.1.1- 3.1.4.1.3), GPR systems use a high frequency (> 50 MHz) electromagnetic pulse comparable with a seismic explosion or air gun which travels inside the media. If there happen to be changes of the dielectric properties of the media on distinct horizons the EM pulse is partly reflected and returns to the receiver antenna of the system. An example for such a horizon would be the ice underside where the media changes from ice to water or the snow-ice interface. During a GPR survey such a wave travel experiment (shot) is recorded every cm along the profile.

Once the antenna has transmitted the EM impulse the receiver starts to acquire the returning signals for some nanoseconds. For interpretation the signal traces of every shot are plotted next to each other in a radargram (Fig. 3.1.18). The grayscale displays the amplitude of the received waveform. After the reflected waveform of the ice underside is identified, the travel time of the wave down and up can be derived (between 20 – 30 ns in this example). With the help of drilling information or using standard values for the propagation velocity, the travel time can be converted into ice thickness. In Figure 3.1.18 the bars represent the drilling information.

3. SEA ICE PHYSICS

The propagation velocity depends on the dielectric permittivity of the media. The reflectivity is related to changes in the dielectric properties, determining the velocity. Apart from the wave travel velocity, the damping of the wave depends on the conductivity of the media and the antenna frequency (50 MHz up to 1.5 GHz). Damping increases with frequency and conductivity.

In Figure 3.1.18 a dominant reflector corresponds nicely with the drilling information. A second reflector at around 10 ms maps the snow-ice interface as the antennas are pulled over the snow surface. Only were the ice gets too thick or consists of many little broken pieces it gets hard to find a reflected signal in the data. For comparison the EMI derived ice thickness for the same profile as in Figure 3.1.18 is shown in Figure 3.1.19. The circles represent the drilled thickness like the bars in the radargram.

Due to its wave characteristics and the small point spacing GPR provides results with higher lateral resolution and accuracy. However, dealing with high salinity ice or not level ice conditions as e.g. pressure ridges, there are problems to retrieve ice thickness information which can be solved with the EMI method. The following table gives an overview of the acquired radar data during ARK 19/1:

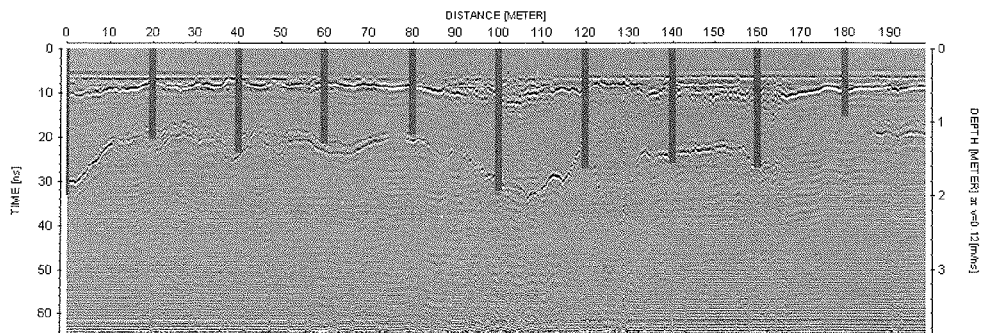


Figure 3.1.18: GPR section (radargram), Antenna: shielded 800 MHz, Date: 20030312. Drilling information plotted as black bars.

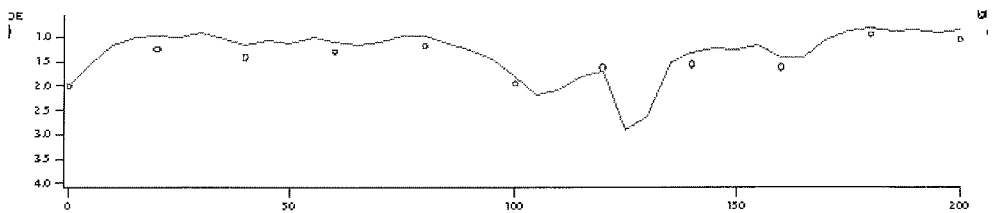


Figure 3.1.19: EMI-derived ice thickness (lines), circles represent drilling data. Date: 20030312. Spacing: 5m.

Sea ice remote sensing, thickness profiling, and ice and snow analyses

Table 3.1.1: GPR measurements performed on ARK 19/1. The crosses in the rows Zs and tt mark if direct snow and/or ice thickness measurements were taken on the GPR profile for validation.

Date	Zs tt	Project name	Antenna	Sampling	Profile	Remarks
12.03.2003	X X	.03031101	800 MHz	10 cm	6 m	System on snow surface
		.03031102	800 MHz	1 cm	1.5 m	All data acquired on 20030312
	.03031103	800 MHz	10 cm	3.6 m		
	.03031104	800 MHz	10 cm	200 m		
	.03031201	800 MHz	10 cm	18 m	System on Ice surface	
			.03031202	800 MHz	5 cm	18 m
17.03.2003	X X	.03031701	800 MHz	5 cm	330 m	
19.03.2003		.03031901	800 MHz	500 ms		Antenna lowered from the bow crane using a rope (Snow thickness ?)
		.03031902	800 MHz	500 ms		
		.03031903	800 MHz	500 ms		
23.03.2003	X X	.03032301	800 MHz	5 cm	200 m	System in Pulka
		.03032302	800 MHz	5 cm	200 m	System on Nansen sledge
01.04.2003	X	.03040101	1 GHz	5 cm	200 m	
07.04.2003		.03040701	800 MHz	250 ms	~ 4000 m	Joint Survey with Kayak
08.04.2003		.03040801	500 MHz	100 ms		Running chris-chross on the floe to test the 500 MHz antenna
		.03040802	500 MHz	100 ms		
11.04.2003		.03041101	500 MHz	100 ms	2000 m	CryoVex I coincident with Kayak
13.04.2003	X X	.03041301	500 MHz	5 cm	200 m	CryoVex I 200 m subset sledge
		.03041302	1 GHz	5 cm	200 m	

3.1.4.2 Preliminary Results

3.1.4.2.1 Storjorden and Barents Sea (Haas)

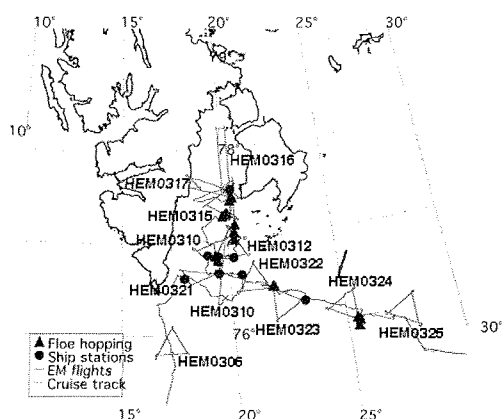


Figure 3.1.20: Map of Storjorden and Barents Sea, showing the locations of ground measurements and tracks and dates of helicopter EM flights.

3. SEA ICE PHYSICS

By means of ground measurements and EM flights, much of the Storfjorden and an almost continuous section across the Barents Sea could be profiled. In total, we sampled 24 floes and performed 12 EM flights (Fig. 3.1.20).

Figure 3.1.21 shows typical ice and snow thickness obtained from ground-measurements versus latitude, i.e. a pseudo profile along Storfjorden and the neighbouring Barents Sea. In Storfjorden, no clear thickness trends from N to S are visible. However, it should be noted that due to the cruise track no measurements were possible in the first-year ice produced in Storfjorden. Typical thicknesses between 0.6 and 1.0 m are in partial agreement with the airborne thickness distributions presented below. However, it becomes clear that the ground measurements were much too sparse to be representative for the overall thickness distribution. In the Barents Sea, a gradual thinning towards the ice edge is visible. However, older and younger ice cannot be separated based on the thickness data alone.

EM flights were very well able to distinguish between the areas of thin ice formed in Storfjord and the thick ice advected from the Arctic Ocean. Figure 3.1.22 shows a comparison of different ice thickness distributions obtained on Flights 0316 (a), 0315 (b&c), and 0312 (d), showing the transition between the different ice regimes (c.f. Fig. 3.1.20). While the grey ice in inner Storfjorden was only 0.2 m thick, the thick ice further to the south had typical thicknesses up to 2.3 m. The modes at small thicknesses represent nilas formed on open water leads.

Figure 3.1.23 shows the transition between the different ice regimes, which was encountered on the W-E flight on 0312. The corresponding thickness distribution is shown in Figure 3.1.22b.

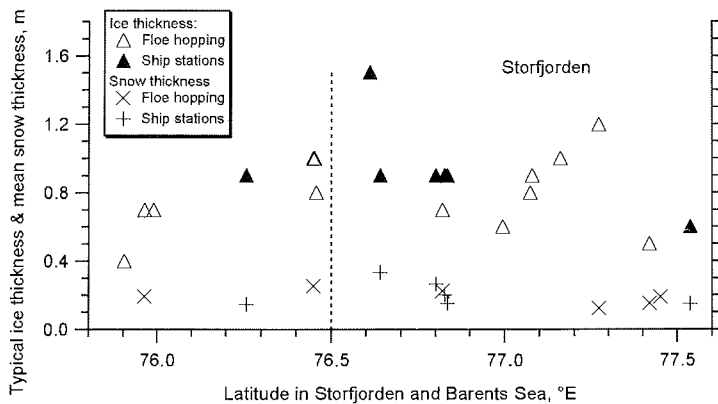


Figure 3.1.21: Typical ice and snow thickness obtained from ground-measurements versus Latitude, between Barents Sea (left) and Storfjorden (right).

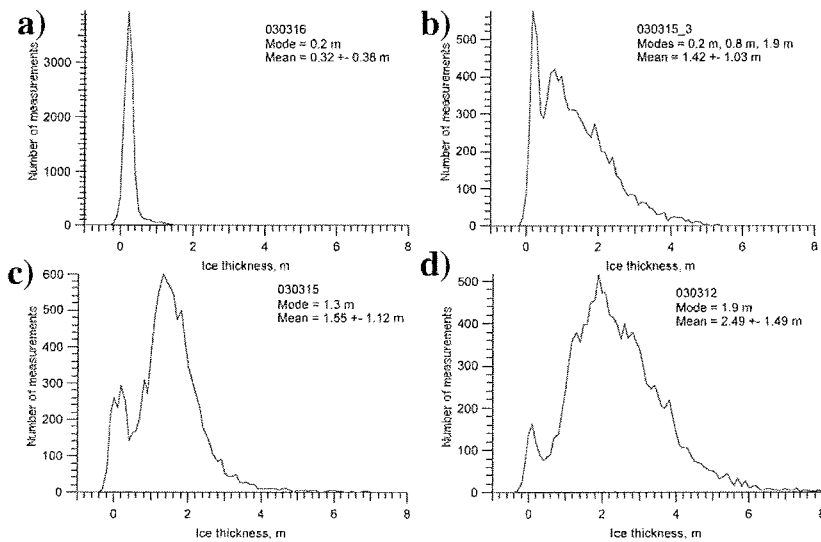


Figure 3.1.22: Ice thickness histograms for different flights in the Storfjorden area (see text) mapping different ice regimes

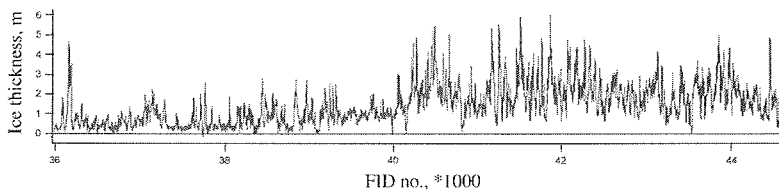


Figure 3.1.23: Thickness profile obtained on March 12 showing the transition from thin first-year ice into thick second- or multiyear ice.

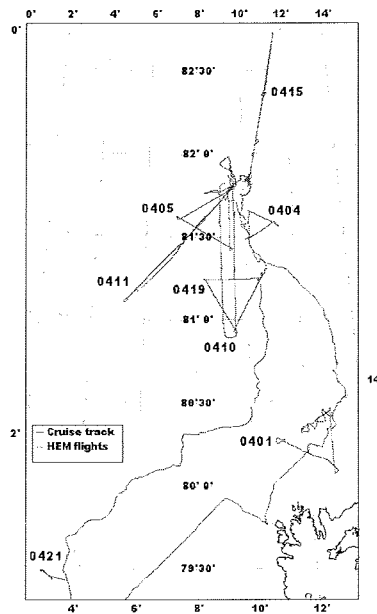
3.1.4.2.2 Fram Strait (Pfaffling, Haas)

During transit from Svalbard into Fram Strait to the drift station on the 1st April a 24 h ice station provided the possibility for a Kayak EM ice thickness profile and the weather also allowed an EM-Bird flight. A failure in the birds altitude display led to a ground contact of the system, which damaged parts of the shell. However, the excellent work of the ship's machine workshop made it possible to conduct the first test flight after the crash only three days later with the repaired bird where it turned out that all systems still worked properly. It was essential for the sea ice team as the most important part of the cruise the CryoVex 2003 campaign was about to come.

3. SEA ICE PHYSICS

On the way back from the drift station we conducted a joint flight with the HeliSCAT system on the 19th April. Using this collocated dataset the dependency of the radar backscatter on sea ice thickness can be studied in more detail than before. Figure 3.1.24 summarizes all flights performed in Fram Strait.

Figure 3.1.24: Map showing HEM flight tracks during ARK 19/1b / CryoVex 2003.



3.1.4.2.3. CryoVex 2003 (Pfaffling, Haas)

The CryoSat Validation Experiment, CryoVex, is a joint effort of the AWI and the European Space Agency, ESA (in cooperation with the National Survey and Cadastre of Denmark, KMS) in order to test possible validation methods to be used on ESAs CryoSat mission.

CryoSat is ESA's first Earth Explorer Opportunity Mission and is aimed at observing changes in the Earth's cryosphere i.e. changes of the ice and snow covered parts of the Earth.

The objective of the CRYOVEX campaign is to provide reference datasets for Cryosat retrieval error studies over sea ice. In particular the campaign is aimed at understanding miscellaneous sources of error: Snow loading, ice density, preferential sampling and various freeboard measurement errors. To meet the validation requirements, the campaign goal is to collect simultaneous and coincident laserscanner / radar height measurements (from the KMS twin otter) and HEM ice

Sea ice remote sensing, thickness profiling, and ice and snow analyses

thickness profiles (from the Polarstern Helicopter) for cross-validation combined with in-situ thickness data from Kayak EM measurements and drillings (done by AWI). During the drift station period two joint CryoVex flights were done. As a consequence of the poor flight weather conditions either on Svalbard or around Polarstern or even both it was very hard to find two suitable days. Figure 3.1.25 shows the tracks of those flights. As the two aircrafts operate at different speeds it is important to find flight concepts to sample the same ice as the sea ice is not stationary but moves with the drift. Therefore the first flight (11th April) was aligned upstream the drift direction. Prior to the Helicopter take off the momentary drift direction and speed was determined from the Polarstern GPS data. For the second flight a heading approx. north was chosen to reach a different ice regime observed from satellite data prior to the flight.

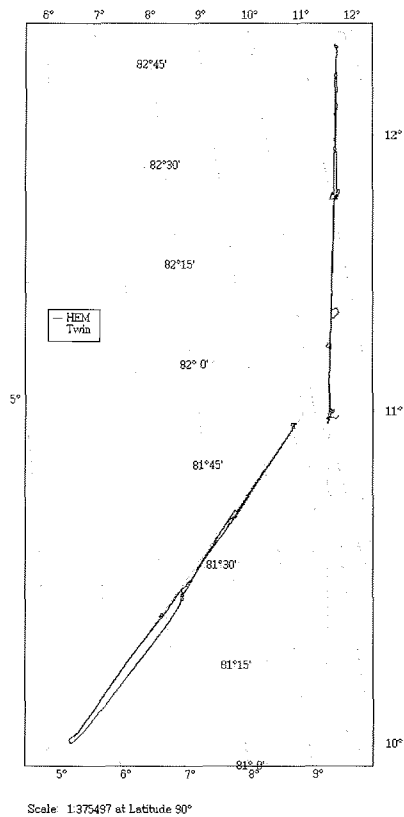
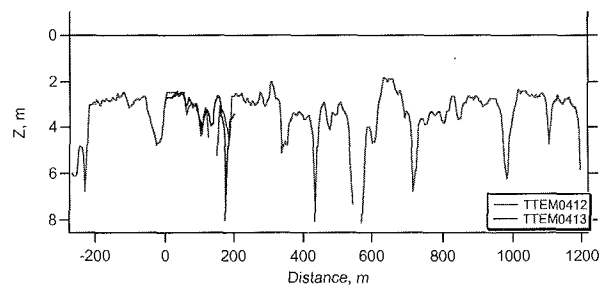


Figure 3.1.25: Flight tracks of the two coincident CryoVex flights on 11th and 15th April. Lines marked as "Twin" indicate tracks of the Danish Laserscanner and D2P radar altimeter on board the Greenland Air Twin Otter. HEM flight lines are labeled as "HEM".

3. SEA ICE PHYSICS

Data from CryoVex I flight on 11th April are shown in Figure 3.1.26. For cross validation of the airborne sea ice data approx. the first 2 km of the flight track were surveyed with the sledge EM, and GPR device combined with a 200m subset of 11 drillings. The excellent agreement between the airborne and ground EM results is shown in Figure 3.1.26a. Studying 30 of the 100 km leg in Figure 3.1.26b thick multiyear floes can be separated from open and refrozen leads. The peaks in the curve up to ten and more meter draft indicate massive ridges within the floes.

a)



b)

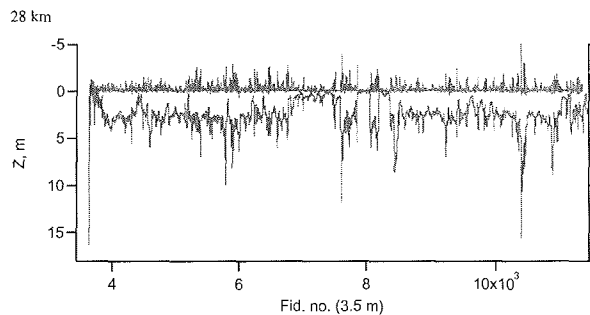


Figure 3.1.26:
a.) subset of the HEM data of the first CryoVex flight on 11.04.2003 compared to the ice thickness derived with the sledge EM.
b.) 30 km ice thickness profile obtained during the joint flight on 11th April 2003.

3.1.5. Laser profiling of pressure ridges (Martin, Haas)

Pressure ridges are the most significant features of sea ice roughness. Ice floes, which collide due to wind forcing or swell, tend to pile up in so called ridges. Ridges are separated into an upper part, the sail, and a lower part below the ice or water surface, the keel. Both features are important for momentum flux from atmosphere and ocean to the ice. Typically the keel is about 4 times deeper as the sail high and also 2-3 times wider.

Sea ice remote sensing, thickness profiling, and ice and snow analyses

The laser measurements performed with the EM bird (Section 3.1.4.1.3) can be processed to obtain height, width and spacing of pressure ridges. During the first part of the cruise in the Storfjord region 12 and during the second part north of Svalbard and north of Fram Strait 8 helicopter flights were performed. The flight tracks ranged from 60 km to 200 km and were in most cases shaped like triangles with equally sized sides. With an intermediate flight speed of 60 knots and a sampling frequency of 100 Hz point spacing results in 0.3 m. The instrument was usually flown about 15 - 20 m above the ground.

The processing of the laser data is complicated by variably vertical motion of the helicopter. That is why the raw data has to be high pass filtered first in order to fit a curve of the helicopter movement. In a second step a profile of the surface is derived. Furthermore mean height, width and spacing of pressure ridges and their number per km along the flight track is calculated as well as width and number per km of ice floes and leads. To define individually identifiable ridges a Rayleigh criterion is used which means that a single ridge must have a crest elevation of more than double the height of the surrounding troughs.

Besides being an Arctic winter expedition this cruise features measurements of young and first year ice on the one hand and multiyear ice on the other hand. The typical difference in surface roughness as revealed by the processed laser data is shown in Figure 3.1.27, comparing level grey ice in Storfjorden with heavily deformed multiyear ice in Fram Strait. Preliminary results show that ice floes in Fram Strait were 30 times larger in diameter than the floes in Storfjorden (100 m average). However, ridge frequency was similar in both regions, amounting to about 22 ridges per km. The smaller floes in Storfjorden allow wind and oceanic currents to produce more leads. The data show a two orders of magnitude higher number of leads in the Storfjorden compared to the Fram Strait profile.

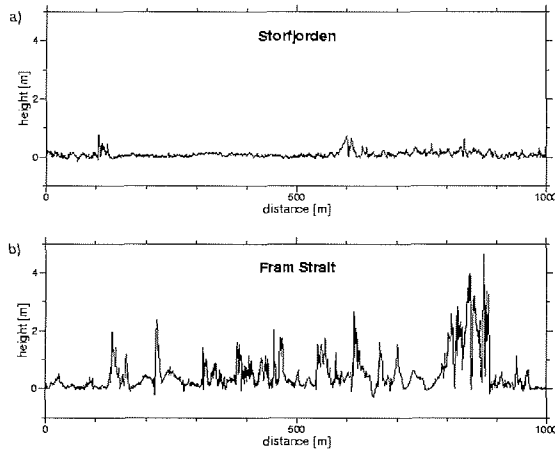


Figure 3.1.27: Comparison of laser derived surface roughness of undeformed grey ice in Storfjorden (a) and heavily deformed multiyear ice in Fram Strait (b). The Fram Strait profile is from the first CryoVex flight.

3. SEA ICE PHYSICS

3.1.6. Ice coring (Haas, Willmes)

Supported by the biological sea ice group 10 ice cores were obtained on different floes visited during thickness work. They were analysed for crystal texture and salinity to better judge age and origin of the sampled floes. In fact, only through these analyses a clear picture of the different young and old ice regimes arose which was not so clear based on thickness profiles alone.

Figure 3.1.28 illustrates the typical C-shaped profiles of first year ice from the Barents Sea and the almost fresh ice typical for multiyear ice in Storfjorden. On March 16, the ice floe consisted of an old floe rafted over a first-year floe.

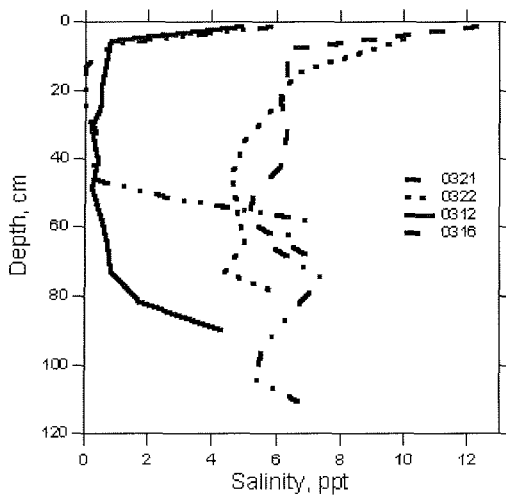


Figure 3.1.28:
Typical salinity profiles of four ice
cores obtained in Storfjorden and
the Barents Sea

3.1.7. Snow measurements (Alexandrov)

Several key snow parameters were measured including snow density and depth. These are important for the interpretation of satellite imagery. During the ice stations snow depth was measured randomly on ice floes of different thickness. Temperature/density profiles were obtained in several snow pits using a special snow density kit.

Altogether 41 snow pits were investigated (Table 3.1.2). These measurements were conducted on different sea ice types: thin, medium, thick first-year and multiyear ice. The temperature profiles of snow were obtained for different snow depths in the wide band from -10°C to -30°C . Snow measurements were supported with photos of ice floes, snow structure, and upper layer of the snow. Studies of typical distribution of snow density, and typical temperature profiles under different air temperatures will be done after the expedition.

Sea ice remote sensing, thickness profiling, and ice and snow analyses

Table 3.1.2: Summary of snow measurements.

N	Date	Coordinates	Number of snow pits	Snow depth	Tair, °C
1	March 7	76° 37'N/17° 57'E	1	Yes	-18.8
2	March 8	76° 35'N/20° 37'E	1	Yes	-13.0
3	March 9	76° 38'N/19° 30'E	1	Yes	-10.7
4	March 10	76° 50'N/19° 02'E	-	Yes	-16.3
5	March 11	76° 50'N/19° 30'E	-	Yes	-26.0
6	March 12	76° 49'N/20° 13'E	2	Yes	-29.0
7	March 16	77° 33'N/20° 21'E	1	Yes	- 9.6
8	March 17	77° 33'N/20° 21'E	3	Yes	- 16.5
9	March 19	77° 17'N/20° 05'E	2	Yes	- 21.8
10	March 21	76° 49'N/19° 23'E	2	Yes	- 4.1
11	March 22	76° 27'N/21° 53'E	2	Yes	-13.8
12	March 23	76° 17'N/23° 22'E	4	Yes	-20.6
13	March 24	75° 58'N/25° 36'E	3	Yes	-19.0
14	March 25	75° 55'N/27° 01'E	1	Yes	-19.0
15	April 1	80° 26'N/12° 50'E	3	Yes	-29.6
16	April 7	81° 54'N/09° 35'E	2	Yes	-21.0; -17.0
17	April 8	81° 54'N/09° 35'E	2	Yes	-17.7; -19.0
18	April 10	81° 49'N/09° 31'E	1	Yes	-20.1
19	April 12	81° 49'N/09° 31'E	3	Yes	- 1.2
20	April 14	81° 49'N/09° 31'E	3	Yes	-7.6; -10.0
21	April 15	81° 47'N/10° 16'E	2	Yes	-13.0
22	April 17	81° 45'N/09° 55'E	2	Yes	-14.9

3.1.8. Wave measurements
(Alexandrov)

Measurements of waves in sea ice were conducted using a wave buoy, consisting of accelerometer and tiltmeters. The objective of this work is to study the statistical characteristics of wave power spectrum/directional wave spectrum within the marginal ice zone (MIZ) with respect to time and different sites within MIZ. A Wave Buoy produced at the Christian Michelsen Research AS (Bergen, Norway) was used for these studies.

Sixteen series of wave measurements were performed during the expedition in the period from March 7 to April 15 (Table 3.1.3).

Five short recordings of about one hour duration have been made on March 7, 8, 9,10,11 and 25. All these recordings were produced on the first-year ice. Descriptions of ice floes were documented, and photos of the buoy location and surroundings were made. Snow thickness measurements and temperature/density profiles of snow near the buoy location were done. Three recordings of several hours duration were

3. SEA ICE PHYSICS

conducted on March 12, 23, and April 1. On March 12 wave measurements were conducted during a long ice station, which took place on a big ice floe approximately 300 m wide and 1 km long with rather level surface. The estimated average thickness amounted to 70 cm. In the place, where the buoy was installed snow thickness was 30-40 cm, and ice thickness 150 cm. Later on the buoy was placed further from Polarstern, where ice thickness was 106 cm, and long-term recording was done there. On March 23 wave measurements, conducted during the long ice station, lasted approximately seven hours. Ice floe diameter was significantly more than one km, and ice thickness was about 90 cm. At the place, where buoy was located, ice thickness was 50 cm and snow depth 15 cm. On April 1 wave measurements were conducted during a long ice station, lasted about 24 hours. Two series of wave measurements were conducted. In the first point measurements lasted 4 hours 7 minutes. The buoy was deployed on rather thick ice floe of approximately 100 m in diameter, surrounded with high ridges, up to 2 meters. The snow depth was about 35 cm. Later on the buoy was replaced to level first year ice floe of 1m thickness, where snow depth was 2-3 cm. Here the 19-hour recording was done. After the buoy was switched off a crack appeared near this place, which then significantly widened up to approximately 50 m. On March 16 wave measurements have been conducted during the long ice station on a big ice floe of approximately 150 m wide and 0.6 km long with rather level surface. Ice thickness near the buoy was 67 cm, and snow depth was about 25 cm. A snow pit was taken near the buoy. The total duration of the record amounts to 20 hours.

Four recordings, each lasting approximately 2 days were conducted during the drifting stage of the expedition. Three of them, starting on April 7, 9, and 12 were done on different parts of the multiyear ice floe. Its thickness varied from 180 cm near Polarstern to 350 cm in some places. Ice surface is quite level, with small hills, but further from the ship it becomes more rough. During the first recording this ice floe turned counter clockwise in approximately twenty degrees, but later on no rotation was observed. The photos of buoy locations and surrounding areas, as well as snow measurements were done. On April 15 the buoy was placed on thin first-year ice of 45 cm thickness, which is located in 5 meters from the multiyear ice floe, and from there it was taken on April 17.

Table 3.1.3: Summary of WAVE BUOY measurements.

Number	Date	Latitude	Longitude	Duration
1	March 7,	76°37'N	17°57'E	50 min
2	March 8,	76°35'N	20°37'E	1h 5 min
3	March 9	76°38'N	19°30'E	50 min
4	March 10	76°50'N	19°02'E	30 min
5	March 11	76°50'N	19°30'E	25 min
6	March 12	76°49'N	20°13'E	3h 50 min
7	March 12	76°49'N	20°13'E	23h 38min
8	March 16	77°33'N	20°21'E	20h 12 min
9	March 23	76°17'N	23°22'E	6h 52 min
10	March 25	75°55'N	27°01'E	53 min

Ice thickness determination using flexural gravity waves

11	April 1	80°26'N	12°50'E	4h 07 min
12	April 1	80°25'N	12°48'E	18h 45 min
13	April 7	81°54'N	09°35'E	48h 10 min
14	April 9	81°50'N	09°43'E	Approx. 48 h
15	April 12	81°51'N	09°56'E	49h 20 min
16	April 15	81°49'N	10°14'E	46h 25 min

3.2 Ice thickness determination using flexural gravity waves

Doble, Mercer, Hughes (SAMS)

Introduction

The cruise represents the first field experiment of the GreenICE project (Greenland Arctic Shelf Ice and Climate Experiment); an EU-funded three-year programme with six partner institutes, co-ordinated by SAMS. The project aims to measure the changes in the structure and dynamics of sea ice that have occurred in a critical region of the Arctic Ocean as a result of a switch in Arctic atmospheric circulation due to the Arctic Oscillation, and to examine whether we can relate these to the long-term (>2000 year) record of variability in the same region retrieved from sediment cores. The project's main experiment will be an ice camp in the Lincoln Sea, north of Greenland, during April 2004.

The Polarstern experiment is a pilot study for this ice camp, allowing extensive in situ testing and optimisation of innovative ice thickness measuring drifters. These are a development of the electronics systems deployed during Polarstern's ANT-XVII/3 cruise leg in the Weddell Sea, modified to investigate the diagnostic use of long-period flexural gravity waves to determine area-averaged ice thickness.

Method

The theory was developed by A.P. Nagurny (Nagurny et al, in press). A continuous ice cover floating on water can be considered as an elastic plate. A wave propagating through it both flexes the ice cover and travels as a gravity wave in the water beneath. This coupled system is known as a flexural gravity wave. A sufficiently long wave ($L \rightarrow \infty$) propagates as if there were no ice cover, and there is also a "critical" or "resonant" wavelength which also travels without hindrance: the internal elastic forces in the plate balance the hydrodynamic and Archimedean forces. Since these waves are attenuated less than other frequencies, the spectrum of the "ice swell" will reflect this critical value, giving a long period peak.

The critical frequency depends on the D , the cylindrical density, of the ice, whose formulation includes the ice thickness (cubed) as well as Young's modulus and Poisson's ratio. The aim of the method is to extract the thickness information without having to determine these hard-to-measure mechanical parameters. This is done by identifying the frequency of purely elastic waves in the ice, excited by impulse events such as ridging or crack formation. Substituting these second wave parameters for the mechanical terms gives a fifth-order non-linear equation in terms of the ice swell

3. SEA ICE PHYSICS

(w_r) and elastic wave (w_s) frequencies. This can only be solved numerically, to give the wave number of the resonant wave. This value is then substituted into an expression which contains only wave-derived and density terms, to give area-averaged ice thickness.

Determination of the ice swell peak is a simple matter of FFTs, whereas the elastic wave frequency can be determined by looking at impulse events such as ridging, formation of cracks etc. This can be difficult if the event is close to the recording site, and requires at least 2 km of intervening ice to damp the non-linear forced vibrations and determine the 'free-vibration' frequency of interest reliably. Identifying these events and generating a reliable elastic wave frequency is the main challenge to developing a remote buoy system.

The scale over which the method averages ice thickness is currently unknown, and an extensive ground-truthing campaign, using both drilling and remote-sensing tools, is necessary.

Instruments

The waves propagating through the ice cover can be measured using several types of instruments. The passage of the waves induces a tilt in the ice surface, and this can be measured with sensitive tilt-meters, which can resolve events of less than 1 microradian. Tiltmeters are perhaps the easiest instruments to use, requiring only an initial levelling on the ice surface, once it has been cleared of snow.

The waves also induce a strain in the ice, proportional to the second spatial derivative of surface elevation, which can be measured with strainmeters. These are fixed into the ice surface at each of two ends, and the change in length across the gauge length of the instrument measured by a sensitive linear variable differential transformer (LVDT). The SAMS instruments incorporate a mechanical lever system to increase their sensitivity, and can resolve strains of 10⁻¹². Though they are time-consuming to install, they have the advantage of also detecting purely compressional events in the ice and are more sensitive than available tiltmeters. A motor-driven re-zeroing system allows a large dynamic range at this very high sensitivity. The units are identical to those used in previous campaigns by the Scott Polar Research Institute, though they have been updated with modern electronics, particularly microprocessor-driven stepper motors in place of the DC motors of the older devices, allowing automatic reconstruction of the data across a re-zero step.

Accelerometers are less useful in this application, as the long periods of the waves in question result in very small vertical accelerations of the ice surface, and are not used here.

The tilt and strain sensors are deployed in arrays of two, orthogonal, and three, 120° separated, devices respectively. The sensors are logged to an embedded microprocessor system, which also controls re-zeroing and communications, at 2 Hz.

Measurements

Ice thickness determination using flexural gravity waves

Data were gathered at each of the four 24-hour ice stations in the Storfjorden area. The area did not provide the necessary conditions for the Nagurny method (which assumes deep water, i.e. $kh \gg 1$, where k is wavenumber and h is water depth) but valuable experience was gained with the instruments, enabling them to be fully operational for the long drift station later. Several mechanical problems were encountered with the equipment in the very low prevailing temperatures (c.-30°C), but these were gradually overcome.

Long period swell waves were observed in each case, with periods ranging from 14 s to 20 s. Most records clearly showed 'beating', from the interaction of closely-spaced frequency components which tended to arrive from entirely separate directions. The spectral coherence of these arrivals was high (>0.6), giving confidence in the derived propagation directions. Wave energy was observed to build and/or decay during the course of three of these ice stations.

Ice Station Two (16/3/03) displayed an initially high amplitude, long period (18 s), peak which decayed at midnight to a largely red-noise character. This less coherent form remained for approximately six hours before the peak was re-established. The six-hour period suggests a tidal interaction with wave propagation into the pack. Though this is not a documented phenomenon, the area is subject to extremely strong tidal flows and further investigation will be carried out on our return.

Ice Station Three (23/3/03) initially took place under relatively-high amplitude wave action – a 15s swell was visible on board ship - and the experimental floe developed several large cracks before midday. Measured wave amplitude then dropped two orders of magnitude, and the floe did not develop any further damage. The beating nature of the time series was not evident in this latter period, with consistently unidirectional wave arrival vectors.

Ice Station Four (1/4/03) was the reverse case, initially being a low-amplitude regime which increased in energy throughout the night. The strains are particularly revealing, showing rapidly increasing elongation in the north-south direction. The instruments were removed at 0700Z, an hour before the floe finally failed less than 10m from the instrument site. The crack rapidly widened to a significant lead, running east-west as might be expected from the strains, allowing recovery of the 'tomato' by going alongside with the ship and using the ship's aft crane.

The Longyearbyen transfer (28/3/03) gave an opportunity to calibrate the strainmeters prior to the long drift station. This had not been possible during the previous ice stations, since the relatively high-amplitude wave regimes did not allow the instruments to settle sufficiently. The SAMS team were able to calibrate one of the two systems during the day, though several problems occurred in the second system. Having one calibrated system at least allowed reliable wave propagation directions to be established during the drift station, in order to direct aircraft operations.

On the long drift station, the two units were initially deployed in poor weather conditions side-by-side to cross-verify measurements between systems. Drilling and

3. SEA ICE PHYSICS

sledge EM measurements around the units established the ice thickness there as 3.2 m. The units were run for three days while several iterations of code were tested, primarily to establish robust re-zeroing behaviour in the strainmeters and to establish radio and Iridium communications with the ship-based modems.

Sledge EM surveys by the AWI group had meanwhile established that the central area of the floe was approximately 2 m thickness, and one unit was redeployed to this area (c.1.5 km from the ship) on 12/4/03, while the other logged the original deployment site. Two SeaBird CTD units (courtesy of the Hamburg IfM group) were deployed into the thermocline (c.80 m) in order to measure any internal waves that may couple to the ice. The second unit was then moved to a similar thickness ice patch approximately 1 km from the first.

Validation of the thickness measured by the Nagurny technique was done in a nested scheme at several scales. A dense grid of direct thickness measurements was taken round the first unit, using the SAMS hot water drill, covering a 50 m grid at 2.5 m spacing. Drilling was later expanded to the diagonals of a 250 m grid, at 10 m spacing. The same area was then covered with the sledge EM, on a 10 m spacing grid. Overflights by the heli-EM covered the entire experimental floe and for c.100 km from the ship. The same area was covered by a Twin Otter flying from Longyearbyen, carrying a swath laser profilometer (300 m swath width) and downward looking radar. Co-incident flights were done with the heli-EM around the area, and the Twin Otter also flew up-wave to the open water, to characterise the complete wave propagation path.

The second unit was moved to a large area of thin ice ($h = 15$ cm) for the last two days of the drift, using the ship's helicopter, to examine the effect of such a dramatic local thickness change on the measurements. The unit radioed its position back to the ship at three-hourly intervals, and a large radar reflector was also set up to ensure the unit could be retrieved. This was successfully done on 18/4/03 during a small weather window in the otherwise unflyable conditions.

References

Nagurny, A.P., V.G.Korostelev, O.M.Johannessen & P.Wadhams, in press. Multiyear variability of sea ice thickness in the Arctic Basin measured by elastic-gravity waves on the ice surface.

4. ATMOSPHERE PHYSICS AND CHEMISTRY

4.1 Convection Over Arctic Leads (COAL)

Lüpkes, Hartmann, Birnbaum, Cohrs (AWI), Yelland, Pascal (SOC), Spieß, Buschmann (TUB)

In Arctic sea ice covered regions the surface temperature is characterized during winter by strong spatial differences. The surface of leads and polynyas can be 30 degrees warmer than the surface of multi year sea ice floes. Such differences generate strong atmospheric convection which penetrates into the stably stratified atmospheric boundary layer (ABL) over sea ice. This process has a strong influence on the exchange of energy, humidity and momentum between the atmosphere, ocean and sea ice. Due to the surface cooling of open water new ice can be formed. With standard parameterization schemes as used in global and regional climate and weather prediction models these processes cannot be taken into account adequately.

Different systems were run to measure the turbulent fluxes of energy and momentum. On Polarstern, sonic anemometers were installed at different masts for the observation of surface fluxes. Three instruments were used permanently, others were additionally run only during ship stations in polynyas or leads. A portable mast was deployed on ice during stations. The upper boundary layer fluxes were measured with the helicopter borne turbulence measuring system Helipod.

4.1.1. Helicopter borne measurements of the ABL over leads and polynyas

The primary aim of the Helipod flights was to measure to what degree leads in the mainly closed sea ice cover influence the boundary layer structure by their heat release. The flights have been carried out in order to study how plumes of heat emanating from the leads are distributed in the BL by turbulent motion. We were interested in the penetration height of the plumes depending on the boundary layer and on lead parameters. How would the lead size and the temperature difference between lead surface and the air affect the convection? Would small leads have an overproportional effect in heat transfer as some studies suggested? And, would parameterisations of convective boundary layers over homogeneous surfaces as e.g. that of Gryanik and Hartmann (2002) be applicable to lead driven convection over sea ice? To answer these questions the Helipod turbulence probe was used during both parts of the cruise under a range of various atmospheric and lead conditions.

The Helipod probe

Helipod is a 5 m long probe carried by a helicopter on a 15 m long rope. It measures at 100 Hz sampling frequency the 3-dimensional wind vector, the surface and air temperatures and the humidity. Furthermore, it records its position, ground speed, height, orientation and attitude by inertial and GPS system. Further details are described in Bange et al. (2002), Figure A shows the Helipod in operation.

4. ATMOSPHERE PHYSICS AND CHEMISTRY

Flight patterns

A total number of 18 Helipod flights were carried out during both parts of the ARKXIX/1 cruise in the Storfjorden area, as well as north of Svalbard. Figure 4.1.B. shows a summary of the positions of these flights.

The main flight pattern consisted of vertically stacked legs of some 10 NM length parallel to the wind. The flights were arranged over a variety of leads ranging in size from a few metres to several kilometres. The boundary layer conditions were always unstable over the lead and both stable and unstable over the adjoining ice. Additionally, several vertical soundings were flown at both ends of the legs. To verify and monitor the consistency and accuracy of the system some calibration patterns have also been flown. Table 1 lists a summary of the flights.

Table 4.1: Helipod flights

Date	Latitude	Longitude	Legs
03-03-09	76.63	19.33	4
03-03-10	76.77	19.33	5
03-03-12	76.8	21.17	5
03-03-15	77.42	20.67	6
03-03-16	77.42	20.45	4
03-03-17	77.47	20.42	4
03-03-19	77.38	20.5	7
03-03-22	76.38	22.06	9
03-03-23	76.22	23.67	8
03-03-24	75.92	25.5	8
03-04-02	80.33	11.67	14 (2 flights)
03-04-03	80.68	13.33	8
03-04-04	81.46	10.17	8
03-04-09	81.82	9.75	8
03-04-10	81.75	9.67	12
03-04-14	81.80	10.5	12
03-04-19	81.27	10.67	10

Flight on 3rd April 2003

As an example of a typical flight pattern, the measurements of the 3rd April, 2003 are shown. The flight was conducted over two elongated leads, both of the same surface temperature, and both oriented orthogonal to the mean boundary layer wind direction. The leads differed only by their width, the upstream one was 1 km wide, while the 5 km further downwind situated lead had a width of 2 km. At both ends of the horizontal flight sections several vertical soundings were flown. Figure 4.1.C. shows the average potential temperature of five soundings together with the mean values resulting from the horizontal flight legs. A well mixed boundary layer of 140 m height can clearly be detected. From Figure 4.1.C. the levels of the horizontal flights with respect to the boundary layer height can also be seen. 6 legs cover the lower two-thirds of the boundary layer, one is at the inversion base and an eighth level well above the boundary layer. The near surface air temperature as well as the surface

Convection over Arctic Leads (COAL)

temperature of the snow-covered ice was $-29\text{ }^{\circ}\text{C}$, while the surface temperature of the leads was $-1.8\text{ }^{\circ}\text{C}$ at the upwind side and slightly lower at the downwind side.

The plumes of turbulent heat flux emanating from both leads is visualised in Figure 4.1.D.. It shows for the stacked horizontal flight legs the low-pass filtered covariance of the fluctuations of the vertical wind velocity and the potential temperature, multiplied by the air density ρ_a and the specific heat of air at constant pressure c_p (thick line in Figure 4.1.D.). The integral of this curve is proportional to the turbulent heat flux. The legs have been flown top to bottom. The abscissa in Figure 4.1.D. is based on geographic coordinates, the moving position of the leads is due to the ice drift during the flight. The airflow is from left to right. In the same graphs the leads are indicated by plotting $\rho_a c_p v(T_a - T_s)$ (v = measured wind velocity, $T_{a,s}$ = temperature at the flight level and at the surface, respectively) representing the bulk parameterization of the heat flux if we assume for simplicity a transfer coefficient $Ch = 1$.

Figure 4.1.D. clearly shows the turbulent heat flux generated by the leads and the advection of plumes towards the leeward side. In case of the smaller lead, near the surface the results of the bulk assumption and of the eddy correlation measurement agree well. In the higher flight legs, the eddy flux decreases rapidly with height over the smaller lead and it nearly vanishes at 88 m (roughly $0.6 z_i$). Over the larger lead, however, the eddy flux near the surface is considerably larger than that resulting from the bulk assumption with $Ch = 1$ indicating a much larger transfer coefficient. And, in contrast to the measured flux over the smaller lead, at 88 m the heat flux still corresponds to the surface flux in magnitude. At the base of the inversion the eddy flux over both leads is vanished.

Results

A more detailed analysis of the large dataset collected is needed in order to draw final conclusions. However, a preliminary inspection of some cases of the measurements, as the one described above, suggests that leads being small with respect to the boundary layer height do not produce a significant plume that is able to rise through the entire BL. Plumes from small leads seem to disappear without much influence on the BL. Plumes from leads that have an extension in the dimension parallel to the wind of several times the boundary layer height are able to fill the entire BL. The averaged turbulent heat flux per unit area of lead surface appears to be larger for large leads than for small leads. The characteristic size that separates small leads from large leads amounts to approximately 10 times the boundary layer height.

4.1.2. Surface fluxes over leads and polynyas

The ship based measurements aimed to quantify the effect of leads and polynyas on the surface layer fluxes in sea ice covered regions. Based on these data, parameterization assumptions such as the relation between the transfer coefficients for heat and momentum or the fetch dependence of fluxes should be investigated. Another important goal was to investigate the dependence of heat fluxes on the thickness of new ice usually formed very quickly in leads. Moreover, some studies

4. ATMOSPHERE PHYSICS AND CHEMISTRY

were carried out in combination with Helipod flights with the possibility to compare the results of both measuring systems.

Equipment used

The AWI turbulence measuring system TMS (Garbrecht et al., 1999, 2002; Garbrecht, 2002) installed permanently on Polarstern consists of a mast at the ship's bow crane which is usually equipped with METEK sonic anemometers and temperature sensors in 5 different heights between 3 m and 20 m above the surface. The mast can be installed in different horizontal distances from the ship's bow. The sonic anemometers measure with a frequency of 17 Hz, temperatures are obtained from PT-100 sensors with 1 Hz. From the sonic anemometer measurements turbulent fluxes of momentum and sensible heat can be derived. Additionally, three masts with sonic anemometers have been installed permanently by SOC: these will be described in the next section. Due to the extremely low temperatures the TMS mast could not be operated with all its sensors in each experiment. For the last measurement only one sonic was used which was installed at the tip of the bow crane (Figure 4.1.H).

Two KT15 radiation thermometers were used in different positions at the ship to register permanently the surface temperature close to the ship. The absolute humidity was measured permanently by a dew point mirror at 10 minute intervals.

The fluxes obtained from the TMS are usually calculated with the eddy correlation method and those from the SOC permanent masts by the dissipation method. A comparison of these different calculation methods is shown in section 3.

Measurements performed

Figure 4.1.E. shows the positions of stations with flux measurements carried out from the ship. Measurements over leads or polynyas were performed in the Storfjorden area and in the Barents Sea at five positions (March 15th, 17th, 19th, 22nd, 24th). In the Fram Strait, north of Svalbard two experiments followed (April, 2nd and 19th) with measurements over leads. Typically, the lead experiments consisted of measurements at one or several positions over sea ice on the downwind side of a lead and in measurements during very slow drift across the lead with stops in a distance of about 500 m to each other. At the end of each experiment measurements over sea ice at the upwind side of the lead were performed to obtain the inflow conditions. The typical duration of stops within the polynya and the measuring periods over ice amounted to 20 minutes. A 3.5 m mast, described in the next section, was installed on the ice at the upwind side of the lead for the entire duration of the experiment.

Drift on 24th of March

One of the drift stations was performed on the 24th of March over the Barents Sea. It is described in the following. Figure 4.1.F contains a photo of the lead which was covered by Nilas of 7.5 cm thickness. The lead was crossed twice by Polarstern, results are shown in Figure 4.1.G for the first drift (circles). Helipod measurements were carried out during two flight legs across the lead at 14 m height (solid lines) when Polarstern had crossed one half of the lead. In Figure 4.1.G the downwind side of the lead is at $x = 0$ m, the upwind end of the lead is at $x = -950$ m. The effect of the

lead is clearly visible in the results of both measuring systems (results of the SOC turbulence sensors are shown in Figure 4.1.1). There is a strong increase of the friction velocity (u), of the heat fluxes and of the drag coefficients. The maximum values of heat fluxes measured by the TMS amount to 75 W/m^2 which is about 20 W/m^2 lower than in the result of the second Helipod flight. However, this difference might be due to the fact that Helipod crossed the channel, Polarstern made in the thin ice cover of the lead. There is also a good agreement between the friction velocities measured by both systems which show an increase from 0.15 m/s over ice on the upwind end of the lead to about 0.3 m/s at its downwind end. Furthermore, the wind velocities obtained from the Helipod and the TMS differ only slightly. Drag coefficients, referring to the measuring height (not stability corrected) shown here for the TMS only, increase also strongly over the lead due to the convective conditions.

Results

As a (preliminary) result of the surface layer measurements we found that the strength of convection over leads depends not only on meteorological parameters but also on the thickness of the new ice formed on leads. Strong convection may still occur over 10 cm ice thickness, whereas a 35 cm ice thickness suppresses heat transport from the ocean to the atmosphere very efficiently. On the other hand, turbulent plumes are advected over the downwind side of the leads by several hundreds of metres which often results also over thick ice in strong heat fluxes directed upward. Due to this effect we measured at a distance of about 300 m from the lead fluxes of sensible heat of still 150 W/m^2 .

The measured data can be used for the validation of small scale models and for comparison with parameterizations of surface fluxes over ice covered regions.

4.1.3. Ship borne continuous measurements

Aims

The Southampton Oceanography Centre (SOC) instrumented the Polarstern prior to the ship leaving Bremerhaven in order to make continuous measurements of the air-sea-ice fluxes of momentum, heat and moisture in addition to various mean meteorological parameters (up- and down-welling short wave radiation, downwelling long wave radiation, air temperature and humidity, surface temperature, air pressure, mean wind speed and direction). As well as contributing to the lead/Polynya studies described above the data obtained during the cruise will be used to:

- a) examine the behaviour of the turbulent fluxes over the wide range of sea-ice concentrations/types and weather conditions encountered.
- b) examine the performance of the inertial dissipation method in unfavourable, i.e. strongly convective conditions.
- c) verify model results of the air flow over the Polarstern (Berry et. al., 2001) and thus quantify and remove any biases in the flux results obtained from the ship-borne sensors.

4. ATMOSPHERE PHYSICS AND CHEMISTRY

- d) extend a separate study into the parameterisation of downwelling long-wave radiation in terms of visual cloud observations (Josey et al., 2002).

Instrumentation

The instruments used for the flux measurements are listed in Table 1 and those used for the mean meteorological measurements are listed in Table 2 along with their location on the ship, the parameter measured and an estimate of the measurement accuracy. Figure 4.1.H shows a schematic of the positions of the masts installed on the ship. All sensors were de-iced daily or as often as required. The ship's navigation data were logged in order to obtain the true wind speed and direction. Sea surface temperature data were obtained from the ship's weather station data and the two thermosalinographs. All data were logged in real time using the AutoFlux system (AutoFlux group, 1996). A webcam was installed on the bridge and digital images of the sea-ice conditions ahead of the ship were obtained every 10 minutes throughout the cruise.

In addition to the ship-borne sensors the SOC group also deployed an on-ice system during the long ice stations as well as during some of the Polynya studies. The on-ice system consisted of a 3.5 m mast which was equipped with a fourth Solent sonic anemometer, a Vaisala sensor for mean air temperature and humidity and a PRT probe for surface temperature. Surface temperatures were also obtained using a hand-held IR sensor. The system was battery-powered and recorded continuous 20 Hz data internally. Table 3 lists the deployment periods of this system..

At the end of the cruise the fast response hygrometer and the two anemometers on the bow/crane masts were removed. In order to obtain additional open-ocean fluxes, the remaining sensors (i.e. the bridge-top anemometer and all the mean meteorological sensors) were left in place and the AutoFlux system configured to operate autonomously for the subsequent cruise from Longyearbyen to Bremerhaven.

Sensor	Manufacturer	Sensor position	Parameter	Sampling rate
R3 Solent sonic anemometer	Gill Instruments Ltd., U.K	6 m mast on bridge	momentum and heat fluxes	20 Hz
R3 Solent sonic anemometer	Gill Instruments Ltd., U.K	2 m crane mast / 6 m bow mast	momentum and heat fluxes	20 Hz
R2 Solent sonic anemometer	Gill Instruments Ltd., U.K	6 m bow mast / 2 m crane mast	momentum flux	20 Hz
IFM hygrometer	KNMI, The Netherlands	6 m bow mast / 2 m crane mast	moisture flux	10 Hz

Convection over Arctic Leads (COAL)

Table 4.1.2: The fast response sensors used to measure the turbulent fluxes

Sensor	Manufacturer	Sensor position	Parameter	Accuracy
R3 Solent sonic anemometer	Gill	6m mast on bridge	Mean wind and direction	1 %
R3 Solent sonic anemometer	Gill	2 m crane mast / 6 m bow mast	Mean wind and direction	1 %
R2 Solent sonic anemometer	Gill	6 m bow mast / 2 m crane mast	Mean wind and direction	1 %
Psychrometer	SOC	bridge mast, 2m above deck	Air temperature, humidity	0.05 °C
Psychrometer	SOC			0.05 °C
Humicap	Vaisala	bridge mast, 2m above deck	Air temperature	0.1 °C
Humicap	Vaisala		Relative humidity	2%
Radiometer	Epply	2m mast, on stbd side bridge	Downwelling long wave radiation	5 W/m ²
Radiometer	Epply			5 W/m ²
Solarimeter x 2	Kipp and Zonen	boomed out, port side above bridge	Up- and down-welling shortwave	< 3%
Solarimeter x 2	Kipp and Zonen	boomed out, stbd side above bridge	Up- and down-welling shortwave	< 3%
Solarimeter x 1	Kipp and Zonen	2m mast, on stbd side bridge	Down-welling shortwave radiation	< 3%
Barometer	Vaisala	observation ally	Air pressure	0.5 mb
IR radiometer	Tasco	Stbd side foredeck	Surface and sky temperature	0.5 °C

Table 4.1.3: The mean meteorological or “slow response” sensors. The columns show, from left to right; sensor type, manufacturer, position on ship, the parameter measured and instrument accuracy. The slow response instruments were all sampled at 0.1 Hz.

Method

Fluxes were obtained using the inertial dissipation (ID) method rather than the eddy correlation (EC) method. Although the ID method is less direct than the EC it has the advantage of using only the high (> 2 Hz) frequency part of the variance spectrum. This means that; 1) the method can be easily employed on a moving ship (Yelland et al., 1994, 1996), and 2) the sampling period required is relatively short (< 1 minute).

4. ATMOSPHERE PHYSICS AND CHEMISTRY

In addition, the flux measurements can be corrected for the effects of the disturbance to the air flow reaching the sensors caused by the presence of the ship (Yelland et al., 1998, 2002). On the other hand, the eddy correlation method has less restrictive assumptions, but can only be applied on stable platforms (stationary ship). Hence both methods complement each other.

Results

Initial results from the ship-borne system show good agreement in the heat and momentum fluxes obtained from the various anemometer. Figure 4.1.1 shows a time series of the preliminary flux results obtained during the 24th March (day 083), the same day which is already described in the previous section. It should be noted that the averaging periods vary for the different sensors and the results are sensitive to the exact period used, but the agreement between them is good nevertheless. The heat fluxes were low (about 20 W/m²) in the morning as the ship approached a nilas-covered Polynya from the downwind side, then increased up to 100 W/m² as the ship performed two transects of the Polynya during the rest of the day.

Date/ month	Start jday and time (GMT)	End jday and time (GMT)	Comment
12/03	071 10:00	072 13:20	24 hr ice station
15/03	074 16:00	074 22:00	Polynya study
16/03	075 16:00	076 12:30	24 hr ice station
22/03	081 16:00	081 20:00	Polynya study
23/03	082 11:30	082 16:10	12 hrs ice station
24/03	083 10:00	083 16:00	Polynya study
01/04	091 11:00	092 08:00	24 hr ice station
07/04	097 11:30	099 10:15	10 day drift station
09/04	099 10:40	103 16:20	moved system to Hamburg site
13/04	103 16:59	106 11:20	moved closer to Hamburg masts
16/04	106 11:20	107 12:33	mast rotated for better alignment with wind
19/04	109 10:50	109 20:00	Polynya study

Table 4.1.4: Deployments of the on-ice flux system.

References

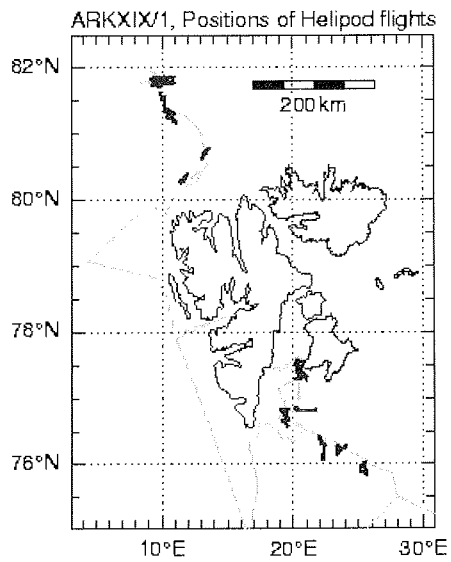
- AutoFlux group, 1996: AutoFlux - an autonomous system for monitoring air-sea fluxes using the inertial dissipation method and ship mounted instrumentation. Proposal to MAST research area C - Marine Technology, 38 pp.
- Bange, J., M. Buschmann, T. Spieß, P. Zittel, P. Vörsmann, 2002: Umrüstung der Hubschrauberschleppsonde Helipod / Vorstellung eines einzigartigen meteorologischen Forschungssystems, Deutscher Luft- und Raumfahrtkongress, Stuttgart, Germany, 23-26 Sept. 2002.
- Berry, D.I., Moat, B. I. and M. J. Yelland, 2001: Airflow distortion at instrument sites on the FS Polarstern. Southampton Oceanography Centre, Southampton, UK. SOC Internal Report No. 69. 36 pp.
- Garbrecht T., C. Lüpkes, E. Augstein, C. Wamser, 1999: Influence of a sea ice ridge on low-level airflow. *J. Geophys. Res.* 104(D20), 24499-24507
- Garbrecht T. 2002: Exchange of momentum and heat between the atmosphere and the ice covered ocean, Dissertation Universität Bremen, Alfred Wegener Institute for polar and marine research, Reports on Polar and Marine Research 410, 113 pp.
- Garbrecht T., C. Lüpkes, J. Hartmann, M. Wolf, 2002: Atmospheric drag coefficients over sea ice – validation of a parameterisation concept, *Tellus*, 54A, 205-219
- Gryanik, V. and Hartmann, J., 2002: A Turbulence Closure for the Convective Boundary Layer Based on a Two-Scale Mass-Flux Approach, *J. Atmos. Sci.*, 59, 2729-2744.
- Josey, S. A., R. W. Pascal, P. K. Taylor and M. J. Yelland, 2003: A new formula for determining the atmospheric longwave flux at the ocean surface at mid-high latitudes. *JGR-Oceans*, 108 (C4), 3108, doi:10.1029/2002 JC001418
- Yelland, M. J., B. I. Moat, R. W. Pascal and D. I Berry, 2002: CFD model estimates of the airflow distortion over research ships and the impact on momentum flux measurements. *J. Atmos. & Oceanic Tech.*, 19 (10), 1477-1499
- Yelland, M. J., B. I. Moat, P. K. Taylor, R. W. Pascal, J. Hutchings and V. C. Cornell, 1998: Wind stress measurements from the open ocean corrected for air flow distortion by the ship. *Journal of Physical Oceanography*, 28 (7), 1511 - 1526
- Yelland, M. J. and P. K. Taylor, 1996: Wind stress measurements from the Open Ocean. *Journal of Physical Oceanography*, 26, 541 - 558.
- Yelland, M. J., P. K. Taylor, I. E. Consterdine and M. H. Smith, 1994: The use of the inertial dissipation technique for shipboard wind stress determination. *Journal of Atm. Ocean Tech*, 11(4), 1093 - 1108.

4. ATMOSPHERE PHYSICS AND CHEMISTRY

Figure 4.1 A:
Helipod in operation.



Figure 4.1.B:
Positions of Helipod
measurements
during ARK19



Convection over Arctic Leads (COAL)

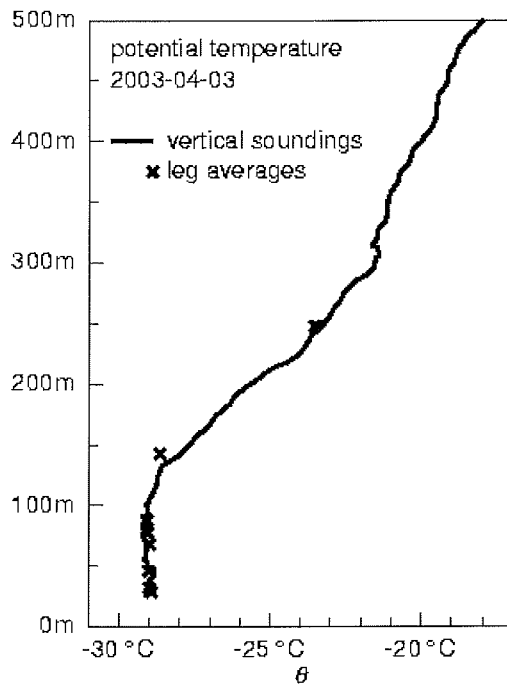


Figure 4.1.C: Profile of potential temperature (average over 5 soundings) and mean values of horizontal flight legs

4. ATMOSPHERE PHYSICS AND CHEMISTRY

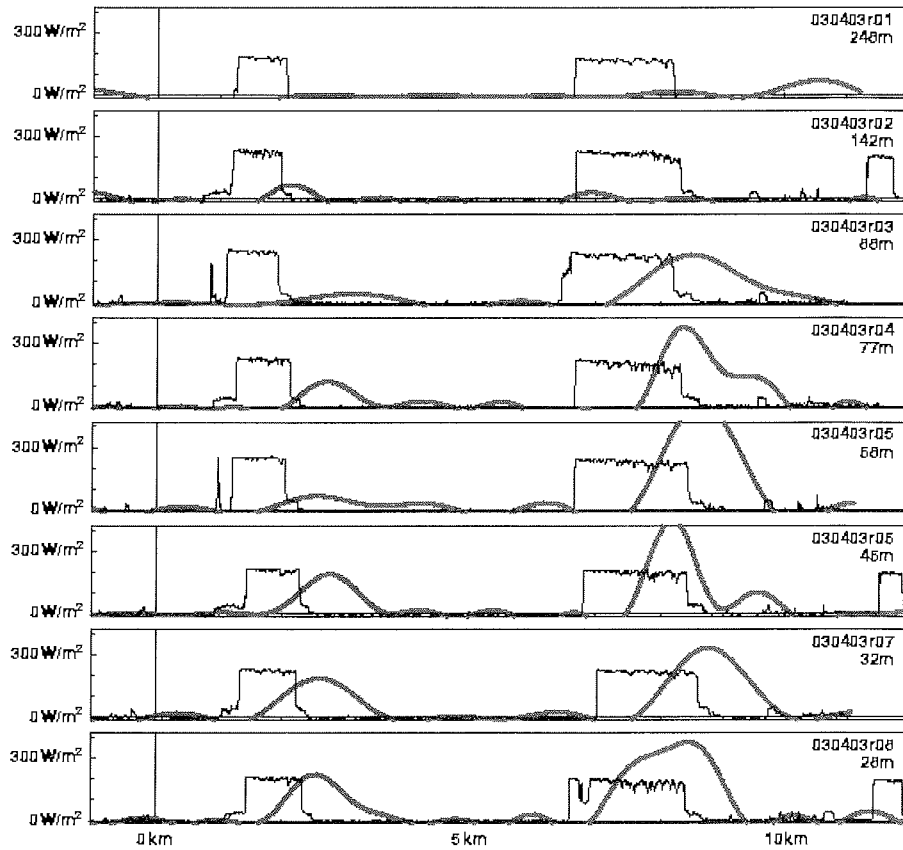


Figure 4.1 D: Low-pass filtered covariance of the fluctuations of the vertical wind velocity and the potential temperature multiplied by the air density and the specific heat of air at constant pressure (thick line). The thin line represents the result of the bulk parameterization of heat fluxes (see text).

Convection over Arctic Leads (COAL)

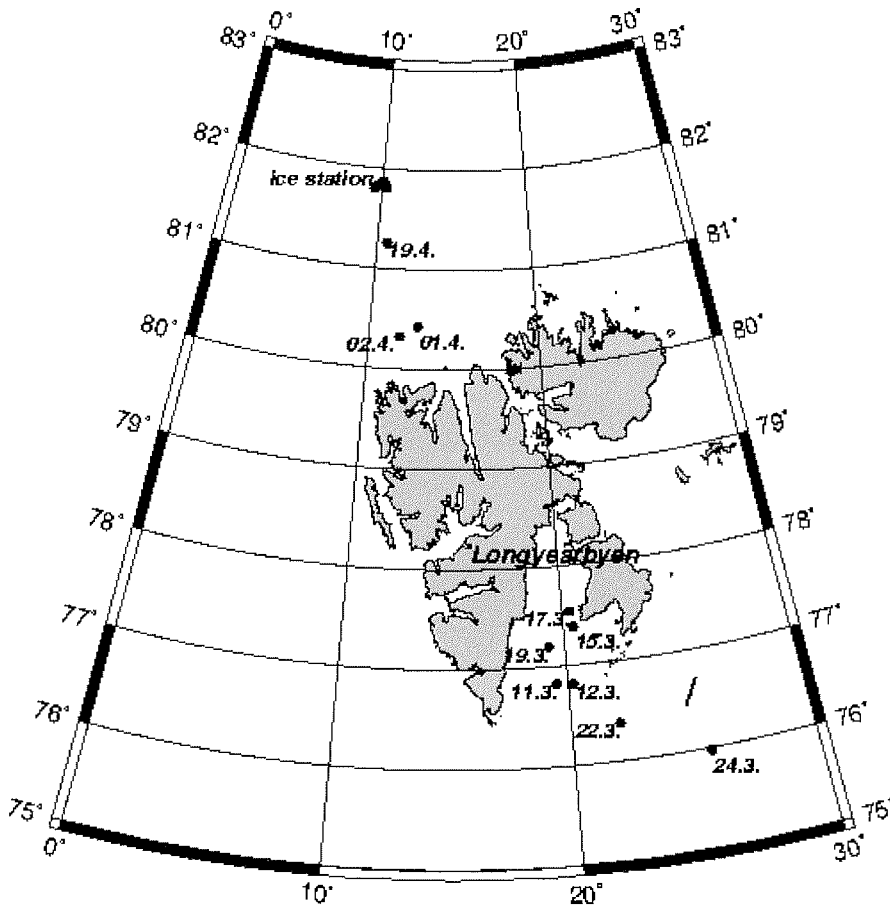


Figure 4.1. E: Positions of stations with flux measurements carried out from the ship. Measurements over leads or polynyas where performed in the Storfjorden area and in the Barents Sea at five positions and in the Fram Strait at two positions.

4. ATMOSPHERE PHYSICS AND CHEMISTRY



Figure 4.1. F: View from Polarstern during the drift station performed on the 24th of March.

Convection over Arctic Leads (COAL)

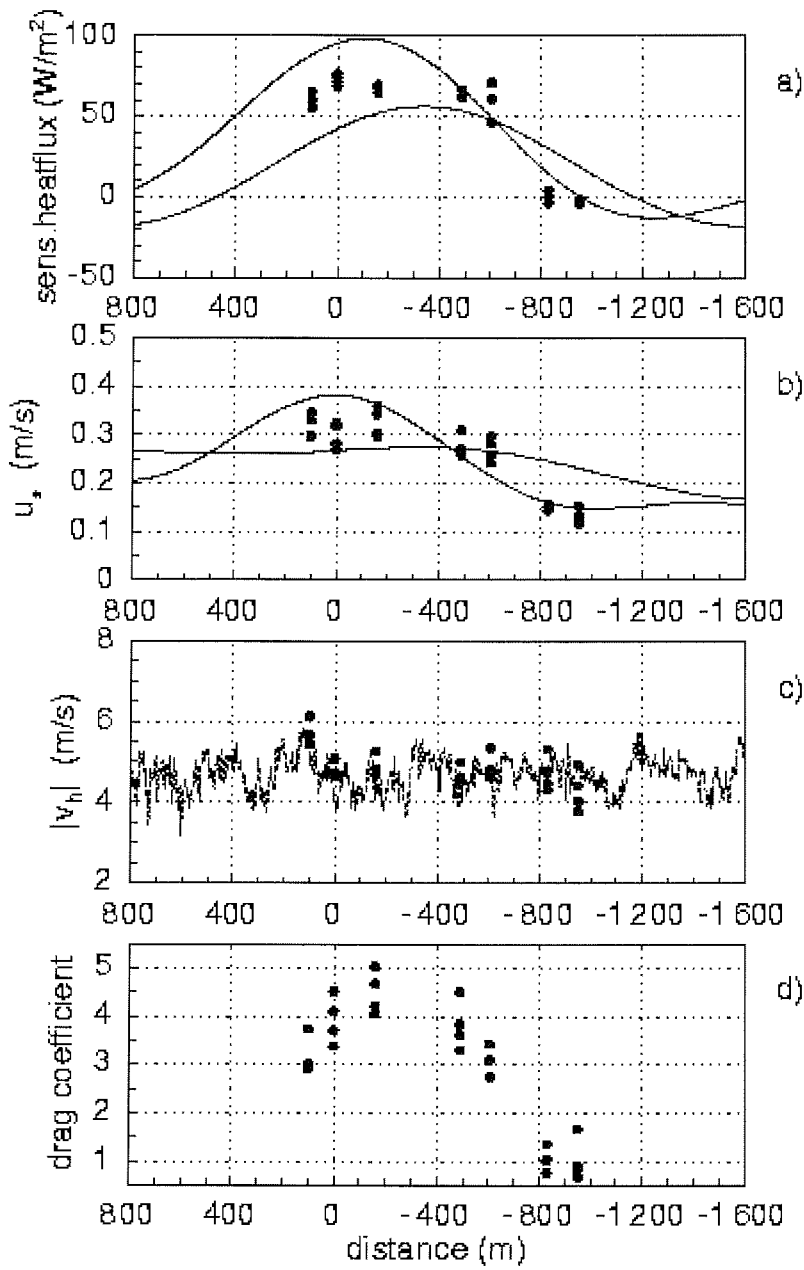


Figure 4.1 G: Results of the TMS measurements obtained from the drift on 24th March.

4. ATMOSPHERE PHYSICS AND CHEMISTRY

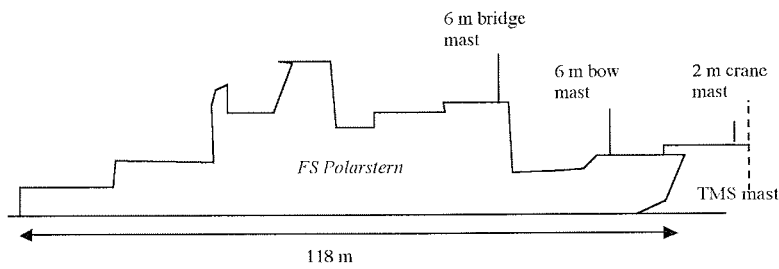


Figure 4.1. H: Location of the masts for measuring turbulent fluxes on the Polarstern.

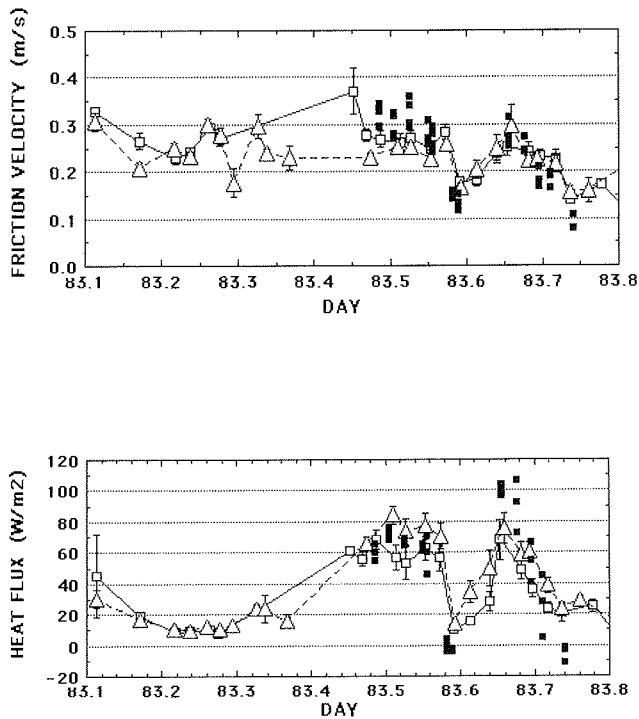


Figure 4.1. I: Time series of (top) friction velocity (square root of the kinematic momentum flux) and (bottom) the heat flux for the 24th March. The open symbols show 30 minutes averaged results from the R3 Solent sonics on the bridge (solid line) and the bow (dashed line). The solid squares show the results from the METEK anemometers on the TMS mast, averaged over the station durations of 15 to 25 minutes.

4.2 Arctic Boundary Layer and Sea Ice Interaction Study (ABSIS)

Kirchgäßner, Eriksson, Offermann, Albert, Seiffert, Bothe, Beeken (MIH, FIMR)

Our measurements on board of the RV Polarstern and during the ice drift station on 'Tomato Island' were a contribution to the ABSIS Project (Arctic Boundary and Sea ice Interaction Study). The goal of ABSIS was to compile a comprehensive data set of simultaneous measurements in the Arctic atmospheric boundary layer, at the air-ice interface, in the sea ice and the underlying ocean. This data set will be used to analyse and quantify the complex interaction processes between Arctic temperature inversions, atmospheric boundary layer and sea ice and thus the dynamic and thermodynamic forcing to the sea ice. This knowledge is necessary to validate and improve the ability to simulate these interaction processes in atmosphere-sea ice-ocean models.

It also includes simultaneous measurements on board the Finnish research vessel Aranda (FIMR, Helsinki, Finland), aircraft measurements of the research aircraft Falcon (DLR, Oberpfaffenhofen, Germany) operating from Longyearbyen and measurements of altogether 11 ARGOS ice buoys. Nine of the 11 buoys (type CALIB: Compact Air Launched Ice Beacon) were deployed by aircraft before the start of the campaign on March 27th and two buoys (type AWS: automatic weather station) were deployed via helicopter from board of RV Polarstern. All buoys are equipped with pressure and temperature sensors. The resulting surface pressure field allows to calculate the geostrophic wind, the tracing of the buoys gives the ice drift. The AWS buoys are additionally equipped with sensors for wind speed and wind direction and thus give information about the influence of the local wind on the ice drift. On April 4th the first AWS buoy was deployed at a position of 81° 51.25' N and 17° 57.29' E. The second AWS buoy was deployed on April 5th at 81° 30.07' N and 12° 04.19' E and could be recovered after the end of the ice drift station on April 19th at a position of 81° 27.88' N and 13° 03.96' E.

4. ATMOSPHERE PHYSICS AND CHEMISTRY

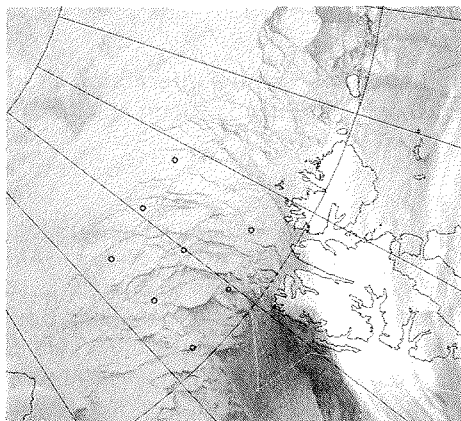


Figure 4.2.A: Position of ice drift buoys and RV Polarstern on April 2nd 2003, 9.31 UTC

Beginning on March 30th hourly observations of meteorological parameters, ice and clouds (type and cover) were carried out and radiosondes were started twice a day at 09.30 UTC and 21.30 UTC. During the period from April 3rd to April 18th radio soundings were carried out every three hours. Afterwards till the end of the cruise radiosondes were launched again twice a day. Radio soundings deliver the vertical profile of air pressure, temperature, relative humidity, wind speed and wind direction between the surface and 15 to 20 km height with a vertical resolution of approximately 20 – 50 m dependent on the ascent rate. These vertical profiles are especially important for the analysis of the structure and the temporal variability of the temperature inversion in the Arctic boundary layer.

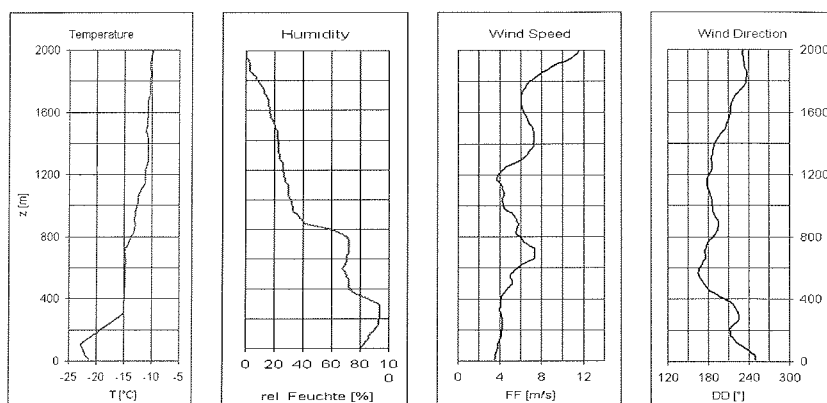


Figure 4.2.B: Example of a vertical radiosonde profile of air temperature T , relative humidity RH , wind speed FF and direction DD in the lower atmosphere (up to 2km) measured on April 7th at 09.43 UTC.

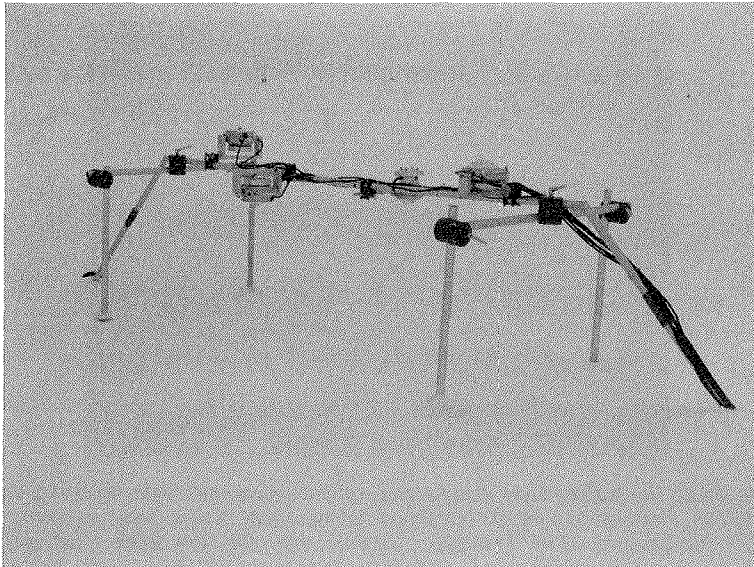
Arctic Boundary Layer and Sea Ice Interaction Study (ABSIS)



Figure 4.2.C: The surface layer measurement and instrumentation site on during the ice drift station. From left to right: 9m-mast and 2m-mast with Sonics, basic meteorological mast, in the background RV Polarstern, between them the 10m profile mast of FIMR, yellow boxes for electricity supply and data storage, precipitation gauge, frame with radiation instruments and tomato for storage of boxes, spades, fuel tanks and other equipment.

After arrival at the planned latitude in the pack ice a proper ice floe and a proper measurement site on it was chosen north of the ship in a distance of approximately 300m. Putting up instruments started on April 7th and was continued on April 8th. Measurements consisted of a meteorological mast, a radiation frame and two sonic instruments (METEK) installed on masts of 2m and 9m height respectively to measure turbulent fluxes. Basic meteorological measurements at the site included temperature of snow and ice at depths of 1cm, 2cm, 5cm and 10cm, surface temperature, air temperature, pressure, humidity, wind speed and direction at a height of 2m. The actual depth of the thermometers below the surface (compared to the initial depth) was observed daily. The radiation frame was equipped with upward and downward looking sensors for long-wave (Eppley) and short-wave radiation (Kipp & Zonen).

4. ATMOSPHERE PHYSICS AND CHEMISTRY



*Figure 4.2.D Frame with the four radiation instruments.
From left to right: upward looking long wave radiometer, downward looking long
wave radiometer, short wave downward and short wave upward looking radiometer.*

The Finnish Institute of Marine Research (FIMR) contributed to the meteorological measurements with a 10 m high profile mast. Wind speed was measured at 5 levels with cup anemometers (Aanderaa Instruments Co.) at heights of 10.10, 4.80, 2.20, 0.95 and 0.40 m above the snow surface. The air temperature was measured at 3 levels (10.10, 2.20, 0.40 m) with platinum film resistor type thermometers (Aanderaa Instruments Co.). Furthermore the wind direction was measured at the top level and the relative humidity at the 4.8 m level. The profile gradients from the mast allow to calculate the fluxes of momentum and sensible heat by the means of a level difference method (LDM). This demands an accurate calibration of the sensors as well as precise knowledge of measuring heights. From the profile data we are able to calculate the aerodynamic roughness length for the surrounding terrain, in this case a ridged sea ice field, and can, together with additional high-quality roughness data, be implemented for modelling parameterisation.

Electricity for all devices except for the profile mast was supplied by a generator. Due to icing by snow drift the generator broke down and had to be replaced by another one on April 8th. Meteorological mast and radiation station data were sampled as 1-minute mean values, sonic turbulence data were measured at a rate of 20 Hz and accumulated to mean values over five-minute intervals.

Determination of Arctic stratospheric ozone losses

Radiation measurements ended on April 16th in the early afternoon. The remaining sensors and equipment were removed from the measurement site in the morning of April 17th, the final day of the ice drift station.

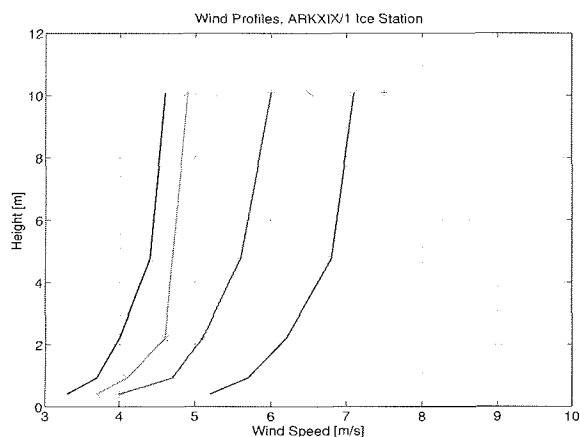


Figure 4.2.E:
Examples of wind speed profiles during the period 10-15.04.2003 measured at the FIMR 10m profile mast. The single data points at the 10-meter level represent gust wind speeds

4.3 Determination of Arctic stratospheric ozone losses Debatin (AWI)

In order to improve our understanding of the wintertime polar ozone losses in the stratosphere, an ozonesonde Match campaign was carried out in the Arctic within the EU funded project "Quantitative Understanding of Ozone Losses by Bipolar Investigations" (QUOBI) from late November 2002 to March 2003. This action was embedded into the first phase of the European study "Validation of International Satellites and Study of Ozone Loss" (VINTERSOL).

The so-called Match technique consists of launching two ozonesondes into the same air mass a few days apart. Fig. 1 illustrates this method. If ozone is chemically destroyed between the two soundings, this will be seen as a small difference in the ozone data. By comparing several hundreds of such ozonesonde pairs one can deduce the degree of ozone loss with good accuracy. The Match technique had already been used to assess the ozone loss during the Arctic winters from 1991/92 to 2000/01.

Since in some of the recent winters we observed more ozone losses than can be explained by state-of-the-art models, this data set together with the data of former campaigns and the data of the first Match campaign in the Antarctic (2003) will be the essential basis for comparisons with several model studies within QUOBI.

4. ATMOSPHERE PHYSICS AND CHEMISTRY

For the first time ever RS Polarstern joined the Match campaign in late February, adding 18 soundings to overall about 450 soundings at approx. 25 ozonesonde stations (cf. Fig.4.3.1). Within the co-ordination procedure it was handled as a moving 'target'. The experience with this new feature was very positive. From the Match point of view we would welcome more RS Polarstern activities in the Arctic winter.

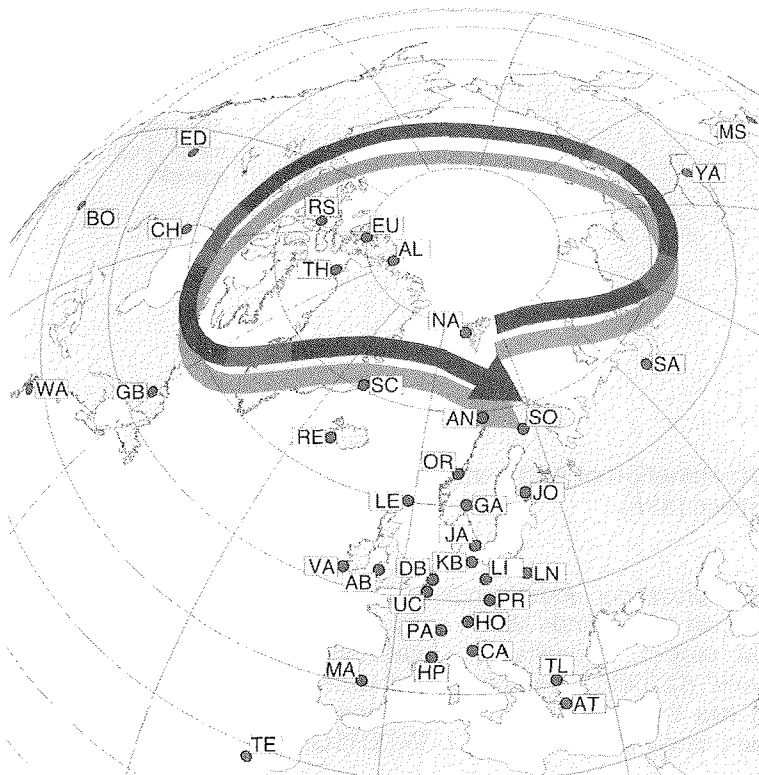


Fig. 4.3.1. Map of ozonesonde stations (RS Polarstern not shown) in the Northern Hemisphere which took part in the Match campaign during the 2002/03 winter. The Match principle is also illustrated. In this example an ozonesonde is launched from the Koldewey station in Ny-Ålesund, Spitsbergen. At the Match headquarter (AWI Potsdam) information about this sonde flight is fed into a trajectory forecast program that uses wind data to predict the course taken by the air mass that was probed by this sonde. If this air mass is predicted to pass close to another station - in this case near Sodankylä/Finland - or RS Polarstern some days later, this second place will be alerted in due time so that a new sonde can be launched into the same air mass.

4.4 Reactive trace compounds in sea ice and in the Arctic troposphere

Jacobi, Dick (AWI)

Introduction

Compared to other remote areas, the composition of the troposphere in the polar regions is modified due to the large snow covered areas. Water-soluble reactive compounds like hydrogen peroxide (H₂O₂) and formaldehyde (HCHO) are present in the snow. These compounds can be transferred from the snow to the atmosphere and vice versa. In addition, solar radiation can penetrate into the top layers of the snow inducing the photochemical production of several reactive compounds. Therefore, the composition of the surface snow is an important parameter for the understanding of atmospheric processes in polar regions.

While some information about the composition of snow in permanently snow-covered areas is available, data about the composition of sea ice or snow on top of sea ice is almost non-existent. Therefore, we determined concentrations of reactive trace compounds in the arctic troposphere, in sea ice, and in the snow cover of ice floes.

Snow-covered sea ice

The snow covers of several ice floes were sampled with a vertical resolution between 2 and 5 cm. These samples are used to determine vertical profiles of density, temperature, and H₂O₂ and HCHO concentrations in the snow cover. In addition, longer ice stations were used to drill ice cores, which were also analyzed for H₂O₂ and HCHO, and to collect further snow samples, which are shipped to Bremerhaven for further analysis regarding the concentrations of anions and cations. Moreover, during three longer ice stations snow samples and ice cores were retrieved for the analysis of the distribution of heavy metals in the snow cover and in the sea ice of the floe. These measurements will also be performed in Bremerhaven. Table 1 contains a detailed list of measured quantities and samples taken for chemical analysis.

Gas phase measurements

Concentrations of ozone (O₃) were continuously measured at a height of approximately 20 m above sea level. The commercial detector (Ansyco GmbH) used the UV absorption at 253.7 nm for determining O₃ concentrations. It was installed in the 'Beobachtungsgang' in front of the meteorological office, while the inlet line was fixed at the railing of the deck behind the 'Peildeck'.

Several longer O₃ depletion episodes with concentrations below the detection limit were encountered (Fig. 4.4.1). One episode started for example on 30 March and lasted until 11 April. This extended episode was only interrupted by short periods with higher O₃ concentrations when winds from southerly directions reached the ship's position.

During the episodes with low O₃ concentrations, balloon-borne O₃ sondes were regularly launched from the helicopter deck (Fig. 4.4.1) to determine the height of the layer with reduced O₃ concentrations. In most cases, low O₃ concentrations were observed in the boundary layer below strong temperature inversions. Profiles measured on 1 April 2003 are shown in Figure 4.4.2. On this day, two sondes were

4. ATMOSPHERE PHYSICS AND CHEMISTRY

launched. At heights above 1500 m O₃ concentrations in the order of 50 ppbv are encountered. These concentrations did not change during the day. Below this height, a dramatic decrease in O₃ occurs. Very steep concentration gradients lead to non-detectable O₃ at a height of around 500 m in the morning. In the afternoon, the height of the layer without ozone further increased to almost 600 m and an additional destruction of O₃ has occurred in the region between 600 and 1500 m.

During the long drift station (PS64/111-2), continuous measurements of gas phase concentrations of O₃ and H₂O₂ were performed directly on the floe. In order to resolve concentration gradients above the floe, two different inlet lines were used to sample ambient air at heights of approximately 90 and 5 cm above the snow surface. In addition, the lower intake line was fixed for 24 h at a depth of - 5 cm below the snow surface to determine concentrations in the interstitial air of the surface snow.

Sea water measurements

Several CTD stations (Tab. 4.4.1) were used to obtain water samples to determine concentrations of H₂O₂ and HCHO in oceanic surface water at high latitudes.

Figure 4.4.1: Preliminary time series of O₃ concentrations measured during the cruise. Red diamonds mark launchings of O₃ sondes.

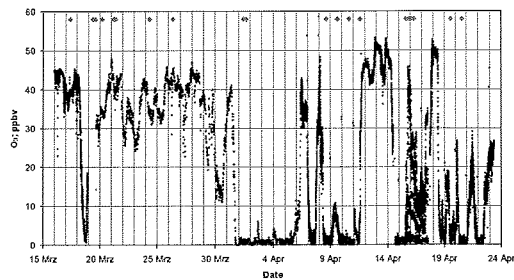
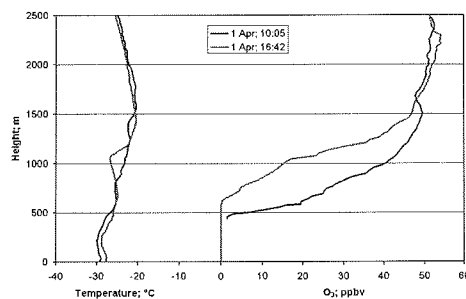


Figure 4.4.2: Temperature and O₃ profiles measured with O₃ sondes in the morning and in the afternoon of 1 April 2003 (80° 25' N; 12° 48' E).



Reactive trace compounds in sea ice and in the Arctic troposphere

Station	[H ₂ O ₂]	[HCHO]	Density	Salinity	Temperature	Anions/ Cations	Heavy metals
PS64/012-1	snow	snow	snow				
014-4	snow	snow	snow				
016-2	snow	snow	snow	surface ice			
021-2	snow	snow	snow	snow, surface ice	snow		
024-1	snow	snow	snow	surface ice	snow		
028-1	snow, ice	snow, ice	snow, ice	surface ice	snow	snow	
031-2	surface	surface					
034-1	surface	surface					
039-1	snow, ice	snow, ice	snow, ice	surface ice	snow	snow	snow, ice
050-1	surface	surface					
052-1	surface	surface					
058-1	surface	surface					
060-1	surface	surface					
062-1	surface	surface					
070-6	snow	snow	snow	surface ice	snow	snow	snow, ice
073-2	snow	snow				snow	
074-1	surface	surface					
075-8	snow	snow	snow	surface ice	snow		
078-1	surface	surface					
079-1	surface	surface					
085-1	surface	surface					
089-1	surface	surface					
093-1	snow, ice	snow, ice	snow, ice			snow	
098-1	surface	surface					
105-1	surface	surface					
106-1	surface	surface					
111-2	gas, snow, ice	snow, ice	snow, ice	surface ice		snow	snow, ice
111-4	surface	surface					
111-8	surface	surface					
112-1	surface	surface					
119-3	surface	surface					
128-1	surface	surface					
133-1	surface	surface					
134-2	surface	surface					
135-1	surface	surface					

Table 4.4.1: List of measured quantities and samples taken for chemical analysis

Snow: snow cover of ice floes; ice: sea ice; surface ice: top of the sea ice; gas: gas phase; surface: seawater

4.5 Meridional aerosol optical depth distribution from 70°S to 80°N

Debatin (AWI)

During the transit from Bremerhaven to Longyearbyen, measurement of aerosol optical depth (AOD) was carried out as a continuation to what had been done in ANT XX/1-4. The aim of this task is to find out the distribution of aerosol optical depth from southern to northern hemisphere, specifically over the Atlantic Ocean. The data can be used for validation activities, like MODIS and SAGE.

AOD was measured using a sunphotometer type SP1A which was coupled to a suntracker type SPTRV2 (both fabricated at Dr. Schulz & Partner GmbH, Germany). The 17 channels of the sunphotometer cover a wavelength range of 351-1062 nm. Measurements were made on 23 days with relatively clear sky and bright sun. The missed days were due to intense cloud throughout the day.

Preliminary results of the measurements in the high northern part of the Atlantic Ocean showed that the AOD level at 1000 nm is mostly below 0.10 (21 cases). Only in two cases the AOD level is extremely high > 0.2 . The measurements during the end of the cruise have been performed at the west side of Spitzbergen and simultaneously AOD data are available at Koldewey station.

Next steps of the data analysis will include comparison of the AOD data obtained from this cruise with that from ARK XIX/1. The horizontal variation will be studied by using trajectory analysis under consideration of the satellite images and aerological data corresponding to the cruises ANT XX/1-4. Finally it is planned to compare with measurements during ANT XIV in 1996/97.

5. WATER MASSES AND CIRCULATION

5.1 Shelf convection in the western Barents Sea and Atlantic water north of Svalbard

Fer, Harms, Martin, Pisarev, Rudels, Schauer, Sirevaag (GIUB, IfMH, AWI, SIM, FIMR)

Introduction

The aim of the oceanographic program was to study wind-induced latent heat polynyas, such as the Storfjord polynya, and sensible heat polynyas, forced by ocean heat as in the Whalers Bay north of Svalbard, during winter.

Shelf/slope convection on and from the Arctic shelf seas constitutes part of the thermohaline overturning in the North Atlantic. It is driven by densification of surface waters through cooling and through their enrichment with brine due to freezing. The Arctic shelf seas provide favorable conditions for the latter process since they are almost ice-free in autumn and have numerous wind-produced polynyas off islands and along the coast throughout the winter. Depending on initial conditions and forcing, shelf/slope convection may form upper layer, intermediate, and deep water

Shelf convection in the western Barents Sea and Atlantic water north of Svalbard

over a broad density range and thereby contribute to a continuous overflow over the Scotland-Greenland sill and trigger convection in subpolar seas.

The first instance, where cold, saline water formed over a shallow shelf could be followed down the continental slope into the deeper layers, was reported from Storfjorden and Storfjordrenna (Quadfasel et al., 1988). Storfjorden located in the southeastern Svalbard Archipelago is approximately 110 km long and 190 m deep at its maximum depth and is enclosed by the islands Spitsbergen, Barentsøya, and Edgeøya. In the south, it is limited by a wide opening and a 120 m deep sill. The other straits are narrow, shallow and dominated by tidal currents. South of Edgeøya, a shallow area separates the deeper southern part of Storfjorden from the Barents Sea. South of the sill the fjord opens to Storfjordrenna, a trough that cuts from the Norwegian Sea into the Barents Sea continental slope and shelf. Storfjordrenna is separated from the main part of the Barents Sea by the shallow Svalbard Bank to the south and the Hopen Bank to the east.

The waters in Storfjorden derive from two sources. Part of the Atlantic Water of the West Spitsbergen Current turns eastward into, and circulates cyclonically around, Storfjordrenna. Some of this Atlantic Water crosses the eastern part of the sill and makes an additional loop into Storfjorden. The second source is the Arctic water of the East Spitsbergen Current that flows south along the eastern coast of Svalbard and turns westward around Edgeøya and passes over the eastern banks, which are too shallow to be flooded by the Atlantic water, and enters Storfjorden from the east. It has a cyclonic circulation in the fjord and joins the West Spitsbergen Current south and west of the southern tip of Spitsbergen. In winter a polynya opens up frequently in the northeastern part of Storfjorden allowing new-ice formation and convective water mass (trans)formations.

In the first part of WARPS we studied the dense water formation in the polynya rich area of Storfjorden, how the heat loss, the ice formation and the salinity increase are related, how the deep depressions are filled, and how the dense water crossing the sill interacts with the ambient waters as it moves towards and down the continental slope.

In the second part we focussed on processes north of Svalbard where the warm Atlantic water of the West Spitsbergen Current encounters and melts sea ice formed in the Arctic Ocean and transported towards Fram Strait. The melt water is stirred into the Atlantic water transforming its upper part into a cold, less saline layer above the warm, saline core of the Fram Strait inflow branch. This upper layer is the embryo of the halocline in the interior of the Arctic Ocean, which inhibits the vertical transport of heat from the Atlantic layer to the ice cover and the atmosphere.

Methods

A total number of 71 CTD (conductivity, temperature, depth) stations were occupied in the Barents Sea (Fig. 5.1.A) and of 46 stations north and west of Svalbard (Fig. 5.1.J). We used a SBE911*plus* system (SN 561) in combination with a rosette SBE 32 (SN 273). The sensors for temperature, SBE 3 (SN 2685), and for conductivity,

5. WATER MASSES AND CIRCULATION

SBE 4 (SN 2446), were calibrated before and after the cruise. The CTD was lowered at a rate of about 0.7 m s^{-1} as close as 2-m to the bottom. For determining the distance to the bottom a Benthos altimeter model 2110-2 was used. The sensor accuracies of the CTD instrument are provided by the manufacturer as 1 dbar, $1 \times 10^{-3} \text{ }^{\circ}\text{C}$, and $3 \times 10^{-4} \text{ Siemens m}^{-1}$ for pressure, temperature and conductivity, respectively. Three moorings were deployed in Storfjorden: 'Ursel' at the western part of the sill, 'Ingo' in the deepest trough, and 'Andreas' at the eastern flank. The details concerning the moorings are summarized in Table 1. The moorings will be recovered in autumn 2003.

Observations in the Barents Sea

Section A (Fig. 5.1.B) was taken from the northern flank of the Svalbard Bank across Storfjordrenna to Sørkapp to detect if any dense water already had reached the continental slope. No such water was observed, and the section was at mid depth dominated by the Atlantic Water with temperatures in excess of 3°C and salinity reaching 35 making its cyclonic loop into Storfjordrenna. The water at the bottom was colder and less saline and could be traces of water cooled on any of the shallow banks surrounding Storfjordrenna.

Section B (Fig. 5.1.C) was south of the sill. Signs of cold water, slightly denser than the Atlantic water, at the western part of the section suggested a flow along the bottom from the sill. Section C (Fig. 5.1D) at or slightly south of the sill showed a stronger presence of dense, cold bottom water. Warmer Atlantic water was present at the eastern part of the section.

After the last station on section C Polarstern turned north and made the south to north section H (Fig. 5.1G) over the flank of the shallow eastern bank toward Edgeøya and an area of open water observed south and west of Edgeøya. The salinity of the upper mixed layer increased slowly towards north, from 34.3 to 34.55 in the polynya area. The temperature was almost invariably at the freezing point. The salinity increase was largest on the shallower stations. The salinity increase of the upper layer was accompanied by a corresponding increase in the bottom layer, which mostly showed a linear salinity gradient towards the bottom, and occasionally a more stepwise salinity increase. The linear increase could be due to local haline convection, while the step like structure implied the presence of more saline water probably formed at still shallower areas and advected along the bottom towards the station.

Section P (Fig. 5.1H) was taken from the polynya towards southwest to and beyond the deepest depression. The temperature was close to freezing in the entire water column on nearly the entire section. Only to the west a layer was observed at mid depth with temperatures slightly above the freezing point. The most saline and dense water was seen at the bottom close to Edgeøya and indicated that saline water was flowing along the bottom toward the depression. Section D passed the southern depression. To the west, the temperature at mid depth was clearly above freezing, indicating remnants of warmer, perhaps Atlantic water, that had entered the fjord at an earlier time.

Shelf convection in the western Barents Sea and Atlantic water north of Svalbard

Polarstern then made a northwest – southeast section from Storfjordrenna over the Hopen Bank and into the Hopen Deep toward the Central Bank. The Central Bank was not reached because of the high ice concentration that impeded the progress during the entire cruise. The Hopen Bank and the western side of the Hopen Deep, down to 100m, was dominated by cold, freezing point, low salinity (34.5) Arctic water, which at least in the Hopen Deep originated from the northern Barents Sea. Further to the east and in the deeper part, the warmer saline Atlantic water entering the Barents Sea at the Bear Island Channel was encountered. A thin, colder, less saline bottom layer that was observed in the deepest part of the Hopen Deep could derive from the Central Bank, where winter convection creates cold, at freezing point, dense water.

Preliminary Results

The temperatures close to, or at, the freezing point and the stable vertical salinity stratification in almost the entire fjord showed that the haline convection was increasing the salinity of the waters in the fjord. The largest increase was found at the shallow areas and within the polynya. Saline, cold water was observed to drain along the bottom towards the deeper depressions. However, salinities as high as those reported from Oden in April 2002 (35.83) were not seen (Rudels, pers.comm.). The highest observed value, 34.965, appears too low for the maximum salinity of the fjord to increase sufficiently within the remaining freezing period to contribute to the Norwegian Sea Deep Water. Less and less dense water is thus expected to be exported from Storfjorden in 2003 than in 2002.

Table 5.1. Mooring properties. Instrument depths are nominal. Here, hab denotes height above bottom.

Mooring	Position		Water Depth (m)	Instrument	Instrument depth (m)	Instrument hab (m)	Deployed Date/ UTC
Ursel	76° 50'N	19° 24.8'E	167	Microcat	161	6	11.03.03 / 07:19
				RCM8	160	7	
				T-chain	158-78	9-89	
				Microcat	151	16	
				RCM4	67	100	
Ingo	77° 12.1'N	19°17.34'E	177	RCM5	78	99	19.03.03 / 20:06
				Microcat	162	15	
				T-chain	170-120	7-57	
				RCM7	172	5	
Andreas	77° 16'N	20° 17.95'E	100	Microcat	173	4	19.03.03 / 07:14
				Seacat	95	5	
				RCM7	94	6	
				Microcat	51	49	
				RCM4	50	50	

5. WATER MASSES AND CIRCULATION

There could be several reasons for this: A more extensive and more stationary ice cover in the fjord the present winter. A situation partly confirmed by the slow progress made by Polarstern through the ice, and by the presence of multi year ice in the southern part of the fjord (Chapter 3.1). The entire water column also appears to have been exchanged in fall 2002 and less saline Arctic water had entered the fjord (Fer, pers.comm.). This would then require a larger ice production and larger brine rejection throughout the winter to reach similar salinities as encountered in April 2002.

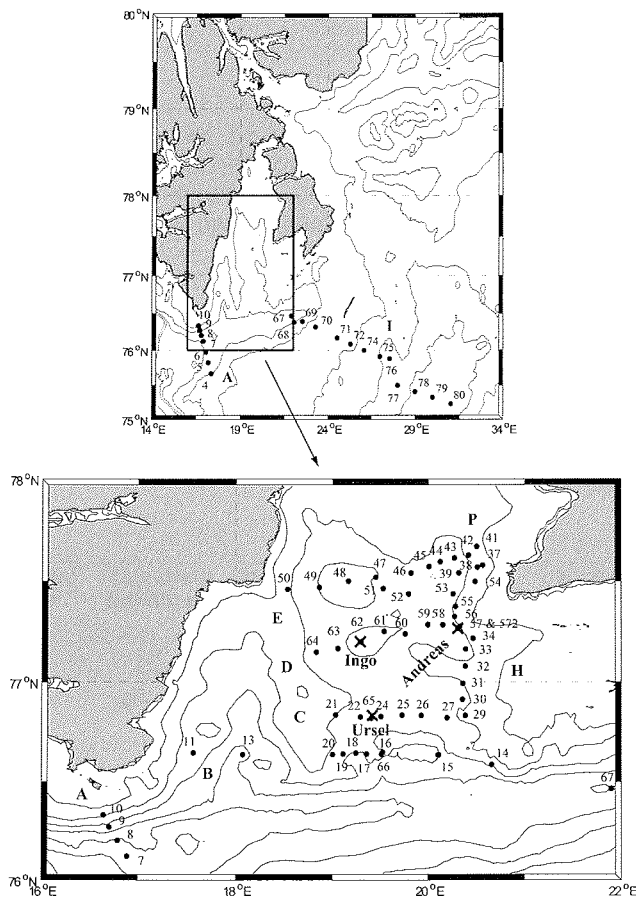


Figure 5.1.A. Bathymetry of the working area with locations of the CTD stations (dots with stations numbers indicated) and the moorings (crosses). The inset is shown in detail for clarity. Isobaths are drawn at 100-m and 50-m intervals for the upper and lower panel, respectively. Sections are labeled A to I, with P denoting the polynya section

Shelf convection in the western Barents Sea and Atlantic water north of Svalbard

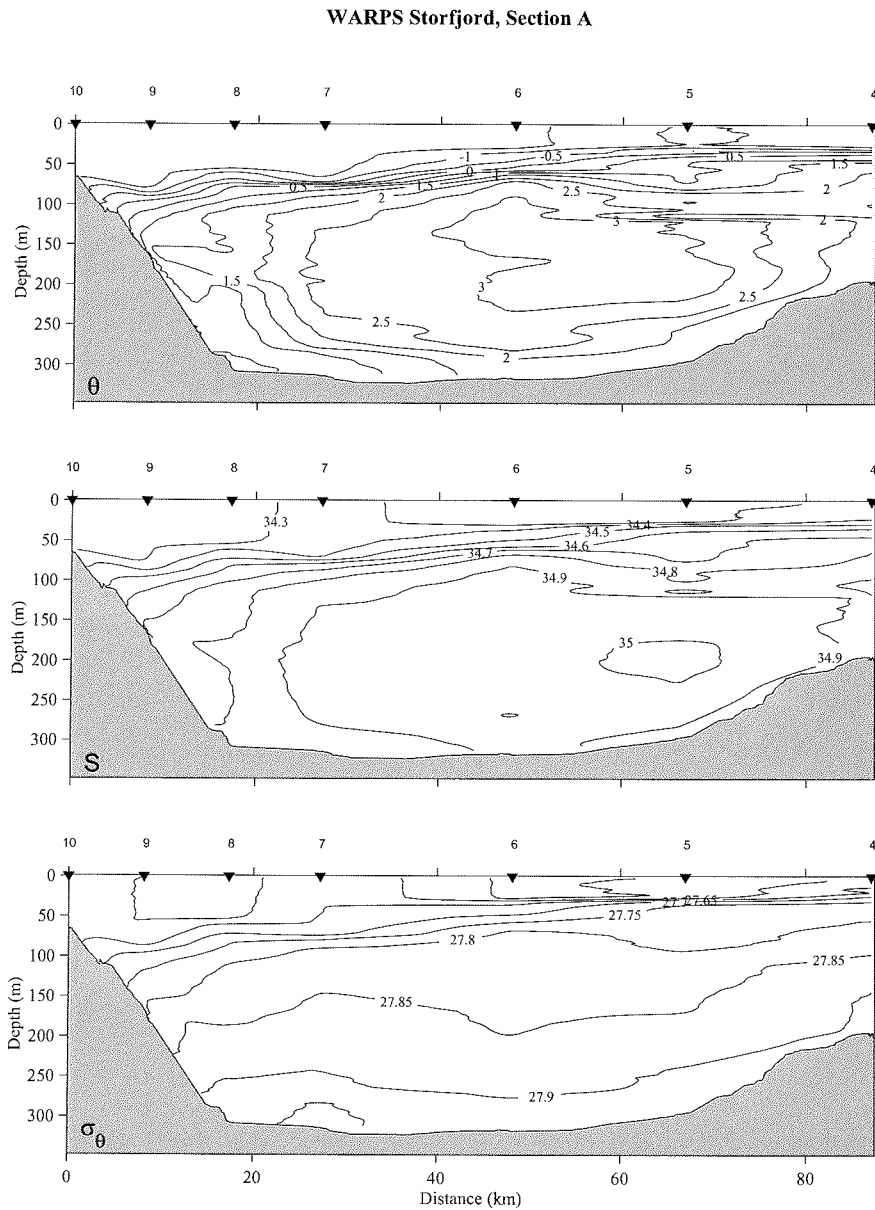


Figure 5.1.B. Distribution of potential temperature, θ , salinity, S , and σ_θ at section A. Contours are drawn at 0.5 °C, 0.1 psu, and 0.05 σ_θ units, respectively. Station numbers are indicated above each panel. Bathymetry is derived from the ship's echo sounder after correcting for section averaged sound velocity.

5. WATER MASSES AND CIRCULATION

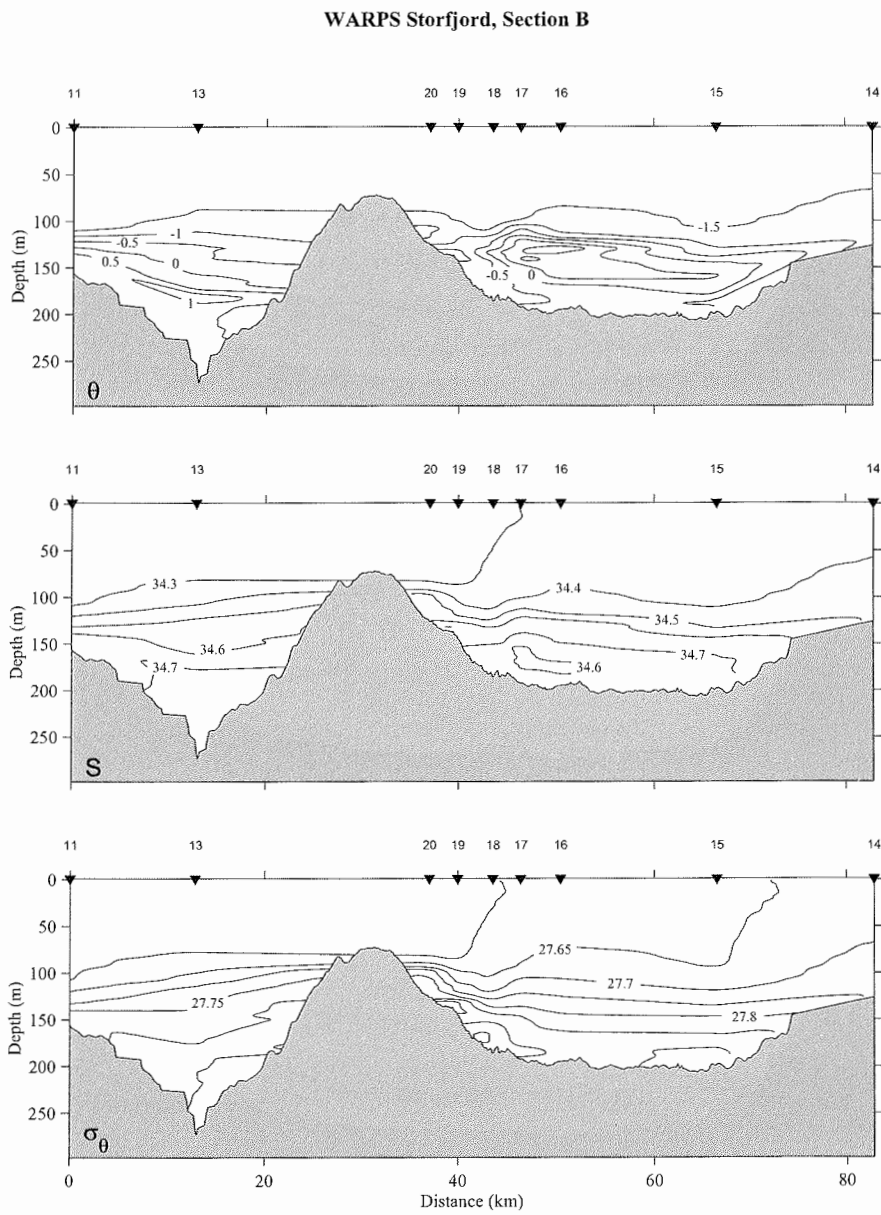


Figure 5.1.C.. Same as Figure 5.1.B, but for section B.

Shelf convection in the western Barents Sea and Atlantic water north of Svalbard

WARPS Storjord, Section C

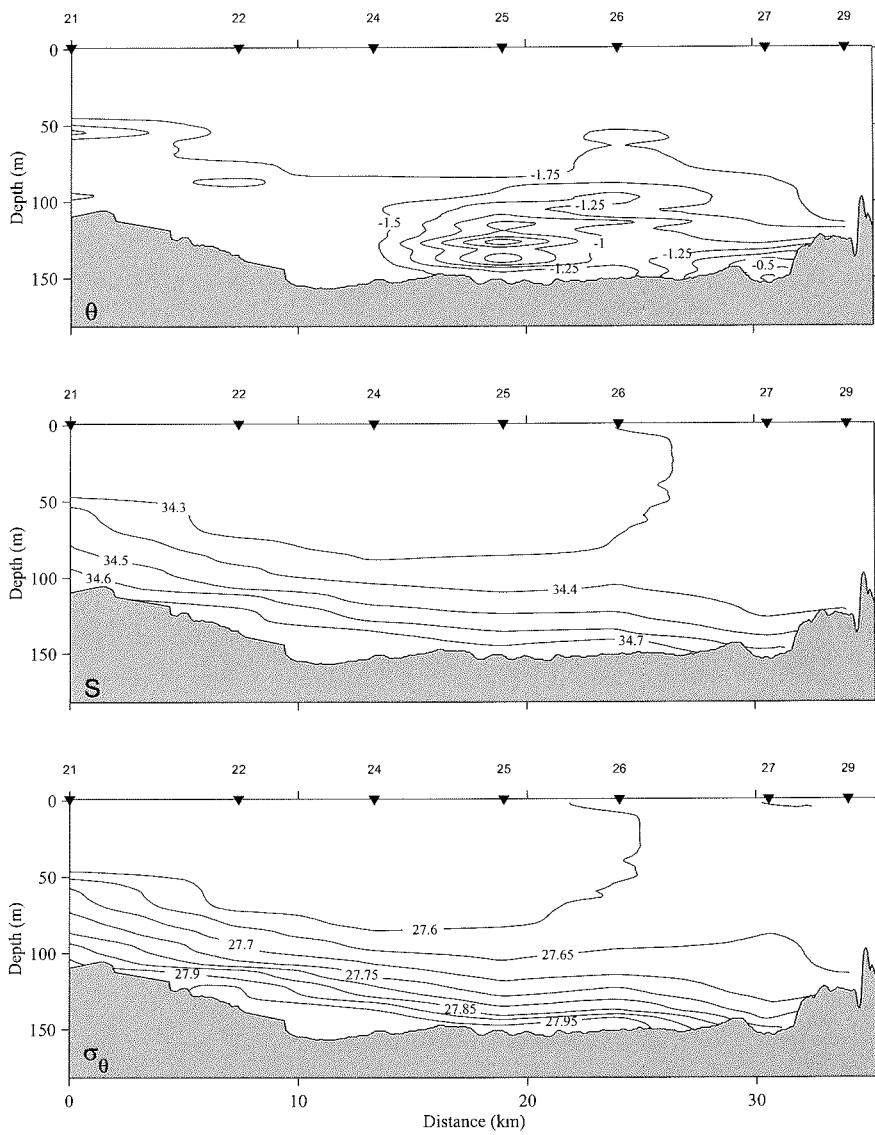


Figure 5.1.D. Same as Figure 5.1.B, but for section C. Here, isotherms are drawn every 0.25° C.

5. WATER MASSES AND CIRCULATION

WARPS Storfjord, Section D

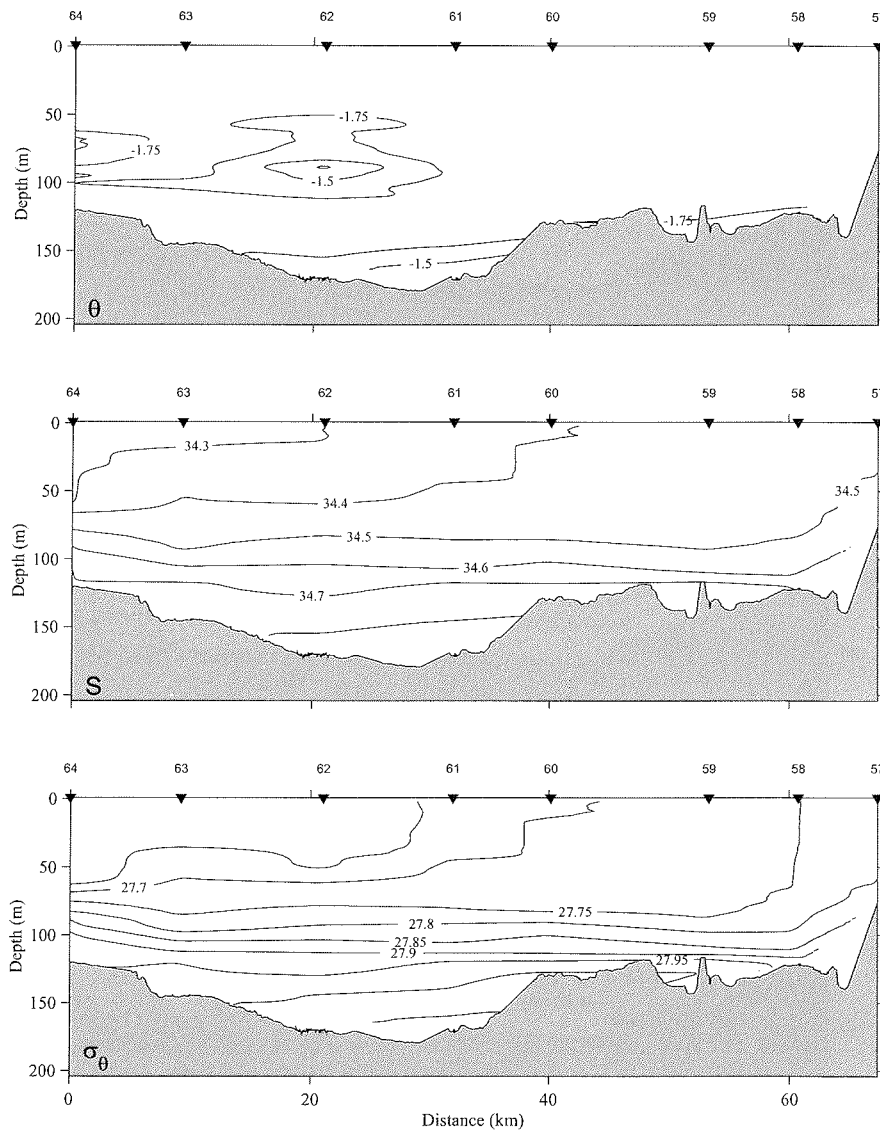


Figure 5.1.E. Same as Figure 5.1.B but for section D with 0.25°C contour intervals in θ .

Shelf convection in the western Barents Sea and Atlantic water north of Svalbard

WARPS Storfjord, Section E

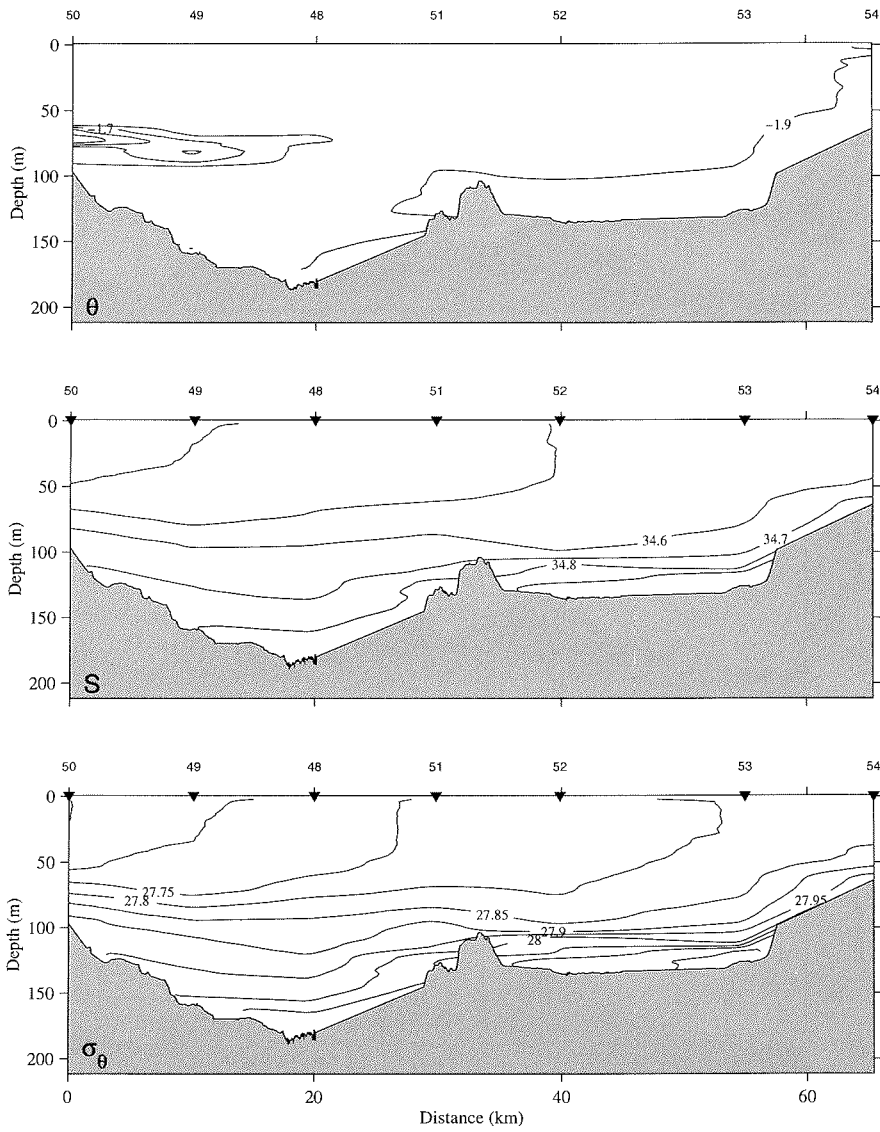


Figure 5.1.F. Same as Figure 5.2. B but for section E. Isotherms are every 0.1° C.

5. WATER MASSES AND CIRCULATION

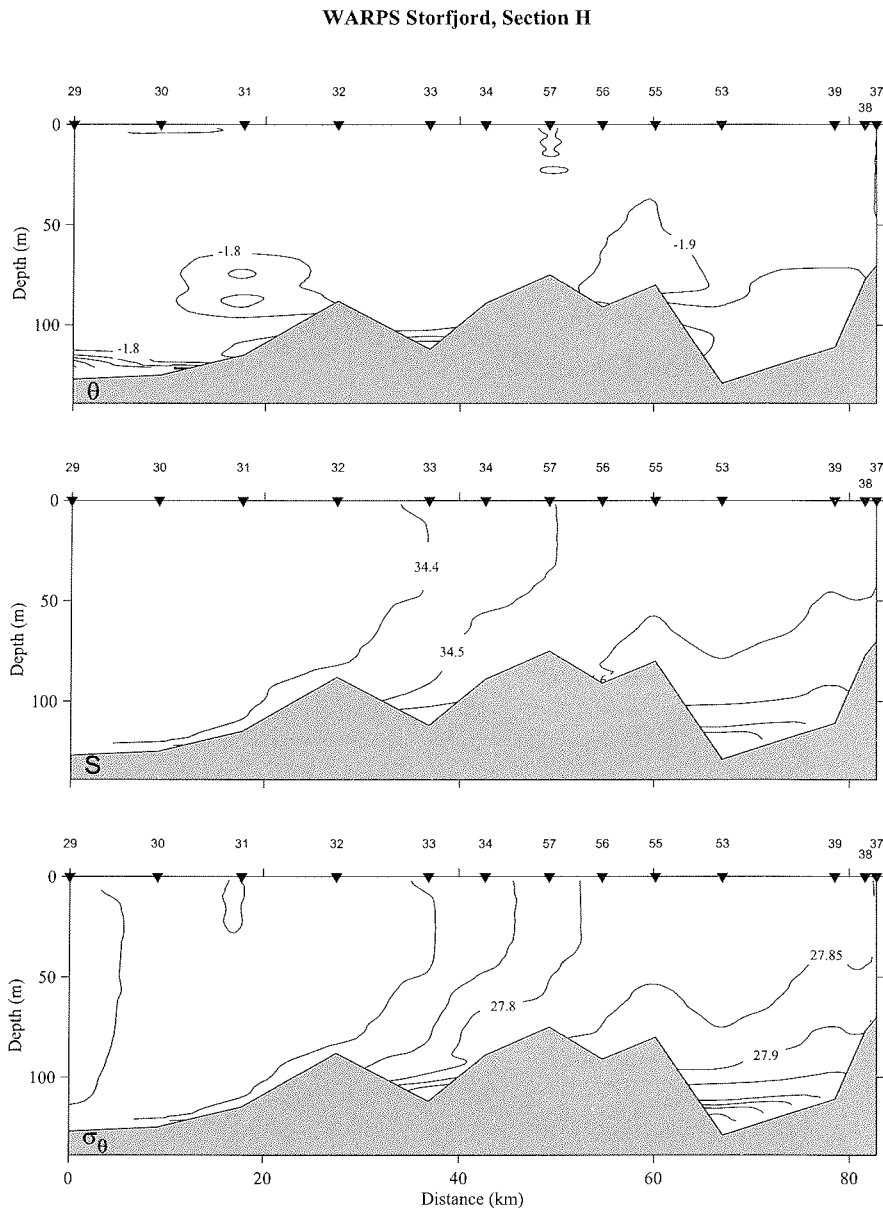


Figure 5.1.G. Same as Figure 5.1.B but for section H. Isotherms are every 0.1°C . Echo sounder derived bathymetry is not available for this section.

Shelf convection in the western Barents Sea and Atlantic water north of Svalbard

WARPS Storffjord, Section P

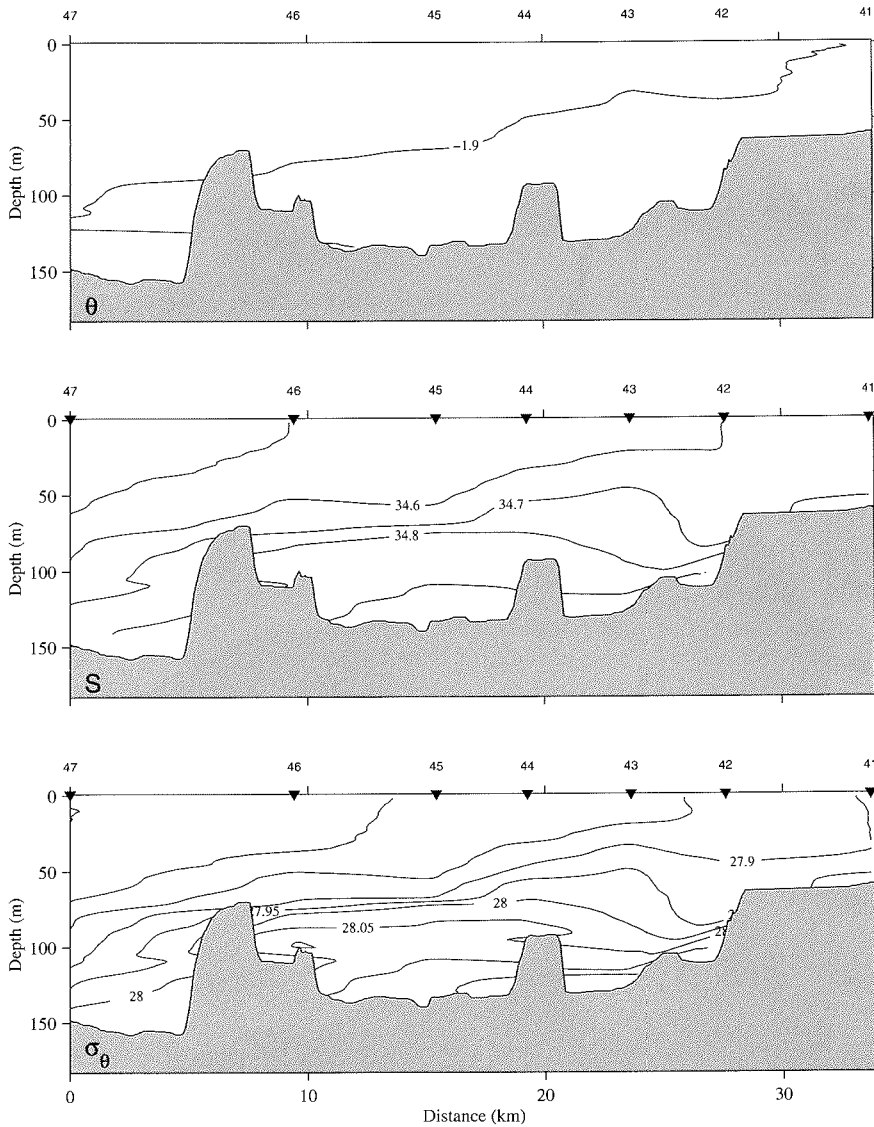


Figure 5.1.H. Same as Figure 5.1.B but for section P. Isotherms are every 0.1°

5. WATER MASSES AND CIRCULATION

WARPS Storfjord, Section I

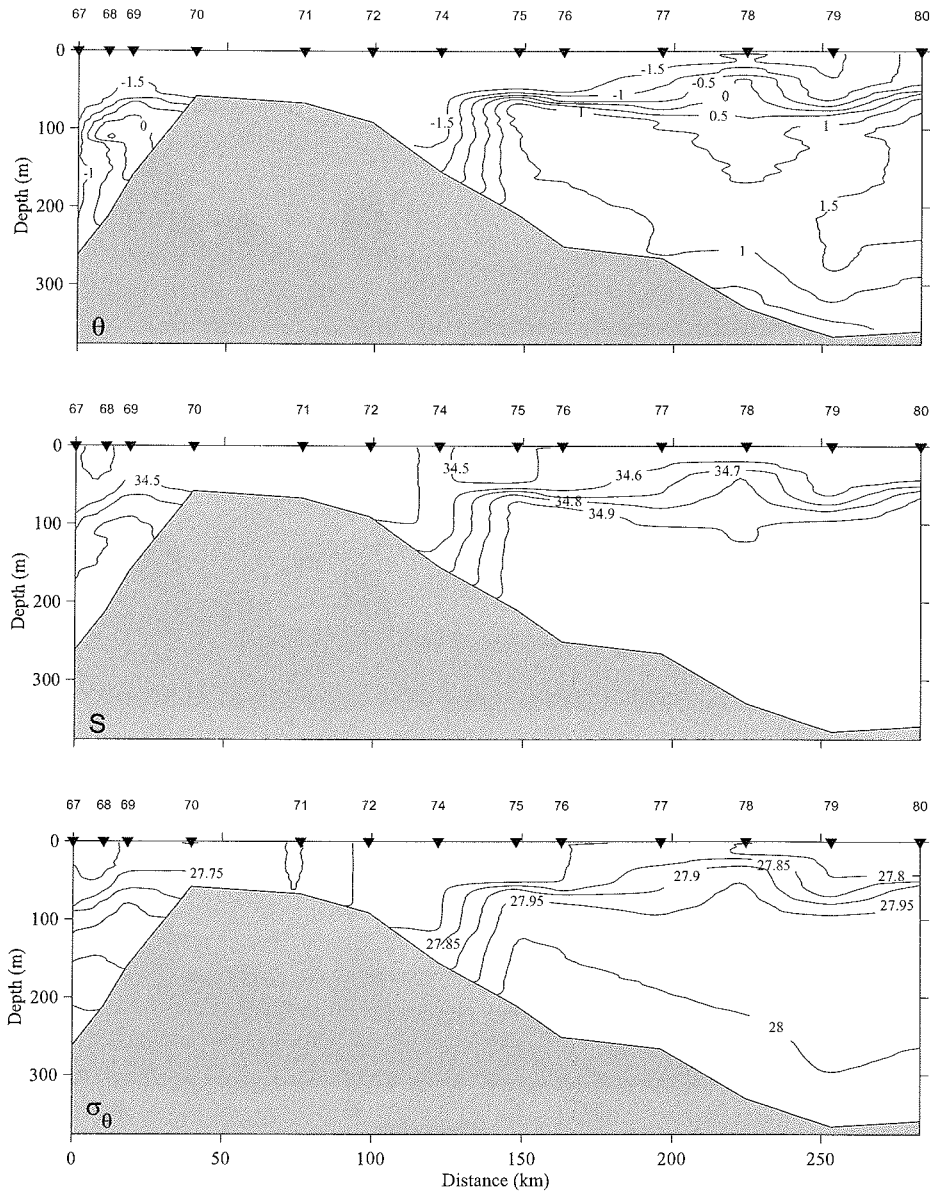


Figure 5.1.1. Same as Figure 5.1.B but for section I. Echo sounder derived bathymetry is not available for this section

Shelf convection in the western Barents Sea and Atlantic water north of Svalbard

OBSERVATIONS north and west of Svalbard

During the second part of WARPS three sections were obtained (Fig. 5.1.J): LT across Whalers Bay and Litke Trough, YP across the southern Yermak Plateau, and a very short section in the "Hausgarten" in Fram Strait (Chapter 6.10). Northerly winds had driven multi-year ice across the Whalers Bay and thereby closed the latent heat polynya for the period of our measurements. However, warm Atlantic water was upwelled near the shelf edge and led to rapid melting (Chapter 5.2). The 27.8-kg/m^3 -isopycnal rose from a depth of 160 m above the Yermak Plateau to 40 m above the shelf edge. While that would have allowed Atlantic Water to be mixed isopycnally to the surface layer and then losing heat to the atmosphere the salinity was not affected and was highest close to the shelf edge.

Consequently it was not too surprising that the warmest water was not found close to the shelf break, as it is typical during summer, but instead a core with temperatures exceeding 3.5°C was met in the center of Litke Trough (Fig. 5.1.K). This water stems from the offshore part of the West Spitsbergen Current which follows the isobaths of the deeper slope in Fram Strait and along the western rim of the Yermak Plateau. The core is visible in the section YP at station 123 (Fig. 5.1.L) although with lower temperature than in the Litke Trough. The branch turns eastward and flows through a gap of the Yermak Plateau which actually is not a plateau but a cliffy structured ridge. Accordingly, the Yermak Plateau branch seems, at least in winter, to form the main source of oceanic heat for the central Arctic Ocean.

5. WATER MASSES AND CIRCULATION

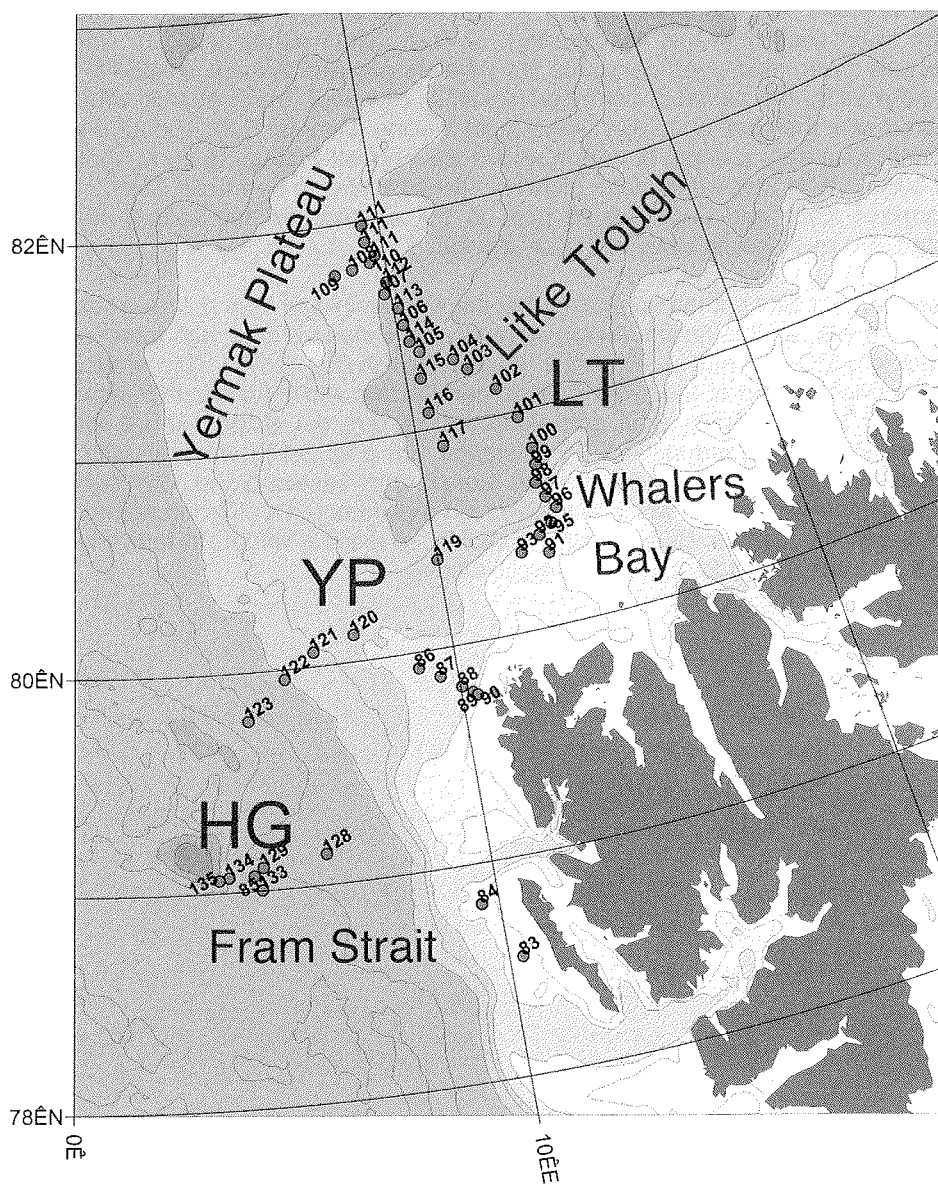


Fig. 5.1.J: Locations of CTD stations north and west of Svalbard

Shelf convection in the western Barents Sea and Atlantic water north of Svalbard

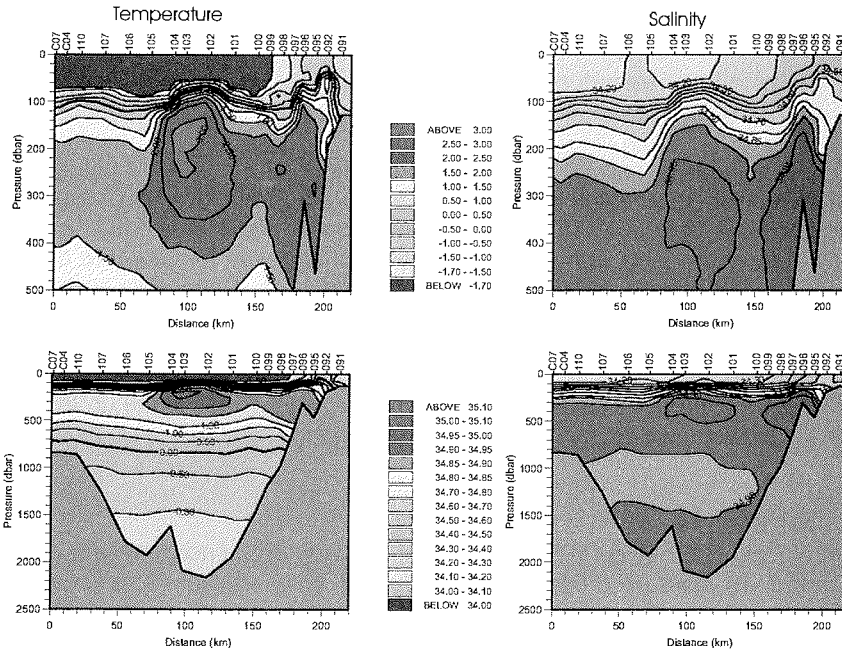


Fig. 5.1.K: Temperature and salinity distribution across Litke Trough in the upper 500 m (upper panels) and over the full water depth (lower panels).

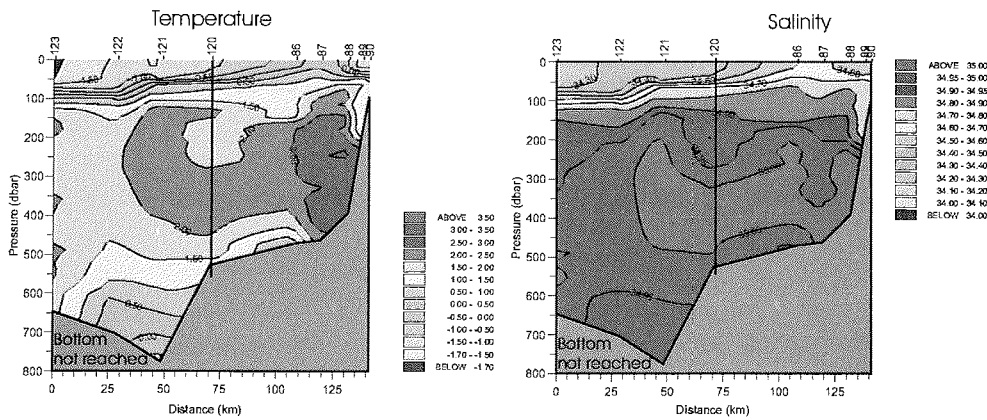


Fig. 5.1.L: Temperature and salinity distribution on the Yermak Plateau.

5. WATER MASSES AND CIRCULATION

5.2 Surface layer turbulence

Sirevaag (GIUB)

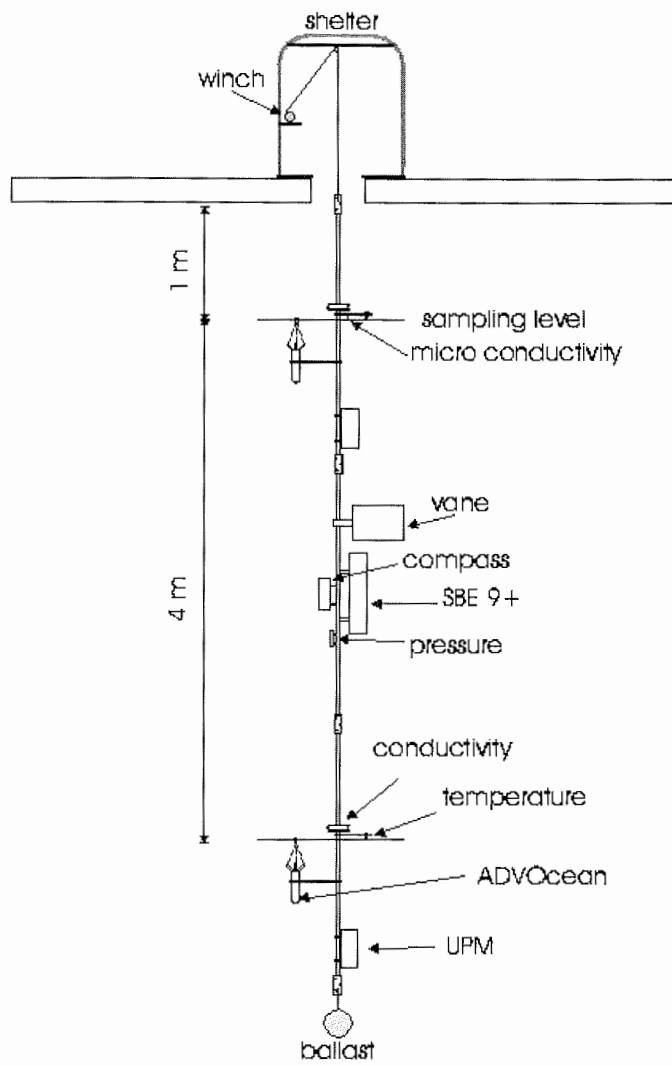
Growth and ablation of sea ice are major components of the surface energy balance for high latitude oceans. Each depends critically on the transfer of both heat and salt at the ice/ocean interface. At the molecular level, salt is much less diffusive than heat (by a factor of about 200), and since most of the changes in temperature and salinity occur across thin layers adjacent to the interface, it is reasonable to expect that double diffusive effects are sometimes important. A primary aim of the joint US/Norway investigations of air-ice-ocean interaction in frozen fjords is to determine plausible ranges of values for the exchange coefficients for heat and salt in bulk formulae. For this purpose mean quantities and turbulent fluxes in the underice boundary layer were measured by means of a turbulent mast.

5.2.1 Instruments

The turbulence mast (Fig. 5.2.A) consisted of two turbulence instrument clusters (TIC) placed 4m apart on a 6m-long vertical mast. Each cluster comprised a Sontek ADV Ocean 5Mhz acoustic Doppler current meter to measure 3-dimensional velocities together with sensitive temperature and conductivity sensors from Sea-Bird. One of the clusters was equipped with a Sea-Bird micro-conductivity sensor to measure rapid changes in salinity. Both ADV's were equipped with an under water processing unit (UPM) and all the data are processed through the SBE9+ to a deck unit on the ice and recorded on a laptop. A compass and a pressure sensor on the middle mast provides direction and right depth.

The mast was deployed by a hand winch through a hole in the ice, giving a stable platform for measurements under sea ice, approximately 200-300 m away from the ship to avoid disturbance from the hull of the ship.

Surface layer turbulence



5. WATER MASSES AND CIRCULATION

5.2.2 Measurements

The mast was deployed at 5 different ice stations: the three first were in fjord conditions in Storfjorden, the fourth in Whaler's Bay north of Spitsbergen while the fifth (C) was a long drift station around 82°N 9°E (Table 1). Some minor technical problems arose every now and then and growing experience during the cruise are reasons for some of the differences in file durations.

At station 4 and station C ice cores were taken to measure temperature and salinity gradients in the ice to compare with heat and salinity fluxes measured under the ice.

Table 1. Stations.

Station	Internal no	position	record length (hours)
28	# 1	76°49'N20°50'E	8
39	# 2	77°32'N20°19'E	8.5
70	# 3	76°17'N23°15'E	4.2
93	# 4	80°25'N12°47'E	13.8
111	# C	81°50'N20°E	133

During the stations in Storfjord (1, 2, 3) and station C, the mixed layer was at the freezing point and downward salt fluxes were measured because of ice formation. Horizontal velocities were in the range 6 to 8 cm/s. One example of vertical heat flux calculated from data obtained on station 2 is shown in figure 5.2.B. The calculations are preliminary since processing will be continued after the cruise. In contrast, at station 4, rapid melting conditions were encountered above the warm Atlantic Water entering the Arctic Ocean along the shelf edge.

Preliminary results of station 2 in Storfjord are shown in Fig. 5.2.B. Calculations at station 4 show heat fluxes to be about 50-100 times larger than at station 2 due to higher temperatures in and below the mixed layer of only approximately 30m depth and higher current velocities close to the ice.

Technetium measurements

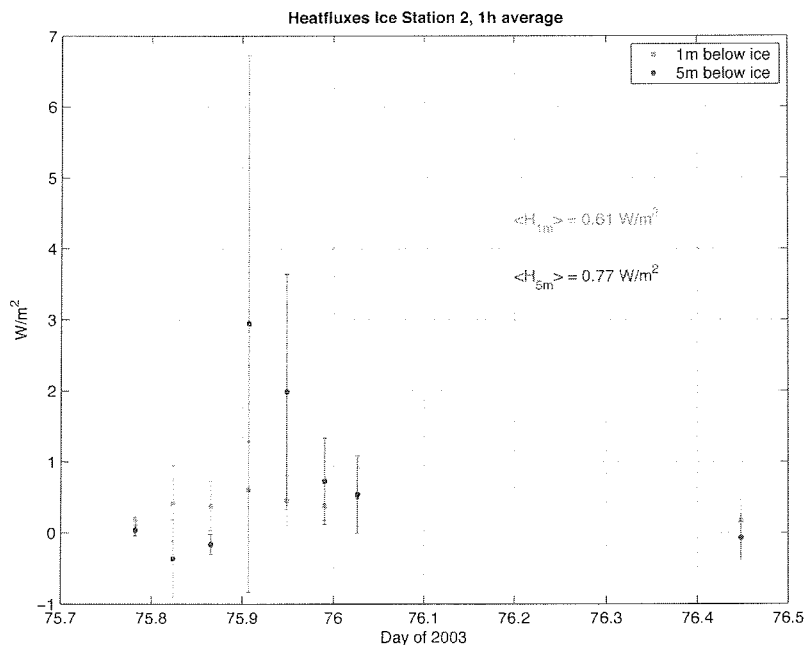


Figure 5.2.B Calculated vertical heat fluxes from ice station 2

5.3. Technetium measurements Karcher (AWI)

Technetium, ⁹⁹Tc, is a highly soluble, beta-emitting man-made radionuclide. The main sources of ⁹⁹Tc are global fallout from nuclear weapons testing and discharges from reprocessing plants for spent nuclear fuel in north-western Europe. Radioactive wastes have been discharged from the reprocessing plants at Sellafield (UK) into the Irish Sea and at La Hague (France) into the English Channel since 1952 and 1966 respectively. The discharges from Sellafield increased in the first quarter of 1994 when a new waste treatment plant, the Enhanced Actinide Removal Plant (EARP), began operation. EARP reduces the discharges of plutonium and americium, allowing the processing of stored Medium Active Concentrate (MAC), but does not significantly remove ⁹⁹Tc. Due to the increased throughput of material for treatment the quantities released of this radionuclide have increased greatly since the commencement of EARP.

⁹⁹Tc behaves conservatively in seawater and is transported from the Irish Sea into the North Sea via the Scottish Coastal Current, which eventually merges with water flowing through the English Channel, labeled with radionuclides from the French nuclear reprocessing plant at La Hague, in Danish waters near the entrance of the Skagerrak. This water becomes incorporated with the Baltic Sea outflow and forms the Norwegian Coastal Current (NwCC). Atlantic Water (AW) of the North Atlantic

Current (NAC) - which has crossed the gaps between Iceland, Faeroes and Scotland from the North Atlantic into the Nordic Seas - continues northward as the Norwegian Atlantic Current (NwAC), and its eastern branch runs parallel to the NwCC. It progressively mixes with the NwCC bearing the radiotracer signal. Near the northernmost end of the Norwegian coast at the western boundary of the Barents Sea (~ 70°N) the NwAC splits into two currents: the northwards flowing West Spitsbergen Current (WSC) and the eastwards flowing North Cape Current (NCC). At present, ⁹⁹Tc can be detected along the NwCC and further north, for example in the Barents Sea and in the WSC, a pattern that was observed in earlier years for ¹³⁷Cs following enhanced discharges of this radionuclide in the 1970s.

The measurements of ⁹⁹Tc have the purpose to monitor the spreading of the 1990s peak of this radionuclide with the Atlantic derived water masses in the Nordic Seas and into the Arctic Ocean. They are a contribution to the project RADNOR (Radioactive dose assessment improvements for the Nordic marine environment: Evaluation of realistic pathways for potential radionuclide releases) and will be used for the validation and improvement of the NRPA box model for radioactive dose assessment and the coupled ice-ocean circulation model NAOSIM of the Alfred Wegener Institute.

Due to the limited analysis capacity only 10 samples could be taken during the cruise. The sampling strategy followed the idea to reveal the basic horizontal structure of ⁹⁹Tc north of Svalbard while at the same time to distinguish between Atlantic Water entering the Arctic with the WSC and Polar surface water which overlays the Atlantic Water while moving south. This made it necessary to sample at the surface and at about 200 m depth. The 10 samples (40 bottles of 25 l each) collected on board are shipped to the NRPA laboratories in Oslo and analysed there.

6. BIOLOGY IN THE SEA-ICE, IN THE WATER COLUMN AND AT THE SEA FLOOR

6.1 Arctic sea-ice biology in winter

Kiko, Scheltz, Schünemann, Werner (IPÖ)

During this cruise measurements of chemical, physical and biological properties in and under different types of pack ice in winter have been conducted. The results will complement our already available data from other seasons. Virtually nothing has been known yet about the abiotic and biotic conditions, e.g. the availability of food sources, in Arctic sea ice of this region in winter, although most of the sympagic species have been believed to live in the ice year-round. Our measurements characterize the ice environment of different ice types and thicknesses in respect to salinity, temperature, inorganic nutrients (PO₄, NH₄, SiO₂) and organic carbon (POC) in the ice and the under-ice water layer. Biological investigations included samples for the determination of species diversity, distribution, abundance and biomass of sympagic (=ice-associated) bacteria, algae and metazoans.

Complete sampling programmes were carried out on three long ice stations in the Storfjorden-Barents Sea area (12.3., 17.3., 23.3.), on one ice station in the West Spitsbergen Current (1.4.), and during the ice-drift station north of Spitsbergen (7.4.–16.4.). This 10-day-station was also used for a study of the spatial and temporal variability of biological sea-ice properties (algal biomass, abundance of organisms).

The Arctic sea-ice environment in winter

The brine channel system of Arctic pack ice is inhabited by the specialized sympagic community. Bacteria, algae, protozoans and metazoans build up a complex food web within this system, which is so far poorly understood. Our biological investigations concentrated on the qualitative and quantitative determination of the meiofaunal community (here: metazoans > 20µm) which will be set into relation to other parameters like salinity, temperature, chlorophyll a content, nutrients and volume of the brine channel system. During the cruise ARK XIX-1 a total of roughly 160 ice cores for biological investigations were drilled at 14 ship- and helicopter-based stations as well as during the ice-drift-station. Ice cores were taken with a SIPRE ice corer (7.5 cm diameter), and temperatures were measured every 5 to 15 cm with a digital thermometer inside the cores immediately after drilling. The same cores were then cut into 1 to 20 cm segments and, after melting in the dark at 4 °C, analysed for salinity, chlorophyll a and phaeopigment contents. Additional ice cores were taken for measurements of inorganic nutrients as well as for the study of species diversity, abundance and biomass of ice algae and heterotrophic protists, which will be conducted by our Finnish cooperation partners (FIMR). For investigations on sea-ice meiofauna three cores were drilled at the same site and cut into 1 to 20 cm segments. These segments were melted in an excess of 0.2 µm filtered sea water in order to avoid osmotic stress to the organisms. After complete melting, the samples were concentrated over a 20 µm sieve and fixed with Bouin's solution (4% final concentration). They will be used for meiofauna investigations (abundances, biomass) and taxonomic studies in the home laboratories. In order to estimate the bacterial concentration subsamples were taken and stained with DAPI. All subsamples were filtered on polycarbonate filters and frozen at –30 °C. Determination of total bacterial numbers will be conducted at home by using epifluorescence microscopical techniques. Furthermore numerous ice undersides were melted and sorted for meiofauna organisms. During the ice-drift-station several cores were taken in order to gain information about the presumably patchy distribution of sympagic meiofauna organisms within one floe.

All temperature measurements in the ice showed similar profiles with lowest temperatures down to - 21 °C at the upper part of the cores and highest values up to –2,5 °C at the lower surface (Fig. 6.1.1H). These temperature profiles are typical for the winter situation within Arctic sea ice. Together with the resulting high brine salinities and small brine volumes, the sea ice therefore represent an extreme habitat during winter. Algal biomass was always very low and did rarely exceed values of 1 µg l⁻¹ (Fig.6.1.2H) indicating no or just beginning primary production in the ice at the end of the study period. However, concentrations in the ice were still one order of magnitude higher than in the underlying water column. All ice cores inspected for meiofauna organisms already onboard showed extremely low abundances. Only single nematods, rotifers and nauplii were observed. This result, which is significantly

6. BIOLOGY IN THE SEA-ICE, IN THE WATER COLUMN AND AT THE SEA FLOOR

different from summer observations, seems to be typical for the winter situation within the Arctic sea ice.

The Arctic under-ice environment in winter

The boundary layer between sea ice and the water column is a unique habitat with special abiotic (e.g. temperature, salinity) and biotic (e.g. food resources) factors, which also vary with season and region. This habitat is colonized by (1) autochthonous under-ice amphipods (*Apherusa glacialis*, *Onisimus* spp., *Gammarus wilkitzkii*), which live directly at the ice underside and complete their entire life-cycle here, and (2) allochthonous sub-ice fauna, means organisms originating either from the ice interior or the pelagic realm, which are found in this boundary layer temporarily, e.g. for feeding or during certain life stages. Aim of this winter cruise was to characterize the environmental conditions of this habitat in winter, and to study the seasonal dynamics and adaptations of the under-ice fauna.

For this purpose, under-ice video, under-ice pumps, several nets and probes were deployed. Life amphipods for experiments (respiration-, excretion rates) were additionally collected from zooplankton nets and baited traps deployed from ice floes. Temperature and salinity profiles were measured in the first 5 metres below the ice on all ice stations (Fig. 6.1.3H). In the Storfjorden-Barents Sea area, the under-ice water was always at the freezing point (e.g. stn 76) representing the expected winter condition, whereas the temperature below the ice in the West Spitsbergen Current (stn 91) was clearly warmer, indicating melting at the ice underside. This observation can be supported from the under-ice video images at this station which showed an ice underside structured like a typical summer floe, with smooth undulations, bulges and depressions. In the under-ice water below the drift-ice-station (e.g. stn 106), a slight stratification in the uppermost metre was observed (Fig. 6.1.3H), however probably not pronounced enough to indicate melting conditions here.

Regarding algal biomass, which is a major food source for many organisms in the under-ice habitat, the expected winter situation with very low values was found. Concentrations of chlorophyll a in the under-ice water were very low everywhere (0.02–0.05 µg l⁻¹). In the lowermost 2 cm of the ice, which is also a feeding ground for the under-ice fauna, concentrations ranged between 0.60–1.02 µg l⁻¹ (Storfjorden), 0.13 µg l⁻¹ (West Spitsbergen Current), and 0.15–3.37 µg l⁻¹ (drift-ice-station), with the higher values occurring to the end of the sampling period. This may indicate the begin of the ice-algal spring bloom, although no significant snow melt had commenced yet.

All four species of the autochthonous under-ice amphipods *Apherusa glacialis*, *Onisimus glacialis*, *O. nanseni* and *Gammarus wilkitzkii* occurred below the ice in all study areas during the cruise. This is the first record of *A. glacialis* and *O. glacialis* in this region in winter, proofing the assumption that these species live in the under-ice habitat year-round. Abundances will be determined by analysis of under-ice video recordings, first estimations point to values not different from summer. The question of how the amphipods survive the winter with limited food sources will be solved by biochemical analysis of lipid content and lipid classes. The hypothesis is that the more herbivorous species (*A. glacialis*, *O. glacialis*) thrive on high amounts of storage lipids which have been accumulated during the summer feeding period. The predominantly omnivorous-carnivorous species *O. nanseni* and *G. wilkitzkii* are most probably feeding on zooplankton and detritus also during winter, as indicated by

faecal pellet production of the collected animals. One egg-bearing female *G. wilkitzkii* was caught, from which 20 juveniles of 2-3 mm length hatched during rearing onboard. At one ice station over shallow water (50 m depth) in Storfjorden, high concentrations of a benthic amphipod (species unknown) were observed directly below the ice. Specimens of this amphipod were recorded on the under-ice video and caught by the under-ice pump but above all by a baited trap (33 individuals) deployed at the ice underside. Determination of gut contents and lipid composition will hopefully show whether these amphipods have been feeding from ice-produced food sources, pointing to the very interesting process of benthos-sympagic coupling. Respiration measurements which have been successfully conducted with all four species of under-ice amphipods as well as with this benthic species will give some insights in the metabolic activity during winter as compared to already available summer data. Altogether, these studies will deliver new information on the overwintering strategies of the Arctic under-ice amphipods.

First inspections of the sub-ice fauna suspended in the water layer directly below the ice (0–5 m depth) showed a very reduced species diversity as compared to other seasons. Mainly small copepods (*Oithona* simil *Pseudocalanus* spp.) were observed as well as copepod nauplii. Both, typical representatives of the larger epipelagic mesozooplankton (*Calanus* spp.) and of the sympagic copepod species (*Halectinosoma* spp., *Cyclopina schneiderii*, *Tisbe* spp.) which occur in this habitat in summer and autumn, seem to be absent or present only in low numbers in this habitat during winter. Later analysis of species and stage composition in the quantitative under-ice pump samples will deliver a more thorough view of the winter composition in this community and, in comparison with existing data from spring, summer and autumn, on the seasonal dynamics of the respective species.

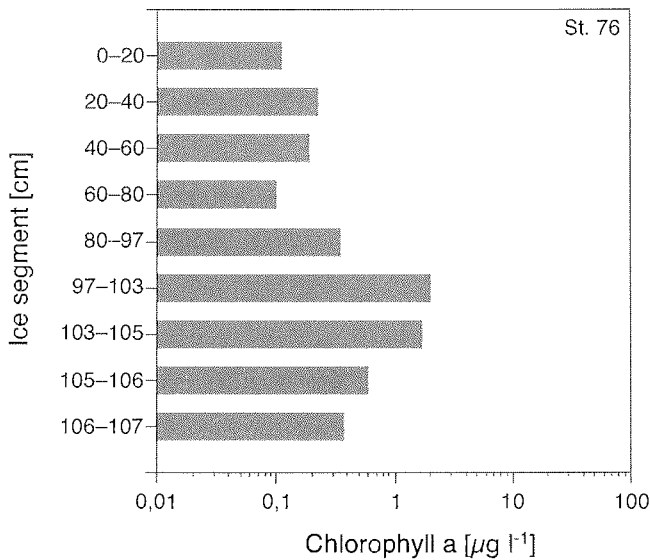


Fig. 6.1.1H: Temperature profile inside the ice at station 76 (Station number = day of the year 2003).

6. BIOLOGY IN THE SEA-ICE, IN THE WATER COLUMN AND AT THE SEA FLOOR

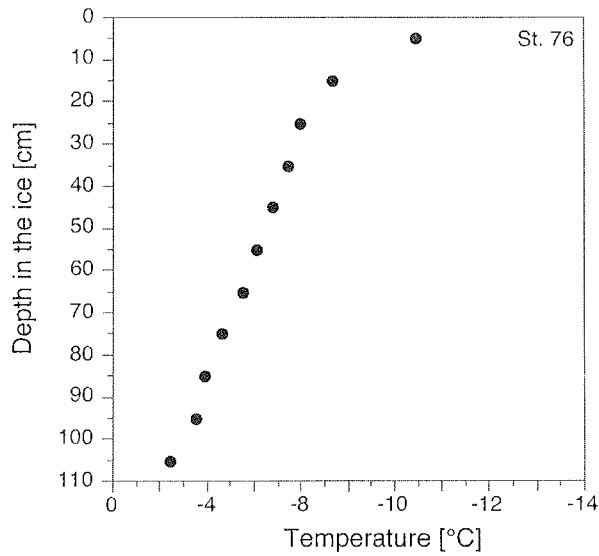


Fig. 6.2.2H: Chlorophyll a profile inside the ice at station 76 (Station number = day of the year 2003)

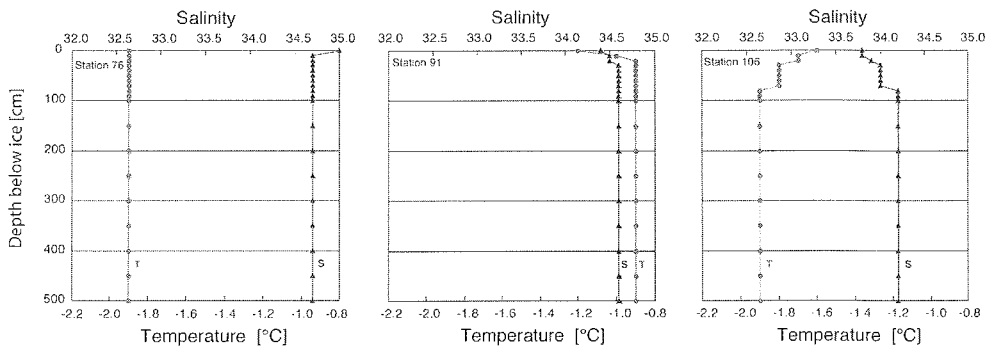


Fig.6.1.3H: Temperature and salinity profiles in the under-ice water (0–5 m depth, starting at the ice underside) in Storfjorden (station 76), in the West Spitsbergeb Current (station 91) and at the ice-drift-station (station 106). Station numbers = days of the year 2003

6.2 Cryo-pelagic coupling in Arctic winter

Auel (UB)

Cryo-pelagic coupling processes were studied under winter conditions (i) in Storfjorden, (ii) in permanent multi-year ice over the Yermak Plateau (central Arctic Ocean), and (iii) in the Marginal Ice Zone of Fram Strait.

A total of 16 multiple opening/closing net hauls (Multinet, mesh size 150 μm) were conducted during the cruise. Most hauls covered the upper 100 m of the water column in high resolution (100-75-50-25-10-0 m). In Storfjorden Multinet samples were collected down to the seafloor. Sampling concentrated on two sections: One transect including five stations from the southern entrance of Storfjorden northward into the central basin of the fjord. Another major section started in heavy multi-year ice at ice station "Tomato Island" on the Yermak Plateau (81° 59' N) and crossed the Marginal Ice Zone on its way southward via seven stations. In addition, Multinet samples were collected at every ice station for comparison to the pelagic under-ice fauna sampled by an under-ice pumping system at the ice/water interface and at five metres depth below the ice. The AWI "Hausgarten" area was sampled twice during the cruise, on March 30th and on April 21st/22nd in order to study the transition from late winter to spring. Strong changes in the vertical distribution of the dominant copepod *Calanus hyperboreus* were observed within these three weeks.

Larger and more mobile species, especially the hyperiid amphipods *Themisto libellula* and *T. abyssorum* were sampled by Rectangular Midwater Trawl (RMT 8, mouth opening: 8 m², mesh size: 4.5 mm) at four stations. Usually, RMT 8 hauls covered the upper 30 m of the water column, since we were interested in the diet composition of little auks and this is the maximum diving depth of this seabird species. In the "Hausgarten" (strn. 124) two successive RMT 8 hauls were collected: one shallow and one 200 m deep.

The zooplankton community in Storfjorden was dominated by polar species, including the copepods *Calanus glacialis* and *Pareuchaeta glacialis*, the amphipod *Themisto libellula* and the pteropods *Clione limacina* and *Limacina helicina*. These indicator species showed that Arctic water masses originating from the northern Barents Sea and East Spitsbergen Current predominated in Storfjorden during the study period. This observation is in contrast to previous studies which showed that at other times species of Atlantic origin, such as *Calanus finmarchicus*, *Pareuchaeta norvegica* and *Themisto abyssorum*, are imported into Storfjorden by a branch of the warm West Spitsbergen Current. The zooplankton community of Storfjorden is apparently very variable and subject to dynamic changes depending on the hydrographic regime. Many females of *T. libellula* caught in Storfjorden carried hatchlings in their brood pouches. Some females released their offspring within a few days after the sampling, and juvenile *T. libellula* of 2-3 mm body length were collected frequently in surface waters during the second half of the expedition. These findings confirm the already established theory that this amphipod species reproduces in winter.

6. BIOLOGY IN THE SEA-ICE, IN THE WATER COLUMN AND AT THE SEA FLOOR

The abundance and distribution pattern of seabirds were studied by standardised sighting intervals of 10 min duration from the bridge. In comparison to previous summer cruises seabird abundance in the investigation area was rather low. Especially in the central part of Storfjorden and during the long-term ice station over the Yermak Plateau only few birds were sighted. Higher abundances of black guillemots, Brünnich's guillemots and little auks, as well as ivory gulls occurred in the marginal ice zone of Fram Strait during the end of the cruise. Little auks were the most abundant seabirds in this region.

Seal sightings were recorded during the seabird survey and during several helicopter flights. Ringed seals were spotted regularly in northern Storfjorden and over the Yermak Plateau. Walrus were present in the shallow areas of northern Storfjorden and close to Mofen island. In contrast to previous cruises in summer and autumn, no seals were sighted in the Marginal Ice Zone of Fram Strait. During other seasons highest concentrations of harp and hooded seals were recorded in this region. One possible explanation for the low seal abundance in this area during the present cruise is that adult individuals of both species gather on the breeding grounds near Jan Mayen during this time of the year. In addition, poor visibility due to sea smoke and strong winds during the only short passage through the Marginal Ice Zone of Fram Strait at the end of the cruise may have contributed to low sighting frequencies in this area.

Narwhals and bowhead whales were sighted several times in open leads in the northern part of the investigation area. They seemed to follow open leads northward and penetrated far into areas permanently covered by heavy sea ice. In one of the leads an adult white whale was seen together with a calf.

Table 1: List of stations with plankton nets.

Station	Date	Time [UTC]	Position Lat.	Position Lon.	Bottom depth [m]	Net type	Max. sampling depth [m]
15	08.03.	20:28	76° 38.12' N	20° 9.48' E	209	Multine	195
28	12.03.	14:00	76° 48.19' N	20° 14.89' E	176	Multine	150
36	16.03.	04:34	77° 29.08' N	20° 16.09' E	125	RMT 8	31
39	17.03.	01:47	77° 32.01' N	20° 18.94' E	111	Multine	100
48	18.03.	07:02	77° 29.90' N	19° 8.84' E	189	Multine	165
62	19.03.	21:19	77° 12.00' N	19° 16.26' E	178	Multine	160
85	30.03.	16:55	79° 3.93' N	4° 17.86' E	2409	Bonqo	1500
85	30.03.	13:00	79° 4.46' N	4° 19.31' E	2338	Multine	2300
85	30.03.	18:43	79° 2.38' N	4° 17.97' E	2540	RMT 8	33
93	02.04.	10:07	80° 21.45' N	12° 14.90' E	184	Multine	173
105	04.04.	10:56	81° 20.89' N	10° 32.21' E	1940	Multine	100
111	08.04.	10:37	81° 58.89' N	9° 25.51' E	840	Multine	100
112	18.04.	16:51	81° 41.96' N	9° 55.37' E	1208	Multine	100
114	19.04.	01:24	81° 25.06' N	10° 18.81' E	1836	Multine	100
115	19.04.	13:14	81° 16.35' N	10° 39.48' E	2028	RMT 8	31
116	19.04.	23:44	81° 4.66' N	10° 27.13' E	1968	Multine	100
118	20.04.	03:20	80° 44.50' N	10° 22.34' E	1415	Multine	100
119	20.04.	10:10	80° 24.69' N	10° 0.43' E	700	Multine	100
120	20.04.	21:27	80° 7.30' N	7° 26.15' E	542	Multine	100

Reproductive biology of calanoid copepods

Station	Date	Time [UTC]	Position Lat.	Position Lon.	Bottom depth [m]	Net type	Max. sampling depth [m]
124	21.04.	14:10	79° 4.21' N	4° 14.99' E	2406	RMT 8	31
124	21.04.	14:41	79° 4.58' N	4° 11.06' E	2436	RMT 8	200
133	22.04.	13:43	78° 59.69' N	4° 27.52' E	2574	Multine	1500

6.3 Reproductive biology of calanoid copepods

Niehoff, Herrmann (AWI)

During ARK XIX/1, three long-term experiments of 2 –3 weeks were carried out focusing on the reproductive biology of the three copepod species, *Calanus finmarchicus*, *C. glacialis* and *C. hyperboreus*, which dominate the zooplankton communities of the northern seas. These copepods overwinter in great depths in a diapause. During late winter they ascend to the surface and start feeding. The winter-spring transition is an important period in the life cycle, however, our knowledge on the physiological processes during the onset of feeding and reproduction is limited.

In order to fill in these gaps, up to 1000 females of each species were sorted immediately after capture from Bongo net hauls taken vertically from 500m (*C. finmarchicus*, *C. glacialis*) or 1500m (*C. hyperboreus*) to the surface. *C. finmarchicus* females were placed in Plexiglas cylinders, suspended in beakers, with net false bottoms to separate females and eggs. *C. glacialis* and *C. hyperboreus* females were transferred in four 50 L containers. Half of the females were fed with algal suspension, the other half was kept in sea-water from below 100m without food. Every day, *C. finmarchicus* females were placed in fresh solutions and the eggs were counted. From each of the large containers, 24 female *C. glacialis* and *C. hyperboreus* were sorted daily and transferred to cell wells (25ml). Their egg production was monitored in 8h intervals in order to reduce the influence of cannibalism. Every 2 or 3 days, the gonad maturity of 24 to 48 females was determined and these females were deep frozen for later analysis of enzyme activity and carbon/nitrogen content. Once a week, 40 to 60 females were deep frozen for lipid analysis. At start and at the end of each of the three experiments, females were preserved in glutaraldehyde/paraformaldehyde buffered with sodium cacodylate (0.1 M) for histological examination of the oocytes. The biochemical and histological analysis will be performed later at the University of Bremen and at the AWI.

During the experiments, starving *C. finmarchicus* females spawned continuously at low rates (1-2 eggs female⁻¹ d⁻¹) whereas the egg production increased to maximum rates of up to 15 eggs female⁻¹ d⁻¹ within 24hrs in feeding females. Starving *C. glacialis* females laid eggs only occasionally. At feeding, egg production increased slowly within 11 d to approx. 20 eggs female⁻¹ d⁻¹. In both species, all feeding females were mature at the end of the experiment whereas the gonad stage of starving females did not change considerably. When *C. hyperboreus* females were captured for the experiment, they were still located in 1500-500m water depth where food is absent or scarce. At the beginning of the experiment, females produced large clutches of up to 323 eggs. Spawning frequency, however, was low, and over the

6. BIOLOGY IN THE SEA-ICE, IN THE WATER COLUMN AND AT THE SEA FLOOR

course of the experiment egg production decreased considerably. No difference, neither in egg production rate nor in gonad development stage, was apparent between starving and feeding females although the later ones ingested the algae provided as they produced 20-40 fecal pellets 1 d⁻¹.

6.4 The pelagic larvae of the invertebrate macrofauna in the Storfjorden and the adjacent Barents Sea Fetzer (AWI)

Introduction

Stability and dynamics of benthic invertebrate communities depend mainly on the recruitment of larvae and juveniles into the community. Only the permanent replacement of old individuals by young ones ensures the survival of a species within the group. For understanding the formation and the variability of benthic communities the understanding of the reproduction modes of bottom living animals is of high importance.

Most species in temperate areas reproduce via pelagic larvae since this ensures a wide distribution and a fast exploitation of new territories (see Fig. 6.4.A). Moreover the planktonic stages are able to enter the euphotic zone and directly utilise the primary production of the upper water layers. Since the pelagic stages are not provided by any energy reserves they very much depend on existing phytoplankton so the timing of their release by the adults is of major importance. Additionally they have to undergo metamorphosis from free-swimming larvae to ready-to-settle juveniles, which make them usually very slow developing.

The second mode of reproduction among benthic animals is to leave out a larval phase and directly produce postlarvae that look like small copies of their adults. Usually this animals of this reproduction type produce few, large, yolky eggs and very often show brooding of the eggs until the small ones hatch. These larvae are normally rather big and well developed when released from their eggs. Since they have no pelagic stage they usually settle in the vicinity of their adults. This ensures that the offspring is not drifted away by prevailing currents but makes it impossible for the species to occupy new favourable sites.

The period of primary production in the Arctic is limited to only a short time in summer, which constrains the feeding period for meroplankters enormously. This and the fact of a long development time needed for pelagic larvae lead to the suggestion that direct development is favoured in high latitudes.

Recent discoveries of an increasing quantity of pelagic larvae in Arctic and Antarctic waters created problems with this generalisation and shows how little is known on the ecology of meroplankton in high latitudes. Until now very little is known about the reproductive adaptation of benthic invertebrates with respect to the temperatures especially of arctic species.

The pelagic larvae of the invertebrate macrofauna in the Storfjorden and the adjacent Barents Sea

The aim of this study is to investigate the meroplankton composition and spatial distribution of benthic invertebrate larvae during late winter in Storfjorden and the adjacent Barents Sea.

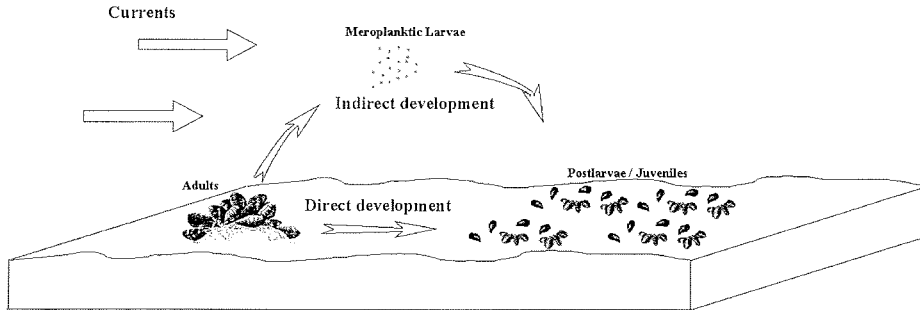


Figure 6.4.A: Reproduction modes of benthic invertebrates

Material and Methods

Larval plankton was collected with a Nansen Closing Net (NCN) with 55µm mesh size at a hauling speed of 0.3 m/sec at 11 Stations (Tab. 1). All those samples were sorted directly onboard since the identification is much enhanced in living material. For species that could not be identified properly digital image were taken with camera mounted to a microscope. To gather information about the spatial occurrence of the larvae in the water column additional Multinet (MN) samples were taken. At stations less 100m depth exclusively NN were taken. All samples were stored in 4% Borax buffered Formaline until further treatment in the laboratory.

Table 1: Overview of meroplankton sampling stations, date, station depth and gear used (MN=Multinet, NN=Nansen Closing Net)

Station	Date	Lat	Lon	Depth [m]	Gear	
006	06.03.03	75° 58.16' N	17° 1.01' E	326.2	MN	NN
015	08.03.03	76° 38.21' N	20° 7.33' E	211.1	MN	NN
025	11.03.03	76° 50.12' N	19° 43.62' E	165.8		NN
048	18.03.03	77° 29.90' N	19° 8.84' E	188.8	MN	NN
062	19.03.03	77° 11.91' N	19° 16.66' E	176.6	MN	
069	22.03.03	76° 23.20' N	22° 29.31' E	158.7	MN	NN
071	24.03.03	76° 10.11' N	24° 27.95' E	67.4		NN
072	24.03.03	76° 4.93' N	25° 19.24' E	94.9		NN
074	24.03.03	75° 59.54' N	26° 3.70' E	164.7	MN	NN
075	25.03.03	75° 54.79' N	26° 58.97' E	220.1	MN	NN
076	25.03.03	75° 52.69' N	27° 31.47' E	258.4	MN	NN

6. BIOLOGY IN THE SEA-ICE, IN THE WATER COLUMN AND AT THE SEA FLOOR

Results and Discussion

In the Nansen Net samples larvae of Gastropoda, Bryozoa, Polychaeta and Bivalves were present although in low numbers. In average about 5-7 individuals were found in each single catch. Larvae of Gastropoda were present at all stations (fig. 6.4.B). Here *Dendronotus* sp., a Nudibranchia, was the most numerous. But also the gastropod *Diaphana minuta* was found especially at the inner parts of the Storfjord. Of the Bivalva not more than one individual was found within a haul. They most probably belong to *Mya truncata* from which the adults are known to be abundant in this area and reproduce the whole year round. All of the found specimens were very small (~100µm) indicating that they have spawned only recently. Of Polychaeta only larvae of the spionid *Prionospio malmgreni* were present. Interestingly they were only present in the deeper parts of Spitsbergen Bank. Here either very young larvae (~300µm) with only three body segments were found or older much bigger ones having up to 18 segments and a size 1300µm were detected. Seemingly this two size classes belong to different releasing events.

Bryozoans (most probably *Membranipora pilorum*) were restricted to the inner Fjord parts and the deeper open Barents Sea.

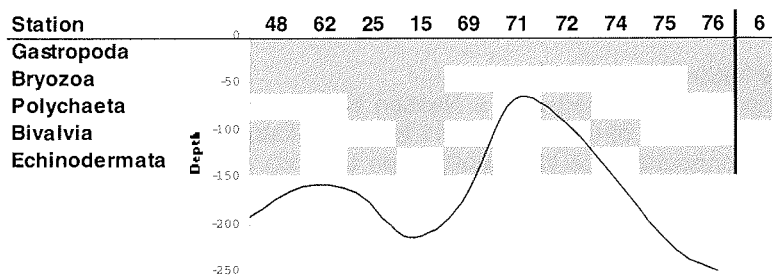


Fig. 6.4.B Presence of larvae of Gastropoda, Bryozoa, Polychaeta, Bivalvia and Echinodermata along a transect following from Station 48 within Storfjord south eastwards to the open Barents Sea. The thin line sketches the depth profile of the transect. Station 6 is excluded since it was located further south outside the transect

Of the Echinodermata rather big larvae of *Asterias* sp., the Common Sea star, were found within the Storfjord. Further outside they were exchanged by juvenile Ophiuroidea (Brittle Stars). They were already fully-grown and did not possess any larval features anymore. Most seemingly were ready to settle soon. Since they were already full developed they have been released by the adults already a long time ago. Of some species of this group it is known that the larvae stay in the water column for up to six months. In the most south-eastern stations of the Barents Sea very young individuals of Brittle Stars have been found, released recently. Only very few larvae were found at the shallow stations of Spitsbergen Bank where the depth were less than 70 meters. But probably here strong prevailing currents may be the causes for such low abundances. Coarse silt at the bottom indicates the presence of strong currents.

6.5 Ocean Optics Schwarz (AWI)

Aims

1a. No visible-wavelength spaceborne sensors, used for detecting algal biomass in surface waters, have sufficient spatial resolution to 'see' between ice floes, and no measurements at all are made during the Arctic winter since these sensors are passive, requiring sunlight. This means that attempts to calculate geochemical fluxes or fields from optical remote sensing data lack any input for the winter and early spring periods. The aim of the ocean optics work during the first leg of this cruise was to measure 'winter situation' optical properties in the surface waters of the Barents Sea, coastal waters of Svalbard and the Fram Strait. Where logistically possible, ice cores were requested from the IPÖ biology group for the measurement of pigment concentrations in the lower 10cm of the ice cores, as well as for taxonomy samples.

1b. The long ice drift station presented a good opportunity for more intensive sampling of ice algae pigments and taxonomy with little time restraint for gathering cores. The spring bloom was expected to begin during this leg of the cruise, and measurements of all optical parameters were planned in surface waters. If temperatures rose above -10°C , deployment of the Trios optical radiometers above the bridge was planned.

Measurements

Phytoplankton Pigments

Samples from the CTD bottles at 10 and $\sim 1.5\text{m}$ depth or from the flow-through supply were stored in opaque bottles. Occasional profiles were taken from the CTD at 0, 10, 20, 30, 50, 70 and 100m depth. Between 750ml and 8 litre aliquots were filtered through 25mm GF/F filters, which were blotted immediately after filtration was complete, and stored in a liquid nitrogen dewar in 2ml cryovials. Duplicate samples were stored in separate dewars. The samples were returned to Bremerhaven for analysis using HPLC.

Absorption by Phytoplankton Pigments

Samples were treated as for phytoplankton pigments. The filters were placed in 27mm diameter tissue capsules and stored in a liquid nitrogen dewar.

Absorption by Coloured, Dissolved Organic Matter and Dissolved Organic Carbon Concentrations.

Samples were collected as for phytoplankton pigments. Using a 'contact free' 47mm glass filtration unit (Sartorius), an initial 250ml aliquot of sample was filtered through a fresh 0.2 μm membrane filter and the sample collection flask rinsed and emptied. A second 250ml aliquot of sample was filtered and used firstly to rinse twice and then to fill a 50ml brown glass sample bottle. Samples were stored at 0°C in a darkened container. During leg 1b, samples were also collected for measurement of DOC concentrations. The filtration strategy was adjusted to include two full rinses of the

6. BIOLOGY IN THE SEA-ICE, IN THE WATER COLUMN AND AT THE SEA FLOOR

filtration equipment using 300 or 500ml of water, and 3 rinses of the sample bottles. DOC samples were stored at -10°C .

Concentration of Suspended Particulate Matter (Organic/Inorganic)

Samples were collected as for phytoplankton pigments. Between 1 and 15 litre aliquots were filtered through precombusted and weighed 47mm GF/F filters. After filtration, the filters were stored at -20°C .

Particle Size Distribution

Samples were collected as for phytoplankton pigments. Aliquots of 250ml were stored in brown glass bottles, conserved with Lugol's iodine, at room temperature.

Taxonomy

Samples were collected as for phytoplankton pigments. Aliquots of 100 or 250ml were preserved with Lugol's iodine and stored at 0°C . Some samples of neat, thawed ice cores were stored in 50ml brown glass bottles and preserved with Lugol's iodine.

All samples will be analysed at the home laboratory.

Station List.

Table 1 shows the stations at which samples were collected. An 'x' indicates a sample of a given parameter was taken. Abbreviations used:

- HPLC: high performance liquid chromatography, for phytoplankton pigment concentrations,
 APHY: absorption by phytoplankton pigments,
 ACDM: absorption by coloured, dissolved organic matter,
 DOC: concentration of dissolved, organic carbon,
 SPM: concentration of suspended, particulate matter (organic/inorganic),
 TAX: phytoplankton taxonomy,
 PSD: particle size distribution,
 POC: concentration of particulate, organic carbon.

Date	Station	Depth (m)	HPLC	APHY	ACDOM	DOC	SPM	TAX	PSD	POC
3.3.03	test	1	x							
		10	x							
		30	x							
		50	x							
6.3.03	5	2	x	x	x		x			
		10	x	x	x		x			
	7	10	x	x	x		x			
		240					x			x
		280					x			x
		308					x			x
8.3.03		Ice core	x							
9.3.03	16	1	x	x	x		x			
		10	x	x	x		x			
		102	x				x			x
		187	x				x			x

Ocean Optics

Date	Station	Depth (m)	HPLC	APHY	ACDOM	DOC	SPM	TAX	PSD	POC
		Ice core	x							
10.3.03	21	Ice core	x							
	22	120	x				x			x
12.3.03	28	Ice core	x					x		
14.3.03	30	1.5	x	x	x		x			x
15.3.03		Ice core	x				x			x
		Ice core			x			x		
16.3.03		Ice core	x				x			x
		Ice core			x			x		
17.3.03		Ice core	0-1cm	x				x		
			1-2cm	x				x		
			2-3cm	x				x		
			3-4cm	x				x		
			4-5cm	x				x		
			5-7cm	x				x		
			7-10cm	x				x		
		Water 0m below ice	x							
		Water 5m below ice	x							
	41	2	x	x	x		x	x	x	x
		58	x	x	x		x	x	x	
18.3.03	45	2	x	x	x		x	x	x	x
		35	x	x	x		x	x	x	x
		80	x		x		x	x	x	x
		131	x		x		x	x	x	x
	47	2	x	x			x	x	x	x
		101	x		x		x	x	x	x
		144	x		x		x	x	x	x
	49	131	x		x		x			x
		155	x		x		x	x	x	x
	52	1.5	x	x	x		x	x	x	x
		bottom	x		x		x	x	x	x
19.3.03	58	2	x	x	x		x	x	x	x
		10	x	x	x		x	x	x	
		120	x		x		x	x	x	x
	60	2	x	x	x		x	x		
		100	x		x		x	x		x
		129	x		x		x	x		x
	62	1.5	x	x	x		x	x		x
		Bottom	x		x		x	x		x
	64	1.7	x	x	x		x			
	65	1	x	x	x		x	x		
		100	x		x		x	x		x
		152	x		x		x	x		x
		Ice core	x					x		
	66	2	x	x	x		x	x		
		187	x		x		x	x		x
22.3.03	67	1.5	x	x	x		x	x		
		bottom	x		x		x	x		x
		Ice core 0-1cm	x					x		
		1-2cm	x					x		
		2-3cm	x					x		
		3-4cm	x					x		
		4-5cm	x					x		
		5-7cm	x					x		

6. BIOLOGY IN THE SEA-ICE, IN THE WATER COLUMN AND AT THE SEA FLOOR

Date	Station	Depth (m)	HPLC	APHY	ACDOM	DOC	SPM	TAX	PSD	POC
		7-10cm	x					x		
	69	1.5	x	x	x		x	x		
		36	x		x					
23.3.03	70	1.5	xxx	x		x	x			
	71	Ice core	x					x		
		Water 0m below ice	x							
		Water 5m below ice	x							
24.3.03	71	1.5	x		x			x		
	72	1.5	x		x			x		
		Ice core	x		x			x		
	74	1.5	x		x					
	75	1.5	x		x					
	76	1.5	x		x			x		
	78	1.5	x		x			x		
	79	1.5	x		x					
26.3.03	80	1.5	x		x			x		
		Surface snow								x
30.3.03	83	1.5	x		x		x	x		
	85	1.5	x		x		x	x		x
	86	1.5	x	x	x		x	x		
	87	1.5	x							
	88	1.5	x	x	x		x			
	89	1.4	x							
	90	1.5	x	x	x		x			
1.4.03	91	1.5	x	x	x		x	x		
	92	1.4	x							
	93	Ice core	x					x		
2.4.03		1.5	x		x		x			
3.4.03	95	1.5	x	x	x		x	x		
	96	1.5	x	x	x		x	x		x
	97	1.5	x	x	x		x	x		
	98	2	x	x	x		x			
	99	1.1	x	x	x		x	x		
		95.4	x		x		x	x		
	100	1.5	x	x	x		x	x		
4.4.03	101	1.5	x	x	x		x	x		
	103	1.5	x	x	x		x			
	105	1.4	x	x	x		x			
	107	2.2	x	x	x		x	x		
5.4.03	109	1.5	x	x	x		x	x		
	110	1.5	x	x	x		x	x		
	111	Drift Station:								
7.4.03		Subsurface snow					x			x
		Surface snow								x
	111-4	1.5	x	x	x	x	x	x		
8.4.03	111-7	1.5	x	x	x	x	x	x		
		9.9	x							
		19.9	x							
		30	x							
		40	x							
		50	x							
		70	x							
		100	x							
		0m below ice	x							

Ocean Optics

Date	Station	Depth (m)	HPLC	APHY	ACDOM	DOC	SPM	TAX	PSD	POC
		5m below ice	x							
		Ice core	x					x		
9.4.03	111-8	1.5	x	x	x	x	x	x		
10.4.03		Ice core	x							
11.4.03		Subsurface snow					x			x
		10.7m flow-thru	x	x	x	x	x			
16.4.03		Snow: 8-13cm								x
		Snow: 13-18cm								x
17.4.03		10.7m flo-thru	x	x	x	x	x	x		
18.4.03	112	1.5	x	x	x	x	x	x		
		10	x							
		20	x							
		30	x							
		50	x							
		70	x							
		100	x							
19.4.03	114	1.5	x	x	x	x	x	x		
		10	x							
		20	x							
		30	x							
		50	x							
		70	x							
		100	x							
	116	1.5	x	x	x	x	x	x		
20.4.03	119	1.5	x	x	x	x	x	x		
		10	x							
		20	x							
		30	x							
		50	x							
		70	x							
		100	x							
	120	1.5	x	x	x	x	x	x		x
21.4.03	128	1.5	x	x	x	x	x	x		x
		10	x							
		20	x							
		30	x							
		50	x							
		70	x							
		100	x							
22.4.03	129	1.5	x	x	x	x	x	x		
	133	1.5	x	x	x	x	x	x		x
		10	x							
		20	x							
		30	x							
		50	x							
	134	1.5	x	x	x	x	x	x		x
		10	x							
		30	x							
	135	1.5	x	x	x	x	x	x		x
		10	x							
		20	x							

6. BIOLOGY IN THE SEA-ICE, IN THE WATER COLUMN AND AT THE SEA FLOOR

6.6 Ecophysiology

Sartoris (AWI)

In the extremely cold waters of the polar regions, where temperature ranges between 0 and -1.9 °C with only little seasonal variation, crustaceans with low extra cellular magnesium levels ($[Mg^{2+}]_e$) like the natant decapoda, amphipoda and isopoda dominate in the crustacean fauna. The capacity to regulate extra cellular magnesium concentrations is likely to be crucial in determining the lower thermal limits of decapod crustaceans. $[Mg^{2+}]_e$ increases with falling temperatures in most crustaceans and, in addition, available evidence suggests that the anaesthetic potency of magnesium increases with decreasing temperature. We therefore propose that the biogeography of marine crustaceans in cold oceans is related to the combined effects of $[Mg^{2+}]_e$ and low temperature. There is only one major exception to the general rule of an inverse correlation between $[Mg^{2+}]_e$ and activity level. The highly active cephalopod molluscs do not regulate $[Mg^{2+}]_e$ at all, however, the haemolymph of cephalopods is characterised by elevated K^+ - levels. One could hypothesise that magnesium excretion in molluscs has never developed to the extent required for an effective reduction of extra cellular levels and that cephalopod molluscs have overcome this constraint by slightly increasing the extra cellular potassium concentration ($[K^+]_e$).

Up to now no experiments have been carried out related to the effects of extra cellular potassium on activity levels of Antarctic crustaceans. During this cruise measurements of respiration rate of a benthic amphipod and the benthic shrimp *Sclerocrangon* were performed to test the hypothesis that the activity level of Antarctic crustaceans is a function of $[Mg^{2+}]_e$ and could be modulated by increasing the extra cellular potassium concentration.

We obtained benthic amphipods and benthic shrimps (*Sclerocrangon*) from various bottom trawls (AGT) in the Store Fjord. They were initially kept at -0.2 ± 0.5 °C in normal sea water containing about 50 mmol Mg^{++}/l and 10 mmol K^+/l and were given several days to acclimatise. After acclimatisation, oxygen consumption of 8 individuals was measured in a closed system (Amphipods) or in a flow through system (*Sclerocrangon*) by optical oxygen microsensors. After measurement the animals were transferred into a different aquarium which contained normal sea water plus 50 mmol Mg^{++}/l and were kept for 24 hours. Afterwards, oxygen consumption was measured as described above. After this treatment, animals were transferred to aquaria with additional 3 mmol K^+/l and they were kept for another 24 hours and tested afterwards. Following this experimental day, they were given 24h in normal sea water to recover and were once again tested under control conditions. This was done to exclude any effect of decreasing condition on the outcome of the experiment. During the experiments, no mortality occurs. After all experimental tests, body length (amphipods) or fresh weight (*Sclerocrangon*) of the eight individuals was measured.

Preliminary results

The increase of magnesium up to a level usually found in reptant decapod crustaceans had a pronounced effect on respiration rate of both species. In both

species oxygen consumption decreases. This result strengthens our hypothesis that the biogeography of marine crustaceans in cold oceans is related to the combined effects of $[Mg^{2+}]_e$ and low temperature. An increase of the Potassium concentration had a stimulating effect on oxygen consumption in both species although control levels were not reached. This results show that an increase in extra cellular potassium has a stimulating effect under the conditions of high extra cellular magnesium not only in molluscs but also in crustaceans. Further experiments concerning the role of extra cellular ion concentrations will be carried out at the AWI with the crustacean species caught during this cruise.

6.7 Arctic zooplankton

Hirche, May (AWI)

The zooplankton investigations in the Barents Sea, Storfjord and Greenland Sea focus on the description of the developmental state of the zooplankton community in winter. Previous studies have revealed early growth and reproduction of several copepod species under the first-year ice of the Barents Sea. Thus it is an interesting question, whether development has started already in March, or whether the community is still in an hibernating condition. The data will be compared with observations on two transects across the ice covered northern Barents Sea in May and June 1997 during ARK 13. Developmental stage composition, gonad maturity and egg production of all dominant copepods were used as parameters of growth and reproduction. Fine mesh were used to collect eggs and young larvae in the water column. Egg production were measured directly in incubation experiments in the laboratory. Concurrent measurements of chlorophyll a in the water column describe the food environment for the zooplankton. Carbon and nitrogen content together with lipids will indicate the physiological condition of dominant copepods. As the zooplankton communities in the three areas differ according to the water masses, comparison of the respective communities will help to reveal the existence of different life cycle strategies.

Copepods often overwinter as resting eggs on the sea floor. Therefore sediment samples from box corer and multicorer were incubated on board ship to follow the development of resting eggs.

6.8 Sea ice microbiology

Gerdes (AWI)

Sea-ice cores were collected at three ice stations and at the 12-day drift station on multi-year ice floes. Additionally one sample from the surface sea water (0,6 m) was taken.

Some sea ice samples were prepared for fluorescent in situ hybridization, DNA – and RNA extraction, and total counts to observe bacterial structure analysis and the differentiation of the active bacterial part at winter conditions. Molecular biological analysis of the prepared samples will be conducted at the home laboratory in Bremerhaven. The winter data will be compared with summer data to see if bacterial

6- BIOLOGY IN THE SEA-ICE, IN THE WATER COLUMN AND AT THE SEA FLOOR

communities differ and which groups are important for the microbial processes during winter.

The remaining sea ice samples were stored at -5°C to study the influence of oil on Arctic sea ice bacteria. Bioremediation experiments will be conducted in the home laboratory in Bremerhaven as well. These investigations in the scope of the ARCOP-project will give information about the toxicity of hydrocarbons on Arctic sea ice communities and about the potential of bacteria to bind, disperse and degrade oil under extreme temperature conditions. Bacteria involved in hydrocarbon degradation will be isolated for more detailed studies.

6.9 Benthos activities during winter

Deubel (AWI)

Benthic organisms are an important component of aquatic ecosystems. Compared to the most phytoplankton, zooplankton as well as smaller benthic taxa like bacteria, nanofauna and meiofauna, the macrofaunal organisms tend to become relatively old. Thus, they are integrating indicators of the environmental conditions and seasonal variabilities. From this point of view macrobenthic organisms are an important link within the processes in the water column and the sea bottom. All sea floor living organisms are dependent on sinking flux of organic matter from the surface waters of the oceans. As there are no fresh plant food resources available at the floor of Arctic seas during the dark winter season, it is anticipated that benthos activities may be lower than in summer. While there is an abundant literature describing benthic nutrient fluxes, most studies have been conducted in either temperate areas or in the summery ice-free shallow environments of the arctic marginal seas. Natural respiration rates of benthic communities in permanent ice covered arctic ecosystems or during wintertime with the strong seasonally sea ice cover are still poorly known. This lack of information constrains our understanding of the functioning and dynamics of benthic marine ecosystems in the Arctic. The final objective of the benthological program was to calculate the benthos activities during wintertime measuring the benthic fluxes of total oxygen uptake rates. To investigate these activities, a multicorer was used to collect cores of sediment in the Barents Sea and Svalbard waters. The samples were taken at 24 stations in water depths ranging from 60 to 267 m. On board two sediment cores were placed in a dark temperature-controlled container ($\approx 0^{\circ}\text{C}$) and incubated for 24 to 80h. The cores were closed with lids with 3 to 34 cm of ambient overlaying circulated bottom water. Oxygen concentrations in the near-bottom water were measured at least before beginning and after finishing the experiments. The benthic respiration rates were calculated as the decrease of the constituent concentration versus time. The oxygen measurements were carried out by using optodes (Microx). After the incubation the macrofauna was separated from the sediment by sieving with a $250\mu\text{m}$ screen and preserved in 7% formaldehyde solution, buffered with borax.

Additional information about macro-zoo benthos activity and reproduction conditions was obtained from Agassiz Trawls (AGT). The macrofauna from the AGTs were pre-sorted in larger taxonomical levels and preserved in formalin. The species identification as well as the lipid and gonads investigations will be done in the home

Seasonal investigations at a deep sea long-term station

laboratory in Bremerhaven. The characters of the benthos assemblages sampled by the AGTs inhabit typical soft bottom communities. The Storfjord was occupied by bottom communities, which were dominated by actinian covered gastropods and larger shrimp like crustacea. Additional higher amounts of *Ciliatocardium ciliatum* (bivalvia), *Ctenodiscus crispatus* (asteroidea) were found. In the Barents Sea most remarkable objects are Echinodermata like *Uasterias linkii*, *Ctenodiscus crispatus* and different species of ophiuroids.

6.10 Seasonal investigations at a deep-sea long-term station

Schewe, Graf, Kolar, Wegner, Wolfahrt (AWI, IFÖN)

Due to its enormous dimensions and inaccessibility, the deep-sea realm remains the world's least known habitat. Even today, numerous of deep ocean processes and their relevance to global climate and ecosystem issues are not sufficiently understood.

Until a few years ago, deep-sea research simply meant the assessment of the present status in a distinct, unexplored region of the world's oceans. Single sampling campaigns or measurements, however, generate only snap shots, not allowing extrapolation on temporal variability. Consequently, ecological assessments are largely confined. Only long-term investigations at selected sites offer the opportunity to identify environmental settings determining the structure, complexity and the development of deep-sea communities.

Since summer 1999, we investigate deep-sea habitats at a polar long-term station in the eastern Framstrait westerly of Spitsbergen (Fig. 6.10.1). Beside a central experimental area at 2500 m water depth (AWI-"Hausgarten"), we regularly sample deep-sea sediments at 9 stations along a depth transect between 1000 - 5500 m, which is revisited yearly to analyse seasonal and interannual variations in biological, geochemical and sedimentological parameters.

Up to now we were only able to examine the special distribution of benthic organisms during the summer months. The expedition ARK XIX/1b gave us the unique opportunity to study benthic activity, abundances, and biomasses of organisms in winter or rather spring time.

Organic matter produced in the euphotic zone or introduced from land is the main food source for deep-sea organisms. To characterise and quantify organic matter fluxes to the seafloor during the spring bloom phase, we deployed a mooring as well as a lander system carrying sedimentation traps. They will record in high resolution such sedimentation events like plankton blooms during the spring and summer time.

Virtually undisturbed sediment samples were taken using a multiple corer, which was equipped with an online video system. Various biogenic compounds from the sediments, sampled with this gear, will be analysed to estimate the total biomass of the smallest sediment-inhabiting organisms as well as the composition of bacterial and meiofaunal communities.

Organism activities (e.g. bacterial exoenzymatic activity) as well as concentrations of sediment bound chloroplastic pigments were immediately examined on board. Preliminary results from the pigment analyses indicate enhanced sedimentation of fresh phytodetritus probably already produced in an early spring bloom phase (Fig.

6. BIOLOGY IN THE SEA-ICE, IN THE WATER COLUMN AND AT THE SEA FLOOR

6.10.2). Especially the high concentrations of refractory phaeopigments give a hint for organic matter laterally transported by the West Spitsbergen Current and probably produced in the Greenland Sea. Bacterial exoenzymatic activities correlate very well with the high availability of potential detrital food (Fig. 6.10.3).

So called colonisation trays for soft bottom fauna (Fig. 6.10.4) were deployed for the first time. These trays are filled with artificial sediments (glass beads) and enriched with various concentrations of particulate food. Deployed for different periods of time (three weeks and three month) these experiments will help to understand the relevance of food availability for the colonisation of deep sea soft bottom habitats by bacteria, meio- and macrofauna organisms. The three weeks experiment was already completed during the cruise, while the deployment of three month experiment will end during the summer cruise ARK XIX/3c.

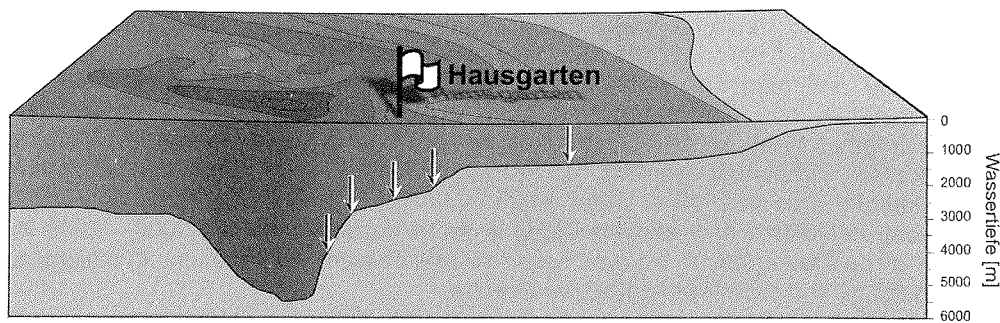


Fig. 6.10.1. "AWI-Hausgarten" depth transect with stations sampled during ARK XIX/1b

Seasonal investigations at a deep-sea long-term station

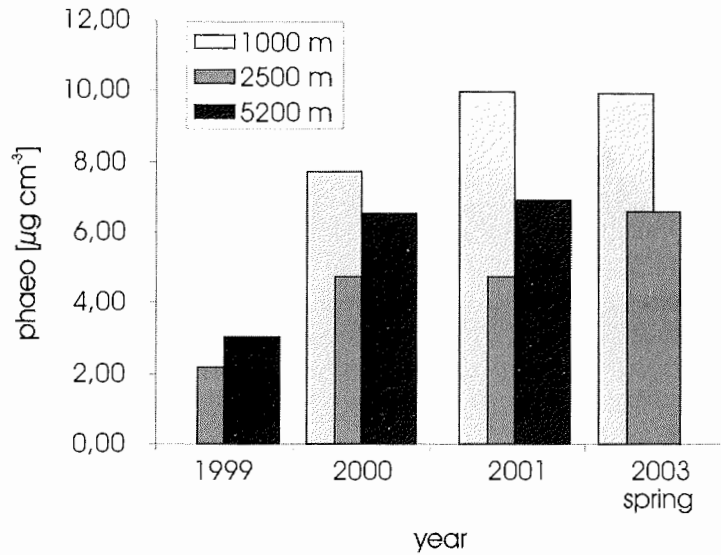


Fig. 6.10.2. concentrations of sediment bound phaeopigments (0-1cm sediment-depth) during several years

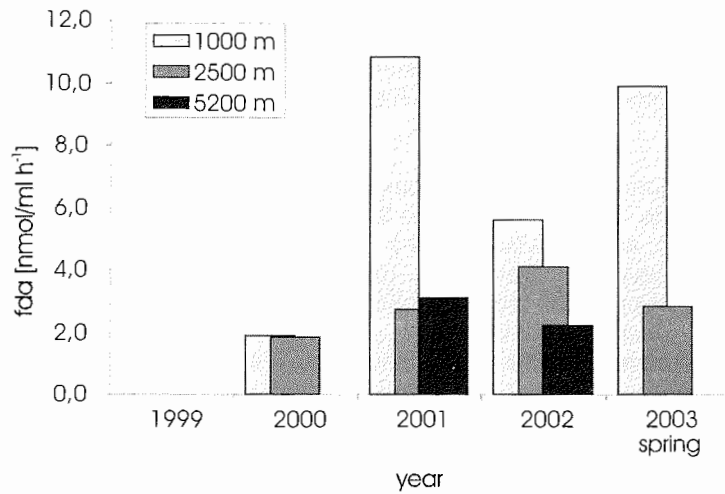


Fig. 6.10.3. bacterial exoenzymatic activities (0-1cm sediment depth) during several years, estimated by esterase turnover rates (FDA)

6. BIOLOGY IN THE SEA-ICE, IN THE WATER COLUMN AND AT THE SEA FLOOR

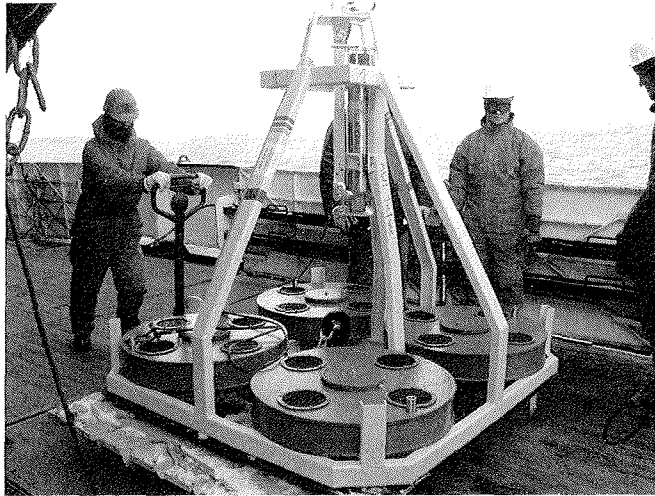


Fig 6.10..4 colonisation tray just recovered

6.11 Methane plumes in the marginal Arctic Ocean - Pathways in the water column and documentation in specific biota

Damm, Wollenburg, Hollmann (AWI)

Goals

Methane is an important greenhouse gas as well as an important component of the global carbon cycle. Methane plumes in the water column and methane enrichments in the sediments are detected on the continental shelf and slope off western Spitsbergen and western Barents Sea. Hence the present marine methane cycle is directly influenced by fossil methane released at gas venting sites in the marginal Arctic Ocean. Since the polar water was supersaturated with respect to the atmospheric methane level this region may act as a source for atmospheric methane, too. However the extension of the plumes are recorded only in a summer situation and the role of seasonal ice coverage and formation of winter-polynyias to the methane pathways in the waters and to the water-atmosphere exchange are not well understood and virtually unknown.

The planned investigations contribute to a better understanding of (1) the potential sources of the detected methane plume in the water column, (2) the different pathways of methane in the hydrosphere, (3) the influence of seasonal ice coverage and a winter polynya to the exchange of methane at the ocean atmosphere boundary, (4) the role of the seasonal ice covered marginal Arctic Ocean as a sink or source for atmospheric methane and (5) the influence of methane released at submarine gas vents on the living benthic fauna and the incorporation of fossil methane into the recent marine carbon cycle in general.

Work at sea

Methane concentrations were measured at 49 stations along the transects in Storfjorden and northwest of Spitsbergen. Water samples were collected in Niskin bottles mounted on a rosette sampler from bottom water depths up to the surface (0.5 m). The dissolved gases were immediately extracted from the water and were analysed for methane by gas chromatograph equipped with a flame ionization detector (FID) on board ship. Gas samples were stored for investigations of the $\delta^{13}\text{CCH}_4$ in the home laboratory. Furthermore 400 water samples for $\delta^{13}\text{CDIC}$ and $\delta^{18}\text{OH}_2\text{O}$ analyses were taken, which will be analyzed during the following months at the AWI. Samples for benthic foraminiferal analyses have been taken in 1-cm-thick slices from the sediment surface down to 10 cm subbottom depth at 19 multicorer sites. During the following months they will be analyzed for their living and dead benthic foraminifera communities. Furthermore, to reveal certain cell characteristics, at each site specimens of selected species were fixated for future transmission electron microscope analyses.

Preliminary results

In the Storfjorden, an extended methane anomaly is indicated by methane concentrations exceeding both, normal marine background values of <5 nM and concentrations in equilibrium with the atmosphere. This points to a complex anomaly formation induced by an interaction of submarine discharge events and several subsequent processes. A submarine venting seep is detected in Storfjorden near Edgeöya. (Fig. 6.11.1). The methane plume is transported laterally and vertically, leading to an extensive anomaly in the whole water column. Simultaneous methane oxidation, dilution by mixing and loss to the atmosphere finally cause the observed spatial variability of the plume and its $\delta^{13}\text{CCH}_4$ heterogeneity. Furthermore, the extension of the plume is influenced by the winter situation. Methane is clearly enriched in surface water below sea-ice as e.g. at the southern part of the P-transect. In comparison, methane is lost to the atmosphere in the ice-free region at the northern part of the P-transect (Fig. 6.11.2).

Preliminary onboard analyzes indicate an increased abundance of benthic foraminifera species described from methane-influenced sites, at sites of increased bottom water methane concentrations. However, comprehensive investigations are needed to show whether this is an accidental phenomenon or a real relationship. By taking these foraminifera samples we also obtained the first winter foraminifera faunas from high northern latitudes. This is especially important because the distribution and abundance of sub-Arctic to Arctic benthic foraminifera is controlled by export production. The dark green protoplasm staining of living foraminifera indicated an unexpectedly high late winter primary production / ice algae production already at the beginning of this cruise. This production is presumably responsible for the surprisingly high standing stock (no. of living specimen). The observation of sexual and asexual reproducing specimen in late winter are a further spectacular observation. The foraminifera fauna of the top most sediment centimeter is dominated by *Nonionellina labradorica*, *Robertinoides charlottensis*, *Recurvoides turbinatus*, *Labrospira crassimargo*, *Globobulimina aculeata*, *Reophax subfusiformis*, *Pyrgo williamsoni*, *Islandiella helenae*, *I. norcrossi*, *Sillicosigmolimina groenlandica*,

6. BIOLOGY IN THE SEA-ICE, IN THE WATER COLUMN AND AT THE SEA FLOOR

Quinqueloculina agglutinata and *Ammotium cassis* (Fig. 6.11.3). Living specimens of these species have been found in summer at highly productive sites. However, during summer they are usually found much deeper in the sediment (>3 cm), whereas the surface centimetre is dominated by different species (e.g. phytodetritus species like *Epistominella vitrea*, *E. exigua* and *E. pusilla*), which are almost absent in the Storfjorden winter fauna.

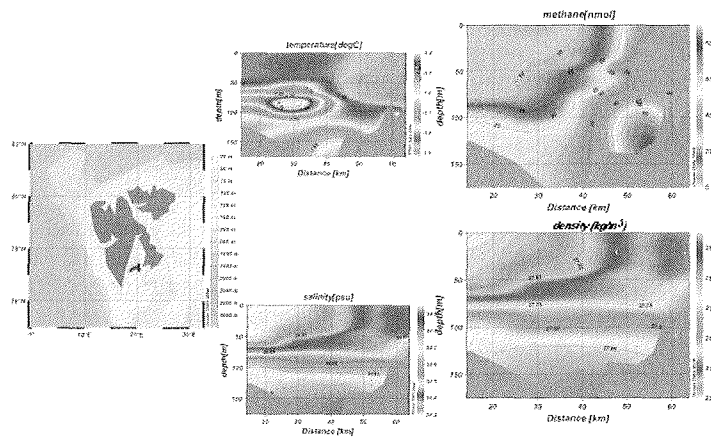


Fig. 6.11.1: Hydrographic data and methane concentration in the Storfjord (transect D, Fig.5.1.A). Near Edgeöya a submarine discharge is indicated by the deep methane maximum.

Methane plumes in the marginal Arctic Ocean

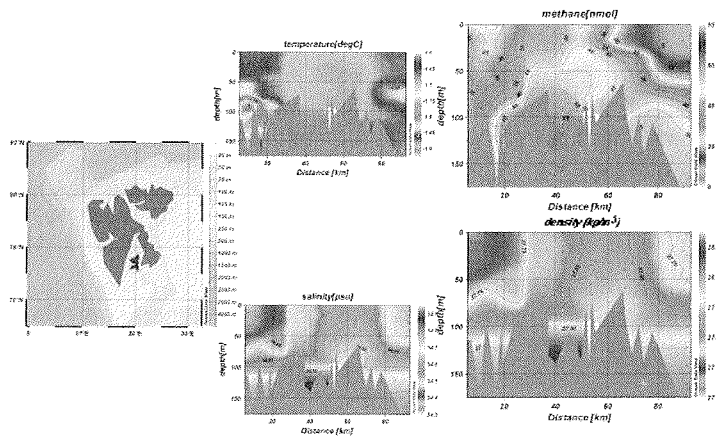


Fig. 6.11.2: Hydrographic data and methane concentration at transect P (Fig.5.1.A). The variation in the surface methane concentration is caused by different ice coverage

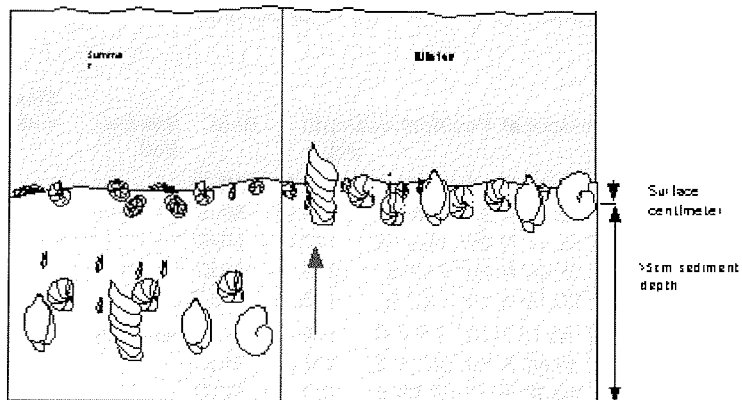


Fig 6.11.3: Living specimens of several species (see text) in summer samples at highly productive sites. During summer they are usually found much deeper in the sediment, whereas the surface is dominated by species which are almost absent in the Storfjorden winter.

7. SEDIMENTOLOGY

Kukina (MMBI)

Reconstructions of the geological history of Svalbard's shelf has fundamental scientific problem, because of peculiarities of evolution of the marine ecosystem in conditions of melting ice sheets, input of the sediment material, intensive sedimentogenesis and changing of sea water salinity in the modern period in connection with anthropogenic influences.

The main directions of the geological investigations:

- Modern periglacial processes and their influence on the geological, geomorphological and sedimentological details of archipelagoes.
- Influence of the ice sheet edge on formation of the frontal zones in the littoral areas.

Preliminary Results

Geological work was carried out at 17 stations (Fig. 1) in the Storfjord. At 2 stations sea-ice sediments were sampled. Smear-slides were prepared from the surface layer (0-1cm) of bottom sediments and from sea-ice sediments in order to obtain the mineralogical composition of the clastic material from the sample material (Table 1).

Table 7.1

Volume of geological works in the ARK XIX/1a expedition

Station	Date	PositionLat	PositionLon	Depth [m]	Gear	Sea-Ice Sed	Smear-slide
PS64/004-2	06.03.03	75° 40.03' N	17° 18.58' E	201.3	MUC		+
PS64/012-2	07.03.03	76° 38.19' N	18° 3.68' E	247.3	MUC		+
PS64/014-2	08.03.03	76° 35.41' N	20° 38.54' E	117.6	MUC		+
PS64/015-8	08.03.03	76° 38.09' N	20° 9.63' E	206.7	MUC		+
PS64/021-3	10.03.03	76° 50.16' N	19° 1.92' E	118.5	MUC		+
PS64/021-2	10.03.03	76° 50.18' N	19° 1.99' E	119.6	ICE	Ice-Core	+
PS64/024-3	11.03.03	76° 49.66' N	19° 30.11' E	167.2	MUC		+
PS64/029-2	14.03.03	76° 49.98' N	20° 22.56' E	130.2	MUC		+
PS64/031-2	14.03.03	76° 59.60' N	20° 21.76' E	117.2	MUC		+
PS64/034-2	15.03.03	77° 13.07' N	20° 28.01' E	91.9	MUC		+
PS64/039-7	17.03.03	77° 31.58' N	20° 19.48' E	111.6	MUC		+
PS64/041-2	17.03.03	77° 40.21' N	20° 29.66' E	61.4	MUC		+
PS64/048-7	18.03.03	77° 29.45' N	19° 4.68' E	188.4	MUC		+
PS64/062-9	19.03.03	77° 12.12' N	19° 14.97' E	177.7	MUC		+
PS64/062-2	19.03.03	77° 17.12' N	20° 02' E	177	ICE	Ice-Core	+
PS64/064-2	20.03.03	77° 8.93' N	18° 50.30' E	124.5	MUC		+

7. SEDIMENTOLOGY

Station	Date	PositionLat	PositionLon	Depth [m]	Gear	Sea-Ice Sed	Smear- slide
PS64/067-6	22.03.03	76° 26.01' N	21° 45.23' E	266.4	MUC		+
PS64/70-5	23.03.03	76° 18.41' N	23° 20.13' E	114.7	MUC		
PS64/72-6	24.03.03	76° 4.82' N	25° 20.67' E	93.3	MUC		

Sea-Ice Sediment Investigation

Sediments in the sea-ice are important for erosion and distribution and consequently are a factor for the sediment budget of the Arctic Ocean.

The main targets of the field work was:

- a) Tracing possible transport pathways of sea-ice sediments based on sedimentological parameters in surface deposits and sea-ice entrained material in source and melt areas.
- b) Identification of sample composition, grain size distributions and mineral assemblages between sea-ice sediments in the different areas of the Arctic Ocean.

During the expedition ARK XIX/1a dirty sea-ice was sampled (Werner I., Schunemann H.). Shipboard sample analyses included:

- 1) Measured volumes of melted ice and water samples were filtered through 0.2mm filter papers (Schwarz J.N.). In the shore-based laboratory the filters will be weighed to quantify the load of sediments.
- 2) Melted ice and water samples were filtered through 0.2mm filters for mineralogical, granulometric analysis and study of morphology of quartz grains.
- 3) Smear-slide description for bulk mineral composition.

Smear-slide description of sea-ice sediments reveal fine-grained composition. Most of the sediment consisted of material less 63 µm in size. Terrigenous components accounted for more than 85% of all counted macerals. The sampled sediments consisted mainly of quartz and feldspar (Tab.2). The quartz was mostly clear, some grains included black minerals and air bubbles. Organic-clay-ferrous aggregates, heavy minerals, clay minerals and microorganisms accounted for 30%. Rock fragments, mica and black ores were generally less abundant (10-12%). Heavy minerals presented amphibole-garnet-black ores association.

Table 7. 2

Mineralogical composition of the sea-ice sediments (%).

Station	Quartz	Feldspar	Mica	Heavy Mineral	Black Ores	Iron-Clay Aggregate	Rock Fragm	Clay Miner	Organic Remain
PS64/21	44	9	6	18	4	3	2	11	3

7. SEDIMENTOLOGY

Surface sediments were taken with the multicorer (MUC, 12 tubes of 6 cm in diameter) for sedimentological (grain size distribution, heavy and light mineralogy and morphology of quartz grain estimates) investigations. In the cruise ARK XIX/1 for sedimentological investigations was sampling surface bottom sediments from multicorer (1 tube). The sediments were described and packed in plastic bags. The smear-slides were also prepared on board and bulk minerals described.

On board RV "Polarstern" the surface sediments cores were described visually. Sediment colours were identified according to the "Munsell Soil Color Chart". Smear-slides were prepared to obtain estimates of the bulk mineral composition, biogenic and terrigenous components.

All sediment surfaces consist of dark olive brown and olive gray mud, the dominant size fraction of which is clay and silt. Only at a few sites (PS64/04, PS64/21, PS64/64, PS64/70) sandy lithology appears. Terrigenous materials (mainly quartz, feldspar, mica and clay minerals) predominate. Heavy minerals include epidote, garnet, pyroxenes and iron hydroxides.

Biogenic components are of minor importance, though diatoms, benthic foraminifera, shell fragments and plant remains were always present. The most abundant organisms were polychaetes.

The uppermost dark brown to olive gray lithological unit of the sediment cores ranges from 2-20 cm in thickness. This strongly bioturbated unit resembles the sediment surface in the multicores and apparently reflects the depth of oxygenation. Below, the sediment color gradually darkened due to Fe precipitation. Bioturbation by living organisms (polychaetes) homogenizing the sediment column was observed down to 10 cm core depth.

Smear-slide analyses showed that quartz is the dominant mineral (24-36%), feldspar, clay minerals and mica were the next most important minerals (Table 3). The heavy minerals composed 14-18% and presented epidote, garnet, pyroxenes and black ores.

7. SEDIMENTOLOGY

Table 7.3.

Mineralogical composition of the surface layer (0-1cm) of bottom sediments (%).

Station	Quartz	Feld Spar	Mica	Calcite	Heavy Min.	Black Ores	Iron-Clay Aggregate	Rock Fragm	Clay Miner	Organic Remain
PS64/04	25.3	13.7	2.1	4.2	15.8	2.1	6.3	1.8	11.6	17.1
PS64/12	30.0	9.8	4.2	5.1	10.9	1.0	5.2	0.8	20.0	13.0
PS64/14	25.5	16.0	3.5	0.5	18.5	5.0	8.5	1.5	14.2	6.8
PS64/15	31.0	14.0	5.1	1.9	18.0	9.0	5.7	0.3	23.0	7.0
PS64/21	27.9	9.7	4.5	3.9	16.9	1.2	6.6	6.5	17.5	4.5
PS64/24	30.0	17.0	4.2	5.8	13.0	3.0	1.5	1.5	18.0	6.0
PS64/29	31.0	9.1	5.2	4.1	9.1	4.1	8.2	0.8	22.4	6.0
PS64/34	27.0	13.0	7.0	4.0	11.4	0.9	3.6	0.2	24.8	8.1
PS64/39	38.0	16.0	8.6	7.4	14.2	0.6	1.8	2.1	3.3	8.0
PS64/41	34.0	12.0	2.8	7.4	16.0	5.6	9.9	0.4	9.9	2.0
PS64/48	39.4	15.6	7.4	2.1	13.3	0.4	1.2	7.6	3.0	11.0
PS64/62	34.2	12.3	5.2	2.3	11.2	1.3	2.6	4.2	15.3	11.4
PS64/64	35.8	15.6	4.5	5.6	16.5	5.4	4.9	2.3	4.0	5.4
PS64/67	34.6	16.2	5.3	5.8	16.2	4.3	8.3	2.8	2.5	4.0

Further detailed sedimentological and mineralogical studies will follow to identify the different source areas.

Future geological investigations in MMBI will include:

- Grain size distribution;
- heavy and light mineralogy
- Morphology of the quartz grain

7. SEDIMENTOLOGY

PS64/04-2 (MUC) Storfjord Svalbard **ARK XIX/1a**
 Recovery: 0.25 cm 75° 40.03N 17° 18.58E Water Depth: 201.3 m

Lithology	Texture	Color	Description
0		2.5Y3/2	0-16 cm Very dark grayish brown, sand silty clay, polychaetes 4-6 cm hard ground 6-8 cm gravel, pebbles 0.5-1 cm in diameter
10			16-25 cm Very dark gray, sand silty clay
20		2.5Y3/0	24-25 cm Boiturbation, pebble 3cm in diameter

PS64/12-2 (MUC) Storfjord Svalbard **ARK XIX/1a**
 Recovery: 0.33 cm 76° 38.19N 18° 3.68E Water Depth: 247.3 m

Lithology	Texture	Color	Description
0		10YR3/2	0-4 cm Very dark grayish brown, silty clay, polychaetes
		2.5Y3/2	4-18 cm Very dark grayish brown, silty clay, polychaetes
10			
20		5Y3/1	18-28 cm Very dark gray, silty clay
30			28-33 cm Boiturbation

PS64/14-2 (MUC) Storfjord Svalbard **ARK XIX/1a**
 Recovery: 0.16 cm 76° 35.41N 20° 38.54E Water Depth: 117.6 m

Lithology	Texture	Color	Description
0		2.5Y4/3	0-6 cm Olive brown, sand silty clay, pebbles 1-3 cm in diameter
10		2.5Y3/2	6-16 cm Very dark grayish brown, silty clay Boiturbation

7. SEDIMENTOLOGY

PS64/15-2 (MUC) Storfjord Svalbard **ARK XIX/1a**
 Recovery: 0.26 cm 76° 38.09N 20° 9.63E Water Depth: 206.7 m

Lithology	Texture	Color	Description
0		2.5Y3/3	0-10 cm Dark olive brown, silty clay, polychaetes
10	5	5Y3/2	10-26 cm Dark olive gray, silty clay, bioturbated
20			

PS64/21-3 (MUC) Storfjord Svalbard **ARK XIX/1a**
 Recovery: 0.20 cm 76° 50.16N 19° 1.92E Water Depth: 118.5 m

Lithology	Texture	Color	Description
0		2.5Y3/3	0-4 cm Dark olive brown, gravel sand silty clay, polychaetes
		2.5Y3/0	0-2 cm dropstone 3 cm in diameter
10			4-20 cm Very dark gray, sand silty clay, bioturbated.
			4-8 cm pebble, gravel 1.5 cm and less in diameter
20			

PS64/24-3 (MUC) Storfjord Svalbard **ARK XIX/1a**
 Recovery: 0.24 cm 76° 49.66N 19° 30.11E Water Depth: 167.2 m

Lithology	Texture	Color	Description
0		2.5Y3/3	0-6 cm Dark olive brown, silty clay
10		2.5Y3/0	6-24 cm Very dark gray, silty clay, bioturbated
20			

7. SEDIMENTOLOGY

PS64/29-2 (MUC) Storfjord Svalbard **ARK XIX/1a**
 Recovery: 0.18 cm 76° 49.98N 20° 22.56E Water Depth: 130.2 m

Lithology	Texture	Color	Description
0		2.5Y3/3	0-6 cm Dark olive brown, silty clay 4-6 cm Oxidized spots
10		5Y3/2	6-18cm Dark olive gray, silty clay, bioturbated
20			

PS64/34-2 (MUC) Storfjord Svalbard **ARK XIX/1a**
 Recovery: 0.28 cm 77° 13.07N 20° 28.01E Water Depth: 91.9 m

Lithology	Texture	Color	Description
0		2.5Y3/3	0-8 cm Dark olive brown, silty clay
10		2.5Y3/0	8-28cm Very dark gray, silty clay, bioturbated 8-16 cm shells fragment, polychaetes
20			
30			

PS64/41-2 (MUC) Storfjord Svalbard **ARK XIX/1a**
 Recovery: 0.28 cm 77° 13.07N 20° 28.01E Water Depth: 91.9 m

Lithology	Texture	Color	Description
0		2.5Y3/3	0-6 cm Dark olive brown, silty clay
10		2.5Y3/0	6-28cm Very dark gray, silty clay, bioturbated
20			
30			

7. SEDIMENTOLOGY

PS64/67-6 (MUC) Storjford Svalbard ARK XIX/1a
 Recovery: 0.25 cm 76 26.01N 21 45.23E Water Depth: 266.4 m

Lithology	Texture	Color	Description
0	[Symbol]	2.5Y3/3	0-3 cm Dark olive brown, clayey sandy silt
		5Y3/2	3-9 cm Dark olive gray, clayey sandy silt,
10	[Symbol]	2.5Y3/0	9-25cm Very dark gray, clayey sandy silt, bioturbated
			20-2cm Shells fragment
			24-25cm Oxidized spots
20	[Symbol]	2.5Y3/0	
30	[Symbol]	2.5Y3/0	

PS64/70-5 (MUC) Storjford Svalbard ARK XIX/1a
 Recovery: 0.18 cm 76 18.41N 23 20.13E Water Depth: 114.7 m

Lithology	Texture	Color	Description
0	[Symbol]	2.5Y3/2	0-3 cm Dark olive brown, silty sand
		5Y3/1	3-18cm Very dark gray, clayey sandy silt, bioturbated, shells fragment
10	[Symbol]	5Y3/1	16-18cm Oxidized spots
20	[Symbol]	5Y3/1	

PS64/72-6 (MUC) Storjford Svalbard ARK XIX/1a
 Recovery: 0.16 cm 76 4.82N 25 20.67E Water Depth: 93.3 m

Lithology	Texture	Color	Description
0	[Symbol]	5Y4/2	0-3 cm Olive gray, gravel, sandy mud,
		5Y3/2	0-1 cm dropstones 3-5 cm in diameter
10	[Symbol]	5Y3/2	3-16cm Dark olive gray, clayey sandy silt, bioturbated, shells fragment
			3-4 cm dropstones 4 sm in diameter (organogenic sandstone)
20	[Symbol]	5Y3/2	

APPENDIX

- A.1 Scientific Participants**
- A.2 Participating Institutions**
- A.3 Ship's Crew**
- A.4 Station List**

A.1 PARTICIPANTS

Name	First Name	Institute	Profession
Albert	Stefanie	MIH	Student
Alexandrov	Vitaly	NERSC	Oceanographer
Auel	Holger	UB	Biologist
Bäsemann	Hinrich	-	Journalist
Beeken	Andreas	MIH	Student
Birnbaum	Gerit	AWI	Meteorologist
Bothe	Oliver	MIH	Student
Buschmann	Marco	AWI	Engineer
Cohrs	Wolfgang	AWI	IT Technician
Damm	Ellen	AWI	Geologist
Debatin	Siegrid	AWI	Technician
Dimmler	Werner	Fielax	Electronic.Technician
Doble	Martin	SAMS	Scientist
Eriksson	Patrick	FIMR	Oceanographer
Fer	Ilker	GIUB	Scientist
Fröb	Ilker	Fielax	Electronic.Technician
Gebauer	Manfred	DWD	Meteorologist
Gerchow	Peter	Fielax	Engineer
Gerdes	Birte	AWI	Ph.D. Student
Graf	Sabine	AWI	Student
Graf	Sabine	AWI	Student
Haas	Christian	AWI	Geophysician
Harms	Ingo	IFMH	Oceanographer
Hartmann	Jörg	AWI	Scientist
Herrmann	Regine	AWI	Student
Hollmann	Beate	AWI	Technician
Hughes	Nicolas	SAMS	Scientist
Jacobi	Hans-Werner	AWI	Chemist
Kern	Stefan	IFMH	Scientist
Kiko	Rainer	IPÖ	Student
Kirchgäßner	Amelie	MIH	Meteorologist
Klein	Boris	AWI	Technician
Kolar	Ingrid	IFÖN	Student
Karcher	Michael	AWI	Oceanographer
Kukina	Natalja	MMBI	Geologist
Lanning	Gisela	AWI	Scientist
Lieser	Jan	AWI	Meteorologist
Lobach	John	AWI	Geophysicist
Lüpkes	Christof	AWI	Meteorologist
Martin	Torge	AWI	Student

Name	First Name	Institute	Profession
May	Philip	AWI	Technician
Mercer	Duncan	SAMS	Engineer
Niehoff	Barbara	AWI	Scientist
Offermann	Michael	MIH	Technician
Olbers	Dirk	AWI	Physicist
Pascal	Robin	SOC	Scientist
Pfaffling	Andreas	AWI	Geophysicist
Pisarev	Sergey	SIO/AWI	Oceanographer
Piskorzynski	Andreas	Fielax	Electron.Technician
Rudels	Bert	FIMR	Oceanographer
Sartoris	Franz Josef	AWI	Biologis
Schauer	Ursula	AWI	Chief Scientist
Scheltz	Annette	IPÖ	Technician
Schewe	Ingo	AWI	Biologist
Schmitz-Köster	Dorothee	RB	Journalist
Schünemann	Henrike	IPÖ	scientific. employee
Schwarz	Jill Nicola	AWI	Scientist
Seiffert	Rita	MIH	Student
Sirevaag	Anders	GIUB	Student
Spieß	Thomas	TUB	Meteorologist
Verhoeven	Roger	Fielax	Electron.Technician
Wegner	Jan	AWI	Technician
Welsch	Andreas	IFMH	Technician
Werner	Iris	IPÖ	Biologist
Willmes	Sascha	AWI	Student
Wolfahrt	Frederike	AWI	Student
Wollenburg	Jutta	AWI	scientific employee
Yelland	Margaret	SOC	Scientist

A.2 PARTICIPATING INSTITUTES

	Adresse / Address
AWI Bremerhaven	Stiftung Alfred-Wegener-Institut für Polar- und Meeresforschung in der Helmholtz-Gemeinschaft Postfach 12 01 61 27515 Bremerhaven
AWI Potsdam	Stiftung Alfred-Wegener-Institut für Polar- und Meeresforschung in der Helmholtz-Gemeinschaft Telegrafenberg A43 D-14473 Potsdam
DWD	Deutscher Wetterdienst Jenfelder Allee 70A 22043 Hamburg
FIMR	Finnish Institute of Marine Research P.O. Box 33 Lyypekinkuja 3A FIN-00931 Helsinki, Finland
GIUB	Geophysical Institute, University of Bergen Allegaten 70 N-5007 Bergen, Norway
HSW	Helicopter Service Wasserthal GmbH Flughafen Hamburg 22335 Hamburg
IfMH	Institut für Meereskunde Universität Hamburg Tropelwitzstrasse 7 22529 Hamburg
IFÖN	Institut für Ökologie und Naturschutz Abt. für Meeresbiologie Althanstr. 14 A-1090 Wien, Austria
IPÖ	Institut für Polarökologie Wischhofstr. 1-3, Geb. 12 24148 Kiel

MIH	Meteorologisches Institut Universität Hamburg Bundesstrasse 55 20146 Hamburg
MMBI	Murmansk Marine Biology Institute RAS 17 Vladimirskaia St. Murmansk, 183010 Russia
NERSC	Nansen Environmental and Remote Sensing Center Edv. Griegsvei 3a N-5059 Bergen, Norway
RB	Radio Bremen Hörfunk Bürgermeister-Spitta-Allee 45 28329 Bremen
SAMS	Scottish Association for Marine Science Dunstaffnage Marine Laboratory Oban, Argyll, PA37 1QA Great Britain
SOC	Southampton Oceanography Centre University of Southampton Waterfront Campus European Way Southampton SO14 3ZH/United Kingdom
TUB	Institut für Luft- und Raumfahrtssysteme Technische Universität Braunschweig Hermann-Blenk-Strasse 23 38108 Braunschweig
SIO	P.P. Shirshov Institute of Oceanology 36, Nachimovsky prosp Moscow, 117851 Russia
UB	Marine Zoology (FB2) University of Bremen P.O. Box 330 440 D-28334 Bremen

A.3 SHIP'S CREW

Reederei F.Laeisz G.m.b.H.
Name of Ship : POLARSTERN
Nationality : GERMAN

Reise **ARK XIX / 1**
28.02.2003 - 24.04.2003
Bremerhaven - Longyearbyen

No.	NAME	RANK	NATION
01.	Pahl, Uwe	Master	German
02.	Grundmann, Uwe	1.Offc.	German
03.	Schulz, Volker	Ch.Eng.	German
04.	Fallei, Holger	2.Offc.	German
05.	Peine, Lutz	2.Offc.	German
06.	Hartung, René	2.Offc.	German
07.	Grigoleit, Urte	Doctor	German
08.	Hecht, Andreas	R.Offc.	German
09.	Erreth, Gyula	1.Eng.	German
10.	Richter, Frank	2.Eng.	German
11.	Simon, Wolfgang	2.Eng.	German
12.	Holtz, Hartmut	Electr.	German
13.	Loidl, Reiner	Boatsw.	German
14.	Neisner, Winfried	Carpenter	German
15.	Bäcker, Andreas	A.B.	German
16.	Schmidt, Uwe	A.B.	German
17.	Winkler, Michael	A.B.	German
18.	Schröder, Norbert	A.B.	German
19.	Bastigkeit, Kai	A.B.	German
20.	Guse, Hartmut	A.B.	German
21.	Hagemann, Manfred	A.B.	German
22.	Niehusen, Arne	Apprent.	German
23.	Beth, Dettlef	Storekeep.	German
24.	Arias Iglesias, Enr.	Mot-man	Chile
25.	Fritz, Günter	Mot-man	Austria
26.	Krösche, Eckard	Mot-man	German
27.	Dinse, Horst	Mot-man	German
28.	Scholl, Christoph	Apprent.	German
29.	Fischer, Matthias	Cook	German
30.	Tupy, Mario	Cooksmate	German
31.	Martens, Michael	Cooksmate	German
32.	Dinse, Petra	1.Stwdess	German
33.	Schöndorfer, Ottilie	Stwdss/KS	German
34.	Streit, Christina	2.Stwdess	German
35.	Schmidt, Maria	2.Stwdess	German
36.	Deuß, Stefanie	2.Stwdess	German
37.	Tu, Jian Min	2.Steward	China
38.	Wu, Chi Lung	2.Steward	German
39.	Yu, Chung Leung	Laundrym.	Hongk.

A.3 STATION LIST

Station PS64/	Date	Time	PositionLat	PositionLon	Depth [m]	Gear	Action	Comment
1-1	03.03.03	14:24	64° 35.46' N	6° 2.45' E	687.6	Multiple net	surface	
1-1	03.03.03	14:45	64° 35.40' N	6° 2.32' E	682.8	Multiple net	at depth	EL 30 / 502m
1-1	03.03.03	14:46	64° 35.40' N	6° 2.32' E	671.2	Multiple net	Hoisting	
1-1	03.03.03	15:05	64° 35.41' N	6° 2.43' E	681.2	Multiple net	on deck	
1-2	03.03.03	15:11	64° 35.44' N	6° 2.47' E	680.4	Bongo net	surface	
1-2	03.03.03	16:02	64° 35.53' N	6° 2.61' E	680.4	Bongo net	on deck	EL 30 / 500m
1-3	03.03.03	16:15	64° 35.56' N	6° 2.78' E	343.2	Multiple net	surface	
1-3	03.03.03	16:19	64° 35.56' N	6° 2.81' E	345.6	Multiple net	at depth	100 m Draht
1-3	03.03.03	16:27	64° 35.55' N	6° 2.87' E	345.2	Multiple net	on deck	
1-4	03.03.03	16:34	64° 35.59' N	6° 2.96' E	342.4	Nansen Net	in the water	
1-4	03.03.03	16:38	64° 35.61' N	6° 3.01' E	342.8	Nansen Net	at depth	100 m Draht
1-4	03.03.03	16:45	64° 35.67' N	6° 3.13' E	342.4	Nansen Net	on Deck	
1-5	03.03.03	16:52	64° 35.72' N	6° 3.21' E	342.0	CTD	surface	
1-5	03.03.03	17:03	64° 35.77' N	6° 3.35' E	339.2	CTD	at depth	317 m Draht
1-5	03.03.03	17:04	64° 35.77' N	6° 3.36' E	339.6	CTD	on deck	
1-6	03.03.03	17:33	64° 35.80' N	6° 3.77' E	341.2	Bongo net	surface	
1-6	03.03.03	17:36	64° 35.81' N	6° 3.81' E	341.2	Bongo net	at depth	50 m
1-6	03.03.03	17:41	64° 35.81' N	6° 3.87' E	341.6	Bongo net	on deck	
2-1	04.03.03	16:36	68° 35.59' N	9° 55.65' E	2806.0	Calibration	start	HELIPOD- Calibration on Helideck; Ship standing still
2-1	04.03.03	17:00	68° 36.06' N	9° 57.03' E	2817.2	Calibration	End	Test aborted - no success
3-1	05.03.03	15:38	72° 30.41' N	14° 14.94' E	1021.9	Calibration	start	
3-1	05.03.03	16:24	72° 30.59' N	14° 15.80' E	1015.0	Calibration	End	Helipod
4-1	06.03.03	11:06	75° 40.14' N	17° 20.14' E	200.0	CTD/rosette	surface	
4-1	06.03.03	11:14	75° 40.13' N	17° 19.73' E	204.2	CTD/rosette	at depth	EL 31 192 m
4-1	06.03.03	11:25	75° 40.07' N	17° 19.29' E	199.6	CTD/rosette	on deck	
4-2	06.03.03	11:30	75° 40.05' N	17° 18.98' E	203.6	Multi corer	surface	
4-2	06.03.03	11:38	75° 40.03' N	17° 18.58' E	201.3	Multi corer	at bottom	200 m GE 52,2
4-2	06.03.03	11:43	75° 40.02' N	17° 18.30' E	200.5	Multi corer	on deck	
5-1	06.03.03	13:30	75° 49.41' N	17° 10.57' E	304.5	CTD/rosette	surface	
5-1	06.03.03	13:40	75° 49.35' N	17° 10.29' E	303.9	CTD/rosette	at depth	EL 31 /292m
5-1	06.03.03	13:54	75° 49.25' N	17° 9.89' E	303.7	CTD/rosette	on deck	
6-1	06.03.03	15:20	75° 58.29' N	17° 1.70' E	327.8	CTD/rosette	surface	
6-1	06.03.03	15:30	75° 58.27' N	17° 1.55' E	328.2	CTD/rosette	at depth	
6-1	06.03.03	15:47	75° 58.22' N	17° 1.22' E	326.9	CTD/rosette	on deck	
6-2	06.03.03	16:00	75° 58.19' N	17° 1.08' E	326.0	Multiple net	surface	
6-2	06.03.03	16:13	75° 58.16' N	17° 1.01' E	326.2	Multiple net	at depth	313 m
6-2	06.03.03	16:34	75° 58.11' N	17° 0.81' E	326.0	Multiple net	on deck	
6-3	06.03.03	16:48	75° 58.04' N	17° 0.74' E	327.0	Bongo net	surface	
6-3	06.03.03	16:59	75° 57.98' N	17° 0.63' E	326.1	Bongo net	at depth	300 m
6-3	06.03.03	17:18	75° 57.91' N	17° 0.52' E	326.7	Bongo net	on deck	
6-4	06.03.03	17:20	75° 57.90' N	17° 0.52' E	326.1	Bongo net	surface	
6-4	06.03.03	17:32	75° 57.84' N	17° 0.46' E	326.1	Bongo net	at depth	300 m
6-4	06.03.03	17:49	75° 57.74' N	17° 0.33' E	325.8	Bongo net	on deck	
6-5	06.03.03	17:58	75° 57.70' N	17° 0.28' E	325.8	Nansen Net	in the water	
6-5	06.03.03	18:13	75° 57.62' N	16° 59.95' E	327.3	Nansen Net	at depth	300m auf Tiefe
6-5	06.03.03	18:30	75° 57.54' N	16° 59.67' E	327.0	Nansen Net	on Deck	
7-1	06.03.03	19:58	76° 7.32' N	16° 53.39' E	324.1	CTD/rosette	surface	
7-1	06.03.03	20:09	76° 7.35' N	16° 53.24' E	323.9	CTD/rosette	at depth	311 m
7-1	06.03.03	20:18	76° 7.35' N	16° 53.11' E	324.6	CTD/rosette	on deck	

Station PS64/	Date	Time	PositionLat	PositionLon	Depth [m]	Gear	Action	Comment
---------------	------	------	-------------	-------------	-----------	------	--------	---------

8-1	06.03.03	21:11	76° 12.20' N	16° 47.49' E	316.8	CTD/rosette	surface	
8-1	06.03.03	21:21	76° 12.22' N	16° 47.01' E	315.5	CTD/rosette	at depth	303 m
8-1	06.03.03	21:31	76° 12.22' N	16° 46.54' E	309.0	CTD/rosette	on deck	
9-1	06.03.03	22:54	76° 16.30' N	16° 42.19' E	170.2	CTD/rosette	surface	
9-1	06.03.03	23:00	76° 16.29' N	16° 41.58' E	165.9	CTD/rosette	at depth	156 m
9-1	06.03.03	23:05	76° 16.30' N	16° 41.17' E	162.7	CTD/rosette	on deck	
10-1	06.03.03	23:47	76° 19.98' N	16° 38.89' E	68.1	CTD/rosette	surface	
10-1	06.03.03	23:51	76° 20.00' N	16° 38.34' E	65.0	CTD/rosette	at depth	58 m
10-1	06.03.03	23:56	76° 20.02' N	16° 37.61' E	64.9	CTD/rosette	on deck	
10-2	07.03.03	00:08	76° 20.01' N	16° 35.68' E	63.7	Multi corer	surface	
10-2	07.03.03	00:11	76° 20.02' N	16° 35.26' E	63.6	Multi corer	at bottom	
10-2	07.03.03	00:15	76° 20.03' N	16° 34.67' E	61.4	Multi corer	on deck	
11-1	07.03.03	06:55	76° 38.81' N	17° 33.84' E	153.2	CTD/rosette	surface	
11-1	07.03.03	07:02	76° 38.80' N	17° 33.76' E	152.4	CTD/rosette	at depth	143 m
11-1	07.03.03	07:12	76° 38.78' N	17° 33.70' E	152.8	CTD/rosette	on deck	
12-1	07.03.03	11:26	76° 37.46' N	17° 59.79' E	228.1	Ice station	Alongside Floe	
12-1	07.03.03	11:32	76° 37.42' N	17° 59.44' E	225.1	Ice station	Gangway on the ice	
12-1	07.03.03	11:46	76° 37.32' N	17° 58.61' E	225.4	Ice station	Scientists on the ice	
12-1	07.03.03	12:49	76° 36.83' N	17° 55.00' E	223.6	Ice station	Scientists on board	
12-1	07.03.03	12:54	76° 36.79' N	17° 54.73' E	224.2	Ice station	Gangway on board	
12-1	07.03.03	12:56	76° 36.77' N	17° 54.63' E	223.1	Ice station	Departure from floe	
13-1	07.03.03	16:35	76° 38.24' N	18° 4.14' E	270.5	CTD/rosette	surface	
13-1	07.03.03	16:44	76° 38.24' N	18° 4.09' E	303.8	CTD/rosette	at depth	
13-1	07.03.03	16:54	76° 38.22' N	18° 3.92' E	249.3	CTD/rosette	on deck	
13-2	07.03.03	17:01	76° 38.21' N	18° 3.78' E	247.3	Multi corer	surface	
13-2	07.03.03	17:07	76° 38.19' N	18° 3.68' E	247.3	Multi corer	at bottom	241 m
13-2	07.03.03	17:14	76° 38.18' N	18° 3.56' E	249.4	Multi corer	on deck	
14-1	08.03.03	12:36	76° 35.34' N	20° 39.31' E	125.5	CTD/rosette	surface	
14-1	08.03.03	12:41	76° 35.37' N	20° 39.24' E	126.6	CTD/rosette	at depth	
14-1	08.03.03	12:46	76° 35.38' N	20° 39.08' E	127.4	CTD/rosette	on deck	
14-2	08.03.03	13:07	76° 35.40' N	20° 38.59' E	116.9	Multi corer	surface	
14-2	08.03.03	13:11	76° 35.41' N	20° 38.54' E	117.6	Multi corer	at bottom	
14-2	08.03.03	13:15	76° 35.41' N	20° 38.50' E	119.3	Multi corer	on deck	
14-3	08.03.03	13:24	76° 35.37' N	20° 38.48' E	120.1	CTD/rosette	surface	
14-3	08.03.03	13:29	76° 35.43' N	20° 37.90' E	121.3	CTD/rosette	at depth	
14-3	08.03.03	13:36	76° 35.46' N	20° 37.63' E	120.1	CTD/rosette	on deck	
14-4	08.03.03	13:56	76° 35.41' N	20° 37.64' E	122.0	Ice station	Alongside Floe	
14-4	08.03.03	14:00	76° 35.43' N	20° 37.55' E	122.2	Ice station	Gangway on the ice	
14-4	08.03.03	14:05	76° 35.45' N	20° 37.47' E	122.4	Ice station	Scientists on the ice	
14-4	08.03.03	15:21	76° 35.60' N	20° 37.13' E	124.0	Ice station	Scientists on board	
14-4	08.03.03	15:22	76° 35.60' N	20° 37.13' E	123.1	Ice station	Gangway on board	
14-4	08.03.03	15:27	76° 35.61' N	20° 37.13' E	123.7	Ice station	Departure from floe	
15-1	08.03.03	17:33	76° 38.24' N	20° 6.13' E	205.3	CTD/rosette	surface	
15-1	08.03.03	17:40	76° 38.23' N	20° 6.32' E	206.1	CTD/rosette	at depth	191 m

Station PS64/	Date	Time	PositionLat	PositionLon	Depth [m]	Gear	Action	Comment
15-1	08.03.03	17:47	76° 38.24' N	20° 6.52' E	208.3	CTD/rosette	on deck	
15-2	08.03.03	18:02	76° 38.22' N	20° 6.69' E	207.5	Multiple net	surface	
15-2	08.03.03	18:13	76° 38.21' N	20° 7.33' E	211.1	Multiple net	at depth	210m gesteckt
15-2	08.03.03	18:28	76° 38.21' N	20° 7.47' E	215.5	Multiple net	on deck	
15-3	08.03.03	18:38	76° 38.19' N	20° 7.59' E	215.8	Bongo net	surface	
15-3	08.03.03	18:45	76° 38.15' N	20° 7.94' E	216.5	Bongo net	at depth	190 m
15-3	08.03.03	18:57	76° 38.19' N	20° 8.40' E	217.7	Bongo net	on deck	
15-4	08.03.03	18:59	76° 38.19' N	20° 8.40' E	217.5	Bongo net	surface	
15-4	08.03.03	19:07	76° 38.16' N	20° 8.45' E	217.4	Bongo net	at depth	190 m
15-4	08.03.03	19:19	76° 38.17' N	20° 8.70' E	216.4	Bongo net	on deck	
15-5	08.03.03	19:21	76° 38.17' N	20° 8.81' E	215.3	Bongo net	surface	
15-5	08.03.03	19:29	76° 38.13' N	20° 9.15' E	216.1	Bongo net	at depth	185 m
15-5	08.03.03	19:41	76° 38.13' N	20° 9.14' E	214.6	Bongo net	on deck	
15-6	08.03.03	19:47	76° 38.13' N	20° 9.19' E	214.0	Nansen Net	in the water	
15-6	08.03.03	19:56	76° 38.13' N	20° 9.25' E	213.7	Nansen Net	at depth	185 m
15-6	08.03.03	20:08	76° 38.13' N	20° 9.34' E	211.2	Nansen Net	on Deck	
15-7	08.03.03	20:20	76° 38.12' N	20° 9.42' E	209.0	Multiple net	surface	
15-7	08.03.03	20:28	76° 38.12' N	20° 9.48' E	209.0	Multiple net	at depth	195 m
15-7	08.03.03	20:38	76° 38.11' N	20° 9.54' E	208.2	Multiple net	on deck	
15-8	08.03.03	20:51	76° 38.10' N	20° 9.61' E	206.8	Multi corer	surface	
15-8	08.03.03	20:57	76° 38.09' N	20° 9.63' E	206.7	Multi corer	at sea bottom	200 m
15-8	08.03.03	21:04	76° 38.09' N	20° 9.66' E	207.6	Multi corer	on deck	
16-1	09.03.03	09:03	76° 38.63' N	19° 30.53' E	198.5	CTD/rosette	surface	
16-1	09.03.03	09:11	76° 38.60' N	19° 30.52' E	198.5	CTD/rosette	at depth	186 m
16-1	09.03.03	09:19	76° 38.59' N	19° 30.53' E	199.0	CTD/rosette	on deck	
16-2	09.03.03	09:41	76° 38.58' N	19° 30.49' E	199.2	Ice station	Alongside Floe	
16-2	09.03.03	09:45	76° 38.58' N	19° 30.48' E	199.5	Ice station	Gangway on the ice	
16-2	09.03.03	09:52	76° 38.57' N	19° 30.46' E	199.3	Ice station	Scientists on the ice	
16-2	09.03.03	10:55	76° 38.44' N	19° 30.05' E	206.0	Ice station	Scientists on board	
16-2	09.03.03	10:58	76° 38.43' N	19° 30.01' E	204.6	Ice station	Gangway on board	
16-2	09.03.03	10:59	76° 38.43' N	19° 30.00' E	204.5	Ice station	Departure from floe	
17-1	09.03.03	13:16	76° 38.51' N	19° 21.59' E	198.5	CTD/rosette	surface	
17-1	09.03.03	13:23	76° 38.49' N	19° 21.34' E	197.1	CTD/rosette	at depth	
17-1	09.03.03	13:35	76° 38.47' N	19° 21.02' E	196.3	CTD/rosette	on deck	
18-1	09.03.03	14:29	76° 38.69' N	19° 14.78' E	182.7	CTD/rosette	surface	
18-1	09.03.03	14:35	76° 38.68' N	19° 14.61' E	183.3	CTD/rosette	at depth	
18-1	09.03.03	14:40	76° 38.67' N	19° 14.46' E	182.6	CTD/rosette	on deck	
19-1	09.03.03	15:50	76° 38.51' N	19° 6.64' E	148.2	CTD/rosette	surface	
19-1	09.03.03	15:56	76° 38.50' N	19° 6.50' E	146.7	CTD/rosette	at depth	
19-1	09.03.03	16:04	76° 38.49' N	19° 6.42' E	146.7	CTD/rosette	on deck	
20-1	09.03.03	20:49	76° 38.30' N	19° 0.06' E	128.0	CTD/rosette	surface	
20-1	09.03.03	20:56	76° 38.27' N	19° 0.01' E	128.2	CTD/rosette	at depth	116 m
20-1	09.03.03	21:02	76° 38.26' N	19° 0.00' E	128.3	CTD/rosette	on deck	
21-1	10.03.03	10:45	76° 50.20' N	19° 2.05' E	119.5	CTD/rosette	surface	Schnitt C
21-1	10.03.03	10:54	76° 50.18' N	19° 2.01' E	119.7	CTD/rosette	at depth	109 m
21-1	10.03.03	10:59	76° 50.18' N	19° 2.00' E	119.7	CTD/rosette	on deck	
21-2	10.03.03	11:00	76° 50.18' N	19° 1.99' E	119.6	Ice station	Scientists on the ice	Mummychair Bb achtern
21-3	10.03.03	11:14	76° 50.17' N	19° 1.93' E	118.7	Multi corer	surface	

Station PS64/	Date	Time	PositionLat	PositionLon	Depth [m]	Gear	Action	Comment
21-3	10.03.03	11:16	76° 50.16' N	19° 1.92' E	118.5	Multi corer	at bottom	120 m
21-3	10.03.03	11:22	76° 50.16' N	19° 1.89' E	118.2	Multi corer	on deck	nicht ausgelöst
21-4	10.03.03	11:25	76° 50.16' N	19° 1.88' E	117.2	Multi corer	surface	
21-4	10.03.03	11:29	76° 50.15' N	19° 1.85' E	117.6	Multi corer	at bottom	122 m
21-4	10.03.03	11:33	76° 50.15' N	19° 1.83' E	117.3	Multi corer	on deck	
21-2	10.03.03	11:50	76° 50.12' N	19° 1.72' E	116.2	Ice station	Scientists on board	
21-2	10.03.03	11:51	76° 50.12' N	19° 1.71' E	116.3	Ice station	Departure from floe	
22-1	10.03.03	19:51	76° 49.60' N	19° 17.46' E	140.9	CTD/rosette	surface	
22-1	10.03.03	20:05	76° 49.59' N	19° 17.47' E	140.6	CTD/rosette	at depth	118 m - Sensore failure - Abbruch
22-1	10.03.03	20:11	76° 49.58' N	19° 17.48' E	140.8	CTD/rosette	on deck	sensors not working - cancelled
22-2	10.03.03	20:37	76° 49.52' N	19° 17.56' E	142.5	CTD/rosette	surface	
22-2	10.03.03	20:42	76° 49.53' N	19° 17.54' E	142.2	CTD/rosette	at depth	127 m
22-2	10.03.03	20:50	76° 49.53' N	19° 17.54' E	141.2	CTD/rosette	on deck	
22-3	10.03.03	20:54	76° 49.53' N	19° 17.54' E	141.0	Mini corer	surface	
22-3	10.03.03	20:58	76° 49.52' N	19° 17.54' E	141.5	Mini corer	at bottom	135 m
22-3	10.03.03	21:02	76° 49.52' N	19° 17.54' E	141.3	Mini corer	on deck	leer
22-4	10.03.03	21:03	76° 49.52' N	19° 17.54' E	141.2	Multi corer	surface	
22-4	10.03.03	21:08	76° 49.52' N	19° 17.53' E	140.8	Multi corer	at bottom	140 m
22-4	10.03.03	21:12	76° 49.51' N	19° 17.53' E	140.8	Multi corer	on deck	
23-1	11.03.03	06:45	76° 50.04' N	19° 24.82' E	167.3	Mooring	surface	Gewicht, Auslöser, Microcat, RCM8, TR7, Beginn T-seit 0626 hrs
23-1	11.03.03	06:49	76° 50.04' N	19° 24.82' E	166.4	Mooring	surface	Microcat
23-1	11.03.03	07:19	76° 50.04' N	19° 24.82' E	167.4	Mooring	surface	RCM 4, 2 Benthos, Ende T-Kette, Toppkugel + Schwimmleine
23-1	11.03.03	07:19	76° 50.04' N	19° 24.82' E	167.4	Mooring	slipped	
24-1	11.03.03	10:30	76° 49.67' N	19° 30.21' E	5440.0	Ice station	Alongside Floe	
24-1	11.03.03	10:37	76° 49.67' N	19° 30.22' E	6582.0	Ice station	Scientists on the ice	
24-1	11.03.03	11:21	76° 49.68' N	19° 30.22' E	8850.0	Ice station	Scientists on board	
24-1	11.03.03	11:27	76° 49.68' N	19° 30.22' E	9223.0	Ice station	Departure from floe	
24-2	11.03.03	12:14	76° 49.65' N	19° 30.31' E	163.2	CTD/rosette	surface	
24-2	11.03.03	12:20	76° 49.65' N	19° 30.30' E	163.2	CTD/rosette	at depth	
24-2	11.03.03	12:58	76° 49.67' N	19° 30.12' E	163.6	CTD/rosette	on deck	
24-3	11.03.03	13:15	76° 49.66' N	19° 30.14' E	166.7	Multi corer	surface	
24-3	11.03.03	13:19	76° 49.66' N	19° 30.11' E	167.2	Multi corer	at bottom	
24-3	11.03.03	13:25	76° 49.67' N	19° 30.10' E	166.0	Multi corer	on deck	

Station PS64/	Date	Time	PositionLat	PositionLon	Depth [m]	Gear	Action	Comment
25-1	11.03.03	17:59	76° 50.11' N	19° 43.63' E	166.2	CTD/rosette	surface	
25-1	11.03.03	18:06	76° 50.12' N	19° 43.62' E	166.8	CTD/rosette	at depth	155m gesteckt
25-1	11.03.03	18:14	76° 50.11' N	19° 43.62' E	166.6	CTD/rosette	on deck	
25-2	11.03.03	18:26	76° 50.12' N	19° 43.62' E	166.3	Nansen Net	in the water	
25-2	11.03.03	18:34	76° 50.12' N	19° 43.62' E	165.8	Nansen Net	at depth	150 m
25-2	11.03.03	18:44	76° 50.12' N	19° 43.62' E	166.0	Nansen Net	on Deck	
25-2	11.03.03	18:46	76° 50.12' N	19° 43.62' E	165.8	Nansen Net	in the water	
25-2	11.03.03	18:54	76° 50.12' N	19° 43.62' E	166.5	Nansen Net	at depth	145 m
25-2	11.03.03	19:03	76° 50.12' N	19° 43.62' E	167.0	Nansen Net	on Deck	
25-3	11.03.03	19:14	76° 50.12' N	19° 43.62' E	166.0	Multi corer	surface	
25-3	11.03.03	19:19	76° 50.12' N	19° 43.62' E	166.0	Multi corer	at bottom	161 m
25-3	11.03.03	19:24	76° 50.12' N	19° 43.62' E	166.0	Multi corer	on deck	
26-1	12.03.03	02:27	76° 50.04' N	19° 55.58' E	165.5	CTD/rosette	surface	
26-1	12.03.03	02:34	76° 50.04' N	19° 55.61' E	166.3	CTD/rosette	at depth	
26-1	12.03.03	02:43	76° 50.04' N	19° 55.63' E	165.6	CTD/rosette	on deck	
26-2	12.03.03	02:55	76° 50.04' N	19° 55.62' E	166.4	Multi corer	surface	
26-2	12.03.03	03:00	76° 50.04' N	19° 55.62' E	165.9	Multi corer	at bottom	
26-2	12.03.03	03:05	76° 50.04' N	19° 55.62' E	165.9	Multi corer	on deck	
27-1	12.03.03	07:12	76° 49.37' N	20° 11.18' E	165.1	CTD/rosette	surface	
27-1	12.03.03	07:16	76° 49.37' N	20° 11.22' E	165.3	CTD/rosette	Information	Hieven und anschließendes Fieren wg. Problemen mit CTD
27-1	12.03.03	07:22	76° 49.37' N	20° 11.22' E	165.0	CTD/rosette	surface	151 m
27-1	12.03.03	07:30	76° 49.37' N	20° 11.26' E	168.0	CTD/rosette	on deck	
28-1	12.03.03	08:20	0° 0.00' N	0° 0.00' E	0.0	Ice station	Alongside Floe	
28-1	12.03.03	08:34	76° 48.71' N	20° 12.68' E	167.0	Ice station	Gangway on the ice	
28-1	12.03.03	08:40	76° 48.70' N	20° 12.73' E	167.9	Ice station	Scientists on the ice	
28-2	12.03.03	09:45	76° 48.66' N	20° 13.38' E	178.3	Turbulenzmesssystem	Start	
28-3	12.03.03	13:09	76° 48.29' N	20° 15.02' E	177.1	Bongo net	surface	
28-3	12.03.03	13:31	76° 48.24' N	20° 14.98' E	176.0	Bongo net	at depth	
28-3	12.03.03	13:39	76° 48.23' N	20° 14.97' E	177.4	Bongo net	on deck	
28-4	12.03.03	13:55	76° 48.20' N	20° 14.91' E	175.6	Multiple net	surface	
28-4	12.03.03	14:00	76° 48.19' N	20° 14.89' E	176.0	Multiple net	at depth	
28-4	12.03.03	14:01	76° 48.19' N	20° 14.88' E	175.5	Multiple net	Hoisting	
28-4	12.03.03	14:09	76° 48.17' N	20° 14.84' E	175.1	Multiple net	on deck	
28-1	12.03.03	16:36	76° 48.11' N	20° 13.89' E	166.7	Ice station	Gangway on board	Mummy Chair stand by für 2 Forscher auf dem Eis
28-1	12.03.03	17:18	76° 48.15' N	20° 13.54' E	166.0	Ice station	Scientists on board	
28-2	12.03.03	20:50	76° 48.46' N	20° 13.32' E	170.4	Turbulenzmesssystem	End of measurement	wegen ungünstiger Windrichtung Mast eingenommen
28-1	12.03.03	23:10	76° 48.64' N	20° 13.61' E	173.6	Ice station	Scientists on the ice	2 Leute bewaffnet zum betanken des Aggrates

Station PS64/	Date	Time	PositionLat	PositionLon	Depth [m]	Gear	Action	Comment
28-1	12.03.03	23:48	76° 48.71' N	20° 13.53' E	170.3	Ice station	Scientists on board	
28-1	13.03.03	12:30	76° 49.31' N	19° 55.17' E	162.1	Ice station	Alongside Floe	
28-1	13.03.03	13:18	76° 48.98' N	19° 53.71' E	163.8	Ice station	Gangway on the ice	
28-1	13.03.03	13:22	76° 48.96' N	19° 53.58' E	162.2	Ice station	Scientists on the ice	
28-1	13.03.03	16:19	76° 47.82' N	19° 48.61' E	158.1	Ice station	Scientists on board	
28-1	13.03.03	16:40	76° 47.72' N	19° 48.11' E	158.5	Ice station	Departure from floe	
29-1	14.03.03	01:50	76° 49.99' N	20° 22.65' E	129.7	CTD/rosette	surface	
29-1	14.03.03	01:55	76° 49.99' N	20° 22.64' E	129.9	CTD/rosette	at depth	
29-1	14.03.03	02:04	76° 49.98' N	20° 22.60' E	129.5	CTD/rosette	on deck	
29-2	14.03.03	02:13	76° 49.98' N	20° 22.57' E	129.7	Multi corer	surface	
29-2	14.03.03	02:16	76° 49.98' N	20° 22.56' E	130.2	Multi corer	at bottom	
29-2	14.03.03	02:20	76° 49.98' N	20° 22.55' E	129.5	Multi corer	on deck	
29-3	14.03.03	02:22	76° 49.98' N	20° 22.54' E	129.8	Multi corer	surface	
29-3	14.03.03	02:26	76° 49.98' N	20° 22.52' E	130.0	Multi corer	at bottom	
29-3	14.03.03	02:30	76° 49.98' N	20° 22.50' E	129.8	Multi corer	on deck	
30-1	14.03.03	09:01	76° 54.89' N	20° 20.90' E	129.2	CTD/rosette	surface	
30-1	14.03.03	09:06	76° 54.89' N	20° 20.95' E	129.6	CTD/rosette	at depth	118 m
30-1	14.03.03	09:13	76° 54.90' N	20° 21.02' E	128.3	CTD/rosette	on deck	
31-1	14.03.03	16:39	76° 59.60' N	20° 21.81' E	118.3	Multi corer	surface	
31-1	14.03.03	16:42	76° 59.60' N	20° 21.76' E	117.2	Multi corer	at bottom	115 m
31-1	14.03.03	16:46	76° 59.60' N	20° 21.69' E	117.9	Multi corer	surface	nicht ausgelöst - 2. Versuch
31-1	14.03.03	16:49	76° 59.60' N	20° 21.64' E	117.5	Multi corer	at bottom	120 m
31-1	14.03.03	16:54	76° 59.60' N	20° 21.56' E	117.7	Multi corer	on deck	
31-2	14.03.03	17:19	76° 59.63' N	20° 21.15' E	119.1	CTD/rosette	surface	
31-2	14.03.03	17:24	76° 59.64' N	20° 21.08' E	119.2	CTD/rosette	at depth	108 m
31-2	14.03.03	17:31	76° 59.65' N	20° 20.96' E	119.3	CTD/rosette	on deck	
32-1	14.03.03	23:49	77° 4.79' N	20° 22.59' E	91.5	CTD/rosette	surface	
32-1	14.03.03	23:54	77° 4.79' N	20° 22.64' E	91.3	CTD/rosette	at depth	81 m
32-1	15.03.03	00:00	77° 4.77' N	20° 22.72' E	90.2	CTD/rosette	on deck	
33-1	15.03.03	02:50	77° 9.85' N	20° 22.83' E	113.3	CTD/rosette	surface	
33-1	15.03.03	02:55	77° 9.84' N	20° 22.89' E	113.7	CTD/rosette	at depth	
33-1	15.03.03	03:04	77° 9.84' N	20° 22.99' E	113.3	CTD/rosette	on deck	
34-1	15.03.03	08:08	77° 13.03' N	20° 27.67' E	90.4	CTD/rosette	surface	
34-1	15.03.03	08:22	77° 13.05' N	20° 27.77' E	90.8	CTD/rosette	at depth	83 m
34-1	15.03.03	08:26	77° 13.05' N	20° 27.81' E	90.7	CTD/rosette	on deck	
34-2	15.03.03	08:42	77° 13.06' N	20° 27.97' E	90.7	Multi corer	surface	
34-2	15.03.03	08:46	77° 13.07' N	20° 28.01' E	91.9	Multi corer	at bottom	97 m
34-2	15.03.03	08:50	77° 13.07' N	20° 28.06' E	92.1	Multi corer	on deck	
35-1	15.03.03	16:20	77° 23.08' N	20° 26.97' E	30.5	Turbulenzmesssystem	Start	
35-1	15.03.03	22:24	77° 24.34' N	20° 18.18' E	97.2	Turbulenzmesssystem	End	Recovery of Ice Mast from floe
36-1	16.03.03	04:30	77° 28.99' N	20° 16.65' E	113.9	Rectangular midwater trawl	surface	
36-1	16.03.03	04:34	77° 29.08' N	20° 16.09' E	125.2	Rectangular midwater trawl	Begin Trawling	

Station PS64/	Date	Time	PositionLat	PositionLon	Depth [m]	Gear	Action	Comment
36-1	16.03.03	04:54	77° 29.36' N	20° 13.30' E	134.8	Rectangular midwater trawl	End of Trawl	
36-1	16.03.03	04:57	77° 29.38' N	20° 12.83' E	135.2	Rectangular midwater trawl	on deck	
36-2	16.03.03	05:18	77° 29.38' N	20° 10.40' E	134.4	Agassiz trawl	surface	
36-2	16.03.03	05:32	77° 29.44' N	20° 13.20' E	136.1	Agassiz trawl	start trawl	450 m Draht
36-2	16.03.03	05:47	77° 29.30' N	20° 14.95' E	134.7	Agassiz trawl	Start hoisting	
36-2	16.03.03	05:59	77° 29.18' N	20° 16.02' E	129.5	Agassiz trawl	Stop Trawl	
36-2	16.03.03	05:59	77° 29.18' N	20° 16.02' E	129.5	Agassiz trawl	off ground	
36-2	16.03.03	06:05	77° 29.11' N	20° 16.59' E	123.1	Agassiz trawl	on deck	
37-1	16.03.03	10:56	77° 34.66' N	20° 33.44' E	72.1	CTD/rosette	surface	
37-1	16.03.03	11:00	77° 34.66' N	20° 33.45' E	71.5	CTD/rosette	at depth	65 m
37-1	16.03.03	11:04	77° 34.66' N	20° 33.45' E	71.9	CTD/rosette	on deck	
37-2	16.03.03	11:12	77° 34.66' N	20° 33.41' E	71.7	Trap, fish	surface	
37-2	16.03.03	11:17	77° 34.66' N	20° 33.39' E	71.7	Trap, fish	at sea bottom	rote Fahne , UKW Sender, 65 m
37-2	16.03.03	11:18	77° 34.66' N	20° 33.39' E	71.9	Trap, fish	Hydrophon to the water	
37-2	16.03.03	11:19	77° 34.66' N	20° 33.39' E	71.8	Trap, fish	released	
37-2	16.03.03	11:21	77° 34.66' N	20° 33.39' E	71.9	Trap, fish	Releaser on Deck	
38-1	16.03.03	11:49	77° 34.05' N	20° 30.17' E	79.3	CTD/rosette	surface	
38-1	16.03.03	11:53	77° 34.05' N	20° 30.19' E	79.1	CTD/rosette	at depth	74 m
38-1	16.03.03	12:00	77° 34.04' N	20° 30.19' E	79.3	CTD/rosette	on deck	
38-2	16.03.03	12:07	77° 34.04' N	20° 30.20' E	79.5	Trap, fish	surface	
38-2	16.03.03	12:10	77° 34.04' N	20° 30.21' E	79.8	Trap, fish	at bottom	
38-2	16.03.03	12:12	77° 34.04' N	20° 30.22' E	79.5	Trap, fish	released	
38-2	16.03.03	12:13	77° 34.04' N	20° 30.22' E	79.5	Trap, fish	Releaser on Deck	
39-1	16.03.03	14:52	77° 33.01' N	20° 21.61' E	123.3	Ice station	Alongside Floe	
39-1	16.03.03	14:58	77° 33.01' N	20° 21.62' E	124.0	Ice station	Gangway on the ice	
39-1	16.03.03	15:08	77° 33.01' N	20° 21.62' E	122.7	Ice station	Scientists on the ice	
39-1	16.03.03	18:30	77° 32.98' N	20° 21.61' E	122.2	Ice station	Scientists on board	
39-2	17.03.03	00:41	77° 32.40' N	20° 18.58' E	113.3	CTD/rosette	surface	
39-2	17.03.03	00:47	77° 32.36' N	20° 18.61' E	112.8	CTD/rosette	at depth	
39-2	17.03.03	00:53	77° 32.33' N	20° 18.64' E	114.1	CTD/rosette	on deck	
39-3	17.03.03	01:43	77° 32.03' N	20° 18.91' E	112.3	Multiple net	surface	
39-3	17.03.03	01:47	77° 32.01' N	20° 18.94' E	111.2	Multiple net	at depth	
39-3	17.03.03	01:48	77° 32.00' N	20° 18.95' E	110.0	Multiple net	Hoisting	
39-3	17.03.03	01:53	77° 31.97' N	20° 18.99' E	109.4	Multiple net	on deck	
39-4	17.03.03	02:15	77° 31.86' N	20° 19.12' E	108.8	Bongo net	surface	
39-4	17.03.03	02:22	77° 31.82' N	20° 19.17' E	108.9	Bongo net	at depth	
39-4	17.03.03	02:28	77° 31.79' N	20° 19.20' E	108.3	Bongo net	on deck	

Station PS64/	Date	Time	PositionLat	PositionLon	Depth [m]	Gear	Action	Comment
39-5	17.03.03	02:32	77° 31.78' N	20° 19.22' E	108.9	Bongo net	surface	
39-5	17.03.03	02:36	77° 31.76' N	20° 19.25' E	109.1	Bongo net	at depth	
39-5	17.03.03	02:40	77° 31.74' N	20° 19.26' E	110.0	Bongo net	on deck	
39-6	17.03.03	02:45	77° 31.72' N	20° 19.28' E	109.6	Nansen Net	in the water	
39-6	17.03.03	02:51	77° 31.70' N	20° 19.29' E	110.0	Nansen Net	at depth	
39-6	17.03.03	02:57	77° 31.67' N	20° 19.31' E	111.7	Nansen Net	on Deck	
39-7	17.03.03	02:59	77° 31.67' N	20° 19.31' E	110.7	Nansen Net	in the water	
39-7	17.03.03	03:04	77° 31.65' N	20° 19.34' E	110.5	Nansen Net	at depth	
39-7	17.03.03	03:10	77° 31.63' N	20° 19.38' E	111.1	Nansen Net	on Deck	
39-7	17.03.03	03:25	77° 31.58' N	20° 19.47' E	112.0	Multi corer	surface	
39-7	17.03.03	03:27	77° 31.58' N	20° 19.48' E	111.6	Multi corer	at sea bottom	
39-7	17.03.03	03:33	77° 31.57' N	20° 19.51' E	111.6	Multi corer	on deck	
39-1	17.03.03	06:10	77° 31.53' N	20° 20.20' E	115.2	Ice station	Gangway on the ice	
39-1	17.03.03	08:04	77° 31.78' N	20° 20.24' E	112.2	Ice station	Scientists on the ice	
39-1	17.03.03	13:22	77° 32.33' N	20° 20.33' E	125.5	Ice station	Scientists on board	
39-1	17.03.03	13:32	77° 32.32' N	20° 20.39' E	126.8	Ice station	Gangway on board	
39-1	17.03.03	13:36	77° 32.32' N	20° 20.48' E	126.8	Ice station	Departure from floe	
38-2	17.03.03	16:04	77° 34.04' N	20° 30.15' E	79.2	Trap, fish	Hydrophon to the water	
38-2	17.03.03	16:14	77° 34.07' N	20° 30.25' E	78.7	Trap, fish	on deck	
37-2	17.03.03	16:45	77° 34.66' N	20° 33.30' E	72.2	Trap, fish	Hydrophon to the water	
37-2	17.03.03	16:49	77° 34.67' N	20° 33.34' E	71.8	Trap, fish	Hydrophon out of the water	no answer
37-2	17.03.03	16:51	77° 34.67' N	20° 33.31' E	71.8	Trap, fish	Hydrophon to the water	
37-2	17.03.03	16:53	77° 34.67' N	20° 33.29' E	72.3	Trap, fish	Hydrophon out of the water	no answer from trap
37-2	17.03.03	17:04	77° 34.63' N	20° 33.19' E	71.4	Trap, fish	Hydrophon to the water	different hydrophon
37-2	17.03.03	17:08	77° 34.63' N	20° 33.19' E	71.1	Trap, fish	Hydrophon out of the water	
37-2	17.03.03	17:17	77° 34.64' N	20° 33.16' E	73.1	Trap, fish	on deck	
40-1	17.03.03	18:32	77° 35.09' N	20° 26.35' E	116.6	Turbulenzmesssystem	Start	
40-1	17.03.03	20:24	77° 35.55' N	20° 30.51' E	101.7	Turbulenzmesssystem	End	
41-1	17.03.03	21:56	77° 40.20' N	20° 29.76' E	61.0	CTD/rosette	surface	
41-1	17.03.03	22:02	77° 40.20' N	20° 29.69' E	61.2	CTD/rosette	at depth	56 m
41-1	17.03.03	22:06	77° 40.20' N	20° 29.67' E	61.9	CTD/rosette	on deck	
41-2	17.03.03	22:13	77° 40.21' N	20° 29.66' E	61.1	Multi corer	surface	
41-2	17.03.03	22:16	77° 40.21' N	20° 29.66' E	61.4	Multi corer	at bottom	63 m
41-2	17.03.03	22:20	77° 40.20' N	20° 29.65' E	61.8	Multi corer	on deck	
42-1	17.03.03	23:24	77° 37.60' N	20° 24.58' E	87.4	CTD/rosette	surface	
42-1	17.03.03	23:31	77° 37.60' N	20° 24.54' E	87.3	CTD/rosette	at depth	80 m
42-1	17.03.03	23:35	77° 37.60' N	20° 24.55' E	87.3	CTD/rosette	on deck	
43-1	18.03.03	00:13	77° 36.86' N	20° 15.69' E	128.3	CTD/rosette	surface	

Station PS64/	Date	Time	PositionLat	PositionLon	Depth [m]	Gear	Action	Comment
43-1	18.03.03	00:18	77° 36.84' N	20° 15.64' E	128.1	CTD/rosette	at depth	
43-1	18.03.03	00:24	77° 36.83' N	20° 15.58' E	129.1	CTD/rosette	on deck	
44-1	18.03.03	01:01	77° 35.69' N	20° 6.96' E	96.4	CTD/rosette	surface	
44-1	18.03.03	01:07	77° 35.66' N	20° 6.91' E	96.7	CTD/rosette	at depth	
44-1	18.03.03	01:09	77° 35.66' N	20° 6.91' E	96.8	CTD/rosette	on deck	
45-1	18.03.03	01:39	77° 34.28' N	20° 0.38' E	139.0	CTD/rosette	surface	
45-1	18.03.03	01:45	77° 34.26' N	20° 0.31' E	138.5	CTD/rosette	at depth	
45-1	18.03.03	01:52	77° 34.22' N	20° 0.24' E	139.4	CTD/rosette	on deck	
46-1	18.03.03	02:44	77° 32.43' N	19° 49.25' E	105.1	CTD/rosette	surface	
46-1	18.03.03	02:50	77° 32.41' N	19° 49.19' E	106.4	CTD/rosette	on deck	
46-1	18.03.03	02:52	77° 32.41' N	19° 49.17' E	107.2	CTD/rosette	surface	
46-1	18.03.03	02:57	77° 32.39' N	19° 49.15' E	108.3	CTD/rosette	at depth	
46-1	18.03.03	03:00	77° 32.39' N	19° 49.12' E	109.8	CTD/rosette	on deck	
47-1	18.03.03	04:16	77° 31.17' N	19° 26.97' E	154.1	CTD/rosette	surface	
47-1	18.03.03	04:23	77° 31.15' N	19° 26.92' E	154.4	CTD/rosette	at depth	140 m
47-1	18.03.03	04:32	77° 31.13' N	19° 26.76' E	154.8	CTD/rosette	on deck	
48-1	18.03.03	06:17	77° 29.97' N	19° 9.99' E	195.3	CTD/rosette	surface	
48-1	18.03.03	06:27	77° 29.95' N	19° 9.77' E	186.9	CTD/rosette	at depth	171 m
48-1	18.03.03	06:42	77° 29.93' N	19° 9.38' E	188.1	CTD/rosette	on deck	
48-2	18.03.03	06:54	77° 29.91' N	19° 9.08' E	188.2	Multiple net	surface	
48-2	18.03.03	07:02	77° 29.90' N	19° 8.84' E	188.8	Multiple net	at depth	168 m
48-2	18.03.03	07:12	77° 29.88' N	19° 8.54' E	188.5	Multiple net	on deck	
48-3	18.03.03	07:27	77° 29.84' N	19° 8.12' E	188.4	Multiple net	surface	
48-3	18.03.03	07:34	77° 29.83' N	19° 7.93' E	188.4	Multiple net	at depth	171 m
48-3	18.03.03	07:45	77° 29.80' N	19° 7.61' E	188.5	Multiple net	on deck	
48-4	18.03.03	07:56	77° 29.77' N	19° 7.30' E	191.3	Bongo net	surface	
48-4	18.03.03	08:07	77° 29.73' N	19° 6.98' E	189.2	Bongo net	at depth	165 m
48-4	18.03.03	08:15	77° 29.70' N	19° 6.74' E	190.5	Bongo net	on deck	
48-5	18.03.03	08:17	77° 29.70' N	19° 6.68' E	189.7	Bongo net	surface	
48-5	18.03.03	08:25	77° 29.67' N	19° 6.44' E	191.0	Bongo net	at depth	165 m
48-5	18.03.03	08:34	77° 29.63' N	19° 6.17' E	192.1	Bongo net	on deck	
48-6	18.03.03	08:42	77° 29.60' N	19° 5.90' E	193.3	Nansen Net	in the water	
48-6	18.03.03	08:51	77° 29.56' N	19° 5.61' E	192.8	Nansen Net	at depth	165 m
48-6	18.03.03	09:02	77° 29.51' N	19° 5.25' E	192.8	Nansen Net	on Deck	
48-7	18.03.03	09:13	77° 29.47' N	19° 4.91' E	192.6	Multi corer	surface	
48-7	18.03.03	09:19	77° 29.45' N	19° 4.68' E	188.4	Multi corer	at bottom	183 m
48-7	18.03.03	09:25	77° 29.42' N	19° 4.43' E	187.1	Multi corer	on deck	
49-1	18.03.03	11:41	77° 28.19' N	18° 51.75' E	165.0	CTD/rosette	surface	
49-1	18.03.03	11:48	77° 28.13' N	18° 51.57' E	165.0	CTD/rosette	at depth	152 m
49-1	18.03.03	11:56	77° 28.06' N	18° 51.38' E	165.7	CTD/rosette	on deck	
50-1	18.03.03	13:38	77° 27.55' N	18° 32.04' E	104.3	CTD/rosette	surface	
50-1	18.03.03	13:43	77° 27.49' N	18° 31.96' E	105.2	CTD/rosette	at depth	
50-1	18.03.03	13:51	77° 27.39' N	18° 31.84' E	103.9	CTD/rosette	on deck	
50-2	18.03.03	14:06	77° 27.25' N	18° 31.58' E	99.2	Multi corer	surface	
50-2	18.03.03	14:09	77° 27.18' N	18° 31.47' E	98.2	Multi corer	at bottom	
50-2	18.03.03	14:12	77° 27.16' N	18° 31.43' E	97.7	Multi corer	on deck	
51-1	18.03.03	19:02	77° 27.78' N	19° 31.56' E	139.0	CTD/rosette	surface	
51-1	18.03.03	19:09	77° 27.74' N	19° 31.41' E	137.1	CTD/rosette	at depth	142 m
51-1	18.03.03	19:15	77° 27.72' N	19° 31.26' E	136.7	CTD/rosette	on deck	
52-1	18.03.03	20:45	77° 26.19' N	19° 47.67' E	140.0	CTD/rosette	surface	
52-1	18.03.03	20:53	77° 26.17' N	19° 47.50' E	139.3	CTD/rosette	at depth	127 m
52-1	18.03.03	21:00	77° 26.15' N	19° 47.36' E	140.1	CTD/rosette	on deck	
53-1	19.03.03	02:29	77° 26.15' N	20° 14.97' E	131.4	CTD/rosette	surface	
53-1	19.03.03	02:35	77° 26.09' N	20° 15.09' E	132.2	CTD/rosette	at depth	
53-1	19.03.03	02:39	77° 26.05' N	20° 15.15' E	132.0	CTD/rosette	on deck	
54-1	19.03.03	03:09	77° 25.93' N	20° 28.71' E	69.4	CTD/rosette	surface	

Station PS64/	Date	Time	PositionLat	PositionLon	Depth [m]	Gear	Action	Comment
54-1	19.03.03	03:13	77° 25.87' N	20° 28.82' E	68.3	CTD/rosette	at depth	
54-1	19.03.03	03:16	77° 25.82' N	20° 28.88' E	68.1	CTD/rosette	on deck	
55-1	19.03.03	03:53	77° 22.66' N	20° 16.15' E	89.4	CTD/rosette	surface	
55-1	19.03.03	04:05	77° 22.55' N	20° 16.50' E	82.8	CTD/rosette	surface	77 m
55-1	19.03.03	04:10	77° 22.50' N	20° 16.60' E	80.6	CTD/rosette	on deck	
56-1	19.03.03	04:55	77° 19.51' N	20° 15.84' E	95.8	CTD/rosette	surface	
56-1	19.03.03	05:00	77° 19.48' N	20° 15.95' E	95.6	CTD/rosette	at depth	88 m
56-1	19.03.03	05:03	77° 19.48' N	20° 16.02' E	96.0	CTD/rosette	on deck	
57-1	19.03.03	05:45	77° 16.58' N	20° 19.03' E	147.1	CTD/rosette	surface	
57-1	19.03.03	05:49	77° 16.56' N	20° 19.16' E	144.5	CTD/rosette	surface	66 m
57-1	19.03.03	05:51	77° 16.55' N	20° 19.19' E	140.9	CTD/rosette	on deck	
57-2	19.03.03	06:21	77° 16.14' N	20° 18.02' E	203.4	CTD/rosette	surface	
57-2	19.03.03	06:34	77° 16.10' N	20° 18.04' E	202.4	CTD/rosette	at depth	Tiefensensor daneben: 102 m Draht 94m
57-2	19.03.03	06:39	77° 16.08' N	20° 18.05' E	201.4	CTD/rosette	on deck	
57-3	19.03.03	06:56	77° 16.04' N	20° 18.02' E	101.1	Mooring	surface	Ankerstein, Releaser, Seacat 3024, RCM 7 11295, 4 Benthos
57-3	19.03.03	07:04	77° 16.03' N	20° 17.99' E	100.4	Mooring	surface	Microcat 2719
57-3	19.03.03	07:12	77° 16.03' N	20° 17.96' E	100.1	Mooring	surface	40 m Meteor, RCM 4 207, 2 Benthos, 5 m Meteor, Toppkugel mit Schwimmleine
57-3	19.03.03	07:14	77° 16.02' N	20° 17.95' E	99.7	Mooring	slipped	
58-1	19.03.03	09:18	77° 17.12' N	20° 8.47' E	127.8	CTD/rosette	surface	
58-1	19.03.03	09:26	77° 17.15' N	20° 8.32' E	127.2	CTD/rosette	at depth	117 m
58-1	19.03.03	09:30	77° 17.17' N	20° 8.24' E	126.1	CTD/rosette	on deck	
59-1	19.03.03	12:02	77° 16.14' N	19° 59.65' E	140.8	CTD/rosette	surface	
59-1	19.03.03	12:07	77° 16.15' N	19° 59.68' E	139.2	CTD/rosette	at depth	
59-1	19.03.03	12:16	77° 16.15' N	19° 59.75' E	137.7	CTD/rosette	on deck	
60-1	19.03.03	14:25	77° 14.41' N	19° 45.50' E	137.3	CTD/rosette	surface	
60-1	19.03.03	14:31	77° 14.38' N	19° 45.63' E	136.4	CTD/rosette	at depth	
60-1	19.03.03	14:36	77° 14.35' N	19° 45.71' E	136.3	CTD/rosette	on deck	
61-1	19.03.03	18:02	77° 15.09' N	19° 32.20' E	178.5	CTD/rosette	surface	
61-1	19.03.03	18:08	77° 15.07' N	19° 32.14' E	179.6	CTD/rosette	at depth	163m gesteckt
61-1	19.03.03	18:16	77° 15.05' N	19° 32.18' E	175.7	CTD/rosette	on deck	
62-1	19.03.03	19:16	77° 11.98' N	19° 17.63' E	176.1	CTD/rosette	surface	
62-1	19.03.03	19:22	77° 12.01' N	19° 17.56' E	176.4	CTD/rosette	at depth	169 m
62-1	19.03.03	19:33	77° 12.03' N	19° 17.55' E	176.8	CTD/rosette	on deck	
62-2	19.03.03	19:40	77° 12.06' N	19° 17.48' E	176.7	Mooring	surface	Ankerstein, Releaser 200, Microcat 2721, RCM 7 11297, TR7, 4 Benthos
62-2	19.03.03	20:04	77° 12.10' N	19° 17.36' E	177.6	Mooring	surface	RCM 5, 2 Benthos, Toppkugel, Schwimmleine
62-2	19.03.03	20:06	77° 12.10' N	19° 17.34' E	177.5	Mooring	slipped	

Station PS64/	Date	Time	PositionLat	PositionLon	Depth [m]	Gear	Action	Comment
62-3	19.03.03	20:23	77° 12.04' N	19° 17.23' E	175.9	Water Sample Bucket	into the water	vom Bugkran
62-4	19.03.03	20:38	77° 11.88' N	19° 16.79' E	176.9	Multiple net	surface	
62-4	19.03.03	20:49	77° 11.91' N	19° 16.66' E	176.6	Multiple net	at depth	163 m
62-4	19.03.03	21:02	77° 11.94' N	19° 16.47' E	178.7	Multiple net	on deck	
62-5	19.03.03	21:10	77° 11.97' N	19° 16.40' E	177.8	Multiple net	surface	
62-6	19.03.03	21:16	77° 11.99' N	19° 16.32' E	176.5	Turbulenzmesssystem	Start	
62-5	19.03.03	21:19	77° 12.00' N	19° 16.26' E	178.0	Multiple net	at depth	161 m
62-5	19.03.03	21:27	77° 12.01' N	19° 16.13' E	177.1	Multiple net	on deck	
62-7	19.03.03	21:44	77° 12.05' N	19° 15.84' E	176.8	Bongo net	surface	
62-7	19.03.03	21:52	77° 12.06' N	19° 15.70' E	178.6	Bongo net	at depth	155 m
62-7	19.03.03	21:59	77° 12.08' N	19° 15.62' E	178.8	Bongo net	on deck	
62-8	19.03.03	22:04	77° 12.08' N	19° 15.55' E	176.9	Nansen Net	in the water	
62-8	19.03.03	22:14	77° 12.10' N	19° 15.40' E	177.5	Nansen Net	at depth	160 m
62-6	19.03.03	22:21	77° 12.08' N	19° 15.32' E	177.4	Turbulenzmesssystem	End	wegen fehlenden Wind Abbruch
62-8	19.03.03	22:24	77° 12.10' N	19° 15.26' E	177.8	Nansen Net	on Deck	
62-9	19.03.03	22:32	77° 12.11' N	19° 15.06' E	177.7	Multi corer	surface	
62-9	19.03.03	22:38	77° 12.12' N	19° 14.97' E	177.7	Multi corer	at bottom	171 m
62-9	19.03.03	22:43	77° 12.13' N	19° 14.87' E	176.0	Multi corer	on deck	
63-1	20.03.03	00:59	77° 10.03' N	19° 3.25' E	150.8	CTD/rosette	surface	
63-1	20.03.03	01:05	77° 10.04' N	19° 3.29' E	151.6	CTD/rosette	at depth	
63-1	20.03.03	01:10	77° 10.04' N	19° 3.32' E	151.5	CTD/rosette	on deck	
64-1	20.03.03	03:25	77° 8.99' N	18° 49.90' E	124.9	CTD/rosette	surface	
64-1	20.03.03	03:31	77° 8.98' N	18° 49.94' E	125.3	CTD/rosette	at depth	
64-1	20.03.03	03:42	77° 8.95' N	18° 50.10' E	124.9	CTD/rosette	on deck	
64-2	20.03.03	03:51	77° 8.94' N	18° 50.26' E	124.3	Multi corer	surface	
64-2	20.03.03	03:55	77° 8.93' N	18° 50.30' E	124.5	Multi corer	at bottom	
64-2	20.03.03	03:59	77° 8.92' N	18° 50.34' E	124.8	Multi corer	on deck	
65-1	21.03.03	09:06	76° 49.28' N	19° 24.39' E	162.4	Water Sample Bucket	into the water	
65-1	21.03.03	09:08	76° 49.28' N	19° 24.34' E	162.1	Water Sample Bucket	into the water	
65-2	21.03.03	09:18	76° 49.24' N	19° 24.28' E	161.0	CTD/rosette	surface	
65-2	21.03.03	09:24	76° 49.24' N	19° 24.36' E	161.7	CTD/rosette	at depth	149 m
65-2	21.03.03	09:34	76° 49.25' N	19° 24.51' E	162.2	CTD/rosette	on deck	
66-1	21.03.03	12:11	76° 38.97' N	19° 31.19' E	197.2	CTD/rosette	surface	
66-1	21.03.03	12:18	76° 38.97' N	19° 31.19' E	198.0	CTD/rosette	at depth	
66-1	21.03.03	12:25	76° 38.97' N	19° 31.21' E	198.0	CTD/rosette	on deck	
67-1	22.03.03	08:12	76° 27.93' N	21° 53.83' E	271.8	CTD/rosette	surface	
67-1	22.03.03	08:23	76° 27.80' N	21° 53.73' E	274.9	CTD/rosette	at depth	258 m
67-1	22.03.03	08:30	76° 27.72' N	21° 53.64' E	272.0	CTD/rosette	on deck	
67-2	22.03.03	08:44	76° 27.55' N	21° 53.38' E	270.6	Multiple net	surface	
67-2	22.03.03	08:57	76° 27.40' N	21° 53.08' E	273.1	Multiple net	at depth	251 m
67-2	22.03.03	09:14	76° 27.20' N	21° 52.52' E	275.5	Multiple net	on deck	
67-3	22.03.03	09:24	76° 27.09' N	21° 52.11' E	270.2	Bongo net	surface	
67-3	22.03.03	09:39	76° 26.93' N	21° 51.40' E	269.7	Bongo net	at depth	240 m
67-3	22.03.03	09:50	76° 26.81' N	21° 50.83' E	270.1	Bongo net	on deck	
67-4	22.03.03	09:54	76° 26.76' N	21° 50.62' E	270.8	Bongo net	surface	
67-4	22.03.03	10:10	76° 26.60' N	21° 49.70' E	270.6	Bongo net	at depth	240 m
67-4	22.03.03	10:21	76° 26.49' N	21° 49.01' E	271.6	Bongo net	on deck	

Station PS64/	Date	Time	PositionLat	PositionLon	Depth [m]	Gear	Action	Comment
67-5	22.03.03	10:28	76° 26.42' N	21° 48.55' E	272.4	Nansen Net	in the water	
67-5	22.03.03	10:45	76° 26.27' N	21° 47.40' E	272.1	Nansen Net	at depth	240 m
67-5	22.03.03	10:59	76° 26.14' N	21° 46.42' E	270.4	Nansen Net	on Deck	
67-6	22.03.03	11:09	76° 26.06' N	21° 45.67' E	267.4	Multi corer	surface	
67-6	22.03.03	11:15	76° 26.01' N	21° 45.23' E	266.4	Multi corer	at bottom	260 m
67-6	22.03.03	11:22	76° 25.95' N	21° 44.70' E	265.3	Multi corer	on deck	
68-1	22.03.03	15:24	76° 22.76' N	22° 2.79' E	222.0	Turbulenzmes ssystem	Start	
68-2	22.03.03	15:40	76° 22.73' N	22° 2.58' E	222.2	Bugkran - Seacat	in the water	
68-1	22.03.03	16:17	76° 22.65' N	22° 2.61' E	220.4	Turbulenzmes ssystem	Information	Beginn Drift Richtung Mitte Polynia
68-3	22.03.03	16:31	76° 22.79' N	22° 2.81' E	223.0	Water Sample Bucket	into the water	
68-4	22.03.03	16:40	76° 22.79' N	22° 2.89' E	222.3	CTD/rosette	surface	
68-4	22.03.03	16:47	76° 22.79' N	22° 3.01' E	221.1	CTD/rosette	at depth	206 m
68-4	22.03.03	16:55	76° 22.78' N	22° 3.19' E	220.4	CTD/rosette	on deck	
68-2	22.03.03	17:31	76° 22.63' N	22° 3.93' E	214.5	Bugkran - Seacat	on Deck	
68-1	22.03.03	17:45	76° 22.59' N	22° 4.27' E	210.9	Turbulenzmes ssystem	Information	Verholen mit kleinster Fahrt an Schollenrand bis Mast über dem Eis
68-1	22.03.03	19:17	76° 22.31' N	22° 6.43' E	205.0	Turbulenzmes ssystem	End	
68-5	22.03.03	20:15	76° 22.01' N	22° 7.76' E	198.4	Ice station	Scientists on the ice	
68-5	22.03.03	20:35	76° 21.80' N	22° 7.43' E	197.0	Ice station	Scientists on board	Ice Mast geborgen
69-1	22.03.03	22:04	76° 23.49' N	22° 31.28' E	165.3	CTD/rosette	surface	
69-1	22.03.03	22:10	76° 23.44' N	22° 30.96' E	165.1	CTD/rosette	at depth	154 m
69-1	22.03.03	22:16	76° 23.39' N	22° 30.64' E	163.9	CTD/rosette	on deck	
69-2	22.03.03	22:27	76° 23.28' N	22° 29.82' E	161.3	Multiple net	surface	
69-2	22.03.03	22:35	76° 23.20' N	22° 29.31' E	158.7	Multiple net	at depth	149 m
69-2	22.03.03	22:46	76° 23.15' N	22° 28.60' E	158.5	Multiple net	on deck	
69-3	22.03.03	22:56	76° 23.08' N	22° 27.72' E	159.8	Bongo net	surface	
69-3	22.03.03	23:11	76° 22.99' N	22° 26.52' E	166.1	Bongo net	at depth	145 m
69-3	22.03.03	23:19	76° 22.96' N	22° 25.86' E	169.8	Bongo net	on deck	
69-4	22.03.03	23:23	76° 22.95' N	22° 25.50' E	160.3	Nansen Net	in the water	
69-4	22.03.03	23:33	76° 22.94' N	22° 24.54' E	176.9	Nansen Net	at depth	145 m
69-4	22.03.03	23:45	76° 22.92' N	22° 23.45' E	175.3	Nansen Net	on Deck	
70-1	23.03.03	06:33	76° 18.95' N	23° 16.19' E	60.7	CTD/rosette	surface	
70-1	23.03.03	06:36	76° 18.93' N	23° 16.43' E	61.2	CTD/rosette	at depth	54 m
70-1	23.03.03	06:39	76° 18.91' N	23° 16.66' E	61.2	CTD/rosette	on deck	
70-2	23.03.03	06:49	76° 18.83' N	23° 17.42' E	60.9	Bongo net	surface	
70-2	23.03.03	06:51	76° 18.81' N	23° 17.58' E	60.0	Bongo net	at depth	50 m
70-2	23.03.03	06:56	76° 18.77' N	23° 17.98' E	61.1	Bongo net	on deck	
70-3	23.03.03	06:59	76° 18.73' N	23° 18.20' E	63.9	Nansen Net	in the water	
70-3	23.03.03	07:03	76° 18.70' N	23° 18.48' E	63.6	Nansen Net	at depth	50 m
70-3	23.03.03	07:07	76° 18.65' N	23° 18.76' E	62.4	Nansen Net	on Deck	
70-4	23.03.03	07:09	76° 18.64' N	23° 18.91' E	62.7	Nansen Net	in the water	
70-4	23.03.03	07:14	76° 18.58' N	23° 19.24' E	131.4	Nansen Net	at depth	50 m

Station PS64/	Date	Time	PositionLat	PositionLon	Depth [m]	Gear	Action	Comment
70-4	23.03.03	07:17	76° 18.55' N	23° 19.42' E	117.7	Nansen Net	on Deck	
70-5	23.03.03	07:26	76° 18.45' N	23° 19.96' E	114.1	Multi corer	surface	
70-5	23.03.03	07:29	76° 18.41' N	23° 20.13' E	114.7	Multi corer	at sea bottom	65 m
70-5	23.03.03	07:33	76° 18.37' N	23° 20.36' E	117.1	Multi corer	on deck	
70-6	23.03.03	08:21	76° 17.70' N	23° 21.95' E	145.7	Ice station	Alongside Floe	
70-6	23.03.03	08:45	76° 17.36' N	23° 22.33' E	63.6	Ice station	Gangway on the ice	
70-6	23.03.03	08:53	76° 17.24' N	23° 22.39' E	64.1	Ice station	Scientists on the ice	
70-6	23.03.03	16:51	76° 16.96' N	23° 11.06' E	52.3	Ice station	Scientists on board	
70-6	23.03.03	17:03	76° 17.00' N	23° 11.68' E	54.7	Ice station	Gangway on board	
70-6	23.03.03	17:09	76° 17.01' N	23° 12.05' E	56.8	Ice station	Departure from floe	
70-7	23.03.03	17:10	76° 17.01' N	23° 12.13' E	56.9	Calibration	start	Kalibrierung SIMS über offenem Wasser
70-7	23.03.03	17:19	76° 17.02' N	23° 12.81' E	54.5	Calibration	End	
71-1	24.03.03	00:11	76° 10.01' N	24° 30.84' E	69.3	CTD/rosette	surface	
71-1	24.03.03	00:15	76° 10.01' N	24° 30.56' E	68.4	CTD/rosette	at depth	
71-1	24.03.03	00:20	76° 10.02' N	24° 30.20' E	70.0	CTD/rosette	on deck	
71-2	24.03.03	00:30	76° 10.02' N	24° 29.60' E	66.9	Bongo net	surface	
71-2	24.03.03	00:34	76° 10.03' N	24° 29.34' E	68.0	Bongo net	at depth	
71-2	24.03.03	00:37	76° 10.04' N	24° 29.15' E	68.3	Bongo net	on deck	
71-3	24.03.03	00:40	76° 10.05' N	24° 28.96' E	68.8	Bongo net	surface	
71-3	24.03.03	00:43	76° 10.06' N	24° 28.78' E	68.3	Bongo net	at depth	
71-3	24.03.03	00:47	76° 10.07' N	24° 28.54' E	67.1	Bongo net	on deck	
71-4	24.03.03	00:54	76° 10.09' N	24° 28.12' E	67.5	Nansen Net	in the water	
71-4	24.03.03	00:57	76° 10.11' N	24° 27.95' E	67.4	Nansen Net	at depth	
71-4	24.03.03	01:00	76° 10.12' N	24° 27.78' E	67.4	Nansen Net	on Deck	
71-5	24.03.03	01:04	76° 10.14' N	24° 27.55' E	67.3	Nansen Net	in the water	
71-5	24.03.03	01:07	76° 10.15' N	24° 27.39' E	67.5	Nansen Net	at depth	
71-5	24.03.03	01:11	76° 10.18' N	24° 27.13' E	68.2	Nansen Net	on Deck	
72-1	24.03.03	05:11	76° 5.00' N	25° 17.26' E	93.5	CTD/rosette	surface	
72-1	24.03.03	05:15	76° 5.00' N	25° 17.42' E	94.3	CTD/rosette	at depth	88 m
72-1	24.03.03	05:19	76° 5.00' N	25° 17.59' E	95.6	CTD/rosette	on deck	
72-2	24.03.03	05:29	76° 4.99' N	25° 18.00' E	94.9	Bongo net	surface	
72-2	24.03.03	05:33	76° 4.99' N	25° 18.17' E	96.0	Bongo net	at depth	80 m
72-2	24.03.03	05:38	76° 4.98' N	25° 18.38' E	97.6	Bongo net	on deck	
72-3	24.03.03	05:40	76° 4.97' N	25° 18.47' E	96.1	Bongo net	surface	
72-3	24.03.03	05:44	76° 4.97' N	25° 18.64' E	94.6	Bongo net	at depth	80 m
72-3	24.03.03	05:49	76° 4.96' N	25° 18.85' E	93.1	Bongo net	on deck	
72-4	24.03.03	05:54	76° 4.94' N	25° 19.06' E	93.3	Nansen Net	in the water	
72-4	24.03.03	05:58	76° 4.93' N	25° 19.24' E	94.9	Nansen Net	at depth	80 m
72-4	24.03.03	06:02	76° 4.92' N	25° 19.41' E	92.8	Nansen Net	on Deck	
72-5	24.03.03	06:06	76° 4.91' N	25° 19.59' E	91.1	Nansen Net	in the water	
72-5	24.03.03	06:11	76° 4.89' N	25° 19.82' E	90.1	Nansen Net	at depth	80 m
72-5	24.03.03	06:17	76° 4.87' N	25° 20.09' E	92.6	Nansen Net	on Deck	
72-6	24.03.03	06:26	76° 4.84' N	25° 20.49' E	92.9	Multi corer	surface	
72-6	24.03.03	06:30	76° 4.82' N	25° 20.67' E	93.3	Multi corer	at bottom	96 m
72-6	24.03.03	06:33	76° 4.81' N	25° 20.81' E	94.3	Multi corer	on deck	

Station PS64/	Date	Time	PositionLat	PositionLon	Depth [m]	Gear	Action	Comment
73-1	24.03.03	11:29	75° 58.41' N	25° 36.52' E	127.9	Turbulenzmesssystem	Start	
73-2	24.03.03	13:31	75° 58.07' N	25° 30.69' E	140.6	Eisfischen	start	
73-3	24.03.03	13:32	75° 58.07' N	25° 30.64' E	141.9	Bugkran - Seacat	in the water	
73-3	24.03.03	13:37	75° 58.06' N	25° 30.42' E	142.5	Bugkran - Seacat	on Deck	
73-2	24.03.03	13:50	75° 58.03' N	25° 29.91' E	142.5	Eisfischen	End	
73-1	24.03.03	16:26	75° 58.12' N	25° 26.96' E	128.9	Turbulenzmesssystem	Information	Reference Mast recovered
73-1	24.03.03	18:01	75° 58.65' N	25° 28.35' E	135.5	Turbulenzmesssystem	End	
74-1	24.03.03	21:59	75° 59.79' N	26° 3.97' E	161.0	CTD/rosette	surface	
74-1	24.03.03	22:06	75° 59.73' N	26° 3.94' E	161.9	CTD/rosette	at depth	148 m
74-1	24.03.03	22:14	75° 59.68' N	26° 3.87' E	163.2	CTD/rosette	on deck	
74-2	24.03.03	22:23	75° 59.61' N	26° 3.79' E	164.5	Multiple net	surface	
74-2	24.03.03	22:31	75° 59.54' N	26° 3.70' E	164.7	Multiple net	at depth	152 m
74-2	24.03.03	22:43	75° 59.46' N	26° 3.56' E	164.0	Multiple net	on deck	
74-3	24.03.03	22:51	75° 59.40' N	26° 3.43' E	156.7	Bongo net	surface	
74-3	24.03.03	22:59	75° 59.34' N	26° 3.27' E	156.2	Bongo net	at depth	140 m
74-3	24.03.03	23:06	75° 59.29' N	26° 3.14' E	157.5	Bongo net	on deck	
74-4	24.03.03	23:11	75° 59.26' N	26° 3.05' E	159.1	Nansen Net	in the water	
74-4	24.03.03	23:21	75° 59.19' N	26° 2.81' E	160.8	Nansen Net	at depth	140 m
74-4	24.03.03	23:30	75° 59.13' N	26° 2.61' E	162.3	Nansen Net	on Deck	
75-1	25.03.03	04:45	75° 54.72' N	26° 58.34' E	216.3	CTD/rosette	surface	
75-1	25.03.03	04:53	75° 54.74' N	26° 58.45' E	217.4	CTD/rosette	at depth	206 m
75-1	25.03.03	05:01	75° 54.75' N	26° 58.60' E	217.8	CTD/rosette	on deck	
75-2	25.03.03	05:10	75° 54.76' N	26° 58.79' E	219.2	Multiple net	surface	
75-2	25.03.03	05:20	75° 54.79' N	26° 58.97' E	220.1	Multiple net	at depth	205 m
75-2	25.03.03	05:35	75° 54.82' N	26° 59.32' E	223.5	Multiple net	on deck	
75-3	25.03.03	05:44	75° 54.85' N	26° 59.54' E	221.0	Bongo net	surface	
75-3	25.03.03	05:48	75° 54.86' N	26° 59.64' E	221.7	Bongo net	surface	100 m
75-3	25.03.03	05:53	75° 54.87' N	26° 59.78' E	223.8	Bongo net	on deck	
75-4	25.03.03	05:59	75° 54.89' N	26° 59.94' E	223.8	Nansen Net	in the water	
75-4	25.03.03	06:13	75° 54.91' N	27° 0.32' E	226.8	Nansen Net	in the water	200 m
75-4	25.03.03	06:24	75° 54.94' N	27° 0.66' E	227.5	Nansen Net	on Deck	
75-5	25.03.03	06:25	75° 54.94' N	27° 0.69' E	228.0	Nansen Net	in the water	
75-5	25.03.03	06:29	75° 54.95' N	27° 0.82' E	228.3	Nansen Net	at depth	60 m
75-5	25.03.03	06:33	75° 54.96' N	27° 0.94' E	227.9	Nansen Net	on Deck	
75-6	25.03.03	06:42	75° 54.97' N	27° 1.22' E	229.3	Multi corer	surface	
75-6	25.03.03	06:47	75° 54.98' N	27° 1.39' E	230.6	Multi corer	at bottom	228 m
75-6	25.03.03	06:54	75° 54.98' N	27° 1.64' E	232.9	Multi corer	on deck	
75-7	25.03.03	07:13	75° 55.14' N	27° 2.74' E	239.5	Agassiz trawl	surface	
75-7	25.03.03	07:26	75° 55.11' N	27° 0.61' E	229.8	Agassiz trawl	start trawl	652 m
75-7	25.03.03	07:41	75° 55.13' N	26° 59.46' E	225.1	Agassiz trawl	Start hoisting	
75-7	25.03.03	07:58	75° 55.14' N	26° 59.11' E	223.0	Agassiz trawl	on deck	
75-8	25.03.03	08:24	75° 55.25' N	26° 59.93' E	229.1	Ice station	Alongside Floe	
75-8	25.03.03	08:29	75° 55.25' N	27° 0.06' E	229.1	Ice station	Scientists on the ice	per Mummychair

Station PS64/	Date	Time	PositionLat	PositionLon	Depth [m]	Gear	Action	Comment
75-8	25.03.03	09:34	75° 55.14' N	27° 1.37' E	231.7	Ice station	Scientists on board	
75-8	25.03.03	09:34	75° 55.14' N	27° 1.37' E	231.7	Ice station	Departure from floe	
76-1	25.03.03	11:21	75° 52.75' N	27° 32.08' E	257.5	CTD/rosette	surface	
76-1	25.03.03	11:29	75° 52.73' N	27° 31.96' E	258.1	CTD/rosette	at depth	245 m
76-1	25.03.03	11:38	75° 52.71' N	27° 31.82' E	257.1	CTD/rosette	on deck	
76-2	25.03.03	11:48	75° 52.69' N	27° 31.61' E	258.0	Multiple net	surface	
76-2	25.03.03	11:59	75° 52.69' N	27° 31.47' E	258.4	Multiple net	at depth	
76-2	25.03.03	12:00	75° 52.69' N	27° 31.46' E	258.5	Multiple net	Hoisting	
76-2	25.03.03	12:16	75° 52.67' N	27° 31.09' E	258.2	Multiple net	on deck	
76-3	25.03.03	12:24	75° 52.66' N	27° 30.87' E	255.6	Nansen Net	in the water	
76-3	25.03.03	12:36	75° 52.65' N	27° 30.55' E	255.6	Nansen Net	at depth	
76-3	25.03.03	12:50	75° 52.65' N	27° 30.19' E	254.0	Nansen Net	on Deck	
76-4	25.03.03	13:02	75° 52.65' N	27° 29.78' E	255.9	Multi corer	surface	
76-4	25.03.03	13:08	75° 52.65' N	27° 29.63' E	257.1	Multi corer	at sea bottom	
76-4	25.03.03	13:13	75° 52.65' N	27° 29.48' E	257.8	Multi corer	on deck	
77-1	25.03.03	16:37	75° 29.92' N	28° 0.17' E	274.2	CTD/rosette	surface	
77-1	25.03.03	16:45	75° 30.00' N	27° 59.99' E	274.3	CTD/rosette	at depth	261 m
77-1	25.03.03	16:52	75° 30.08' N	27° 59.74' E	273.1	CTD/rosette	on deck	
77-2	25.03.03	17:02	75° 30.20' N	27° 59.32' E	274.0	Trap, fish	surface	
77-2	25.03.03	17:08	75° 30.28' N	27° 59.02' E	274.0	Trap, fish	Hydrophon to the water	255 m Draht
77-2	25.03.03	17:11	75° 30.32' N	27° 58.92' E	272.7	Trap, fish	Hydrophon out of the water	Funktionsstörung des Hydrophon
77-2	25.03.03	17:13	75° 30.35' N	27° 58.81' E	269.5	Trap, fish	Hydrophon to the water	
77-2	25.03.03	17:14	75° 30.36' N	27° 58.76' E	269.7	Trap, fish	released	
77-2	25.03.03	17:15	75° 30.37' N	27° 58.71' E	271.9	Trap, fish	Hydrophon out of the water	
77-2	25.03.03	17:18	75° 30.42' N	27° 58.60' E	272.1	Trap, fish	Releaser on Deck	
77-3	25.03.03	17:43	75° 30.69' N	27° 59.66' E	272.9	Trap, fish	surface	
77-3	25.03.03	17:46	75° 30.74' N	27° 59.54' E	272.2	Trap, fish	at bottom	
77-3	25.03.03	17:59	75° 30.92' N	27° 59.42' E	270.2	Trap, fish	Releaser on Deck	
78-1	25.03.03	20:26	75° 24.60' N	28° 59.95' E	343.3	CTD/rosette	surface	
78-1	25.03.03	20:37	75° 24.72' N	28° 59.92' E	340.4	CTD/rosette	at depth	326 m
78-1	25.03.03	20:46	75° 24.85' N	28° 59.67' E	339.7	CTD/rosette	on deck	
79-1	25.03.03	23:14	75° 19.49' N	30° 0.23' E	379.5	CTD/rosette	surface	
79-1	25.03.03	23:26	75° 19.67' N	29° 59.63' E	378.3	CTD/rosette	at depth	364 m
79-1	25.03.03	23:33	75° 19.75' N	29° 59.35' E	377.6	CTD/rosette	on deck	
80-1	26.03.03	03:09	75° 13.64' N	31° 0.23' E	368.5	CTD/rosette	surface	
80-1	26.03.03	03:21	75° 13.83' N	30° 59.89' E	366.8	CTD/rosette	at depth	
80-1	26.03.03	03:31	75° 13.97' N	31° 0.02' E	367.6	CTD/rosette	on deck	
77-2	26.03.03	10:04	75° 30.21' N	27° 58.83' E	273.9	Trap, fish	Hydrophon to the water	
77-2	26.03.03	10:07	75° 30.21' N	27° 58.84' E	273.3	Trap, fish	released	
77-2	26.03.03	10:14	75° 30.19' N	27° 59.11' E	273.2	Trap, fish	Hydrophon to the water	
77-2	26.03.03	10:18	75° 30.15' N	27° 59.25' E	274.5	Trap, fish	Releaser on Deck	

Station PS64/	Date	Time	PositionLat	PositionLon	Depth [m]	Gear	Action	Comment
77-2	26.03.03	10:30	75° 30.36' N	27° 58.71' E	272.0	Trap, fish	Hydrophon to the water	
77-2	26.03.03	11:06	75° 30.00' N	27° 59.84' E	273.4	Trap, fish	on deck	
77-3	26.03.03	11:20	75° 30.77' N	27° 59.30' E	270.7	Trap, fish	Hydrophon to the water	
77-3	26.03.03	11:22	75° 30.75' N	27° 59.41' E	272.2	Trap, fish	released	
77-3	26.03.03	11:38	75° 30.76' N	27° 59.98' E	271.3	Trap, fish	Hydrophon out of the water	
77-3	26.03.03	12:21	75° 30.65' N	27° 59.90' E	271.1	Trap, fish	Searching by helicopter	
77-3	26.03.03	12:48	75° 30.38' N	27° 58.83' E	272.5	Trap, fish	Hydrophon to the water	
77-3	26.03.03	12:49	75° 30.37' N	27° 58.80' E	270.0	Trap, fish	Hydrophon out of the water	stb
77-3	26.03.03	12:54	75° 30.31' N	27° 58.63' E	276.7	Trap, fish	Hydrophon to the water	
77-3	26.03.03	12:56	75° 30.30' N	27° 58.59' E	275.7	Trap, fish	Hydrophon out of the water	
77-3	26.03.03	12:58	75° 30.29' N	27° 58.52' E	275.3	Trap, fish	Aborted, trap not afloat	
81-1	26.03.03	13:11	75° 30.24' N	27° 58.13' E	274.6	Agassiz trawl	surface	
81-1	26.03.03	13:26	75° 30.74' N	27° 59.57' E	272.6	Agassiz trawl	start trawl	
81-1	26.03.03	13:26	75° 30.74' N	27° 59.57' E	272.6	Agassiz trawl	AGT on ground	
81-1	26.03.03	13:41	75° 30.99' N	28° 0.36' E	269.7	Agassiz trawl	Stop Trawl	
81-1	26.03.03	13:42	75° 31.00' N	28° 0.40' E	269.5	Agassiz trawl	Start hoisting	
81-1	26.03.03	13:52	75° 31.08' N	28° 0.64' E	269.2	Agassiz trawl	AGT off ground	
81-1	26.03.03	14:05	75° 31.30' N	28° 1.18' E	267.8	Agassiz trawl	on deck	
82-1	28.03.03	18:00	77° 53.95' N	11° 2.80' E	142.8	Calibration	start	Magnetik Drehkreise: 1x über Stb, 1x über Bb; Radius 1nm, v=7 kn
82-1	28.03.03	18:44	77° 53.47' N	11° 4.11' E	123.2	Calibration	Information	Beginnen 2. Drehkreis
82-1	28.03.03	19:33	77° 53.38' N	11° 4.85' E	119.2	Calibration	End	
83-1	30.03.03	00:39	78° 32,91' N	10° 18,84' E	102,6	CTD/rosette	surface	
83-1	30.03.03	00:44	78° 32,86' N	10° 18,67' E	93,1	CTD/rosette	at depth	
83-1	30.03.03	00:51	78° 32,75' N	10° 18,50' E	84,1	CTD/rosette	on deck	
84-1	30.03.03	03:25	78° 48,93' N	9° 35,43' E	96,6	CTD/rosette	surface	
84-1	30.03.03	03:30	78° 48,85' N	9° 35,28' E	99,5	CTD/rosette	at depth	
84-1	30.03.03	03:36	78° 48,79' N	9° 35,04' E	100,2	CTD/rosette	on deck	
85-1	30.03.03	10:16	79° 4,04' N	4° 20,22' E	2373,0	CTD/rosette	surface	

Station PS64/	Date	Time	PositionLat	PositionLon	Depth [m]	Gear	Action	Comment
85-1	30.03.03	11:03	79° 4,20' N	4° 19,24' E	2368,0	CTD/rosette	at depth	2317 m
85-1	30.03.03	11:36	79° 4,31' N	4° 18,95' E	2359,0	CTD/rosette	on deck	
85-2	30.03.03	11:45	79° 4,35' N	4° 18,90' E	2354,0	Multiple net	surface	
85-2	30.03.03	13:00	79° 4,46' N	4° 19,31' E	2338,0	Multiple net	at depth	
85-2	30.03.03	14:19	79° 4,32' N	4° 19,66' E	2344,0	Multiple net	on deck	
85-3	30.03.03	14:28	79° 4,27' N	4° 19,69' E	2350,0	Multiple net	surface	
85-3	30.03.03	14:38	79° 4,29' N	4° 19,71' E	2349,0	Multiple net	Error - Restart	
85-3	30.03.03	14:45	79° 4,31' N	4° 19,74' E	2345,0	Multiple net	surface	
85-3	30.03.03	15:03	79° 4,29' N	4° 19,85' E	2346,0	Multiple net	Hoisting	
85-3	30.03.03	15:03	79° 4,29' N	4° 19,85' E	2346,0	Multiple net	at depth	
85-3	30.03.03	15:21	79° 4,30' N	4° 19,83' E	2345,0	Multiple net	on deck	
85-4	30.03.03	15:33	79° 4,35' N	4° 19,84' E	2342,0	Colonization Tray	to water	
85-4	30.03.03	15:43	79° 4,41' N	4° 19,92' E	2332,0	Colonization Tray	slipped	
85-5	30.03.03	16:02	79° 4,47' N	4° 15,92' E	2387,0	Bongo net	surface	
85-5	30.03.03	16:55	79° 3,93' N	4° 17,86' E	2409,0	Bongo net	at depth	1500 m
85-5	30.03.03	18:17	79° 3,10' N	4° 19,91' E	2457,0	Bongo net	on deck	
85-6	30.03.03	18:40	79° 2,32' N	4° 17,49' E	2549,0	Rectangular midwater trawl	surface	
85-6	30.03.03	18:43	79° 2,38' N	4° 17,97' E	2540,0	Rectangular midwater trawl	Begin Trawling	33 m
85-6	30.03.03	19:03	79° 2,52' N	4° 20,39' E	2508,0	Rectangular midwater trawl	End of Trawl	
85-6	30.03.03	19:06	79° 2,57' N	4° 20,81' E	2498,0	Rectangular midwater trawl	on deck	
86-1	31.03.03	06:03	79° 55,66' N	9° 0,49' E	483,7	CTD/rosette	surface	
86-1	31.03.03	06:15	79° 55,55' N	9° 1,17' E	483,8	CTD/rosette	at depth	467 m
86-1	31.03.03	06:31	79° 55,36' N	9° 1,96' E	484,7	CTD/rosette	on deck	
87-1	31.03.03	07:21	79° 52,50' N	9° 31,63' E	477,7	Water Sample Bucket	into the water	
87-2	31.03.03	07:32	79° 52,47' N	9° 31,63' E	476,5	CTD/rosette	surface	
87-2	31.03.03	07:43	79° 52,44' N	9° 31,56' E	476,8	CTD/rosette	at depth	458 m
87-2	31.03.03	07:56	79° 52,39' N	9° 31,49' E	475,6	CTD/rosette	on deck	
88-1	31.03.03	08:55	79° 48,75' N	10° 1,68' E	403,4	CTD/rosette	surface	
88-1	31.03.03	09:07	79° 48,70' N	10° 2,15' E	400,7	CTD/rosette	at depth	386 m
88-1	31.03.03	09:22	79° 48,66' N	10° 2,53' E	398,8	CTD/rosette	on deck	
89-1	31.03.03	10:10	79° 46,77' N	10° 17,66' E	233,7	CTD/rosette	surface	
89-1	31.03.03	10:17	79° 46,75' N	10° 17,88' E	200,3	CTD/rosette	at depth	172 m
89-1	31.03.03	10:23	79° 46,78' N	10° 18,03' E	197,0	CTD/rosette	on deck	
90-1	31.03.03	10:46	79° 45,80' N	10° 24,42' E	96,0	Water Sample Bucket	into the water	
90-2	31.03.03	10:55	79° 45,74' N	10° 24,43' E	94,2	CTD/rosette	surface	
90-2	31.03.03	11:00	79° 45,71' N	10° 24,37' E	92,1	CTD/rosette	at depth	91 m
90-2	31.03.03	11:10	79° 45,66' N	10° 24,26' E	96,8	CTD/rosette	on deck	
91-1	01.04.03	02:50	80° 20,09' N	13° 0,21' E	126,6	CTD/rosette	surface	

Station PS64/	Date	Time	PositionLat	PositionLon	Depth [m]	Gear	Action	Comment
91-1	01.04.03	02:57	80° 20,09' N	13° 0,29' E	126,9	CTD/rosette	at depth	
91-1	01.04.03	03:06	80° 20,09' N	13° 0,40' E	128,1	CTD/rosette	on deck	
92-1	01.04.03	04:55	80° 25,44' N	12° 51,14' E	195,6	CTD/rosette	surface	
92-1	01.04.03	05:01	80° 25,43' N	12° 51,15' E	194,7	CTD/rosette	at depth	188 m
92-1	01.04.03	05:09	80° 25,43' N	12° 51,16' E	193,6	CTD/rosette	on deck	
93-1	01.04.03	08:35	80° 26,17' N	12° 49,44' E	289,3	Ice station	Alongside Floe	
93-1	01.04.03	08:56	80° 26,13' N	12° 49,38' E	281,9	Ice station	Gangway on the ice	
93-1	01.04.03	08:58	80° 26,12' N	12° 49,36' E	281,3	Ice station	Scientists on the ice	
93-1	01.04.03	17:51	80° 25,18' N	12° 47,20' E	192,2	Ice station	Scientists on board	
93-1	01.04.03	19:43	80° 24,76' N	12° 43,73' E	184,8	Ice station	Scientists on the ice	Tomato Team - 2 Persons
93-1	01.04.03	20:46	80° 24,45' N	12° 40,64' E	188,6	Ice station	Scientists on board	
93-1	01.04.03	23:41	80° 23,56' N	12° 30,90' E	201,4	Ice station	Scientists on the ice	zur Tomate Auftanken etc
93-1	02.04.03	00:23	80° 23,40' N	12° 28,94' E	193,4	Ice station	Scientists on board	
93-1	02.04.03	06:10	80° 22,61' N	12° 21,63' E	179,3	Ice station	Scientists on the ice	
93-1	02.04.03	07:23	80° 22,36' N	12° 20,12' E	182,1	Ice station	Scientists on board	
93-1	02.04.03	07:59	80° 22,21' N	12° 19,13' E	178,9	Ice station	Scientists on the ice	Meteomast abbergen
93-1	02.04.03	08:21	80° 22,13' N	12° 18,56' E	176,2	Ice station	Scientists on board	
93-1	02.04.03	08:22	80° 22,13' N	12° 18,53' E	177,0	Ice station	Ice Gangway on board	
93-1	02.04.03	08:46	80° 21,98' N	12° 16,84' E	189,4	Ice station	Alongside Floe	
93-1	02.04.03	08:47	80° 21,97' N	12° 16,80' E	189,5	Ice station	Scientists on the ice	mummychair tomato team
93-1	02.04.03	08:58	80° 21,93' N	12° 16,47' E	188,8	Ice station	Scientists on the ice	
93-1	02.04.03	08:59	80° 21,92' N	12° 16,45' E	188,0	Ice station	Departure from floe	
93-2	02.04.03	09:10	80° 21,82' N	12° 16,47' E	181,2	CTD/rosette	surface	
93-2	02.04.03	09:17	80° 21,75' N	12° 16,61' E	182,7	CTD/rosette	at depth	176 m
93-2	02.04.03	09:34	80° 21,72' N	12° 16,44' E	184,0	CTD/rosette	on deck	
93-3	02.04.03	10:00	80° 21,51' N	12° 15,24' E	184,5	Multiple net	surface	
93-3	02.04.03	10:07	80° 21,45' N	12° 14,90' E	184,2	Multiple net	at depth	173 m
93-3	02.04.03	10:15	80° 21,40' N	12° 14,58' E	185,4	Multiple net	on deck	
93-4	02.04.03	10:36	80° 20,90' N	12° 1,60' E	198,3	Water Sample Bucket	into the water	
94-1	02.04.03	14:50	80° 19,59' N	11° 46,68' E	198,3	Turbulenzmesssystem	Start	
94-1	02.04.03	19:50	80° 19,11' N	11° 47,95' E	196,4	Turbulenzmesssystem	End	

Station PS64/	Date	Time	PositionLat	PositionLon	Depth [m]	Gear	Action	Comment
95-1	03.04.03	06:01	80° 27,95' N	13° 14,86' E	466,5	CTD/rosette	surface	
95-1	03.04.03	06:16	80° 27,93' N	13° 14,79' E	464,6	CTD/rosette	at depth	449 m
95-1	03.04.03	06:33	80° 27,89' N	13° 14,45' E	463,3	CTD/rosette	on deck	
96-1	03.04.03	07:45	80° 31,83' N	13° 28,23' E	306,6	CTD/rosette	surface	
96-1	03.04.03	07:54	80° 31,85' N	13° 28,19' E	307,1	CTD/rosette	at depth	295 m
96-1	03.04.03	08:04	80° 31,83' N	13° 28,01' E	311,3	CTD/rosette	on deck	
96-1	03.04.03	08:04	80° 31,83' N	13° 28,01' E	311,3	CTD/rosette	surface	
97-1	03.04.03	08:59	80° 35,34' N	13° 15,35' E	634,7	CTD/rosette	surface	
97-1	03.04.03	09:18	80° 35,28' N	13° 14,97' E	641,0	CTD/rosette	at depth	627 m
97-1	03.04.03	09:35	80° 35,22' N	13° 14,60' E	647,6	CTD/rosette	on deck	
98-1	03.04.03	10:32	80° 39,67' N	13° 5,12' E	981,8	CTD/rosette	surface	
98-1	03.04.03	10:51	80° 39,64' N	13° 4,50' E	986,9	CTD/rosette	at depth	955 m
98-1	03.04.03	11:07	80° 39,58' N	13° 4,08' E	989,7	CTD/rosette	on deck	
99-1	03.04.03	18:47	80° 44,38' N	13° 12,23' E	1190,0	CTD/rosette	surface	
99-1	03.04.03	19:11	80° 44,47' N	13° 11,99' E	1196,0	CTD/rosette	at depth	1158 m
99-1	03.04.03	19:34	80° 44,42' N	13° 11,48' E	1201,0	CTD/rosette	on deck	
100-1	03.04.03	20:21	80° 49,29' N	13° 13,59' E	1484,0	CTD/rosette	surface	
100-1	03.04.03	20:49	80° 49,17' N	13° 12,98' E	1481,0	CTD/rosette	at depth	1436 m
100-1	03.04.03	21:16	80° 49,06' N	13° 12,34' E	1478,0	CTD/rosette	on deck	
101-1	03.04.03	22:42	80° 58,59' N	13° 1,89' E	1967,0	CTD/rosette	surface	
101-1	03.04.03	23:18	80° 58,42' N	13° 1,04' E	1962,0	CTD/rosette	at depth	1913 m
101-1	03.04.03	23:54	80° 58,23' N	13° 0,34' E	1955,0	CTD/rosette	on deck	
102-1	04.04.03	01:27	81° 7,44' N	12° 35,45' E	2219,0	CTD/rosette	surface	
102-1	04.04.03	02:08	81° 7,30' N	12° 34,72' E	2219,0	CTD/rosette	at depth	
102-1	04.04.03	02:51	81° 7,10' N	12° 33,99' E	2216,0	CTD/rosette	on deck	
103-1	04.04.03	04:18	81° 14,58' N	11° 52,90' E	2100,0	CTD/rosette	surface	
103-1	04.04.03	05:00	81° 14,41' N	11° 52,33' E	2099,0	CTD/rosette	at depth	2046m
103-1	04.04.03	05:40	81° 14,25' N	11° 51,70' E	2101,0	CTD/rosette	on deck	
104-1	04.04.03	06:28	81° 18,08' N	11° 31,15' E	1620,0	CTD/rosette	surface	
104-1	04.04.03	06:58	81° 17,93' N	11° 30,56' E	1644,0	CTD/rosette	at depth	1582m
104-1	04.04.03	07:19	81° 17,83' N	11° 30,13' E	1663,0	CTD/rosette	on deck	
105-1	04.04.03	09:04	81° 21,93' N	10° 32,83' E	1936,0	CTD/rosette	surface	
105-1	04.04.03	09:38	81° 21,69' N	10° 32,78' E	1939,0	CTD/rosette	at depth	1887 m
105-1	04.04.03	10:07	81° 21,40' N	10° 32,45' E	1944,0	CTD/rosette	on deck	
105-2	04.04.03	10:52	81° 20,91' N	10° 32,17' E	1940,0	Multiple net	surface	
105-2	04.04.03	10:56	81° 20,89' N	10° 32,21' E	1940,0	Multiple net	at depth	103 m
105-2	04.04.03	11:02	81° 20,83' N	10° 32,18' E	1941,0	Multiple net	on deck	
106-1	04.04.03	13:28	81° 30,07' N	10° 12,80' E	1793,0	CTD/rosette	surface	
106-2	04.04.03	13:32	81° 30,03' N	10° 12,66' E	1792,0	seacat	Start Profile	Bugkran, zu Wasser
106-1	04.04.03	14:02	81° 29,83' N	10° 12,46' E	1794,0	CTD/rosette	at depth	
106-2	04.04.03	14:19	81° 29,75' N	10° 12,02' E	1791,0	Seacat	Finish profile	Hand-ADCP ein
106-1	04.04.03	14:27	81° 29,72' N	10° 12,07' E	1790,0	CTD/rosette	on deck	
107-1	04.04.03	16:59	81° 39,20' N	9° 48,30' E	1284,0	CTD/rosette	surface	
107-1	04.04.03	17:25	81° 39,00' N	9° 47,90' E	1284,0	CTD/rosette	at depth	1247m
107-1	04.04.03	17:44	81° 38,90' N	9° 47,70' E	1278,0	CTD/rosette	on deck	
108-1	05.04.03	01:12	81° 47,41' N	8° 54,53' E	820,1	CTD/rosette	surface	
108-1	05.04.03	01:28	81° 47,34' N	8° 54,38' E	821,2	CTD/rosette	at depth	
108-1	05.04.03	01:41	81° 47,27' N	8° 54,27' E	825,2	CTD/rosette	on deck	
109-1	05.04.03	02:31	81° 46,24' N	8° 19,66' E	832,7	CTD/rosette	surface	
109-1	05.04.03	02:50	81° 46,17' N	8° 19,77' E	832,8	CTD/rosette	at depth	
109-1	05.04.03	03:06	81° 46,11' N	8° 19,87' E	832,4	CTD/rosette	on deck	

Station PS64/	Date	Time	PositionLat	PositionLon	Depth [m]	Gear	Action	Comment
110-1	06.04.03	02:38	81° 48,27' N	9° 29,47' E	871,1	CTD/rosette	surface	
110-1	06.04.03	02:56	81° 48,33' N	9° 29,90' E	869,4	CTD/rosette	at depth	
110-1	06.04.03	03:10	81° 48,38' N	9° 30,20' E	872,1	CTD/rosette	on deck	
111-1	06.04.03	14:00	81° 51,85' N	9° 34,02' E	864,0	English TurbMasts	Begin	
111-1	06.04.03	21:37	81° 54,99' N	9° 25,64' E	847,8	English Turb Masts	End	unterbrechen für Anlegen
111-2	06.04.03	22:15	81° 55,37' N	9° 29,53' E	862,1	Ice station	Alongside Floe	
111-2	06.04.03	22:22	81° 55,38' N	9° 29,33' E	862,0	Ice station	Scientists on the ice	Ausbringen Tilt&Strainmeter, Observation durch Meteogruppe
111-2	07.04.03	00:36	81° 55,28' N	9° 27,41' E	854,5	Ice station	Scientists on board	
111-2	07.04.03	00:36	81° 55,28' N	9° 27,41' E	854,5	Ice station	Departure from floe	
111-1	07.04.03	01:06	81° 55,08' N	9° 23,59' E	842,0	English Turb Masts	Begin	
111-1	07.04.03	08:06	81° 53,88' N	9° 31,50' E	857,5	English Turb Masts	End	
111-3	07.04.03	08:30	81° 53,90' N	9° 34,17' E	855,8	Ice station	Alongside Floe	
111-3	07.04.03	08:40	81° 53,88' N	9° 34,07' E	855,4	Ice station	Gangway on the ice	
111-3	07.04.03	08:44	81° 53,87' N	9° 34,07' E	856,1	Ice station	Scientists on the ice	
111-4	07.04.03	17:21	81° 54,14' N	9° 27,14' E	845,0	CTD/rosette	surface	
111-4	07.04.03	17:37	81° 54,18' N	9° 26,43' E	844,0	CTD/rosette	at depth	812 m
111-4	07.04.03	17:52	81° 54,23' N	9° 25,75' E	843,4	CTD/rosette	on deck	
111-3	07.04.03	18:24	81° 54,33' N	9° 24,12' E	841,5	Ice station	Scientists on board	
111-3	08.04.03	08:00	81° 58,95' N	9° 21,94' E	828,5	Ice station	Scientists on the ice	
111-5	08.04.03	10:33	81° 58,89' N	9° 25,51' E	838,2	Multiple net	surface	
111-5	08.04.03	10:37	81° 58,89' N	9° 25,51' E	839,5	Multiple net	at depth	102 m
111-5	08.04.03	10:42	81° 58,88' N	9° 25,51' E	840,8	Multiple net	on deck	
111-6	08.04.03	10:58	81° 58,83' N	9° 25,53' E	843,1	Nansen Net	in the water	
111-6	08.04.03	11:06	81° 58,81' N	9° 25,54' E	842,4	Nansen Net	at depth	200 m
111-6	08.04.03	11:17	81° 58,78' N	9° 25,54' E	842,4	Nansen Net	on Deck	
111-7	08.04.03	11:27	81° 58,75' N	9° 25,52' E	842,4	CTD/rosette	surface	
111-7	08.04.03	11:41	81° 58,71' N	9° 25,46' E	840,1	CTD/rosette	at depth	808 m
111-7	08.04.03	11:59	81° 58,66' N	9° 25,31' E	840,1	CTD/rosette	on deck	
111-7	08.04.03	11:59	81° 58,66' N	9° 25,31' E	840,1	CTD/rosette	on deck	
111-3	08.04.03	21:39	81° 56,65' N	9° 27,10' E	849,1	Ice station	Scientists on board	Gangway hoch
111-3	08.04.03	22:22	81° 56,35' N	9° 27,01' E	852,0	Ice station	Scientists on the ice	Auftanken
111-3	08.04.03	23:07	81° 56,03' N	9° 27,31' E	859,1	Ice station	Scientists on board	

Station PS64/	Date	Time	PositionLat	PositionLon	Depth [m]	Gear	Action	Comment
111-3	09.04.03	00:15	81° 55,53' N	9° 28,17' E	863,1	Ice station	Scientists on the ice	Tanken
111-3	09.04.03	00:30	81° 55,41' N	9° 28,36' E	860,5	Ice station	Scientists on board	
111-3	09.04.03	02:48	81° 54,33' N	9° 30,25' E	867,2	Ice station	Scientists on the ice	
111-3	09.04.03	03:07	81° 54,18' N	9° 30,61' E	865,1	Ice station	Scientists on board	
111-3	09.04.03	07:21	81° 52,55' N	9° 35,95' E	870,5	Ice station	Scientists on the ice	
111-3	09.04.03	08:00	81° 52,31' N	9° 36,90' E	877,7	Ice station	Scientists on board	
111-3	09.04.03	08:30	81° 52,12' N	9° 37,50' E	880,5	Ice station	Scientists on the ice	
111-8	09.04.03	13:22	81° 50,14' N	9° 41,66' E	888,0	CTD/rosette	surface	
111-8	09.04.03	13:41	81° 50,00' N	9° 41,73' E	893,1	CTD/rosette	at depth	
111-8	09.04.03	14:00	81° 49,87' N	9° 41,77' E	894,8	CTD/rosette	on deck	
111-9	09.04.03	14:11	81° 49,79' N	9° 41,78' E	894,2	Multi corer	surface	Video/über A-Galgen
111-9	09.04.03	14:21	81° 49,73' N	9° 41,81' E	898,0	Multi corer	information	Abbruch/Telemetriedefekt
111-9	09.04.03	14:35	81° 49,63' N	9° 41,83' E	896,2	Multi corer	on deck	
111-3	09.04.03	15:01	81° 49,46' N	9° 41,80' E	898,8	Ice station	Scientists on board	
111-3	09.04.03	15:02	81° 49,45' N	9° 41,80' E	899,5	Ice station	Gangway on board	
111-3	09.04.03	15:05	81° 49,43' N	9° 41,80' E	903,1	Ice station	Departure from floe	
111-3	09.04.03	16:28	81° 48,92' N	9° 41,37' E	898,1	Ice station	Alongside Floe	
111-3	09.04.03	16:51	81° 48,80' N	9° 40,97' E	902,4	Ice station	Gangway on the ice	
111-3	09.04.03	16:56	81° 48,77' N	9° 40,90' E	900,1	Ice station	Scientists on the ice	
111-3	09.04.03	17:03	81° 48,74' N	9° 40,81' E	904,0	Ice station	Information	Positionieren neu an der Scholle
111-3	09.04.03	17:30	81° 48,62' N	9° 40,32' E	904,0	Ice station	Fast on ice anchors	
111-3	09.04.03	18:00	81° 48,51' N	9° 39,79' E	908,1	Ice station	Scientists on the ice	
111-3	09.04.03	23:00	81° 48,28' N	9° 34,17' E	885,5	Ice station	Scientists on board	
111-3	10.04.03	00:20	81° 48,36' N	9° 33,42' E	881,8	Ice station	Scientists on the ice	
111-3	10.04.03	00:45	81° 48,38' N	9° 33,17' E	880,7	Ice station	Scientists on board	
111-3	10.04.03	06:18	81° 48,58' N	9° 30,95' E	872,4	Ice station	Scientists on the ice	
111-3	10.04.03	06:36	81° 48,58' N	9° 30,93' E	871,2	Ice station	Scientists on board	
111-3	10.04.03	08:30	81° 48,57' N	9° 31,09' E	868,8	Ice station	Scientists on the ice	

Station PS64/	Date	Time	PositionLat	PositionLon	Depth [m]	Gear	Action	Comment
---------------	------	------	-------------	-------------	-----------	------	--------	---------

111-3	10.04.03	11:57	81° 48,39' N	9° 31,45' E	875,2	Ice station	Scientists on board	
111-3	10.04.03	12:22	81° 48,36' N	9° 31,48' E	874,8	Ice station	Scientists on the ice	
111-10	10.04.03	13:24	81° 48,26' N	9° 31,60' E	876,5	Multi corer	surface	mit Telemetrie
111-10	10.04.03	13:43	81° 48,22' N	9° 31,63' E	879,8	Multi corer	at sea bottom	
111-10	10.04.03	13:51	81° 48,21' N	9° 31,66' E	879,0	Multi corer	information	3 Versuche und nicht ausgelöst / Hieven
111-10	10.04.03	14:10	81° 48,17' N	9° 31,64' E	879,8	Multi corer	on deck	
111-3	10.04.03	16:21	81° 47,85' N	9° 31,38' E	883,5	Ice station	Scientists on board	
111-3	10.04.03	16:30	81° 47,82' N	9° 31,33' E	882,5	Ice station	Scientists on the ice	
111-3	10.04.03	19:42	81° 47,29' N	9° 29,22' E	881,7	Ice station	Scientists on board	
111-3	10.04.03	21:15	81° 47,19' N	9° 27,81' E	879,7	Ice station	Scientists on the ice	
111-3	10.04.03	22:15	81° 47,15' N	9° 27,15' E	880,1	Ice station	Scientists on board	
111-3	10.04.03	23:04	81° 47,11' N	9° 26,91' E	878,8	Ice station	Scientists on the ice	
111-3	11.04.03	01:41	81° 46,92' N	9° 26,54' E	877,0	Ice station	Scientists on board	
111-3	11.04.03	06:23	81° 46,99' N	9° 27,77' E	881,5	Ice station	Scientists on the ice	
111-3	11.04.03	07:00	81° 47,04' N	9° 28,13' E	883,0	Ice station	Scientists on board	
111-3	11.04.03	08:10	81° 47,14' N	9° 28,93' E	884,7	Ice station	Scientists on the ice	
111-11	11.04.03	08:48	81° 47,17' N	9° 29,26' E	885,5	Multi corer	surface	
111-11	11.04.03	09:08	81° 47,19' N	9° 29,39' E	885,4	Multi corer	at sea bottom	859 m
111-11	11.04.03	09:25	81° 47,20' N	9° 29,48' E	887,7	Multi corer	on deck	
111-3	11.04.03	17:17	81° 47,57' N	9° 29,18' E	878,8	Ice station	Information	Forschung nur noch in unmittelbarer Schiffsnähe, wenig Sicht
111-3	11.04.03	17:36	81° 47,60' N	9° 29,23' E	878,5	Ice station	Scientists on board	
111-3	11.04.03	18:20	81° 47,70' N	9° 29,40' E	879,2	Ice station	Scientists on the ice	
111-3	11.04.03	19:10	81° 47,86' N	9° 29,67' E	877,8	Ice station	Scientists on board	
111-3	11.04.03	19:32	81° 47,94' N	9° 29,87' E	874,7	Ice station	Scientists on the ice	

Station PS64/	Date	Time	PositionLat	PositionLon	Depth [m]	Gear	Action	Comment
111-3	11.04.03	20:42	81° 48,26' N	9° 30,84' E	875,7	Ice station	Scientists on board	
111-3	12.04.03	00:23	81° 49,29' N	9° 37,17' E	880,4	Ice station	Scientists on the ice	
111-3	12.04.03	00:52	81° 49,39' N	9° 38,21' E	883,8	Ice station	Scientists on board	
111-3	12.04.03	08:32	81° 50,62' N	9° 51,83' E	925,5	Ice station	Scientists on the ice	
111-3	12.04.03	09:46	81° 50,76' N	9° 53,65' E	936,9	Ice station	Scientists on board	
111-3	12.04.03	10:21	81° 50,80' N	9° 54,40' E	940,7	Ice station	Scientists on the ice	
111-3	12.04.03	18:06	81° 50,91' N	9° 55,11' E	942,2	Ice station	Scientists on board	
111-3	12.04.03	18:30	81° 50,93' N	9° 54,73' E	940,2	Ice station	Scientists on the ice	
111-3	12.04.03	18:52	81° 50,96' N	9° 54,43' E	934,7	Ice station	Scientists on board	
111-3	13.04.03	00:22	81° 51,35' N	9° 53,41' E	943,8	Ice station	Scientists on the ice	
111-3	13.04.03	00:44	81° 51,37' N	9° 53,43' E	946,4	Ice station	Scientists on board	
111-3	13.04.03	06:24	81° 51,65' N	9° 52,46' E	938,7	Ice station	Scientists on the ice	
111-3	13.04.03	06:45	81° 51,66' N	9° 52,49' E	934,9	Ice station	Scientists on board	
111-3	13.04.03	08:30	81° 51,75' N	9° 52,96' E	936,1	Ice station	Scientists on the ice	
111-3	13.04.03	11:58	81° 51,84' N	9° 54,16' E	940,7	Ice station	Scientists on board	
111-3	13.04.03	12:33	81° 51,84' N	9° 54,27' E	939,7	Ice station	Scientists on the ice	
111-3	13.04.03	14:00	81° 51,83' N	9° 54,12' E	939,9	Ice station	Free from ice anchors	
111-3	13.04.03	14:39	81° 51,82' N	9° 53,96' E	941,2	Ice station	Information	Verholen 2 Schiffslängen achteraus
111-3	13.04.03	14:40	81° 51,82' N	9° 53,95' E	941,1	Ice station	Gangway on board	
111-3	13.04.03	14:44	81° 51,81' N	9° 53,91' E	941,8	Ice station	Departure from floe	
111-3	13.04.03	15:55	81° 52,01' N	9° 55,99' E	944,2	Ice station	Alongside Floe	
111-3	13.04.03	16:06	81° 52,00' N	9° 55,90' E	945,5	Ice station	Ice Gangway on the ice	
111-3	13.04.03	17:00	81° 51,97' N	9° 55,38' E	942,8	Ice station	Fast on ice anchors	keine Anker ausgebracht - Fest an Scholle
111-3	13.04.03	17:14	81° 51,97' N	9° 55,22' E	941,1	Ice station	Scientists on board	

Station PS64/	Date	Time	PositionLat	PositionLon	Depth [m]	Gear	Action	Comment
111-3	13.04.03	18:20	81° 51,94' N	9° 54,48' E	938,9	Ice station	Scientists on the ice	
111-3	13.04.03	19:19	81° 51,93' N	9° 53,69' E	940,2	Ice station	Scientists on board	
111-3	14.04.03	00:16	81° 52,11' N	9° 54,16' E	941,4	Ice station	Scientists on the ice	
111-3	14.04.03	01:01	81° 52,12' N	9° 54,61' E	943,1	Ice station	Scientists on board	
111-3	14.04.03	06:24	81° 52,16' N	9° 58,23' E	949,4	Ice station	Scientists on the ice	
111-3	14.04.03	08:13	81° 52,13' N	10° 0,21' E	959,4	Ice station	Scientists on board	
111-3	14.04.03	08:52	81° 52,10' N	10° 1,15' E	956,5	Ice station	Scientists on the ice	
111-12	14.04.03	10:00	81° 52,02' N	10° 3,13' E	963,1	Turbulenzmesssystem	Start	
111-3	14.04.03	19:08	81° 50,38' N	10° 15,16' E	1043,0	Ice station	Scientists on board	
111-3	14.04.03	20:30	81° 50,12' N	10° 15,03' E	1040,0	Ice station	Scientists on the ice	
111-3	15.04.03	00:22	81° 49,51' N	10° 14,83' E	1030,0	Ice station	Scientists on the ice	
111-3	15.04.03	01:18	81° 49,42' N	10° 14,75' E	1031,0	Ice station	Scientists on board	
111-3	15.04.03	06:20	81° 49,02' N	10° 13,14' E	1020,0	Ice station	Scientists on the ice	
111-3	15.04.03	06:54	81° 48,95' N	10° 13,00' E	1017,0	Ice station	Scientists on board	
111-3	15.04.03	08:36	81° 48,79' N	10° 12,81' E	1013,0	Ice station	Scientists on the ice	
111-3	15.04.03	15:45	81° 48,91' N	10° 18,74' E	1052,0	Ice station	Scientists on board	
111-3	15.04.03	16:21	81° 48,91' N	10° 18,78' E	1051,0	Ice station	Scientists on the ice	
111-12	15.04.03	16:29	81° 48,91' N	10° 18,76' E	1053,0	Turbulenzmesssystem	End	
111-3	15.04.03	19:23	81° 48,72' N	10° 18,18' E	1048,0	Ice station	Scientists on board	
111-3	16.04.03	00:25	81° 48,04' N	10° 18,72' E	1084,0	Ice station	Scientists on the ice	
111-3	16.04.03	01:27	81° 47,94' N	10° 18,73' E	1081,0	Ice station	Scientists on board	
111-3	16.04.03	06:22	81° 47,38' N	10° 17,19' E	1091,0	Ice station	Scientists on the ice	
111-3	16.04.03	07:19	81° 47,26' N	10° 16,81' E	1090,0	Ice station	Scientists on board	
111-3	16.04.03	08:27	81° 47,10' N	10° 16,41' E	1094,0	Ice station	Scientists on the ice	
111-3	16.04.03	18:00	81° 46,06' N	10° 12,63' E	1105,0	Ice station	Scientists on board	
111-3	16.04.03	18:27	81° 45,97' N	10° 12,03' E	1111,0	Ice station	Scientists on the ice	

Station PS64/	Date	Time	PositionLat	PositionLon	Depth [m]	Gear	Action	Comment
111-3	16.04.03	19:26	81° 45,78' N	10° 10,56' E	1116,0	Ice station	Scientists on board	
111-3	17.04.03	00:17	81° 45,08' N	10° 5,49' E	1139,0	Ice station	Scientists on the ice	
111-3	17.04.03	00:59	81° 45,06' N	10° 5,40' E	1140,0	Ice station	Scientists on board	
111-3	17.04.03	06:12	81° 45,15' N	10° 3,82' E	1133,0	Ice station	Scientists on the ice	
111-3	17.04.03	06:48	81° 45,14' N	10° 3,26' E	1131,0	Ice station	Scientists on board	
111-3	17.04.03	09:10	81° 45,05' N	10° 0,53' E	1120,0	Ice station	Scientists on the ice	
111-3	17.04.03	17:00	81° 45,16' N	9° 55,17' E	1113,0	Ice station	Scientists on board	
111-3	17.04.03	17:03	81° 45,16' N	9° 55,14' E	1105,0	Ice station	Gangway on board	
111-3	17.04.03	17:06	81° 45,16' N	9° 55,11' E	1108,0	Ice station	Departure from floe	
112-1	18.04.03	15:49	81° 42,39' N	9° 54,85' E	1193,0	CTD/rosette	surface	
112-1	18.04.03	16:12	81° 42,23' N	9° 55,06' E	1201,0	CTD/rosette	at depth	
112-1	18.04.03	16:35	81° 42,07' N	9° 55,23' E	1204,0	CTD/rosette	on deck	
112-2	18.04.03	16:46	81° 41,99' N	9° 55,34' E	1212,0	Multiple net	surface	
112-2	18.04.03	16:51	81° 41,96' N	9° 55,37' E	1208,0	Multiple net	at depth	104m
112-2	18.04.03	16:57	81° 41,92' N	9° 55,40' E	1212,0	Multiple net	on deck	
112-3	18.04.03	17:04	81° 41,87' N	9° 55,44' E	1212,0	Nansen Net	in the water	
112-3	18.04.03	17:17	81° 41,77' N	9° 55,52' E	1216,0	Nansen Net	at depth	201m
112-3	18.04.03	17:29	81° 41,69' N	9° 55,53' E	1218,0	Nansen Net	on Deck	
112-4	18.04.03	17:42	81° 41,60' N	9° 55,40' E	1223,0	Multi corer	surface	
112-4	18.04.03	18:08	81° 41,42' N	9° 55,39' E	1232,0	Multi corer	at sea bottom	1191m gesteckt
112-4	18.04.03	18:30	81° 41,28' N	9° 55,35' E	1237,0	Multi corer	on deck	
113-1	18.04.03	20:33	81° 34,71' N	10° 8,80' E	1712,0	CTD/rosette	surface	
113-1	18.04.03	20:56	81° 34,56' N	10° 8,67' E	1710,0	CTD/rosette	at depth	995 m
113-1	18.04.03	21:10	81° 34,52' N	10° 8,72' E	1716,0	CTD/rosette	on deck	
114-1	19.04.03	00:26	81° 25,05' N	10° 17,92' E	1835,0	CTD/rosette	surface	
114-1	19.04.03	00:46	81° 25,04' N	10° 18,09' E	1835,0	CTD/rosette	at depth	
114-1	19.04.03	01:07	81° 25,04' N	10° 18,37' E	1835,0	CTD/rosette	on deck	
114-2	19.04.03	01:16	81° 25,06' N	10° 18,59' E	1836,0	Multiple net	surface	
114-2	19.04.03	01:24	81° 25,06' N	10° 18,81' E	1836,0	Multiple net	at depth	
114-2	19.04.03	01:34	81° 25,06' N	10° 18,96' E	1836,0	Multiple net	on deck	
115-1	19.04.03	13:11	81° 16,33' N	10° 40,14' E	2028,0	Rectangular midwater trawl	surface	
115-1	19.04.03	13:14	81° 16,35' N	10° 39,48' E	2028,0	Rectangular midwater trawl	Begin Trawling	
115-1	19.04.03	13:34	81° 16,50' N	10° 35,44' E	2028,0	Rectangular midwater trawl	End of Trawl	
115-1	19.04.03	13:38	81° 16,48' N	10° 35,24' E	2027,0	Rectangular midwater trawl	on deck	

Station PS64/	Date	Time	PositionLat	PositionLon	Depth [m]	Gear	Action	Comment
115-2	19.04.03	15:15	81° 15,33' N	10° 37,43' E	2029,0	Turbulenzmesssystem	Start	Mast nicht ausgeklappt
115-2	19.04.03	15:33	81° 15,22' N	10° 37,45' E	2028,0	Turbulenzmesssystem	Information	Verholen für Neubeginn der Messung - ungünstige Winde
115-2	19.04.03	15:49	81° 15,10' N	10° 35,72' E	2028,0	Turbulenzmesssystem	Information	Ende Verholen
115-2	19.04.03	18:44	81° 14,36' N	10° 30,73' E	2002,0	Turbulenzmesssystem	Information	Drehen in Wind für HEM-Bird Landung
115-2	19.04.03	20:30	81° 14,60' N	10° 28,34' E	2001,0	Turbulenzmesssystem	End	
115-3	19.04.03	20:45	81° 14,56' N	10° 27,80' E	2000,0	Eisfischen	start	
115-3	19.04.03	21:04	81° 14,47' N	10° 27,26' E	1997,0	Eisfischen	End	
115-4	19.04.03	21:11	81° 14,42' N	10° 27,03' E	1992,0	CTD/rosette	surface	
115-4	19.04.03	21:23	81° 14,38' N	10° 26,66' E	1995,0	CTD/rosette	at depth	437 m
115-4	19.04.03	21:32	81° 14,34' N	10° 26,38' E	1993,0	CTD/rosette	on deck	
116-1	19.04.03	23:06	81° 4,78' N	10° 29,25' E	1999,0	CTD/rosette	surface	
116-1	19.04.03	23:19	81° 4,70' N	10° 28,63' E	1988,0	CTD/rosette	at depth	
116-1	19.04.03	23:28	81° 4,69' N	10° 28,04' E	1980,0	CTD/rosette	on deck	
116-2	19.04.03	23:40	81° 4,66' N	10° 27,33' E	1972,0	Multiple net	surface	
116-2	19.04.03	23:44	81° 4,66' N	10° 27,13' E	1968,0	Multiple net	at depth	
116-2	19.04.03	23:45	81° 4,65' N	10° 27,08' E	1966,0	Multiple net	Hoisting	
116-2	19.04.03	23:50	81° 4,63' N	10° 26,78' E	1959,0	Multiple net	on deck	
117-1	20.04.03	01:23	80° 54,86' N	10° 43,66' E	1491,0	CTD/rosette	surface	
117-1	20.04.03	01:33	80° 54,88' N	10° 43,49' E	1492,0	CTD/rosette	at depth	
117-1	20.04.03	01:47	80° 54,80' N	10° 42,86' E	1470,0	CTD/rosette	on deck	
118-1	20.04.03	03:18	80° 44,51' N	10° 22,45' E	1417,0	Multiple net	surface	
118-1	20.04.03	03:20	80° 44,50' N	10° 22,34' E	1415,0	Multiple net	at depth	107 m
118-1	20.04.03	03:29	80° 44,50' N	10° 22,11' E	1404,0	Multiple net	on deck	
119-1	20.04.03	09:55	80° 24,88' N	10° 0,93' E	703,5	Water Sample Bucket	into the water	
119-2	20.04.03	10:04	80° 24,76' N	10° 0,68' E	701,7	Multiple net	surface	
119-2	20.04.03	10:10	80° 24,69' N	10° 0,43' E	700,0	Multiple net	at depth	106 m
119-2	20.04.03	10:17	80° 24,59' N	10° 0,10' E	700,8	Multiple net	on deck	
119-3	20.04.03	10:26	80° 24,47' N	9° 59,75' E	699,1	CTD/rosette	surface	
119-3	20.04.03	10:54	80° 24,08' N	9° 58,39' E	700,8	CTD/rosette	on deck	
120-1	20.04.03	20:42	80° 7,35' N	7° 25,93' E	542,0	CTD/rosette	surface	
120-1	20.04.03	20:56	80° 7,44' N	7° 26,01' E	542,4	CTD/rosette	at depth	523 m
120-1	20.04.03	21:10	80° 7,38' N	7° 25,91' E	542,4	CTD/rosette	on deck	
120-2	20.04.03	21:22	80° 7,32' N	7° 26,12' E	542,8	Multiple net	surface	
120-2	20.04.03	21:27	80° 7,30' N	7° 26,15' E	542,4	Multiple net	at depth	104 m
120-2	20.04.03	21:34	80° 7,28' N	7° 26,20' E	542,0	Multiple net	on deck	
120-3	20.04.03	21:38	80° 7,28' N	7° 26,26' E	542,4	Water Sample Bucket	into the water	
121-1	20.04.03	23:49	80° 4,01' N	6° 19,38' E	787,6	Water Sample Bucket	into the water	
121-2	20.04.03	23:55	80° 3,92' N	6° 19,26' E	789,6	CTD/rosette	surface	

Station PS64/	Date	Time	PositionLat	PositionLon	Depth [m]	Gear	Action	Comment
------------------	------	------	-------------	-------------	--------------	------	--------	---------

121-2	21.04.03	00:12	80° 3,93' N	6° 18,86' E	790,8	CTD/rosette	at depth	
121-2	21.04.03	00:26	80° 3,90' N	6° 18,56' E	792,8	CTD/rosette	on deck	
122-1	21.04.03	02:09	79° 57,38' N	5° 29,81' E	1058,0	CTD/rosette	surface	
122-1	21.04.03	02:24	79° 57,33' N	5° 29,22' E	1062,8	CTD/rosette	at depth	
122-1	21.04.03	02:39	79° 57,29' N	5° 29,04' E	1064,8	CTD/rosette	on deck	
123-1	21.04.03	05:28	79° 46,66' N	4° 27,63' E	2396,8	CTD/rosette	surface	
123-1	21.04.03	05:42	79° 46,62' N	4° 27,78' E	2397,2	CTD/rosette	at depth	642m
123-1	21.04.03	05:53	79° 46,63' N	4° 27,87' E	2396,8	CTD/rosette	on deck	
85-4	21.04.03	12:23	79° 4,40' N	4° 19,31' E	2331,2	Colonization Tray	hydrophon into water	
85-4	21.04.03	12:30	79° 4,25' N	4° 19,51' E	2343,6	Colonization Tray	released	
85-4	21.04.03	12:31	79° 4,23' N	4° 19,52' E	2346,0	Colonization Tray	hydrophon on deck	
85-4	21.04.03	12:49	79° 4,35' N	4° 19,86' E	2328,8	Colonization Tray	hydrophon into water	Posi eben an Stb. 50m
85-4	21.04.03	13:01	79° 4,10' N	4° 20,00' E	2355,2	Colonization Tray	information	Wellen sind ausgekuppelt
85-4	21.04.03	13:04	79° 4,00' N	4° 19,87' E	2368,0	Colonization Tray	hydrophon on deck	nichts gehört
85-4	21.04.03	13:10	79° 3,80' N	4° 19,53' E	2393,6	Colonization Tray	information	eingekuppelt
85-4	21.04.03	13:21	79° 3,88' N	4° 18,42' E	2398,8	Colonization Tray	on surface	
85-4	21.04.03	13:32	79° 4,19' N	4° 18,67' E	2360,8	Colonization Tray	mooring alongside	
85-4	21.04.03	13:36	79° 4,14' N	4° 18,70' E	2367,6	Colonization Tray	information	am Haken
85-4	21.04.03	13:52	79° 3,86' N	4° 18,23' E	2400,4	Colonization Tray	on deck	
124-1	21.04.03	14:06	79° 4,15' N	4° 15,83' E	2402,8	Rectangular midwater trawl	surface	
124-1	21.04.03	14:10	79° 4,19' N	4° 15,17' E	2406,8	Rectangular midwater trawl	Begin Trawling	
124-1	21.04.03	14:30	79° 4,58' N	4° 12,11' E	2423,6	Rectangular midwater trawl	End of Trawl	
124-1	21.04.03	14:33	79° 4,60' N	4° 11,76' E	2426,8	Rectangular midwater trawl	on deck	
124-2	21.04.03	14:41	79° 4,57' N	4° 11,20' E	2434,4	Rectangular midwater trawl	surface	
124-2	21.04.03	14:53	79° 4,75' N	4° 9,21' E	2455,6	Rectangular midwater trawl	heave	200m gefiert
124-2	21.04.03	15:08	79° 5,00' N	4° 6,72' E	2484,0	Rectangular midwater trawl	on deck	
125-1	21.04.03	15:48	79° 4,41' N	4° 19,94' E	2322,4	Colonization Tray	to water	

Station PS64/	Date	Time	PositionLat	PositionLon	Depth [m]	Gear	Action	Comment
125-1	21.04.03	15:49	79° 4,40' N	4° 19,91' E	2323,6	Colonization Tray	Driftmeter in the water	
125-1	21.04.03	15:51	79° 4,37' N	4° 19,86' E	2327,2	Colonization Tray	information	Freq.: 160,725
125-1	21.04.03	15:58	79° 4,29' N	4° 19,57' E	2338,4	Colonization Tray	to water	Toppeinheit
125-1	21.04.03	16:00	79° 4,28' N	4° 19,47' E	2340,8	Colonization Tray	slipped	
126-1	21.04.03	16:31	79° 3,64' N	4° 9,91' E	2497,2	Algae Frame	in the water	
126-1	21.04.03	18:01	79° 2,80' N	4° 5,50' E	2641,6	Algae Frame	at depth	2609m
126-1	21.04.03	18:07	79° 2,79' N	4° 5,15' E	2644,8	Algae Frame	Hydrophon in the water	
126-1	21.04.03	18:09	79° 2,78' N	4° 5,04' E	2646,4	Algae Frame	released	
126-1	21.04.03	18:11	79° 2,76' N	4° 4,92' E	2648,4	Algae Frame	Information	Posidonia-Test nicht erfolgreich - abgebrochen
126-1	21.04.03	18:13	79° 2,75' N	4° 4,82' E	2649,2	Algae Frame	Hydrophon on deck	
126-1	21.04.03	18:50	79° 2,43' N	4° 2,11' E	2683,2	Algae Frame	Releaser on deck	
127-1	21.04.03	19:26	79° 2,83' N	4° 14,14' E	2531,6	Bottom lander	surface	mit Sedimentfalle UKWSEnder 160,725 funktioniert
128-1	21.04.03	22:06	79° 8,31' N	6° 6,10' E	1290,3	CTD/rosette	surface	
128-1	21.04.03	22:14	79° 8,39' N	6° 5,86' E	1293,2	CTD/rosette	at depth	299m
128-1	21.04.03	22:25	79° 8,41' N	6° 5,69' E	1293,6	CTD/rosette	on deck	
128-2	21.04.03	22:37	79° 8,35' N	6° 5,65' E	1292,0	Multi corer	surface	
128-2	21.04.03	23:06	79° 8,46' N	6° 5,55' E	1296,5	Multi corer	at sea bottom	
128-2	21.04.03	23:31	79° 8,45' N	6° 5,38' E	1296,0	Multi corer	on deck	
128-3	22.04.03	00:03	79° 8,32' N	6° 5,33' E	1292,1	Trap, fish	surface	Sender 160,725 MHz getestet, o.B.
128-3	22.04.03	00:54	79° 8,26' N	6° 4,98' E	1290,7	Trap, fish	Hydrophon to the water	
128-3	22.04.03	00:55	79° 8,25' N	6° 4,98' E	1290,9	Trap, fish	released	
128-3	22.04.03	00:59	79° 8,24' N	6° 4,96' E	1290,4	Trap, fish	Hydrophon out of the water	keine Antwort, nochmaliger Test an Deck
128-3	22.04.03	01:01	79° 8,24' N	6° 4,93' E	1290,4	Trap, fish	Hydrophon to the water	

Station PS64/	Date	Time	PositionLat	PositionLon	Depth [m]	Gear	Action	Comment
128-3	22.04.03	01:04	79° 8,26' N	6° 4,86' E	1282,0	Trap, fish	Hydrophon out of the water	gosh, no reply
128-3	22.04.03	01:37	79° 8,33' N	6° 4,30' E	1293,6	Trap, fish	Releaser on Deck	
129-1	22.04.03	03:36	79° 6,35' N	4° 33,79' E	1806,8	CTD/rosette	surface	
129-1	22.04.03	03:44	79° 6,25' N	4° 33,17' E	1781,6	CTD/rosette	at depth	303m
129-1	22.04.03	03:51	79° 6,22' N	4° 32,74' E	1806,4	CTD/rosette	on deck	
129-2	22.04.03	04:04	79° 6,17' N	4° 32,03' E	1826,0	Multi corer	surface	
129-2	22.04.03	04:54	79° 6,11' N	4° 29,67' E	1868,0	Multi corer	at sea bottom	1845m
129-2	22.04.03	05:31	79° 6,03' N	4° 28,11' E	1901,6	Multi corer	on deck	
130-1	22.04.03	07:26	79° 3,72' N	4° 10,59' E	2481,2	Multi corer	surface	
130-1	22.04.03	08:09	79° 3,67' N	4° 10,78' E	2483,2	Multi corer	at sea bottom	2435 m
130-1	22.04.03	08:46	79° 3,68' N	4° 9,67' E	2496,4	Multi corer	on deck	
131-1	22.04.03	09:20	79° 3,45' N	4° 19,38' E	2424,8	Colonization Tray	to water	UKW 154,585 KHz Test erfolgreich
131-1	22.04.03	09:21	79° 3,44' N	4° 19,33' E	2425,6	Colonization Tray	Driftmeter in the water	
131-1	22.04.03	09:26	79° 3,39' N	4° 19,02' E	2430,0	Colonization Tray	information	Toppeinheit 6 gelbe, 6 orange Benthoskugeln
131-1	22.04.03	09:27	79° 3,39' N	4° 18,95' E	2431,2	Colonization Tray	slipped	
132-1	22.04.03	10:24	79° 0,06' N	4° 28,98' E	2550,8	Mooring	surface	FEVI; mit Ankerstein voran über Stb.
132-1	22.04.03	10:29	79° 0,04' N	4° 28,97' E	2551,6	Mooring	action	SM + 5 Benthos z.W. ; 150m
132-1	22.04.03	10:39	78° 60,00' N	4° 28,95' E	2553,2	Mooring	action	Sedimentfalle z.W.,
132-1	22.04.03	10:47	78° 59,98' N	4° 28,80' E	2555,2	Mooring	action	5 Benthos
132-1	22.04.03	11:13	78° 59,99' N	4° 28,07' E	2561,2	Mooring	action	1000m & 5 Benthos z.W.
132-1	22.04.03	11:36	78° 59,94' N	4° 27,76' E	2565,2	Mooring	action	1000m + Sedimentfalle z.W.
132-1	22.04.03	11:47	78° 59,95' N	4° 27,50' E	2567,2	Mooring	action	150m, 9 Benthos, ARGOS- Toppeinheit z.W.
132-1	22.04.03	11:49	78° 59,95' N	4° 27,44' E	2568,0	Mooring	slipped	
133-1	22.04.03	12:14	79° 0,11' N	4° 29,66' E	2544,0	CTD/rosette	surface	
133-1	22.04.03	12:25	79° 0,17' N	4° 29,51' E	2543,6	CTD/rosette	at depth	
133-1	22.04.03	12:39	79° 0,16' N	4° 29,05' E	2547,6	CTD/rosette	on deck	

Station PS64/	Date	Time	PositionLat	PositionLon	Depth [m]	Gear	Action	Comment
133-2	22.04.03	12:50	79° 0,10' N	4° 28,90' E	2550,8	Multiple net	surface	
133-2	22.04.03	13:43	78° 59,69' N	4° 27,52' E	2574,4	Multiple net	at depth	
133-2	22.04.03	13:44	78° 59,69' N	4° 27,49' E	2574,4	Multiple net	Hoisting	
133-2	22.04.03	14:38	78° 59,28' N	4° 26,49' E	2591,6	Multiple net	on deck	
134-1	22.04.03	15:55	79° 4,01' N	3° 42,68' E	2899,3	CTD/rosette	surface	
134-1	22.04.03	16:03	79° 3,99' N	3° 42,47' E	2919,1	CTD/rosette	at depth	296m gesteckt
134-1	22.04.03	16:10	79° 3,96' N	3° 42,39' E	2937,6	CTD/rosette	on deck	
134-2	22.04.03	16:18	79° 3,95' N	3° 42,30' E	2935,6	Multi corer	surface	
134-2	22.04.03	17:14	79° 3,77' N	3° 41,62' E	3003,2	Multi corer	at sea bottom	2962m
134-2	22.04.03	18:17	79° 3,65' N	3° 40,81' E	3038,0	Multi corer	on deck	
135-1	22.04.03	18:51	79° 3,49' N	3° 28,73' E	3995,6	CTD/rosette	surface	
135-1	22.04.03	18:57	79° 3,47' N	3° 28,65' E	4006,4	CTD/rosette	at depth	304 m
135-1	22.04.03	19:08	79° 3,42' N	3° 28,46' E	4025,2	CTD/rosette	on deck	
135-2	22.04.03	19:18	79° 3,48' N	3° 28,33' E	4036,0	Multi corer	surface	
135-2	22.04.03	20:38	79° 3,62' N	3° 28,23' E	4067,2	Multi corer	at sea bottom	4051 m
135-2	22.04.03	22:21	79° 3,89' N	3° 27,82' E	3990,0	Multi corer	on deck	
136-1	23.04.03	00:30	79° 5,77' N	4° 40,01' E	2014,0	Multi corer	surface	
136-1	23.04.03	00:37	79° 5,73' N	4° 39,82' E	2037,2	Multi corer	on deck	Galgenblock fest gefroren
136-1	23.04.03	00:41	79° 5,68' N	4° 39,68' E	2046,0	Multi corer	surface	Block wieder gangbar
136-1	23.04.03	01:22	79° 5,96' N	4° 39,88' E	1959,2	Multi corer	at sea bottom	
136-1	23.04.03	02:14	79° 6,10' N	4° 39,19' E	1949,1	Multi corer	on deck	
128-3	23.04.03	04:37	79° 8,25' N	6° 5,30' E	1290,4	Trap, fish	Hydrophon to the water	
128-3	23.04.03	04:43	79° 8,23' N	6° 5,24' E	1290,0	Trap, fish	Information	Prop.wellen ausgekuppelt
128-3	23.04.03	04:47	79° 8,21' N	6° 5,36' E	1289,6	Trap, fish	released	
128-3	23.04.03	04:49	79° 8,20' N	6° 5,42' E	1289,6	Trap, fish	Hydrophon out of the water	
128-3	23.04.03	05:45	79° 8,47' N	6° 5,45' E	1296,8	Trap, fish	on deck	

ARK XIX/2

April 24 to May 14, 2003

Longyearbyen - Bremerhaven

Fahrtleiter / Chief Scientist

Gerhard Kattner

Koordinator / Coordinator

Eberhard Fahrbach

1.	FAHRTABSCHNITT / CRUISE LEG ARK XIX/2	
1.1	Zusammenfassung und Fahrtverlauf	165
	<i>Itinerary and summary</i>	166
1.2	Weather conditions	168
1.3	Hydrographic conditions in the Greenland Sea	169
1.4	Nutrient distribution in the Greenland Sea	172
1.5	Transport of terrigenous organic carbon in the East Greenland Current	174
1.6	Carbon isotopes of dissolved organic matter in the Arctic Ocean: disaggregation of the terrestrial component	175
1.7	Ocean Optics	176
1.8	Optical measurements	181
1.9	Zooplankton	188
1.10	Station list	189
1.11	Participants	192
1.12	Participating Institutions	193
1.13	Ship's Crew ARK XIX/2	194

1. FAHRTABSCHNITT / CRUISE LEG ARK XIX/2

1.1 Zusammenfassung und Fahrtverlauf (AWI)

Der 2. Fahrtabschnitt der 19. Polarstern-Expedition in die Arktis startete am 24. April 2003 in Longyearbyen auf Spitzbergen. Von dort ging es zunächst in Richtung Bäreninsel, wo die ozeanographischen Untersuchungen mit einem Schnitt entlang 75°N begonnen wurden, der bis zum grönländischen Schelfgebiet führte (Fig. 1.1.1). Dieser Schnitt wird jährlich wiederholt, um Veränderungen der Wassermassen insbesondere der Tiefen- und Bodenwassermassen der Grönlandsee langfristig untersuchen zu können. In diesem Jahr konnte aufgrund der frühen Jahreszeit die großräumige hydrographische Struktur unmittelbar nach den Konvektionseignissen im Winter erfasst werden. Die sehr komplexen Vorgänge sollen zum einen durch die Untersuchungen während der 75° Schnittfahrten und zum anderen durch autonome Jojo-Verankerungen geklärt werden. Die Verankerungen ermöglichen die detaillierte Aufzeichnung der Prozesse während des ganzen Jahres. Das herausragende Ergebnis der diesjährigen Untersuchungen war das Auffinden und Vermessen eines konvektiven Wirbels, der die größte Konvektionstiefe hatte, die in den letzten Jahren gefunden wurde. Das Temperaturmaximum, das normalerweise bei etwa 1700 m liegt, lag hier in einer Tiefe von 2700 m.

Neben den hydrographischen Untersuchungen wurden während des 75° Schnitts sowie auf dem grönländischen Schelf und am Hang die Nährsalzkonzentrationen gemessen, um im Vergleich zu früheren Fahrten die saisonalen und jährlichen Veränderungen bestimmen zu können. Nitrat und Phosphat, deren Verhältnis sowie Silicat haben sich als gute Tracer für den Ausstrom arktischen Oberflächenwassers, das zum Teil auch pazifischen Ursprung hat, erwiesen. Während dieser Expedition wurden jedoch keine Anteile pazifischen Wassers gefunden. Ein weiterer Schwerpunkt war die Erfassung von Fluoreszenzprofilen im Ostgrönlandstrom und die Korrelation der Fluoreszenzsignale mit den hydrographischen und chemischen Daten. Mit diesen Untersuchungen werden wir eine bessere Abschätzung des Volumentransports an terrigenem Material im Ostgrönlandstrom erzielen können.

Die optischen Eigenschaften des Meerwassers wurden bestimmt, um eine direkte Validierung von Fernerkundungsdaten vorzunehmen. Dazu gehörten die Messung der Strahlungsdichte über dem Wasser und der Konzentration von Stoffen, die optisch aktiv sind sowie die Bestimmung der optischen Eigenschaften. Ziel der Untersuchungen war es, das Verständnis der Variabilität von optischen Eigenschaften zu verbessern und Daten für der Entwicklung und Verbesserung von Fernerkundungsalgorithmen zu sammeln.

Ziel der biologischen Arbeiten war die Untersuchung der Vertikalverteilung des Zooplanktons in der Grönlandsee in Fortsetzung der Arbeiten auf dem vorherigen Fahrtabschnitt. Da die älteren Stadien den Winter in tiefem Wasser verbringen, sollen die Daten aus dem Frühjahr Aufschlüsse über den Zeitpunkt des Aufstiegs in die euphotische Zone und über die Gonadenreife ergeben, um bessere Informationen über den zeitlichen Verlauf der Reproduktionsbiologie zu erhalten.

Itinerary and summary

Nach Beendigung der Arbeiten auf dem grönländischen Schelf brauchte Polarstern dann noch 5 Tage, um am 14. Mai 2003 wieder in Bremerhaven einzulaufen.

Itinerary and summary

The second leg of the Polarstern expedition ARK XIX to the Arctic started in Longyearbyen on Spitsbergen on the 24th of April 2003. We steamed towards Bear Island to the eastern end of the transect along 75°N across the Greenland Sea (Fig. 1.1.1). The hydrographic observations are repeated for many years to investigate the variability and changes of the Greenland Sea water masses with respect to deep and bottom water formation. During the expedition the large scale hydrographic structure was assessed immediately after the winter cooling period. The complex conditions were studied by oceanographic measurements during the Greenland Sea transect and by autonomous Jojo-moorings. These moorings allow detailed records of a complete yearly cycle. The most outstanding single feature of the survey in the Greenland Sea was the convective eddy. This feature represents the deepest convection level observed in recent years. The ubiquitous temperature maximum (found usually at medium depth levels of about 1700 m) was displaced downwards to 2700 m.

Along the 75°N transect and on the Greenland shelf nutrient concentrations were determined to monitor interannual and spatial variability. Nitrate and phosphate and its ratio as well as silicate are good tracers for the outflow of upper halocline Arctic surface water flowing along the Greenland continental slope. Part of this water mass is probably of Pacific origin but during this expedition no signature of water masses from the Pacific could be detected. Another topic was the determination of fluorescence profiles in the East Greenland Current (EGC) and their correlation with hydrographic and chemical data. These studies will allow a better estimate on the amount of terrigenous carbon transported from the Arctic Ocean via the EGC to the North Atlantic.

The optical properties of seawater were determined for direct validation of optical remotely-sensed data. The radiance above the water was measured, which mimics the satellite-borne sensors. Concentrations of optically active constituents in the water and optical properties of these constituents were determined. The primary objective was to acquire data for improving our understanding of the ocean optical properties and for developing/refining ocean colour algorithms for the investigated polar waters.

Biological work focused on the seasonal ontogenetic migrations of zooplankton continuing work started on the previous cruise leg. This time series will allow to determine the timing of developmental ascent after overwintering and gonad maturation and will reveal better information of the reproduction biology of zooplankton species.

After finishing our research in the East Greenland shelf area Polarstern needed 5 days back to Bremerhaven, where she arrived on the 14th of May 2003.

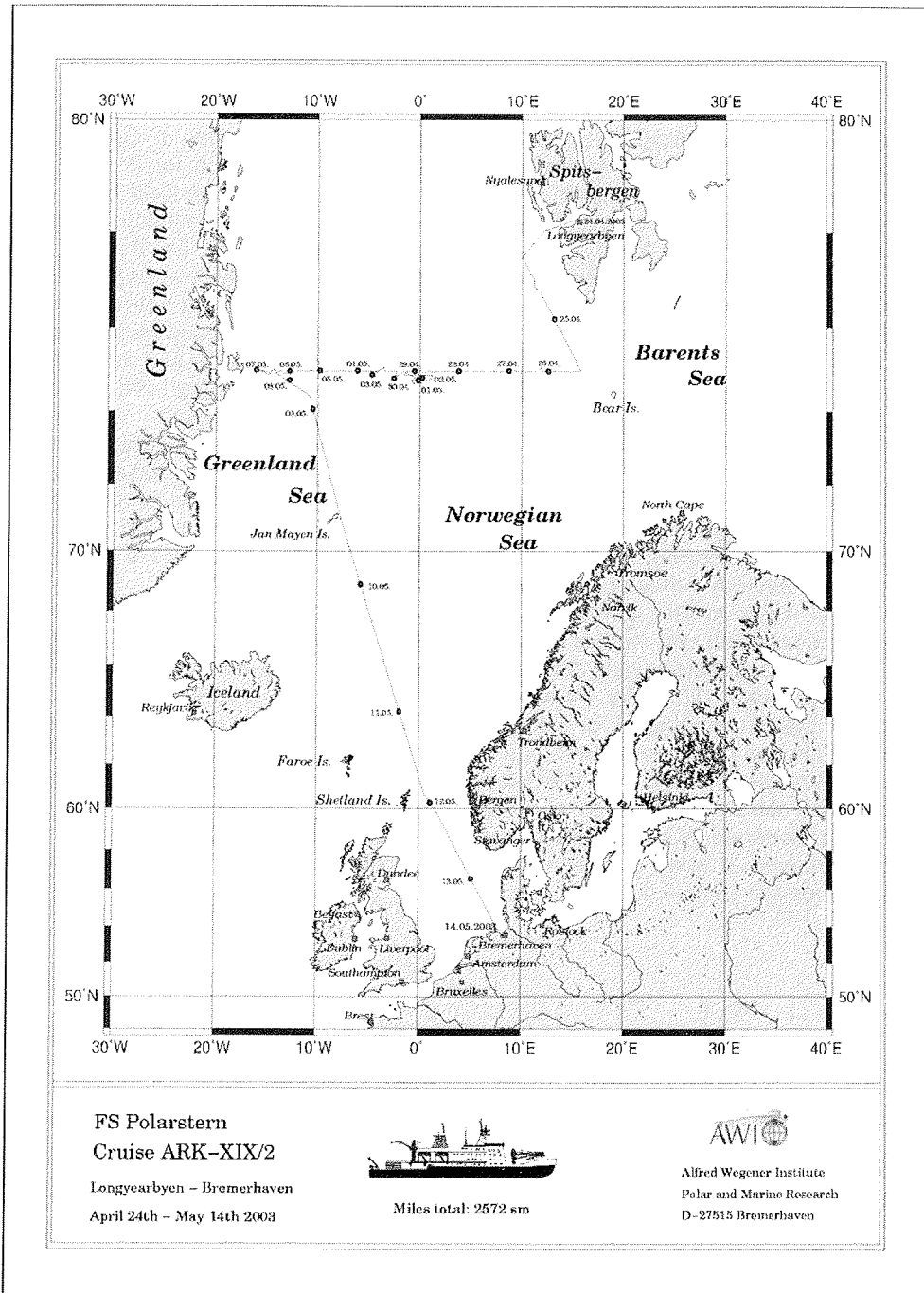


Fig. 1.1.1 Cruise track of RV Polarstern during the ARK XIX/2 expedition

Weather conditions

1.2 Weather conditions

E. Knuth (DWD)

On April 24 at about 18:00 local time RV Polarstern left the Isfjorden on Spitsbergen under sunny conditions and temperatures of minus 10°C heading for Bear Island. The transit to the 75°N transect north of Bear Island was influenced by a high pressure system over Greenland. On the evening of April 25 the investigations began along 75°N, going west. Moderate to fresh easterly winds and a sea of about 2 m occurred. The following work was dominated by a stable northerly flow, accompanied by some heavy snow showers. The temperatures encountered were between minus 10 and minus 3°C. For a short time the investigations were influenced by small polar lows, which developed southwest of Spitsbergen and caused winds of 7 to 8 Bft and a sea of 4 to 4.5 m. The synoptic situation was dominated by a high with northerly winds of 4 to 5 Bft and a sea of 2-3 m over north and central Greenland.

During the night from May 2 to 3 RV Polarstern encountered the first light sea-ice of this leg. From May 5 light to moderate south easterly winds predominated and did not hinder the station work within the ice. In the afternoon of May 7 the most westerly station was reached near 75°N 16.3°W. The weather was sunny and only light southerly winds occurred. At noon of May 9 the last investigations were completed under south easterly winds of Bft 2 and temperatures of minus 4°C.

The cruise back to Bremerhaven began with light to moderate winds. The ice coverage decreased and the last ice was observed during the following night. Late on May 9 a light to moderate wind came from westerly directions and veered northerly in the following night. Then RV Polarstern came near to the northern flank of a low pressure system southwest of Iceland, which moved slowly east. This weather condition caused northerly to north easterly winds of Bft 4 to 6. From May 11 until the end of the cruise a trough over the Hebrides and Irish Sea moved slowly east. Under its influence the wind turned to southerly, later south westerly directions. The wind force was moderate to strong, accompanied by local showers. RV Polarstern arrived in Bremerhaven at noon of May 14. Frequency of wind speeds and directions are given in Figs 1.2.1 and 1.1.2.

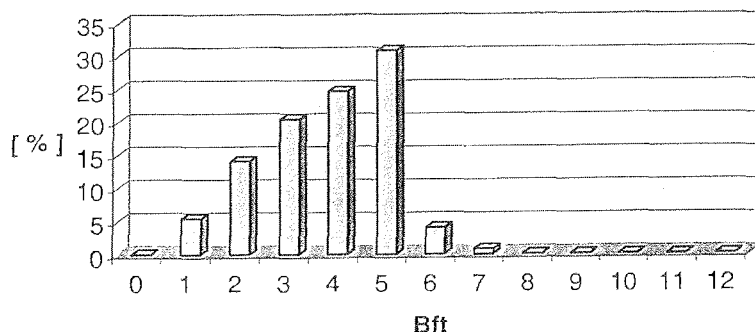


Fig. 1.2.1 Frequency of wind speeds during ARK XIX/2

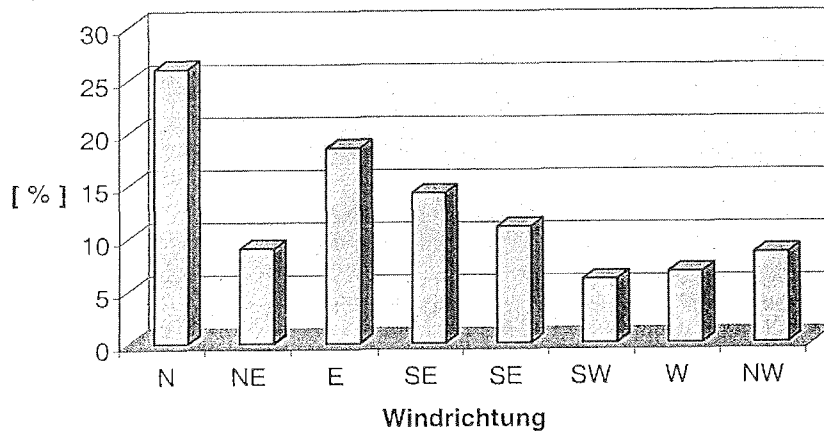


Fig. 1.2.2 Frequency of wind directions during ARK XIX/2

1.3 Hydrographic conditions in the Greenland Sea

G. Budéus, S. Ronski, R. Plugge, J. Schwarz, L. Gerull,
J. Otto, S. Breitenbach (AWI)

Bottom water renewal in the Greenland Sea by deep convection in interplay with ice coverage and atmospheric forcing is a major element of the water mass modification in the Arctic Mediterranean. Effects influence both the central Arctic Ocean and the overflow waters into the Atlantic. Since the hydrographic observations became more frequent in the late 1980s, no bottom water renewal by winter convection took place. However, under these conditions, the deep water properties changed towards higher temperatures and salinities. Furthermore, the doming structure in the Greenland Gyre, as it was observed in the mid-80s, was superseded by an essentially 2-layered water mass arrangement with a marked density step which is located presently at about 1700 m. The specific objectives of the project, which is incorporated in the EU funded 'CONVECTION', are to investigate the relative importance of atmospheric forcing parameters for winter convection, to clarify whether ice coverage inhibits or facilitates deep convection, to build a long term observational basis about deep water changes in the Greenland Gyre, and to contribute to the decision which deep water exchange mechanisms are at work under the absence of deep winter convection. A special focus is put on a long-lived submesoscale coherent vortex (SCV). Within this eddy, winter convection penetrates usually to considerably greater depths (about 2600 m) than in the surrounding waters. The eddy has a diameter of only 20 km, and as it shows no surface signal it is difficult to detect.

Hydrographic conditions in the Greenland Sea

Work at sea

In the central Greenland Sea, a long term zonal CTD transect at 75°N has been performed with a regular station spacing of 10 nautical miles. This distance has not been reduced at frontal zones in order to gain time for a couple of stations dedicated to the search and investigation of the SCV. CTD and water sampler (SBE 911+ with duplicate sensors, SBE Carousel 24 bottles of 12 L each) worked faultlessly. Additional sensors were attached for oxygen concentrations, chlorophyll fluorescence, and Gelbstoff fluorescence.

It is not possible to describe the full details of calibration and data procedures here. A few hints may suffice to give an idea about the general procedure. We use the same sensors already for a number of years and checked for their performance with respect to unwanted cross dependencies. According to this, one of the temperature sensors shows a pressure sensitivity of roughly 1.5 mK/4000 dbar while no pressure or temperature dependence of the conductivity sensors could be found. To identify the latter is close to impossible in the field (within the polar oceans) because of the high gradients in the upper water column where temperature differences occur. The locations of in-situ comparisons have been chosen carefully by checking for each data point whether a comparison is allowed or inhibited. Time alignment has been optimised for each flow path separately (reference station 138) and will be applied together with final post cruise calibration. The difference between pre-cruise and post-cruise calibration is normally in the range of a few mK and a few 1/1000 in salinity. Bottle sample salinities of quadruple samples are determined as a rough check on board, in the lab on land, and by Ocean Scientific.

We started to search for the convective eddy (SCV) at April 27th. A triangle grid formed by equidistant station points was constructed, where the distance between each station pair was 7 nautical miles. This seemed to be the largest allowed distance when looking for a feature of 20 km diameter. As instruments we used deep cast XBTs which have a nominal range of 1850 m (T5, Sippican). Frequently they provided data to 2000 m. Ship speed has to be reduced to about 7 knots when throwing them. Since the cast duration is only about 5 minutes, this does not seriously effect the ship's progress. Software has been used which was specially modified for the actual task of our eddy search. It contains an optional one degree Celsius temperature range with a free choice of the lower temperature scale value. So the vertical structure with the surface warm layer (or its lack) and the mid depth temperature maximum (and its depth) could easily be recognized. Starting at 20:00 in the evening, we were so lucky to detect the eddy already during the next morning at about 5 o'clock and threw XBTs with the double frequency then in order to localize the eddy as well as possible with this rough tool.

The position of the eddy core was 74°50.5 'N, 00°03.5'W on 29 April 2003, and we performed a south-north and an east-west transect (of 8 stations each) across its centre. Transect plots of preliminarily calibrated data are shown in Fig. 1.3.1.

Three in house developed EP/CC (externally powered/compressibility compensated) Jojo-moorings have been exchanged during the worst weather conditions encountered within this cruise. Nevertheless, work went smoothly and no loss of instruments occurred.

First results

The most outstanding single feature of the survey in the Greenland Sea was certainly the convective eddy. This feature represents the deepest convection level observed in recent years. It was found close to the 0° meridian a few miles south of 75°N with the ubiquitous temperature maximum (found usually at medium depth levels of some 1700 m) displaced downwards to 2700 m. The eddy contains water which is denser than the surrounding at low pressure levels (about 600 m), but considerably less dense at higher pressures. This indicates that the water within the eddy is not a good candidate for bottom water replacement. Its lifetime by now exceeds two years. As is true for the background of the Greenland Gyre interior, the eddy is not well ventilated

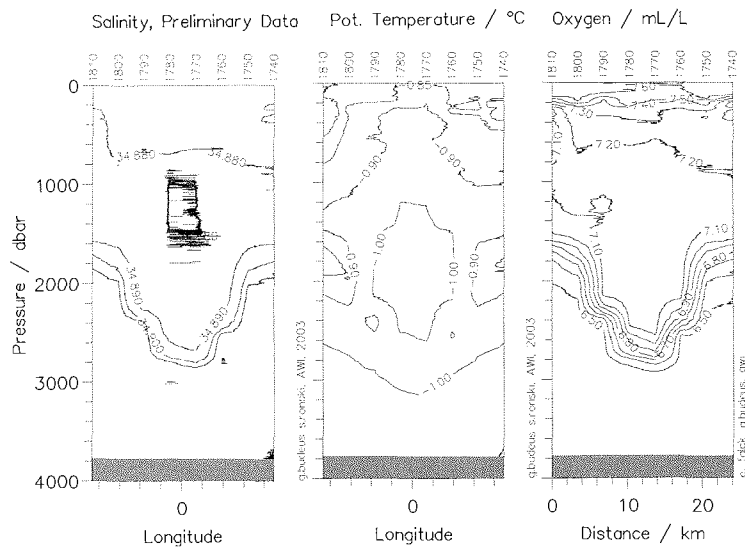


Fig. 1.3.1 Salinity, temperature and oxygen distribution in the convective eddy (SCV)

during the preceding winter, which may initiate eventually its decay. The extent of the cold temperature core has diminished, the core temperature is not colder than last year, the bottom density step is not found at a deeper level than before, and there is no station with vertically homogeneous profiles.

The general situation was characterized by spring conditions. A stable surface layer had already established, largely due to melting pack ice floes which were encountered already at 2°W. It is difficult to determine the exact depth to which winter convection has proceeded, and this has to be analysed later. At first sight, convection seems to have affected only a few hundred metres. The bottom water temperature increase continued, but in a different fashion than observed before. There is no descend of the temperature maximum, and the lower water column showed higher temperatures than before only within the down most 100 to 200 m. As this effect is presumably due to vertical diffusion, the present situation will allow to investigate its specific contribution to the deep water changes in the Greenland Gyre. This was not

Nutrient distribution in the Greenland Sea

feasible during the preceding years when vertical displacement dominated the time variability.

The work on the East Greenland shelf revealed another striking result. The near surface Arctic outflow normally contains waters of Pacific origin and a silicate maximum below, and both were intended to investigate with this cruise. Although the ship went as close to the Greenland coast as possible (20 miles distance) in spite of severe ice conditions, these types of Polar Waters could not be found. Minimum salinities were just below 34.0, whereas the above mentioned waters typically show salinities of about 33.1. As at the same time the area coverage with old pack ice floes was extreme for the last 10 years, this observation might indicate a change in the Arctic surface current system, resulting in an increasing release of ice through Fram Strait and different surface water paths. This, at present speculative, suggestion is supported by the observed Gelbstoff concentrations which were unusually high and located close to the surface.

1.4 Nutrient distribution in the Greenland Sea

M. Behrends, E. Falck, C. Hartmann, G. Kattner, M. Stürcken (AWI)

The distribution of nutrients is closely connected with physical and planktological investigations. The development of phytoplankton blooms is especially dependent on the availability of nutrients. On the other hand nutrients are good tracers for the identification of water masses. Nitrate and phosphate as well as its ratio are good tracers for the outflow of upper halocline Arctic surface water flowing along the East Greenland continental slope. Part of this water mass is probably of Pacific origin. In addition, high concentrations of silicate are typical for water masses in the East Greenland Current. In comparison with similar transects in former years, the seasonal and interannual variability will be determined.

Nutrient concentrations were measured during the 75°N Greenland Sea transect and across the Greenland shelf and slope. To determine the structure of the water masses along the Greenland coast and slope a second transects was conducted back from the Greenland coast and downwards the slope.

Work at sea

From all water samples, taken with the CTD rosette sampler at different depth, the nutrients - nitrate, nitrite, phosphate and silicate - were determined immediately on board with an Autoanalyser-system according to standard methods. In addition, some samples were taken for dissolved organic carbon determination and some of the material was enriched on C-18 resin for latter characterisation of the chemical structure of dissolved organic material.

Preliminary results

The distribution of phosphate, nitrate and silicate is shown in Fig. 1.4.1. The surface concentrations were relatively high and reflect the typical spring situation where nutrients are not depleted because phytoplankton growth has not been started. The small convective eddy was also detected in the nutrient distribution so that lower concentrations reached deeper than in the surrounding water. Another interesting results was found on the East Greenland shelf and slope were usually enhanced

Nutrient distribution in the Greenland Sea

silicate concentrations occurred and water of Pacific origin can be detected by nitrate to phosphate ratios. During this cruise, however, no comparable signals were found. It might be speculated that the circulation of the upper water masses in the Arctic Ocean was different compared to former years.

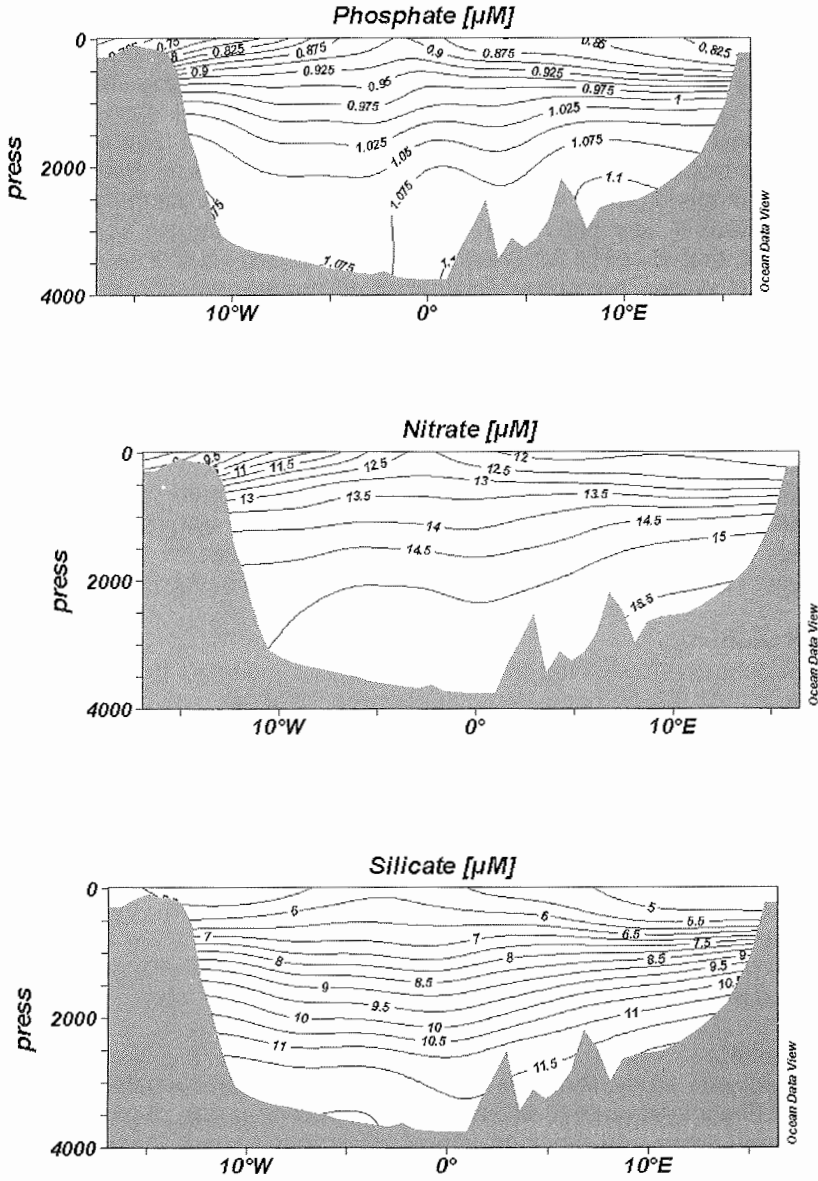


Fig. 1.4.1 Nutrient distribution along the 75°N Greenland Sea transect.

1.5 Transport of terrigenous organic carbon in the East Greenland Current

B. Meon (AWI)

Introduction

The Arctic Ocean holds about 1% of the world's ocean volume but receives a disproportionately large amount (11%) of worldwide river discharge rendering it a unique place to study land-ocean interactions and address the flux and fate of terrigenous organic matter. Eurasian and North American rivers together transport about 23 Tg of dissolved organic carbon (DOC) to the Arctic Ocean. Based on lignin phenol measurements (Opsahl et al. 1999) and more recently fluorescent profiles (Amon et al. 2003) it has been shown that a significant portion of terrigenous dissolved organic material (TDOM) leaves the Arctic Ocean via the East Greenland Current (EGC). However, the current estimates on annual transport of TDOM are based on measurements in August/September thus lacking seasonal resolution. Furthermore, the measurement of specific components of DOM and fluorescence properties of TDOM alone are not sufficient to distinguish between TDOM originating from the Eurasian or North American rivers.

The focus of our current study was to measure fluorescence profiles on the Greenland slope and shelf along the 75°N transect in the EGC. In addition to improving our seasonal resolution of TDOM export estimates to the North Atlantic we intend to use hydrographic data (Budéus and coworkers) and inorganic nutrient measurements (Kattner and coworkers) to link water masses of elevated TDOM concentrations to their Eurasian and/or North American/Pacific origin.

Material and Methods

Fluorescence data were collected in situ using a CTD-mounted probe with a high specificity for TDOM (broad band excitation between 350-460 nm, emission at 550 nm). At selected stations and from various depths DOM was concentrated to conduct lignin phenol measurements in order to calibrate the fluorescent signals against concentrations of vascular plant material that comprises a specific marker for material of terrestrial origin. In short, 10-17 liters of 0.2 µm-filtered seawater was acidified to a pH of 2.5 and passed through a C18 resin using a peristaltic pump and a flow of 1 ml/min. The C18 columns were stored at -20°C for subsequent elution of the adsorbed material with methanol and measurement of lignin phenol oxidation products by gas chromatography-mass spectrometry. Samples for the determination of DOC concentrations were filtered through combusted GF/F-filters and stored frozen in sealed borosilicate ampoules.

Preliminary results

Similar to a previous study (Amon et al. 2003) TDOM fluorescence signals were highest on the Greenland shelf (0.65 relative fluorescence units), decreasing on the steep and narrow slope and reaching almost background levels towards the open Greenland Sea (0.45). The signal intensities were higher than measured before when maximum values on the Greenland shelf at 75°N reached 0.55 fluorescence units (Amon et al. 2003) indicating temporal variations and maybe seasonality in the transport of TDOM with increased TDOM concentrations in spring relative to

Carbon isotopes of dissolved organic matter in the Arctic Ocean: disaggregation of the terrestrial component

summer. A further difference to previous measurements is the location of maximum signal intensities in the depth profiles. Maximum fluorescent values in August/September were located in a distinct core between 50 and 150 m (Amon et al. 2003). In contrast, fluorescence during this year's measurements was highest at the surface and decreased with depth. Interestingly these changes in the vertical distribution of the fluorescence signals coincide with the absence of a typical Polar Water layer of Pacific origin that is characterized by a salinity of about 33 and high silicate concentrations. Thus, the even higher TDOM fluorescence measured this year is likely to derive from material discharged by Eurasian rivers.

In summary there appear to be significant differences between this year's measurements and those conducted in previous years with respect to TDOM concentrations and distribution in the EGC. This may be due to seasonal variations or because of recent changes in the current system of the Arctic Ocean. A closer and quantitative evaluation of the fluorescence data together with nutrient and lignin phenol concentrations will allow a more detailed interpretation of variations in fluxes and the origin of TDOM on the Greenland shelf and slope.

References

Amon, R.M.W., Budéus, G., and B. Meon. 2003. Dissolved organic carbon distribution and origin in the Nordic Seas: Exchanges with the Arctic Ocean and the North Atlantic. *Journal of Geophysical Research-Oceans*. In press.

Opsahl, S., Benner, R., and R.M.W. Amon. 1999. Major fluxes of terrigenous dissolved organic matter through the Arctic Ocean. *Limnology and Oceanography*, 4, 2017-2023.

1.6 Carbon isotopes of dissolved organic matter in the Arctic Ocean: disaggregation of the terrestrial component

H. Köhler (IBM)

Introduction

Analyses of the carbon isotopes ^{13}C and ^{14}C in parallel have the potential to disaggregate terrestrial and marine dissolved organic carbon (DOC) due to their distinct isotopic signatures. The combination of the "source indicator" ^{13}C and the "age indicator" ^{14}C will allow us to reconstruct the fate and relative proportion of terrigenous organic matter in the Arctic Ocean and to assess its flux to the North Atlantic. Isotopic studies of this kind are complementary to optical and biomarker approaches, with the advantage that the bulk DOM is taken into account. In previous studies we found the terrigenous DOM on the Arctic shelf to be refractory and of high molecular weight, whereas DOM of marine origin was predominantly abundant as low molecular weight compounds. During this cruise our research activity focused on the isolation and separation of DOM into different molecular weight fractions. The comparison of carbon isotopes in these fractions of different Arctic water masses will enable us to evaluate the dynamics of DOM in the Arctic Ocean in terms of sources and cycling times.

Methods

Five stations representing water masses of the Atlantic, the Greenland Sea and the East Greenland Current were sampled. Large volume water samples (90-120 litres) for analysis of DOM were taken using a CTD-rosette-sampler. Particles were removed by sequential passage through cartridge filters of 3 and 0.2 μm pore size. The filtrate was then separated by membrane filtration into 3 nominal size fractions: HMW DOM (1 kDa to 0.2 μm , high molecular weight DOM), a medium size fraction (0.5 kDa to 1 kDa) and a fraction of low molecular weight (<0.5 kDa). Size fractionation was performed by a tangential-flow ultrafiltration unit (Pall-Rochem) equipped with Osmonics ultrafilters (Desal GE, Desal DK respectively). Immediately following initial fractionation and concentration, retentate samples were desalted using about 5 l of low organic deionized water. Samples for DOC analysis were collected from the <0.2 μm filtrate and each DOM size fraction. Sample retentates of about 2 l were stored frozen at -20°C after desalination.

A newly developed continuous-flow technique based on high-temperature catalytic combustion for further isotope ratio mass spectrometric detection will allow us to determine carbon isotope data directly on the retentate samples as well as on the permeate samples. Thus, our measurements will cover the total size spectrum of dissolved organic matter, even the low molecular weight fraction, which escaped isotopic measurements in seawater so far.

1.7 Ocean Optics

J. Schwarz, I. Kolar (AWI)

Introduction

Ocean colour satellites, such as SeaWiFS and MoDIS, offer unrivalled temporal and spatial coverage of the surface ocean. These data provide the basis for global estimates of parameters such as phytoplankton biomass and particulate organic carbon, as well as shedding light on seasonal changes and many other phenomena. However, no signal is received in the polar winter or in the presence of large-scale cloud and ice cover, and the signal is especially difficult to interpret when small, sub-pixel-sized clouds or ice fragments are present. In the Atlantic Arctic sector, the spring phytoplankton bloom occurs at the ice edge, making it difficult for satellite sensors to see. A further drawback to ocean colour products is their current reliance on empirical algorithms which are based on measurements in the mid-latitudes. This means that any variability in pigment composition or depth of the chlorophyll maximum, for example, is not included in the algorithms, possibly leading to unrealistic parameter estimates and leaving the ocean colour product quality uncertain.

During this leg of the cruise we worked in collaboration with the group from Scripps Institute of Oceanography: Malgorzata Stramska, Ben Allison and Slawomir Kaczmarek (on loan from the Polish Academy of Sciences Institute of Oceanology, Poland). While we focused on spatial coverage, the Scripps group used profiling instruments to gather information about variability with depth. These datasets should be viewed as complementary.

Aims

Our aims during ARK XIX/2 were:

- to gather as many suites of optical measurements as possible, to add to the sparse knowledge of optical parameters in this region and give a good statistical basis for evaluating algorithm performance during the Arctic springtime.
- to sample the regions with low-percentage ice-cover to estimate errors in satellite data in the presence of sub-pixel ice,
- to sample the ice-covered regions to judge the quality of global estimates of, for example, productivity, which are based solely on ocean colour data.

Methods

Water was taken at 10 m from the CTD where possible. Owing to high demand for water from different groups, samples were occasionally taken from the flow-through supply at 10.7 m, or using a bucket to gather surface water. Samples were taken for:

concentration of phytoplankton pigments (HPLC),
absorption by phytoplankton pigments,
concentration of dissolved, organic carbon,
absorption by coloured, dissolved organic matter,
concentration of organic and inorganic suspended particulates,
particle size distribution (Coulter Counter),
concentration of particulate organic carbon,
concentration of bacteria, and
phytoplankton taxonomy.

Phytoplankton Pigments: Samples were stored in opaque bottles. Between 500 ml and 5 litre aliquots were filtered through 25 mm GF/F filters, which were blotted immediately after filtration was complete, and stored in a liquid nitrogen dewar in 2 ml cryovials. Duplicate and, when possible, triplicate samples were stored in separate dewars. The samples were returned to Bremerhaven for analysis using HPLC.

Absorption by Phytoplankton Pigments: Samples were treated as for phytoplankton pigments. The filters were placed in 27 mm diameter tissue capsules and stored in a liquid nitrogen dewar. At two stations, a series of filtrations was carried out with aliquots of 0 to 1.5 litres of seawater (0.2 μm filtered seawater was filtered for the blank). The purpose of these experiments was to provide information on the particle concentration effect when measuring absorption, for which a correction, the beta-correction factor, must be applied.

Absorption by Coloured, Dissolved Organic Matter and Dissolved Organic Carbon Concentrations: Samples were collected as for phytoplankton pigments. Using a 'contact free' 47 mm glass filtration unit (Sartorius), two 300 to 500 ml aliquots of sample water were filtered through a fresh 0.2 μm membrane filter to rinse the sample collection flask. A third aliquot of sample was filtered and used firstly to rinse thrice and then to fill two 50 ml brown glass sample bottles. For DOC, the sample bottle was half-full, and the bottles were frozen at -25°C , then stored at -10°C . CDOM samples were stored at 4°C .

Concentration of Suspended Particulate Matter (organic/Inorganic): Samples were collected as for phytoplankton pigments. Between 1 and 10 litre aliquots were filtered through precombusted and weighed 47 mm GF/F filters. After filtration, the filters were stored at -25°C. When possible, triplicate samples were taken, together with a blank.

Concentration of Particulate Organic Carbon: Samples were collected as for phytoplankton pigments. Between 0.5 and 5 litre aliquots were filtered through precombusted, 25 mm diameter GF/F filters. The filters were folded and stored in foil wrappings at -25°C. Blanks were taken every 1 to 5 days.

Particle Size Distribution: Samples were collected as for phytoplankton pigments. Aliquots of 250 ml were stored in brown glass bottles, conserved with Lugol's iodine, at room temperature.

Taxonomy: Samples were collected as for phytoplankton pigments. Aliquots of 100 or 250ml were preserved with Lugol's iodine.

Concentration of Bacteria: Samples were collected as for phytoplankton pigments. After rinsing a brown glass bottle three times with sample water, aliquots of 100 ml were preserved using 10 drops of 37% formaldehyde and stored at 4°C.

All samples will be analysed at the home laboratory. Table 1.7.1 indicates which parameters were sampled at each station. All samples are from one or more CTD rosette bottles closed at approximately 10 m depth, except: Stations 168, 169, 174, 175 – taken from the surface using a bucket, and Stations 151, 158, 162, 199, 211, 212, 225, 228, underway 1-13 – all or partially taken from the ship's surface supply (10.7 m).

Table 1.7.1 Parameters sampled at each station during ARK XIX/2

Date	Time (UTC)	Station	HP LC	AP HY	AC DOM	DOC	SPM	POC	PSD	TAX	BAC	PHO
25.04.	14:40	138	x	x	x	x	x		x	x		
		139	x	x	x	x	x	x	x	x		
		140	x	x	x	x	x	x	x	?	?	
26.04.	05:00	141	x	x	x	x	x	x	x	x		
		142	x	x	x	x	x	x	x	x		
		143	x	x	x	x	x	x	x	x		
		144	x	x	x	x	x	x	x	x		
		145	x	x	x	x	x	x	x	x		
		146	x	x	x	x	x	x	x	x		
27.04.	10:20	146	x	x	x	x	x	x	x			
	01:30	147	x	x	x	x	x	x	x	x		
		148	x	x	x	x	x	x	x	x		
		149	x	x	x	x	x	x	x	x		
		150	x	x	x	x	x	x	x	x		
		151	x	x	x	x	x	x	x	x		
		152	x	x	x	x	x	x	x	x		
		153	x	x	x	x	x	x	x	x		
154		x	x	x	x	x	x	x	x			
28.04.	01:40	155	x	x	x	x	x	x	x			

Ocean Optics

Date	Time (UTC)	Station	HP LC	AP HY	AC DOM	DOC	SPM	POC	PSD	TAX	BAC	PHO
	04:30	156	x	x	x	x	x		x	x		
	08:45	157	x	x	x	x	x	x	x	x		
	14:00	158	x	x	x	x	x	x	?	?		
	17:00	159	x	x	x	x	x	x	x	x		
		160	x	x	x	x	x	x	?	?		
	21:40	161	x	x	x	x	x	x	x	x		
29.04.	00:40	162	x	x	x	x	x	x	x	x		
	03:50	163	x	x	x	x	x	x	x	x		
	08:30	164	x	x	x	x	x	x	x	x		
	16:00	165	x	x	x	x	x	x	x	x		
30.04.	13:30	168	x	x	x	x	x	x	x	x		
	16:00	169	x	x	x	x	x	x	x	x		
	19:00	170	x	x	x	x	x	x	x	x		
	23:40	172	x	x	x	x	x	x	x	x		
	02:40	173	x	x	x	x	x	x	x	x		
01.05.	06:15	174	x	x	x	x	x	x	x	x		
	11:30	175	x	x	x	x	x	x	x	x		
	14:45	176	x	x	x	x	x	x	x	x		
	20:00	178	x	x	x	x	x	x	x			
02.05.	01:00	180	x	x	x	x	x	x	x			
		182	x	x	x	x	x	x	x	x		
	19:20	184	x	x	x	x	x	x	x	x	x	
	21:40	185	x	x	x	x		x	x	x		
03.05.	01:00	186	x	x	x	x	x	x	x	x		
	20:30	189-2	x	x	x	x	x	x	x	x		
04.05.	02:15	190	x	x	x	x		x	x	x		
	05:30	191	x	x	x	x	x	x	x	x		
	12:00	192	x	x	x	x	x	x	x	x		
	16:15	193	x	x	x	x	x	x	x	x		
	19:40	194	x	x	x	x	x	x	x	x		
	21:10	195	x	x	x	x	x	x	x	x		
05.05.	00:40	196	x	x	x	x	x	x	x	x		
	04:15	197	x	x	x	x	x	x	x	x	x	
	11:15	198	x	x	x	x	x	x	x	x	x	
	17:45	199	x	x	x	x	x	x	x	x	x	
	20:30	200	x	x	x	x	x	x	x	x	x	
	22:50	201	x	x	x	x	x	x	x	x	x	
06.05.	01:50	202	x	x	x	x	x	x	x	x	x	
	04:55	203	x	x	x	x	x	x	x	x	x	
	08:30	204	x	x	x	x	x	x	x	x	x	
	10:45	205	x	x	x	x	x	x	x	x	x	
	13:20	206	x	x	x	x	x		x	x	x	
	17:00	207	x	x	x	x	x	x	x	x	x	
	19:00	208	x	x	x	x	x	x	x	x	x	
	21:20	209	x	x	x	x	x		x	x	x	

Ocean Optics

Date	Time (UTC)	Station	HP LC	AP HY	AC DOM	DOC	SPM	POC	PSD	TAX	BAC	PHO	
07.05.	01:00	210	x	x	x	x	x	x	?	?	x		
	08:30	211	x	x	x	x	x	x	x	x	x		
	13:30	212	x	x	x	x	x		x	x	x		
		213								x		x	
		214	x	x	x	x	x		x	x	x		
	21:15	215	x	x	x	x	x		x	x	x		
	22:35	216	x	x	x	x	x		x	x	x		
08.05.	00:16	218	x	x	x	x	x		x	x	x		
	01:20	219	x	x	x	x	x		x	?	?		
	03:10	221	x	x	x	x	x		x	x	x		
	04:35	222	x	x	x	x	x		x	x	x		
	05:50	223	x	x	x	x	x		x	x	x		
	08:20	224	x	x	x	x	x		x	x	x		
	10:20	225	x	x	x	x	x		x	x	x		
	13:00	226	x	x	x	x	x	x	x	x	x		
	16:25	227	x	x	x	x	x	x	x	x	x		
	20:40	228	x	x	x	x	x	x	x	x	x		
	23:30	229	x	x	x	x	x	x	x	x	x		
	09.05.	02:30	230	x	x	x	x	x	x	x	x	x	
		06:00	231	x	x	x	x	x	x	x	x	x	
09:40		232	x	x	x	x	x	x	x	x	x		
12:00		Uway1	x	x	x	x	x	x	x	x	x	x	
14:00		Uway2	x	x	x	x	x	x	x	x	x	x	
18:00		Uway3	x	x	x	x	x	x	x	x	x	x	
22:00		Uway4	x	x	x	x	x	x	x	x	x	x	
10.05.	02:00	Uway5	x	x	x	x	x	x	x	x	x	x	
	06:00	Uway6	x	x	x	x	x	x	x	x	x	x	
	10:00	Uway7	x	x	x	x	x	x	x	x	x	x	
	14:00	Uway8	x	x	x	x	x	x	x	x	x	x	
	18:00	Uway9	x	x	x	x	x	x	x	x	x	x	
22:00	Uway10	x	x	x	x	x	x	x	x	x	x		
11.05.	02:00	Uway11	x	x	x	x	x	x	x	x	x	x	
	06:00	Uway12	x	x	x	x	x	x	x	x	x	x	
	10:00	Uway13	x	x	x	x	x	x	x	x	x	x	

1.8 Optical measurements

M. Stramska (USC), D. B. Allison (SIO), S. Kaczmarek (IOPAS)

Our operational objective during the cruise was to carry out a set of in-water optical measurements and to collect discrete water samples for various biochemical analyses (more information about collected data is given below). This work was done in collaboration with Dr. Jill Schwarz from AWI during the second leg of ARK XIX cruise. Our near-future goal is to use the collected data to develop sound bio-optical relationships for the north polar regions. Such bio-optical relationships will be useful for quantitative interpretation of in-situ and satellite optical data in terms of the concentration of optically active water components such as chlorophyll (Chl), particulate organic carbon (POC) and total suspended matter (TSM). Note, that present global ocean colour remote sensing algorithms are based largely on data sets collected in mid- and low-latitudes and there is a concern that satellite remote sensing of phytoplankton biomass in polar regions may be subject to significant errors. Therefore we plan to use our data for validation of the standard ocean colour algorithms in the investigated region. We also expect that our data set will allow us to design refined and new algorithms, and to study the mechanisms driving the observed bio-optical variability. For example, one of our efforts will focus on the development of algorithms for POC determination from satellite data. While pigment algorithms are a routine application of ocean colour remote sensing, the capability to estimate POC from optical remote sensing represents a relatively new idea. Because carbon is of direct interest for the studies on biogeochemical cycles in the oceans, we believe that our goal to develop remote sensing capabilities for estimating POC will be of major significance for advancing our understanding of the role of the oceans in global climate change.

Measurements

The overall cruise schedule allowed for one full optical station and at least two additional short optical stations per day. Data collected at these stations included in water optical measurements with our profiling instruments and filtration of water samples from the ship's CTD for analysis of various water constituents. These are all described in more detail below.

During the full optical station we made vertical profiles using a freefall radiometer (SPMR, Satlantic – RAD on the cruise station logs) for measurements of spectral downwelling irradiance (E_d) and upwelling radiance (L_u) at 13 wavebands (339, 380, 411, 443, 470, 490, 510, 531, 555, 590, 619, 666, and 684 nm). We also measured vertical profiles of the physical and inherent optical water properties with the Multisensor Datalogger System (MDS– OP on the cruise station logs). This system includes a SeaBird Sealogger 25 with temperature, conductivity, and pressure sensors, two single-wavelength (488 and 660 nm) beam transmissometers (WetLabs), chlorophyll fluorometer (WetLabs), Quantum Scalar Irradiance (PAR) sensor (QSP-200PD, Biospherical), the spectral backscattering meter Hydrosat-6 (HobiLabs) allowing determination of backscattering coefficient (b_b) at six wavelengths (442, 470, 555, 589, 620, and 671 nm), and two a-beta (HobiLabs) instruments for measurements of total absorption (a) and backscattering coefficients at

Optical measurements

one waveband each (420 and 510 nm). Typically, the SPMR downcasts ended at 60-m and the MDS downcast ended at 150-m depth.

Short optical stations included vertical profiles of physical and inherent optical water properties with the MDS package in surface water (30-50 m). In addition to the regular short optical stations we were able to increase the frequency of these casts on the transect out of the Greenland shelf. In this case the MDS casts were done on every regular ship's CTD station (PS64/214 - PS64/232) down to 100-m depth.

At most of the optical stations discrete water samples were taken from the ship's CTD bottles at selected depths within the euphotic zone for various analyses. Typically during the full optical station discrete water samples were collected at 5 depths while only 2 depths were sampled at the short optical stations. In addition to the optical stations, we sampled water from the ship's flow-through sea water system (ca. 10 m depth) at opportune times. In particular, we observed spring bloom conditions at the ice edge, and water was sampled from the ship's flow-through water supply for some time after the regular CTD stations ended.

All the discrete water samples will be analysed at the appropriate facilities at our home institutions. Particulate ($a_p(l)$) and phytoplankton ($a_{ph}(l)$), absorption spectra from 300 to 800 nm will be measured with a double-beam bench-top spectrophotometer using a filter-pad technique. The dry weight of total suspended matter (*TSM*) will be obtained by standard gravimetric technique. Standard procedures will be used to measure pigments (HPLC and fluorometry) and POC (combustion of dry sample filters). At selected stations water samples were also preserved for microscopic analysis of plankton. A list of optical stations and their geographical positions are shown in Table 1.8.1 and Figure 1.8.1.

Additionally, in few cases when we observed clear sky conditions (during a station or when ship was underway) we made above-water optical measurements of direct sun radiance with a portable hand-held sun photometer MicroTops (Solar Light). This instrument includes 5 wavebands: 440, 500, 675, 870, and 940 nm, and allows the determination of atmospheric aerosol optical thickness for proper correction of direct atmospheric transmittance. Aerosol optical thickness at the time of satellite overpass is essential for verifying the atmospheric correction of ocean colour.

Preliminary Results

Full interpretation of our data will be only possible after we finish processing the optical and physical data from the vertical profiles and discrete water samples are analysed in the appropriate facilities. However, preliminary results indicate that in the open ocean waters we observed mostly low chlorophyll concentrations characteristic of pre-bloom conditions. Higher concentrations of phytoplankton were present only at the ice edge on the way into and out of the East Greenland Current. Examples of concurrent vertical profiles of water temperature, salinity, density, fluorescence, and beam transmission at 488 and 660 nm are shown in Figures 1.8.2 – 1.8.7. Stations shown in Figures 1.8.2 – 1.8.5 were collected on the 75°N transect, while stations shown in Figures 1.8.6 and 1.8.7 represent bloom conditions observed on the ice edge on the way out of the Greenland shelf. Interestingly, it is evident from the data shown in Figures 1.8.2 – 1.8.7 that there is a good correspondence between the physical and optical features in the vertical profiles observed in surface waters of the various oceanic regions visited during our cruise.

Optical measurements

Table 1.8.1 List of full and short optical stations.

SIO Number	Station AWI Number	Station Date [GMT]	Time	Latitude [°]	Longitude [°]
full stations					
1	PS64/138	4/25/2003	14:04	75.9183	13.8742
2	PS64/144	4/26/2003	10:51	74.9985	12.5977
5	PS64/150	4/27/2003	11:21	75.0002	8.7365
8	PS64/157	4/28/2003	08:44	74.9973	4.2347
11	PS64/164	4/29/2003	08:30	75.0003	-0.3038
18	PS64/189	5/03/2003	20:25	75.0010	-4.1233
20	PS64/192	5/04/2003	10:05	75.0012	-6.0660
22	PS64/198	5/05/2003	09:27	75.0023	-9.9283
29	PS64/213	5/07/2003	15:47	74.9978	-16.0050
41	PS64/225	5/08/2003	09:18	74.7552	-13.0620
short stations					
12	PS64/165	4/29/2003	14:17	74.9987	-0.9333
13	PS64/168	4/30/2003	11:25	74.7682	-0.1278
14	PS64/169	4/30/2003	14:34	74.7995	-0.1295
16	PS64/175	5/01/2003	09:45	74.8418	0.3132
23	PS64/199	5/05/2003	14:58	75.9990	-10.5877
24	PS64/204	5/06/2003	07:37	74.9783	-12.4870
25	PS64/205	5/06/2003	10:06	74.9900	-12.6292
26	PS64/207	5/06/2003	17:00	74.9547	-13.2487
27	PS64/211	5/07/2003	08:23	75.0032	-15.6675
28	PS64/212	5/07/2003	13:10	74.9987	-16.3323
30	PS64/214	5/07/2003	17:40	74.9830	-15.6947
32	PS64/215	5/07/2003	20:56	74.9708	-15.3545
33	PS64/216	5/07/2003	22:35	74.9215	-14.9567
34	PS64/217	5/07/2003	23:23	74.9277	-14.6838
35	PS64/219	5/08/2003	01:15	74.9353	-14.1185
36	PS64/220	5/08/2003	02:15	74.9072	-13.8538
37	PS64/221	5/08/2003	03:09	74.8543	-13.6178
38	PS64/222	5/08/2003	04:35	74.8037	-13.2275
39	PS64/223	5/08/2003	05:31	74.7870	-13.1695
40	PS64/224	5/08/2003	07:59	74.7713	-13.1330
42	PS64/226	5/08/2003	11:59	74.7785	-12.8190
43	PS64/227	5/08/2003	13:57	74.7223	-12.6920
43	PS64/227	5/08/2003	13:57	74.7223	-12.6920
44	PS64/228	5/08/2003	19:42	74.6613	-12.4815
45	PS64/229	5/08/2003	22:09	74.6270	-12.2085
46	PS64/230	5/09/2003	01:05	74.5838	-11.8910
47	PS64/231	5/09/2003	04:26	74.5000	-11.3940
48	PS64/232	5/09/2003	07:59	74.3950	-10.8620

Optical measurements



Figure 1.8.1 Map showing the locations of the optical stations covered by the Scripps group. Full optical stations are indicated by circles, short stations by dots, and the ship's positions on the way back to Bremerhaven when water samples were collected from the flow-through sea water system are indicated by crosses.

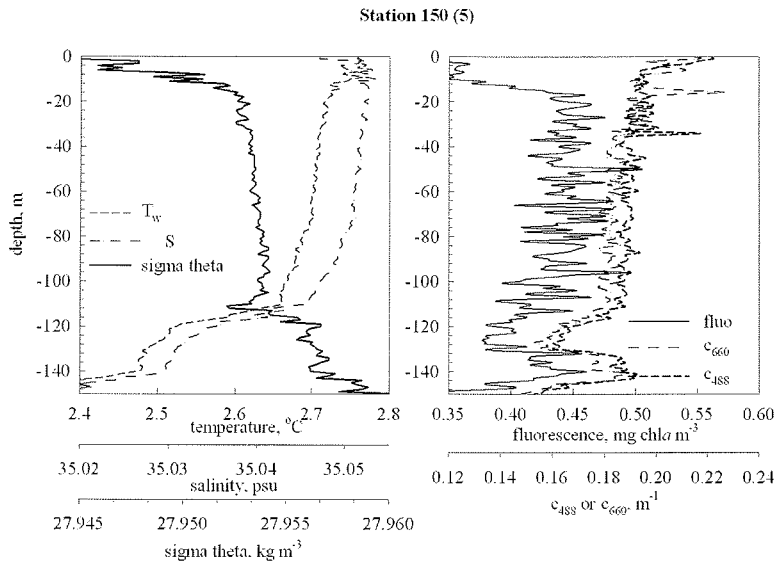


Figure 1.8.2 Vertical profiles of water temperature (T_w), salinity (S), density (sigma theta), beam attenuation at 488 nm (c_{488}) and 660 nm (c_{660}), and fluorescence (fluo) measured at station 150 (75.001°N , 8.7365°E). The number in parenthesis indicates Scripps station number (SIO station 5). Fluorescence has been tentatively converted to mg chl a m^{-3} based on the fluorometer calibrations from our previous experiments

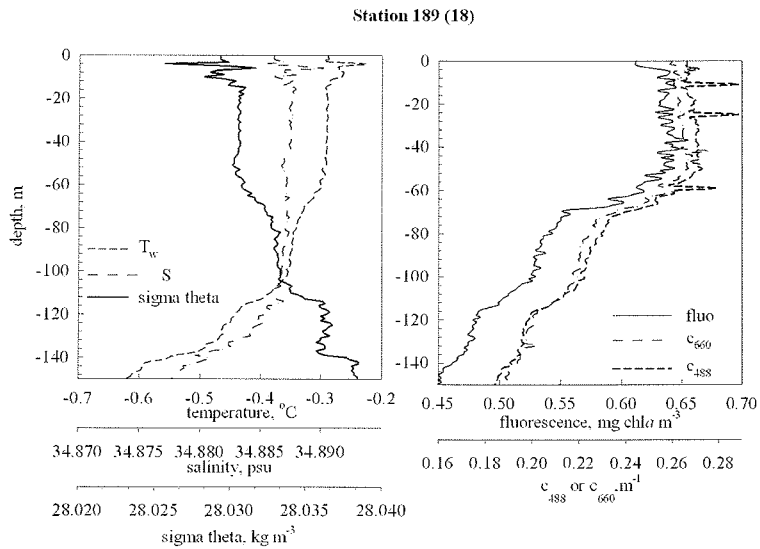


Figure 1.8.3 As in Figure 1.8.2, but for station 189 (75.001°N , 4.1233°E).

Optical measurements

Station 198 (22)

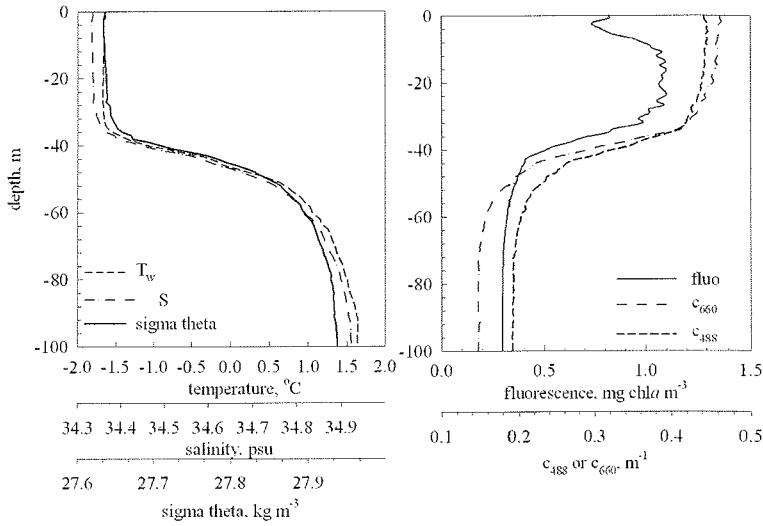


Figure 1.8.4 As in Figure 1.8.2, but for station 198 (75.0023N, 9.9283W).

Station 205 (25)

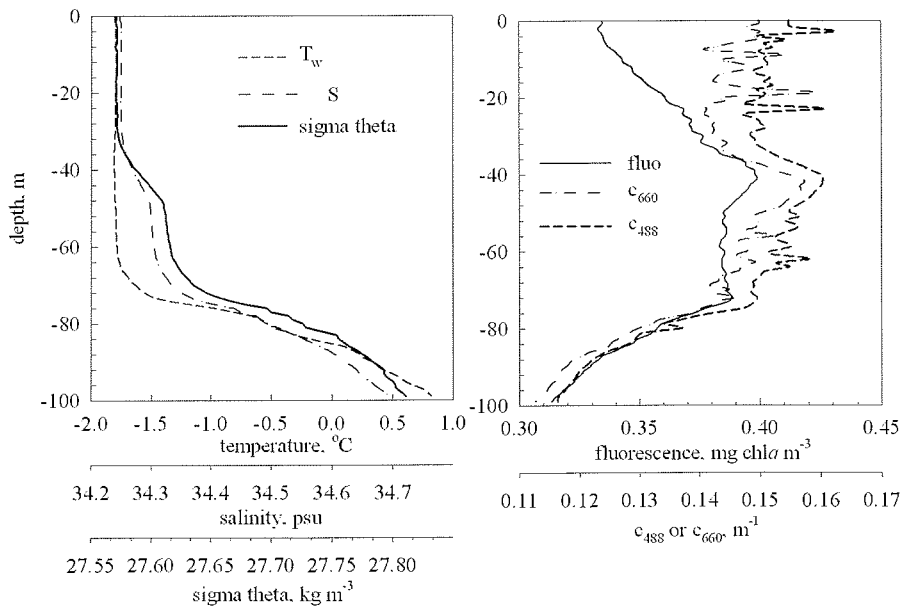


Figure 1.8.5 As in Figure 1.8.2, but for station 205 (74.99N, 12.629W).

Optical measurements

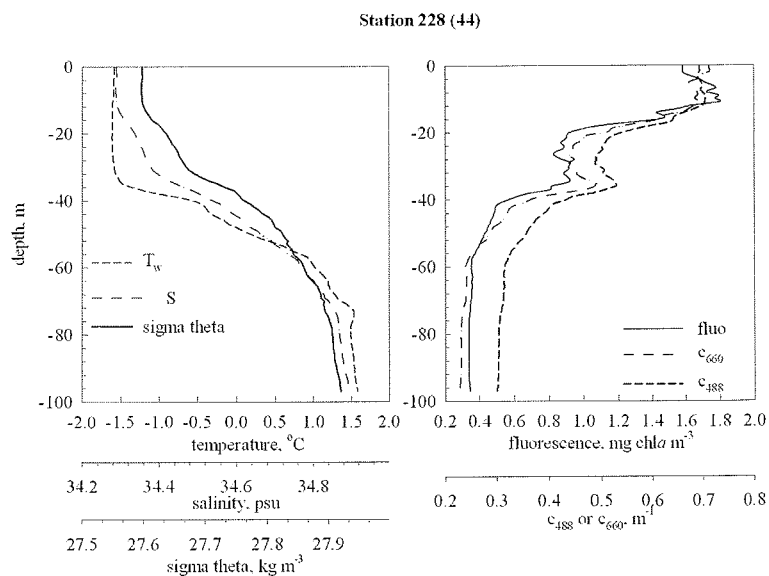


Figure 1.8.6 As in Figure 1.8.2, but for station 228 (74.661N, 12.4815W).

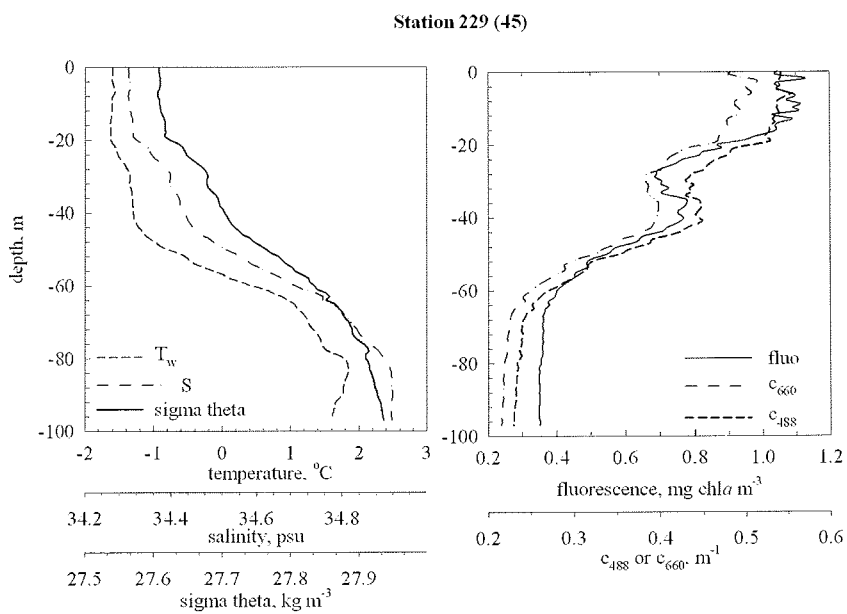


Figure 1.8.7 As in Figure 1.8.2, but for station 229 (74.627N, 12.2085W).

Zooplankton

1.9 Zooplankton

R. Alheit, U. Babst (AWI)

To further clarify the reproductive biology of calanoid copepods from the Greenland Sea a number of zooplankton net samples were taken. A multiple opening and closing net with 150 μm mesh size was employed down to a depth of 2200 m, and the water column sampled vertically at 9 given depths, in both Atlantic and Arctic water masses.

Parallel catches were made down to 200 m, using a fine mesh (55 μm) Nansen Net for population genetic studies. Daily fine mesh (55 μm) Nansen samples, (a total of 14), were taken to collect eggs and young larval stages. Both sets of samples were conserved for further analysis. For gonad maturity and egg production investigation daily samples were taken using a 310 μm mesh size Bongo net. Fifty female *Calanus hyperboreus* were removed from each Bongo catch (total catches = 11) and kept in the laboratory as a time series for in-situ-investigation of gonad maturity and egg production.

Additional experiments with differing food regimes were started to compare gonadal development of *C. hyperboreus* females from 2 different water masses. Further samples were taken for carbon and nitrogen analyses.

Stationlist

1.10 Station list

Station	Date	Time (UTC)		Position	Position	Depth [m]	Gear Abbreviation
		Start	End	Lat	Lon		
138	25.04.03	14:04	15:22	75° 55.10' N	13° 52.45' E	822.4	CTD/RO, OP, RAD
139	25.04.03	22:38	23:00	74° 59.90' N	15° 50.23' E	266.9	CTD/RO
140	26.04.03	00:21	01:16	74° 59.88' N	15° 8.33' E	1052.0	CTD/RO
141	26.04.03	02:23	03:21	75° 0.08' N	14° 29.95' E	1449.0	CTD/RO
142	26.04.03	04:30	06:44	75° 0.02' N	13° 51.76' E	1811.0	CTD/RO, BO, NN
143	26.04.03	08:09	09:31	75° 0.01' N	13° 13.14' E	2023.0	CTD/RO, OP, RAD
144	26.04.03	10:51	13:13	74° 59.91' N	12° 35.86' E	2191.0	CTD/RO
145	26.04.03	14:33	20:50	75° 0.04' N	11° 55.82' E	2345.0	CTD/RO, OP, NN, MN
146	26.04.03	22:20	00:03	74° 59.84' N	11° 17.97' E	2467.0	CTD/RO
147	27.04.03	01:27	02:58	75° 0.05' N	10° 38.24' E	2548.0	CTD/RO
148	27.04.03	04:15	05:43	74° 59.96' N	9° 59.82' E	2595.0	CTD/RO
149	27.04.03	07:11	09:48	75° 0.11' N	9° 22.81' E	2610.0	CTD/RO, OP, NN, BO
150	27.04.03	11:21	13:25	75° 0.01' N	8° 44.19' E	2683.0	CTD/RO, OP, RAD
151	27.04.03	14:42	16:41	74° 59.89' N	8° 4.62' E	3538.0	CTD/RO, OP
152	27.04.03	17:47	19:16	74° 59.97' N	7° 25.61' E	2489.0	CTD/RO
153	27.04.03	20:24	21:44	75° 0.11' N	6° 46.94' E	2280.0	CTD/RO
154	27.04.03	22:58	00:26	74° 59.98' N	6° 7.59' E	2876.0	CTD/RO
155	28.04.03	01:39	03:13	74° 59.93' N	5° 29.76' E	3127.0	CTD/RO
156	28.04.03	04:29	07:26	74° 59.99' N	4° 51.58' E	3275.0	CTD/RO, Op, NN, BO
157	28.04.03	08:44	11:03	74° 59.84' N	4° 14.08' E	3140.0	CTD/RO, OP, RAD
158	28.04.03	12:17	14:14	74° 59.98' N	3° 34.86' E	3492.0	CTD/RO, OP
159	28.04.03	15:37	17:18	74° 59.84' N	2° 55.77' E	2550.0	CTD/RO
160	28.04.03	18:48	20:31	74° 59.92' N	2° 17.04' E	2966.0	CTD/RO
161	28.04.03	21:39	23:28	75° 0.03' N	1° 38.03' E	3164.0	CTD/RO
162	29.04.03	00:39	02:44	75° 0.03' N	0° 59.37' E	3791.0	CTD/RO
163	29.04.03	03:53	07:12	74° 59.94' N	0° 21.01' E	3791.0	CTD/RO, OP, NN, BO
164	29.04.03	08:30	13:24	75° 0.02' N	0° 18.23' W	3788.0	CTD/RO, OP, RAD
165	29.04.03	14:17	16:44	74° 59.92' N	0° 56.00' W	3747.0	CTD/RO, OP
166	29.04.03	17:28	06:54	74° 59.98' N	1° 15.00' W	3660.0	XBT
167	30.04.03	07:54	10:28	74° 44.17' N	0° 7.74' W	3619.0	CTD/RO, NN
168	30.04.03	11:25	13:52	74° 46.09' N	0° 7.67' W	3801.0	CTD/RO, OP
169	30.04.03	14:34	16:45	74° 47.97' N	0° 7.77' W	3782.0	CTD/RO, OP
170	30.04.03	17:30	19:43	74° 50.08' N	0° 7.58' W	3796.0	CTD/RO
171	30.04.03	20:36	22:49	74° 51.96' N	0° 7.51' W	3790.0	CTD/RO
172	30.04.03	23:37	01:47	74° 54.00' N	0° 7.40' W	3790.0	CTD/RO
173	01.05.03	02:38	04:44	74° 56.01' N	0° 7.56' W	3790.0	CTD/RO
174	01.05.03	06:14	09:03	74° 50.43' N	0° 26.79' E	3795.0	CTD/RO, OP, NN, BO
175	01.05.03	09:45	12:15	74° 50.51' N	0° 18.79' E	3792.0	CTD/RO, OP
176	01.05.03	12:53	14:51	74° 50.48' N	0° 11.50' E	3793.0	CTD/RO
177	01.05.03	15:30	17:37	74° 50.54' N	0° 3.48' E	3792.0	CTD/RO
178	01.05.03	18:07	20:03	74° 50.51' N	0° 3.91' W	3792.0	CTD/RO
179	01.05.03	20:35	22:36	74° 50.51' N	0° 11.54' W	3790.0	CTD/RO
180	01.05.03	23:17	01:11	74° 50.54' N	0° 18.65' W	3795.0	CTD/RO

Stationlist

Station	Date	Time (UTC)		Position Lat	Position Lon	Depth [m]	Gear Abbreviation
		Start	End				
181	02.05.03	02:02	03:52	74° 50.35' N	0° 26.16' W	3789.0	CTD/RO
182	02.05.03	06:20	08:21	75° 0.04' N	1° 34.76' W	3745.0	CTD/RO, OP
183	02.05.03	10:32	15:17	74° 50.12' N	2° 30.46' W	3715.0	MOR
184	02.05.03	17:12	20:29	75° 0.01' N	2° 13.01' W	3656.0	CTD/RO, BO, NN
185	02.05.03	21:38	23:42	75° 0.03' N	2° 50.94' W	3709.0	CTD/RO
186	03.05.03	01:05	03:08	75° 0.04' N	3° 30.28' W	3682.0	CTD/RO
187	03.05.03	04:03	07:45	75° 5.13' N	3° 27.43' W	3685.0	MOR
188	03.05.03	10:37	14:14	74° 54.98' N	4° 37.96' W	3631.0	MOR
189	03.05.03	15:26	01:00	75° 0.03' N	4° 8.23' W	3662.0	MN
190	04.05.03	02:15	04:15	74° 59.95' N	4° 47.14' W	3628.0	CTD/RO
191	04.05.03	05:26	08:43	75° 0.02' N	5° 25.03' W	3590.0	CTD/RO, OP, NN, BO
192	04.05.03	10:05	12:50	75° 0.07' N	6° 3.96' W	3543.0	CTD/RO, OP, RAD
193	04.05.03	14:16	16:21	74° 59.93' N	6° 43.04' W	3507.0	CTD/RO, OP
194	04.05.03	17:40	19:39	74° 59.93' N	7° 20.78' W	3458.0	CTD/RO
195	04.05.03	21:08	23:02	74° 59.91' N	8° 1.73' W	3410.0	CTD/RO
196	05.05.03	00:41	02:39	74° 59.97' N	8° 39.85' W	3373.0	CTD/RO
197	05.05.03	04:16	07:12	74° 59.74' N	9° 18.90' W	3308.0	CTD/RO, NN, BO
198	05.05.03	09:27	12:10	75° 0.14' N	9° 55.70' W	3228.0	CTD/RO, OP, RAD
199	05.05.03	14:58	16:53	74° 59.94' N	10° 35.26' W	3084.0	CTD/RO, OP
200	05.05.03	18:31	20:38	74° 59.89' N	11° 2.02' W	2752.0	CTD/RO
201	05.05.03	22:50	00:34	75° 0.15' N	11° 28.25' W	2333.0	CTD/RO
202	06.05.03	01:47	03:17	75° 0.05' N	11° 52.05' W	1912.0	CTD/RO
203	06.05.03	04:55	05:48	74° 57.78' N	12° 18.86' W	1489.0	CTD/RO
204	06.05.03	07:37	09:32	74° 58.70' N	12° 29.22' W	1154.0	CTD/RO, OP, NN, BO
205	06.05.03	10:06	11:26	74° 59.40' N	12° 37.75' W	878.2	CTD/RO, OP, RAD
206	06.05.03	11:57	12:30	74° 59.43' N	12° 46.60' W	573.5	CTD/RO
207	06.05.03	17:00	17:22	74° 57.28' N	13° 14.92' W	274.2	CTD/RO, OP
208	06.05.03	18:45	19:03	75° 0.25' N	13° 40.24' W	206.1	CTD/RO
209	06.05.03	21:03	22:05	75° 0.80' N	14° 18.49' W	168.2	CTD/RO
210	07.05.03	01:01	01:15	74° 59.02' N	14° 59.30' W	119.3	CTD/RO
211	07.05.03	08:23	10:04	75° 0.19' N	15° 40.05' W	201.8	CTD/RO, OP, NN, BO
212	07.05.03	13:10	14:32	74° 59.92' N	16° 19.94' W	326.3	CTD/RO, OP, EF
213	07.05.03	15:47	16:46	74° 59.87' N	16° 0.30' W	266.4	CTD/RO, OP, RAD
214	07.05.03	17:40	17:58	74° 58.98' N	15° 41.68' W	206.9	CTD/RO, OP
215	07.05.03	20:56	21:19	74° 58.25' N	15° 21.27' W	159.2	CTD/RO, OP
216	07.05.03	22:35	22:49	74° 55.29' N	14° 57.40' W	143.4	CTD/RO, OP
217	07.05.03	23:23	23:44	74° 55.66' N	14° 41.03' W	180.6	CTD/RO, OP
218	08.05.03	00:16	00:30	74° 56.21' N	14° 25.39' W	173.4	CTD/RO
219	08.05.03	01:15	01:28	74° 56.12' N	14° 7.11' W	177.1	CTD/RO, OP
220	08.05.03	02:08	02:23	74° 54.45' N	13° 51.20' W	190.6	CTD/RO, OP
221	08.05.03	03:09	03:25	74° 51.26' N	13° 37.07' W	270.0	CTD/RO, OP
222	08.05.03	04:35	05:07	74° 48.22' N	13° 13.65' W	606.8	CTD/RO, OP
223	08.05.03	05:31	07:30	74° 47.22' N	13° 10.17' W	854.5	CTD/RO, OP, NN, BO
224	08.05.03	07:59	08:45	74° 46.28' N	13° 7.98' W	1046.0	CTD/RO, OP
225	08.05.03	09:18	10:42	74° 45.31' N	13° 3.72' W	1289.0	CTD/RO, OP, RAD
226	08.05.03	11:59	12:56	74° 46.71' N	12° 49.14' W	1522.0	CTD/RO, OP
227	08.05.03	13:57	18:26	74° 43.34' N	12° 41.52' W	1915.0	CTD/RO, OP
228	08.05.03	19:42	21:07	74° 39.68' N	12° 28.89' W	2316.0	CTD/RO, OP

Stationlist

Station	Date	Time (UTC)		Position	Position	Depth [m]	Gear Abbreviation
		Start	End	Lat	Lon		
229	08.05.03	22:09	23:38	74° 37.62' N	12° 12.51' W	2582.0	CTD/RO, OP
230	09.05.03	01:05	02:43	74° 35.03' N	11° 53.46' W	2852.0	CTD/RO, OP
231	09.05.03	04:26	06:15	74° 30.00' N	11° 23.64' W	3073.0	CTD/RO, OP
232	09.05.03	07:59	09:48	74° 23.70' N	10° 51.72' W	3132.0	CTD/RO, OP

CTD probe

RO = Rosette water sampler

OP = Optics Package: Multi Sensor Data Logger (mit CTD)

NN = Nansen net MN = Multiple net

BO = Bongo net

XBT = Expendable bathythermograph

RAD = Seawifs Profiling Multi Wavelength Radiometer

MOR = Mooring

Participants

1.11 Participants

Name	Institute
Alheit, Ruth	AWI
Allison, David Ben	SIO
Babst, Ulrike	AWI
Behrens, Melanie	AWI
Brauer, Irene	SBG
Breitenbach, Sebastian	AWI
Budéus, Gereon	AWI
Falck, Eva	AWI
Gerull, Linda	AWI
Hartmann, Carmen	AWI
Kaczmarek, Slawomir	IOPAS
Kattner, Gerhard	AWI
Knuth, Edmund	DWD
Köhler, Hayo	IBM
Kolar, Ingrid	AWI
Kolk, Annette	BIA
Lannig, Gisela	AWI
Meon, Benedikt	AWI
Metzger, Rebecca	AWI
Otto, Juliane	AWI
Plugge, Rainer	AWI
Ronski, Stephanie	AWI
Schwarz, Jill Nicola	AWI
Stöckert-Stüve, Axel	AWI
Stramska, Malgorzata	USC
Stürcken, Marthi	AWI

1.12 Participating Institutions

AWI Alfred-Wegener-Institut für Polar- und Meeresforschung
Columbusstrasse
27568 Bremerhaven, Germany

BIA Berufsgenossenschaftliches Institut für Arbeitssicherheit
Alte Heerstr. 111
53757 St. Augustin, Germany

DWD Deutscher Wetterdienst
Bernhard-Nocht-Straße
20359 Hamburg, Germany

IBM Institut für Biogeochemie und Meereskunde
Universität Hamburg
Bundesstraße 55
20146 Hamburg

IOPAS Institute of Oceanology
Polish Academy of Sciences
Powstancow Warszawy 55
P.O. Box 68
81-712 Sopot, Poland

SBG See-Berufsgenossenschaft
Reimerstwiete 2
20457 Hamburg, Germany

SIO Marine Physical Laboratory
Scripps Institute of Oceanography
La Jolla, CA 92093 – 0238, USA

USC University of Southern California
Mancock Institute for Marine Studies
Los Angeles, CA 90089 – 0371, USA

Ship's Crew

1.13 Ship's Crew ARK XIX/2

Pahl, Uwe	Master
Schwarze, Stefan	1. Offc.
Schulz, Volker	Ch.Eng.
Fallei, Holger	2. Offc.
Hartung, René	2. Offc.
Szepanski, Nico	2. Offc.
Kohlberg, Eberhard	Doctor
Hecht, Andreas	R.Offc.
Erreth Monostori, G.	1. Eng.
Richter, Frank	2. Eng.
Simon, Wolfgang	2. Eng.
Baier, Ulrich	FielaxElo
Dimmler, Werner	FielaxElo
Fröb, Martin	FielaxElo
Holtz, Hartmut	ElecTech.
Piskorzynski, Andreas	FielaxElo
Clasen, Burkhard	Boatsw.
Neisner, Winfried	Carpenter
Burzan, Gerd-Ekkeh.	A.B.
Guse, Hartmut	A.B.
Kreis, Reinhard	A.B.
Moser, Siegfried	A.B.
Schmidt, Uwe	A.B.
Schröder, Norbert	A.B.
Schultz, Ottomar	A.B.
Beth, Detlef	Storek.
Arias Iglesias, Enr.	Mot-man
Dinse, Horst	Mot-man
Fritz, Günter	Mot-man
Krösche, Eckard	Mot-man
Fischer, Matthias	Cook
Martens, Michael	Cooksmate
Tupy, Mario	Cooksmate
Dinse, Petra	1. Stwdess
Schöndorfer, Ottilie	Stwdess/Kr
Deuß, Stefanie	2. Stwdess
Schmidt, Maria	2. Stwdess
Streit, Christina	2. Stwdess
Tu, Jian-Min	2. Steward
Wu, Chi Lung	2. Steward
Yu, Chung Leung	Laundrym.
Niehusen, Arne	Trainee/D
Scholl, Christoph	Trainee/D